Electronic Supplementary Information (ESI)

Selective synthesis of diazacyclooctane-containing flexible ladder polymers with symmetrically or unsymmetrically substituted side chains

Keiki Inoue, Fumitaka Ishiwari* and Takanori Fukushima*

*To whom correspondence should be addressed.
E-mail: ishiwari@chem.eng.osaka-u.ac.jp (F.I.), fukushima@res.titech.ac.jp (T.F)

Table of Contents

Materials and methods

1. Materials. Unless otherwise stated, all commercial reagents were used as received. PIM-EA-TB (M_n = 3.0 × 10^4 Da, M_w/M_n = 1.69) was prepared according to previously reported procedure[1] and unambiguously characterized by nuclear magnetic resonance (NMR) spectroscopy[2] and size exclusion chromatography-multi angle light scattering (SEC-MALS) measurement.

2. General. NMR spectroscopy measurements were carried out on a Bruker AVANCE-500 spectrometer (500 MHz for ^{1}H and 125 MHz for ^{13}C) or AVANCE-400 spectrometer (400 MHz for ^{1}H and 100 MHz for ^{13}C). Chemical shifts (δ) are expressed relative to the resonances of the residual non-deuterated solvents for ^{1}H [$CDCl_3$: $^1H(\delta)$ = 7.26 ppm, DMSO-d_6: $^1H(\delta)$ = 2.50 ppm] and ^{13}C [$CDCl_3$: $^{13}C(\delta)$ = 78.0 ppm, DMSO-d_6: $^{13}C(\delta)$ = 39.52 ppm]. Absolute values of the coupling constants are given in Hertz (Hz), regardless of their sign. Multiplicities are abbreviated as singlet (s), doublet (d), triplet (t), multiplet (m), and broad (br). Infrared (IR) spectra were recorded at 25 °C on a JASCO FT/IR-660$_{Plus}$ Fourier-transform infrared spectrometer. APCI-TOF Mass spectrometry measurements were performed on a Bruker microTOF II mass spectrometer equipped with an atmospheric pressure chemical ionization (APCI) probe. SEC-MALS measurements were performed on a TOSOH GPC-8020 system, equipped with a column (Shodex LF-804), a Wyatt Technology, DAWN HELEOS multiangle laser light scattering photometer with a He−Ne laser (λ_0 = 658 nm), and a Wyatt Technology Optilab rEX differential refractometer, using chloroform ($CHCl_3$) as an eluent at a flow rate of 1.0 mL/min. The SEC-MALS profiles were recorded and analyzed using ASTRA software (ver.6.1.1, Wyatt Technology). Differential refractive index increment ($\partial n/\partial c$) for the polymer in $CHCl_3$ was determined based on the peak area of the refractive index chromatograms and the polymer mass concentration (c) of an injected solution assuming that the injected polymer was fully recovered. The $\partial n/\partial c$ value of PIM-EA-TB was determined to be 0.197 cm^3/g at λ_0 = 658 nm. Angular dependences of the scattering intensity were analyzed using the Debye plot in a scattering angle ranging from 45.8° to 138.8°, to give the weight-averaged molecular weight (M_w) of PIM-EA-TB.

3. Synthesis

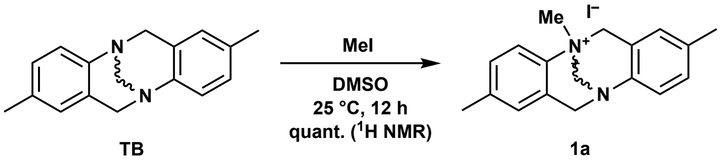

1a:[2] MeI (5.8 μL, 93.3 μmol) was added at 25 °C to a DMSO-d_6 solution (0.45 mL) of **TB** (4.7 mg, 18.8 μmol) in a NMR tube, and the mixture was stirred for 12 h at 25 °C. NMR spectroscopic data of the reaction mixture was measured to confirm quantitative conversion of **TB** into **1a**. The reaction mixture was used for the next step. Spectroscopic data of obtained **1a** were identical to those reported previously.[2] Analytical data (^{1}H and ^{13}C NMR spectra, H-H COSY, HMQC and HMBC correlations) of **1a** are shown in Figures S7–S11.

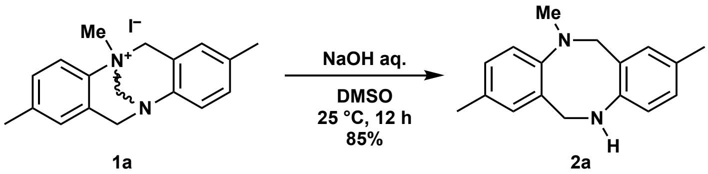

2a:[2] A solution of **1a** (18.8 μmol) in DMSO was poured into a NaOH aqueous solution (1.0 M, 15 mL) at 25 °C, and the mixture was stirred for 12 h at 25 °C. The resultant white precipitate was collected by filtration, washed with water, and then dried under reduced pressure to afford **2a** (85% yield) as a white solid (4.0 mg, 15.9 μmol). Spectroscopic data of obtained **2a** were identical to those reported previously.[2] Analytical data (^{1}H and ^{13}C NMR spectra, HMQC and HMBC correlations, FT-IR spectrum, and high-resolution APCI-TOF mass spectra) of **2a** are shown in Figures S12–S17.

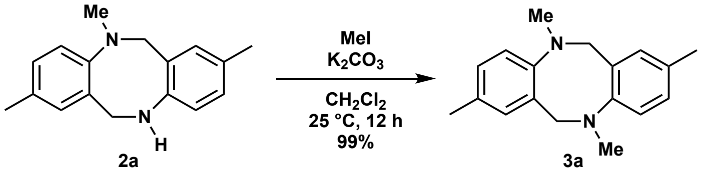

3a: MeI (20.2 μL, 325 μmol) was added at 25 °C to a CH_2Cl_2 solution (1.0 mL) of **2a** (8.2 mg, 32.5 μmol) and K_2CO_3 (22.9 mg, 166 mmol)), and the mixture was stirred for 12 h at 25 °C. The resulting mixture was poured into water (10 mL) and extracted with CH_2Cl_2 (15 mL, eight times). The organic extract was washed successively with water and brine, and then evaporated to dryness under reduced pressure to afford **3a** (99% yield) as a white solid (8.6 mg, 32.2 μmol): ^{1}H NMR (400 MHz, DMSO-d_6): δ (ppm) 6.93 (d, J = 6.2 Hz, 2H), 6.92 (s, 2H), 6.70 (d, J = 8.8 Hz, 2H), 4.21 (s, 4H), 2.70 (s, 6H), 2.20 (s, 6H). ^{13}C NMR (125 MHz, DMSO-d_6): δ (ppm) 148.0, 131.8, 128.2, 126.7, 125.9, 114.8, 57.8, 39.2, 20.0.

FT-IR (KBr): ν (cm^{-1}) 3224, 3056, 2997, 2972, 2945, 2911, 2896, 2856, 2782, 2728, 2593, 2371, 2342, 1882, 1854, 1816, 1786, 1765, 1743, 1726, 1710, 1691, 1678, 1659, 1641, 1613, 1566, 1552, 1509, 1477, 1466, 1449, 1428, 1409, 1379, 1344, 1296, 1247, 1216, 1185, 1128, 1105, 1083, 1041, 1013, 977, 936, 926, 899, 873, 820, 808, 764, 748, 732, 711, 687, 669, 647, 615, 574, 516, 500, 479, 470, 455, 439, 424, 415, 406. High-resolution ACPI-TOF mass: calcd. for $C_{18}H_{23}N_2$ $[M+H]^+$: m/z = 267.1856, found: 267.1847. Analytical data (^{1}H and ^{13}C NMR spectra, HMQC and HMBC correlations, FT-IR spectrum, and high-resolution APCI-TOF mass spectra) of **3a** are shown in Figures S18–S23.

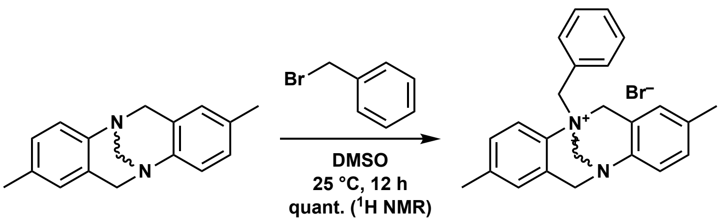

TB **1c**

1c:[3–7] Benzyl bromide (18.2 μL, 153 μmol) was added at 25 °C to a DMSO-d_6 solution (0.45 mL) of **TB** (36.4 mg, 146 μmol) in a NMR tube, and the mixture was stirred for 12 h at 25 °C. NMR spectroscopic data of the reaction mixture was measured to confirm quantitative conversion of **TB** into **1c**. The reaction mixture was used for the next step: ^{1}H NMR (500 MHz, DMSO) δ (ppm) 8.45 (d, J = 8.7 Hz, 1H), 7.56 (d, J = 7.6 Hz, 1H), 7.56 (d, J = 7.6 Hz, 1H), 7.44 (dd, J = 7.6, 7.6 Hz, 1H), 7.41 (dd, J = 7.6, 7.6 Hz, 1H), , 7.39 (dd, J = 7.6, 7.6 Hz, 1H), 7.33 (d, J = 8.7 Hz, 1H), 7.18 (d, J = 8.3 Hz, 1H), 7.09 (d, J = 8.3 Hz, 1H), 6.94 (s, 1H), 6.92 (s, 1H), 5.67 (d, J = 13.2 Hz, 1H), 5.56 (d, J = 13.2 Hz, 1H), 5.44 (d, J = 15.8 Hz, 1H), 5.34 (d, J = 11.4 Hz, 1H), 5.09 (d, J = 11.4 Hz, 1H), 5.06 (d, J = 15.8 Hz, 1H), 4.68 (d, J = 17.2 Hz, 1H), 4.16 (d, J = 17.2 Hz, 1H), 2.19 (s, 3H), 2.15 (s, 3H). ^{13}C NMR (126 MHz, DMSO) δ 140.3, 134.0, 135.8, 134.6, 133.2, 130.3, 129.9, 129.4, 129.1, 128.8, 128.3, 127.4, 127.0, 124.1, 123.1, 121.9, 73.9, 65.5, 64.7, 56.6, 20.3. Analytical data (^{1}H and ^{13}C NMR spectra, H-H COSY, HMQC and HMBC correlations) of **1c** are shown in Figures S24–S28.

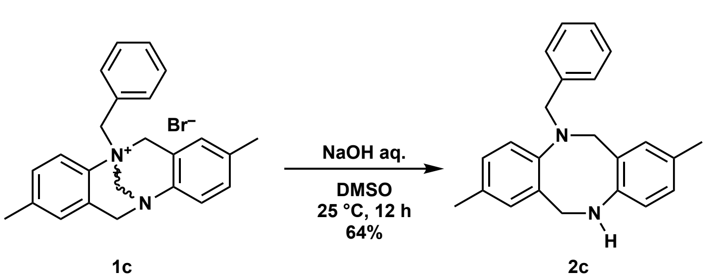

1c **2c**

2c:[3] A solution of **1c** (146 μmol) in DMSO was poured into a NaOH aqueous solution (1.0 M, 20 mL) at 25 °C, and the mixture was stirred for 12 h at 25 °C. The resultant white precipitate was collected by filtration, washed with water, and then dried under reduced pressure to afford **2c** (64% yield) as a white solid (30.7 mg, 93.5 μmol): ^{1}H NMR (400 MHz, CDCl$_3$): δ (ppm) 7.31 (dd, J = 7.3, 7.1 Hz, 2H), 7.25 (d, J = 7.3 Hz, 2H), 7.23 (dd, J = 7.1, 7.1 Hz, 1H), 6.89 (d, J = 8.0 Hz, 1H), 6.88 (s, 1H), 6.86 (d, J = 7.8 Hz, 1H), 6.80 (d, J = 7.8 Hz, 1H), 6.65 (s, 1H), 6.56 (d, J = 8.0 Hz, 1H), 4.44 (s, 2H), 4.38 (s, 2H), 4.37 (s, 2H), 4.12 (s, 1H), 2.23 (s, 3H), 2.17 (s, 3H). ^{13}C NMR (125 MHz, CDCl$_3$): δ (ppm) 147.7, 145.7, 139.4, 132.8, 131.6, 129.2, 128.7, 128.7, 128.5, 128.1, 127.6, 127.5, 126.8, 123.9, 117.8, 117.1, 55.9, 54.7, 51.1, 20.5, 20.4. FT-IR (KBr): ν (cm^{-1}) 3396, 3318, 3083, 3060, 3023, 2999, 2955, 2921, 2894, 2853, 2731, 1952, 1873, 1815, 1728, 1654, 1614, 1567, 1509, 1452, 1412, 1392, 1360, 1342, 1313, 1268, 1226, 1190, 1163, 1122, 1075, 1028, 973, 951, 938, 878, 811, 768, 724, 697, 668, 613, 593, 572, 556, 537, 515, 498, 483, 461, 442, 421, 405. High-resolution ACPI-TOF mass: calcd. for $C_{23}H_{25}N_2$ [M+H]$^+$: m/z = 329.2012, found: 329.1997. Analytical data (^{1}H and ^{13}C NMR spectra, H-H COSY, HMQC and HMBC correlations, FT-IR spectrum, and high-resolution APCI-TOF mass spectra) of **2c** are shown in Figures S29–S35.

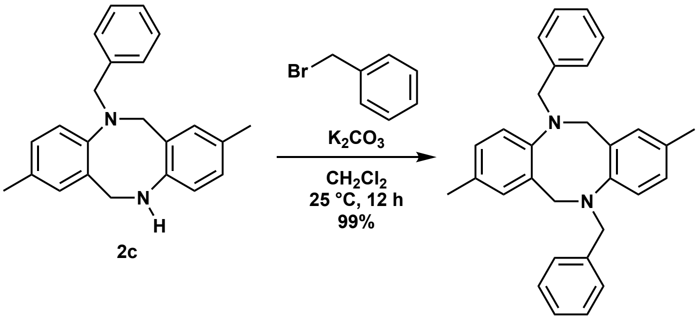

3c

3c: Benzyl bromide (7.30 μL, 61.5 μmol) was added at 25 °C to a CH_2Cl_2 solution (1.0 mL) of **2c** (10.0 mg, 30.5 μmol) and K_2CO_3 (9.1 mg, 65.1 μmol), and the mixture was stirred for 12 h at 25 °C. The resulting mixture was poured into water (10 mL) and extracted with CH_2Cl_2 (15 mL, eight times). The organic extract was washed successively with water and brine, and then evaporated to dryness under reduced pressure at 50 °C to afford **3c** (99% yield) as a white solid (12.6 mg, 30.1 μmol): ^{1}H NMR (400 MHz, CDCl$_3$): δ (ppm) 7.34 (dd, J = 7.3, 7.3 Hz, 4H), 7.27 (dd, J = 7.3, 7.3 Hz, 2H), 7.23 (d, J = 7.3 Hz, 4H), 6.94 (dd, J = 8.2, 1.6 Hz, 2H), 6.82 (d, J = 8.2 Hz, 2H), 6.75 (d, J = 1.6 Hz, 2H), 4.48 (s, 4H), 4.36 (s, 4H), 2.23 (s, 6H). ^{13}C NMR (125 MHz, CDCl$_3$): δ (ppm) 147.8, 139.4, 132.9, 128.7, 128.5, 127.5, 127.3, 126.8, 126.1, 116.4, 55.5, 55.1, 20.4. FT-IR (KBr): ν (cm^{-1}) 3081, 3061, 3028, 2991, 2912, 2885, 2856, 2732, 1951, 1875, 1862, 1834, 1806, 1787, 1765, 1739, 1725, 1710, 1691, 1678, 1659, 1641, 1612, 1564, 1552, 1511, 1493, 1468, 1452, 1441, 1409, 1359, 1299, 1275, 1259, 1246, 1228, 1212, 1191, 1170, 1144, 1118, 1073, 1040, 1028, 1001, 963, 945, 910, 899, 882, 872, 845, 810, 799, 764, 747, 736, 724, 699, 658, 617, 594, 575, 518, 461, 443, 434, 423, 415, 406. High-resolution ACPI-TOF mass: calcd. for $C_{30}H_{31}N_2$ [M+H]$^+$: m/z = 419.2482, found: 419.2495. Analytical data (^{1}H and ^{13}C NMR spectra, H-H COSY, HMQC and HMBC correlations, FT-IR spectrum, and high-resolution APCI-TOF mass spectra) of **3c** are shown in Figures S36–S42.

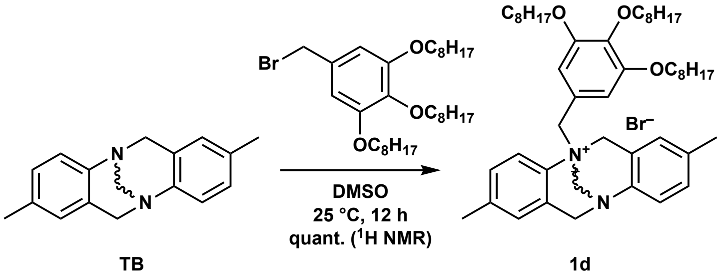

1d: 3,4,5-trioctyloxybenzyl bromide (31.7 mg, 57.1 μmol) was added at 25 °C to a DMSO-*d*$_6$ solution (0.45 mL) of **TB** (13.9 mg, 55.5 μmol) in a NMR tube, and the mixture was stirred for 12 h at 25 °C. NMR spectroscopic data of the reaction mixture was measured to confirm quantitative conversion of **TB** into **1d**. The reaction mixture was used for the next step: ^{1}H NMR (400 MHz, DMSO-*d*$_6$): δ (ppm) 8.22 (d, J = 8.1 Hz, 1H), 7.38 (d, J = 7.5 Hz, 1H), 7.18 (d, J = 7.5 Hz, 1H), 7.12 (d, J = 8.4 Hz, 1H), 7.01 (s, 1H), 6.95 (s, 1H), 6.69 (s, 2H), 5.31 (d, J = 13.9 Hz, 1H), 5.27 (d, J = 13.5 Hz, 1H), 5.18 (d, J = 16.8 Hz, 1H), 5.14 (d, J = 15.0 Hz, 1H), 4.91 (d, J = 15.4 Hz, 1H), 4.74 (d, J = 11.9 Hz, 1H), 4.68 (d, J = 16.7 Hz, 1H), 4.19 (d, J = 17.8 Hz, 1H), 3.92 (m, 2H), 3.81 (m, 2H), 3.78 (m, 2H), 2.24 (s, 3H), 2.20 (s, 3H), 1.67 (m, 6H), 1.59 (m, 6H), 1.26 (m, 24H), 0.86 (m, 9H). ^{13}C NMR (125 MHz, DMSO-*d*$_6$): δ (ppm) 152.3, 140.1, 134.0, 138.5, 136.5, 134.5, 129.8, 129.3, 129.1, 128.2, 127.1, 124.1, 123.1, 122.1, 122.0, 111.4, 79.4, 74.1, 72.2, 68.3, 65.4, 64.7, 56.5, 54.8, 31.3, 31.2, 29.8, 28.9, 28.8, 28.8, 28.7, 25.7, 25.6, 22.1, 20.3, 20.2, 13.8, 13.7. Analytical data (^{1}H and ^{13}C NMR spectra, H-H COSY, HMQC and HMBC correlations) of **1d** are shown in Figures S43–S47.

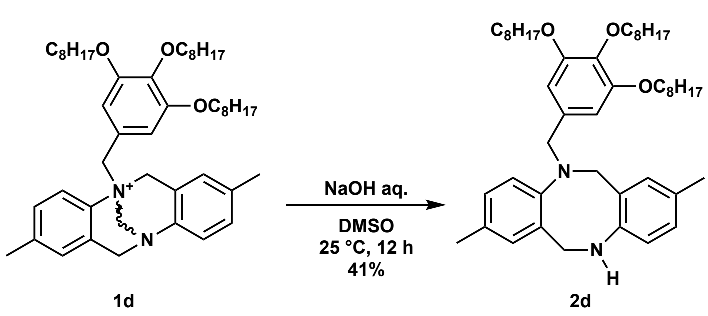

2d: A solution of **1d** (1.01 mmol) in DMSO was poured into a NaOH aqueous solution (1.0 M, 20 mL) at 25 °C, and the mixture was stirred for 12 h at 25 °C. The resultant yellowish precipitate was collected by filtration, washed with water, and then dried under reduced pressure. The obtained residue was subjected to column chromatography on SiO$_2$ (ethyl acetate /*n*-hexane; v/v = 1:20), to allow isolation of **2d** (41% yield) as an yellowish oil (249 mg, 349 μmol) and **3d** (5.8% yield) as an colorless oil (58.9 mg, 49.6 μmol). ^{1}H NMR (400 MHz, $CDCl_3$): δ (ppm) 6.91 (dd, *J* = 8.2, 1.6 Hz, 1H), 6.87 (d, *J* = 1.7 Hz, 1H), 6.85 (dd, *J* = 7.7, 2.0 Hz, 1H), 6.84 (d, *J* = 7.8 Hz, 1H), 6.67 (d, *J* = 1.7 Hz, 1H), 6.53 (d, *J* = 7.9 Hz, 1H), 6.43 (s, 2H), 4.43 (s, 2H), 4.35 (s, 2H), 4.26 (s, 2H), 4.09 (s, 1H), 3.92 (t, *J* = 6.7 Hz, 2H), 3.86 (t, *J* = 6.5 Hz, 4H), 2.23 (s, 3H), 2.17 (s, 3H), 1.74 (tt, *J* = 6.6, 6.6 Hz, 6H), 1.44 (m, 6H), 1.30 (m, 24H), 0.88 (t, *J* = 6.8 Hz, 9H). ^{13}C NMR (125 MHz, $CDCl_3$): δ (ppm) 153.1, 147.7, 145.7, 136.9, 134.5, 132.8, 131.5, 129.3, 128.7, 128.2, 127.5, 124.0, 118.1, 117.0, 106.0, 73.5, 69.0, 56.5, 54.9, 51.1, 32.0, 31.9, 30.4, 29.7, 29.5, 29.4, 26.2, 22.8, 22.8, 20.4, 20.4, 14.2. FT-IR (KBr): ν (cm^{-1}) 3384, 3006, 2925, 2855, 2730, 1741, 1693, 1614, 1590, 1509, 1467, 1435, 1415, 1380, 1359, 1327, 1269, 1226, 1171, 1113, 1064, 1039, 1012, 955, 896, 876, 811, 768, 744, 724, 669, 614, 591, 575, 553, 516, 499, 484, 461, 444, 427, 407. High-resolution ACPI-TOF mass: calcd. for $C_{47}H_{73}N_2O_3$ $[M+H]^+$: *m*/*z* = 712.5537, found: 712.5530. Analytical data (^{1}H and ^{13}C NMR spectra, H-H COSY, HMQC and HMBC correlations, FT-IR spectrum, and high-resolution APCI-TOF mass spectra) of **2d** are shown in Figures S48–S54.

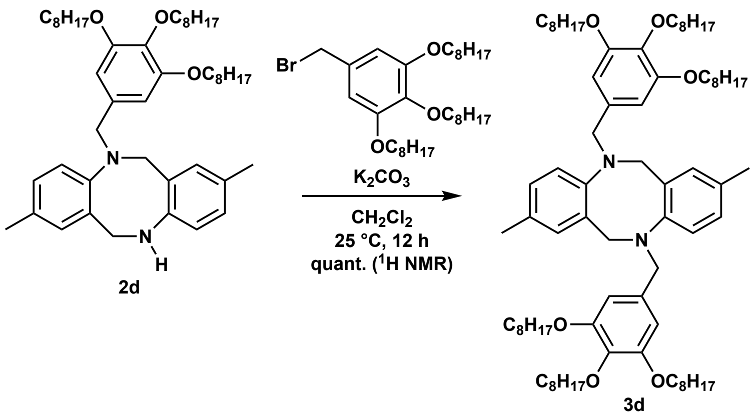

3d: 3,4,5-Trioctyloxybenzyl bromide (20.0 mg, 36.0 μmol) was added at 25 °C to a CH_2Cl_2 solution (8.0 mL) of **2d** (14.0 mg, 19.6 μmol) and K_2CO_3 (5.2 mg, 37.6 μmol), and the mixture was stirred for 12 h at 25 °C. The resulting mixture was poured into water (10 mL) and extracted with CH_2Cl_2 (15 mL, three times). The organic extract was washed successively with water and brine, and then evaporated to dryness under reduced pressure. The obtained residue was subjected to column chromatography on SiO_2 (ethyl acetate /*n*-hexane; v/v = 1:20), to allow isolation of **3d** (98% yield) as a colorless oil (22.8 mg, 19.2 μmol): ^{1}H NMR (500 MHz, $CDCl_3$): δ (ppm) 6.94 (d, *J* = 8.1 Hz, 2H), 6.86 (d, *J* = 8.1 Hz, 2H), 6.72 (s, 2H), 6.38 (s, 4H), 4.41 (s, 4H), 4.22 (s, 4H), 3.96 (t, *J* = 6.6 Hz, 4H), 3.86 (t, *J* = 6.4 Hz, 8H), 2.22 (s, 6H), 1.77 (m, 12H), 1.47 (m, 12H), 1.32 (m, 48H), 0.91 (m, *J* = 3.3 Hz, 18H). ^{13}C NMR (125 MHz, $CDCl_3$): δ (ppm) 153.2, 147.9, 137.1, 134.4, 132.9, 128.7, 127.4, 126.6, 116.7, 73.5, 69.1, 55.9, 55.5, 32.0, 31.9, 30.5, 29.7, 29.5, 29.5, 29.4, 26.2, 22.8, 22.8, 20.4, 14.2. FT-IR (KBr): *ν* (cm^{-1}) 3397, 2953, 2925, 2855, 1612, 1590, 1549, 1509, 1467, 1453, 1436, 1410, 1379, 1326, 1228, 1169, 1113, 1040, 959, 899, 873, 809, 783, 724, 657, 614, 584. High-resolution ACPI-TOF mass: calcd. for $C_{78}H_{127}N_2O_6$ $[M+H]^+$: *m*/*z* = 1187.9689, found: 1187.9631. Analytical data (^{1}H and ^{13}C NMR spectra, HMQC and HMBC correlations, FT-IR spectrum, and high-resolution APCI-TOF mass spectra) of **3d** are shown in Figures S55–S60.

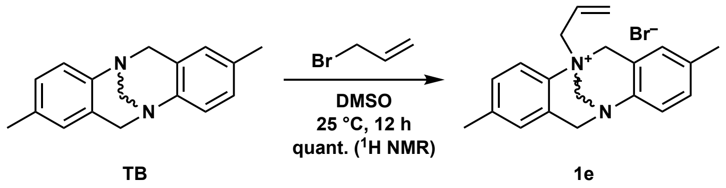

1e: Allyl bromide (11.2 μL, 133 μmol) was added at 25 °C to a DMSO-*d*$_6$ solution (0.45 mL) of **TB** (31.6 mg, 126 μmol) in a NMR tube, and the mixture was stirred for 12 h at 25 °C. NMR spectroscopic data of the reaction mixture was measured to confirm quantitative conversion of **TB** into **1e**. The reaction mixture was used for the next step: ^{1}H NMR (500 MHz, DMSO-*d*$_6$): *δ* (ppm) 8.03 (d, *J* = 8.7 Hz, 1H), 7.25 (d, *J* = 8.9 Hz, 1H), 7.23 (d, *J* = 8.4 Hz, 1H), 7.12 (d, *J* = 8.3 Hz, 1H), 7.01 (s, 1H), 6.91 (s, 1H), 5.81 (tdd, *J* = 16.9, 10.0, 6.9 Hz, 1H), 5.67 (d, *J* = 16.9 Hz, 1H), 5.49 (d, *J* = 10.1 Hz, 1H), 5.48 (d, *J* = 12.3 Hz, 1H), 5.39 (d, *J* = 15.5 Hz, 1H), 5.21 (dd, *J* = 13.9, 7.4 Hz, 1H), 5.11 (d, *J* = 11.3 Hz, 1H), 4.90 (d, *J* = 17.1 Hz, 1H), 4.84 (d, *J* = 15.3 Hz, 1H), 4.75 (dd, *J* = 13.9, 6.5 Hz, 1H), 4.22 (d, *J* = 17.1 Hz, 1H), 2.20 (s, 3H), 2.17 (s, 3H). ^{13}C NMR (125 MHz, DMSO-*d*$_6$): *δ* (ppm) 140.2, 140.1, 135.3, 134.6, 129.8, 129.4, 129.0, 128.2, 127.4, 126.9, 125.6, 124.2, 122.8, 121.9, 74.1, 66.0, 63.3, 56.2, 20.3, 20.2. Analytical data (^{1}H and ^{13}C NMR spectra, H-H COSY, HMQC, HMBC correlations) of **1e** are shown in Figures S61–S65.

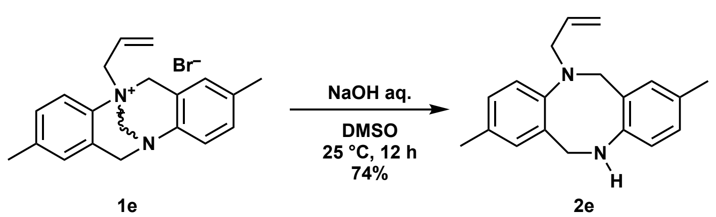

2e: A solution of **1e** (12.6 μmol) in DMSO was poured into a NaOH aqueous solution (1.0 M, 10 mL) at 25 °C, and the mixture was stirred for 12 h at 25 °C. The resultant white precipitate was collected by filtration, washed with water, and then dried under reduced pressure to afford **2e** (74% yield) as an off-white powder (25.9 mg, 93.0 mmol): ^{1}H NMR (400 MHz, $CDCl_3$): *δ* (ppm) 6.94 (dd, *J* = 8.2, 1.8 Hz, 1H), 6.88 (dd, *J* = 8.2, 1.5 Hz, 1H), 6.86 (d, *J* = 1.6 Hz, 1H), 6.85 (d, *J* = 1.5 Hz, 1H), 6.82 (d, *J* = 8.2 Hz, 1H), 6.55 (d, *J* = 7.9 Hz, 1H), 5.89 (tdd, *J* = 17.2, 10.3, 5.2 Hz, 1H), 5.24 (tdd, *J* = 9.1, 1.7, 1.7 Hz, 1H), 5.21 (td, *J* =

3.9, 1.7 Hz, 1H), 4.42 (s, 2H), 4.36 (s, 2H), 3.75 (d, $J = 5.1$ Hz, 2H), 2.24 (s, 3H), 2.24 (s, 3H). ^{13}C NMR (125 MHz, $CDCl_3$): δ (ppm) 147.6, 145.8, 135.2, 132.7, 131.6, 128.9, 128.7, 128.6, 127.8, 127.6, 124.2, 117.4, 117.2, 116.5, 54.4, 54.1, 51.1, 20.4, 20.4. FT-IR (KBr): ν (cm^{-1}) 3374, 3285, 3177, 3076, 3005, 2974, 2914, 2896, 2857, 2731, 1876, 1835, 1758, 1635, 1614, 1568, 1509, 1477, 1448, 1429, 1411, 1393, 1359, 1344, 1312, 1288, 1268, 1248, 1227, 1171, 1124, 1107, 1060, 1032, 991, 953, 942, 916, 879, 824, 814, 769, 760, 727, 708, 668, 648, 613, 566, 506, 485, 461, 453, 422, 409. High-resolution ACPI-TOF mass: calcd. for $C_{19}H_{23}N_2$ $[M+H]^+$: $m/z = 279.1856$, found: 279.1848. Analytical data (^{1}H and ^{13}C NMR spectra, H-H COSY, HMQC, HMBC correlations, FT-IR spectrum, and high-resolution APCI-TOF mass spectra) of **2e** are shown in Figures S66–S72.

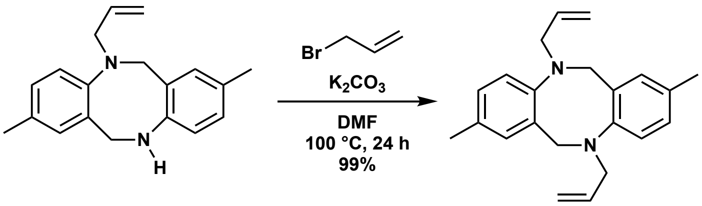

2e **3e**

3e: Allyl bromide (54.8 μL, 650 μmol) was added at 25 °C to a DMF solution (3.0 mL) of **2e** (36.2 mg, 130 μmol) and K_2CO_3 (98.8 mg, 715 μmol), and the mixture was stirred for 12 h at 25 °C. The resulting mixture was poured into water (80 mL) and extracted with CH_2Cl_2 (15 mL, eight times). The organic extract was washed successively with water and brine, and then evaporated to dryness under reduced pressure to afford **3e** (99% yield) as a yellow powder (40.9 mg, 128 mmol): ^{1}H NMR (400 MHz, $CDCl_3$): δ (ppm) 6.95 (d, $J = 8.1$ Hz, 2H), 6.87 (s, 2H), 6.78 (d, $J = 8.1$ Hz, 2H), 5.79 (tdd, $J = 16.6, 10.7, 5.3$ Hz, 2H), 5.18 (s, 2H), 5.15 (dd, $J = 7.2, 1.6$ Hz, 4H), 4.33 (s, 4H), 3.64 (d, $J = 4.5$ Hz, 4H), 2.25 (s, 6H). ^{13}C NMR (125 MHz, $CDCl_3$): δ (ppm) 147.6, 135.2, 132.7, 128.5, 126.9, 126.3, 116.3, 116.1, 54.7, 53.6, 20.4. FT-IR (KBr): ν (cm^{-1}) 3082, 3006, 2980, 2915, 2857, 2729, 1641, 1612, 1564, 1549, 1510, 1484, 1461, 1427, 1409, 1360, 1342, 1291, 1255, 1229, 1174, 1162, 1122, 1059, 1033, 999, 960, 943, 934, 920, 909, 879, 869, 811, 666, 614, 567, 556. High-resolution ACPI-TOF mass: calcd. for $C_{22}H_{27}N_2$ $[M+H]^+$: $m/z = 319.2169$, found: 319.2161. Analytical data (^{1}H and ^{13}C NMR spectra, H-H COSY, HMQC and HMBC correlations, FT-IR spectrum, and high-resolution APCI-TOF mass spectra) of **3e** are shown in Figures S73–S79.

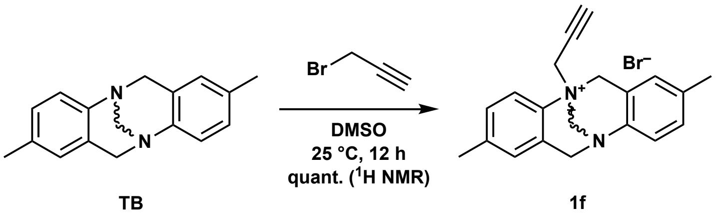

1f: Propargyl bromide (9.2 M toluene solution, 14.3 μL, 131 μmol) was added at 25 °C to a DMSO-d_6 solution (0.45 mL) of **TB** (31.3 mg, 125 μmol) in a NMR tube, and the mixture was stirred for 12 h at 25 °C. NMR spectroscopic data of the reaction mixture was measured to confirm quantitative conversion of **TB** into **1f**. The reaction mixture was used for the next step: ^{1}H NMR (400 MHz, DMSO-d_6): δ (ppm) 8.06 (d, J = 8.7 Hz, 1H), 7.30 (d, J = 8.6 Hz, 1H), 7.25 (d, J = 8.3 Hz, 1H), 7.14 (d, J = 9.1 Hz, 1H), 7.03 (s, 1H), 6.92 (s, 1H), 5.66 (dd, J = 16.8, 2.1 Hz, 1H), 5.45 (d, J = 15.5 Hz, 1H), 5.44 (d, J = 10.2 Hz, 1H), 5.26 (d, J = 11.1 Hz, 1H), 5.20 (dd, J = 16.9, 2.1 Hz, 1H), 4.91 (d, J = 17.3 Hz, 1H), 4.86 (d, J = 15.2 Hz, 1H), 4.27 (d, J = 17.2 Hz, 1H), 3.87 (s, 1H), 2.22 (s, 3H), 2.17 (s, 3H). ^{13}C NMR (125 MHz, DMSO-d_6): δ (ppm) 140.5, 139.9, 136.0, 134.8, 130.0, 129.7, 128.8, 128.1, 126.9, 124.3, 121.9, 121.5, 82.9, 75.3, 72.2, 65.3, 56.3, 51.6, 20.3, 20.2. Analytical data (^{1}H and ^{13}C NMR spectra, HMQC, HMBC correlations) of **1f** are shown in Figures S80–S83.

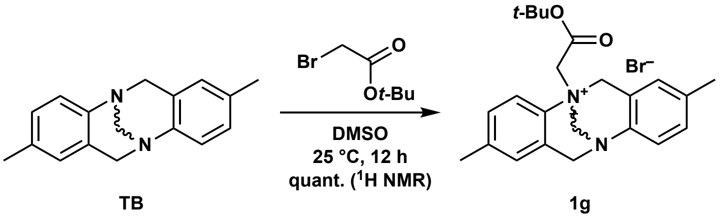

1g: *tert*-Butyl bromoacetate (19.3 μL, 131 μmol) was added at 25 °C to a DMSO-d_6 solution (0.45 mL) of **TB** (31.2 mg, 125 μmol) in a NMR tube, and the mixture was stirred for 12 h at 25 °C. NMR spectroscopic data of the reaction mixture was measured to confirm quantitative conversion of **TB** into **1g**. The reaction mixture was used for the next step: ^{1}H NMR (500 MHz, DMSO-d_6): δ (ppm) 7.89 (d, J = 8.6 Hz, 1H), 7.28 (d, J = 8.6 Hz, 1H), 7.26 (d, J = 8.8 Hz, 1H), 7.16 (d, J = 8.1 Hz, 1H), 7.05 (s, 1H), 6.92 (s, 1H), 5.72 (d, J = 11.0 Hz, 1H), 5.55 (d, J = 16.9 Hz, 1H), 5.42 (d, J = 15.5 Hz, 1H), 5.13 (d, J = 11.0 Hz, 1H), 5.00 (d, J = 17.0 Hz, 1H), 4.80 (d, J = 17.1 Hz, 1H), 4.78 (d, J = 15.0 Hz, 1H), 4.32 (d, J = 17.2 Hz, 1H), 2.22 (s, 3H), 2.20 (s, 3H), 1.24 (s, 9H). ^{13}C NMR (125 MHz, DMSO-d_6): δ (ppm) 162.6, 140.1, 140.0, 137.3, 134.9, 130.1, 129.7, 128.3, 128.2, 126.8, 124.2, 121.4, 120.1, 84.2, 76.7, 67.1, 60.4, 56.4, 27.2, 20.3. Analytical data (^{1}H and ^{13}C NMR spectra, HMQC, HMBC correlations) of **1g** are shown in Figures S84–S87.

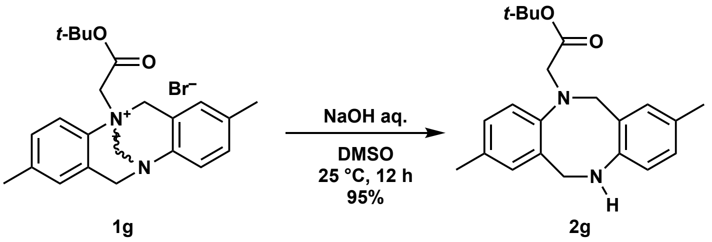

2g: A solution of **1g** (2.01 mmol) in DMSO was poured into a NaOH aqueous solution (1.0 M, 20 mL) at 25 °C, and the mixture was stirred for 12 h at 25 °C. The resultant white precipitate was collected by filtration, washed with water, and then dried under reduced pressure to afford **2g** (95% yield) as a white solid (670 mg, 1.90 mmol): ^{1}H NMR (400 MHz, $CDCl_3$): δ (ppm) 6.93 (d, J = 9.0 Hz, 1H), 6.88 (d, J = 8.5 Hz, 1H), 6.87 (s, 1H), 6.85 (s, 1H), 6.64 (d, J = 8.6 Hz, 1H), 6.54 (d, J = 7.6 Hz, 1H), 4.47 (s, 2H), 4.42 (s, 2H), 4.08 (br s, 1H), 3.68 (s, 2H), 2.24 (s, 3H), 2.23 (s, 3H), 1.51 (s, 9H). ^{13}C NMR (125 MHz, $CDCl_3$): δ (ppm) 171.5, 146.8, 145.6, 132.6, 131.5, 129.1, 128.9, 128.6, 128.6, 127.6, 123.5, 117.2, 117.2, 81.4, 55.4, 54.1, 50.8, 28.3, 20.4, 20.4. FT-IR (KBr): ν (cm^{-1}) 3394, 3366, 3320, 3078, 3004, 2975, 2917, 2866, 2733, 1877, 1818, 1741, 1724, 1614, 1570, 1509, 1475, 1455, 1419, 1392, 1367, 1346, 1335, 1309, 1285, 1255, 1220, 1175, 1152, 1124, 1054, 1041, 960, 934, 916, 896, 880, 846, 815, 776, 763, 743, 727, 705, 685, 668, 618, 573, 512, 502, 478, 462, 451, 427, 409. High-resolution ACPI-TOF mass: calcd. for $C_{22}H_{29}N_2O_2$ $[M+H]^+$: m/z = 353.2224, found: 353.2240. Analytical data (^{1}H and ^{13}C NMR spectra, HMQC and HMBC correlations, FT-IR spectrum, and high-resolution APCI-TOF mass spectra) of **2g** are shown in Figures S88–S93.

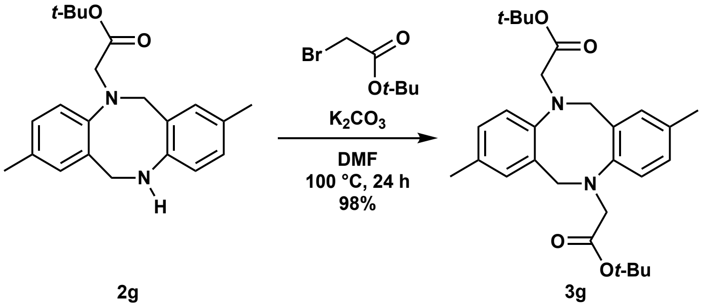

3g: *tert*-Butyl bromoacetate (96.0 μL, 650 μmol) was added at 25 °C to a DMF solution (3.0 mL) of **2g** (45.1 mg, 128 μmol) and K_2CO_3 (97.2 mg, 703 μmol), and the mixture was stirred for 12 h at 25 °C. The resulting mixture was poured into water (80 mL) and extracted with CH_2Cl_2 (15 mL, seven times). The organic extract was washed successively with water and brine, and then evaporated to dryness under reduced pressure at 50 °C to afford **3g** (98% yield) as a yellow powder (58.8 mg, 125 μmol): ^{1}H NMR (400 MHz, $CDCl_3$): δ (ppm) 6.96 (d, J = 8.4 Hz, 2H), 6.90 (s, 2H), 6.60 (d, J = 8.0 Hz, 2H), 4.43 (s, 4H), 3.54 (s, 4H), 2.26 (s, 6H), 1.50 (s, 18H). ^{13}C NMR (125 MHz, $CDCl_3$): δ (ppm) 171.4, 147.0, 132.6, 128.8, 127.8, 125.9, 116.1, 81.3, 55.7, 53.6, 28.2, 20.4. FT-IR (KBr): ν (cm^{-1}) 3082, 3004, 2976, 2918, 2859, 2727, 1737, 1678, 1649, 1642, 1615, 1567, 1548, 1513, 1478, 1460, 1453, 1424, 1401, 1392, 1369, 1343, 1309, 1259, 1221, 1148, 1043, 966, 953, 910, 884, 873, 847, 800, 764, 740, 698, 681, 613, 590, 576, 522, 460. High-resolution ACPI-TOF mass: calcd. for $C_{28}H_{39}N_2O_4$ $[M+H]^+$: m/z = 467.2904, found: 467.2915 Analytical data (^{1}H and ^{13}C NMR spectra, H-H COSY, HMQC and HMBC correlations, FT-IR spectrum, and high-resolution APCI-TOF mass spectra) of **3g** are shown in Figures S94–S100.

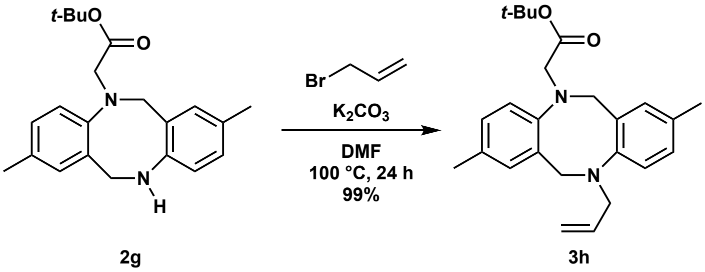

3h: Allyl bromide (21.3 μL, 253 μmol) was added at 25 °C to a dimethylformamide solution (3.0 mL) of **2g** (17.8 mg, 50.5 μmol) and K_2CO_3 (34.7 mg, 251 μmol), and the mixture was stirred for 24 h at 100 °C. The resulting mixture was poured into water (80 mL) and the resultant yellow precipitate was collected by filtration, washed with water, and then dried under reduced pressure to afford **3h** (99% yield) as a yellow powder (19.8 mg, 50.4 mmol): ^{1}H NMR (400 MHz, $CDCl_3$): δ (ppm) 6.95 (d, J = 8.2 Hz, 1H), 6.95 (d, J = 8.2 Hz, 1H), 6.90 (s, 1H), 6.87 (s, 1H), 6.78 (d, J = 8.1 Hz, 1H), 6.60 (d, J = 8.2 Hz, 1H), 5.77 (tdd, J = 12.1, 5.6, 5.0 Hz, 1H), 5.17 (dd, J = 3.9, 1.7 Hz, 1H), 5.13 (dd, J = 10.8, 1.6 Hz, 1H), 4.45 (s, 2H), 4.32 (s, 2H), 3.63 (d, J = 4.8 Hz, 2H), 3.55 (s, 2H), 2.26 (s, 3H), 2.25 (s, 3H), 1.51 (s, 9H). ^{13}C NMR (125 MHz, $CDCl_3$): δ (ppm) 171.5, 147.5, 147.1, 135.1, 132.7, 132.7, 128.7, 128.7, 127.8, 127.0, 126.6, 125.7, 116.4, 116.2, 116.1, 81.3, 55.9, 54.5, 53.6, 28.3, 20.4, 20.4. FT-IR (KBr): ν (cm^{-1}) 3407, 3077, 2976, 2919, 2860, 2731, 1875, 1855, 1834, 1817, 1777, 1740, 1690, 1677, 1659, 1641, 1613, 1571, 1548, 1510, 1480, 1460, 1452, 1410, 1393, 1367, 1345, 1286, 1256, 1231, 1213, 1149, 1122, 1035, 990, 963, 947, 917, 875, 848, 808, 774, 734, 688, 667, 615, 573, 510, 498, 479, 461, 451, 439, 425, 415, 406. High-resolution ACPI-TOF mass: calcd. for $C_{25}H_{33}N_2O_2$ $[M+H]^+$: m/z = 393.2537, found: 393.2546. Analytical data (^{1}H and ^{13}C NMR spectra, H-H COSY, HMQC and HMBC correlations, FT-IR spectrum, and high-resolution APCI-TOF mass spectra) of **3h** are shown in Figures S101–S107.

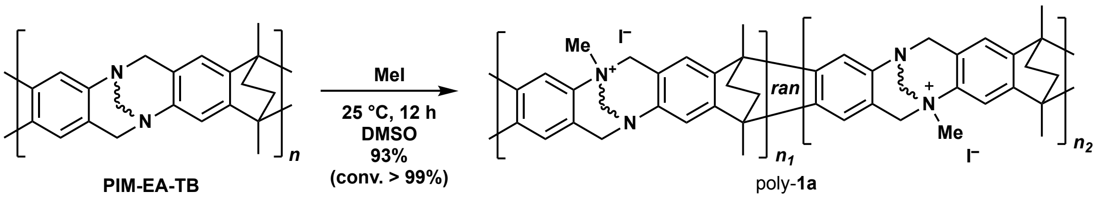

Poly-**1a**:[2] MeI (117 μL, 1.88 mmol) was added at 25 °C to a DMSO solution (1.8 mL) of **PIM-EA-TB** (57.0 mg, 190 μmol), and the mixture was stirred for 12 h at 25 °C. The reaction mixture was poured into water, and the precipitate formed was collected by filtration, washed with water and MeOH, and dried under reduced pressure to afford poly-**1a** (93% yield) as an off-white powder (78.2 mg, 177 μmol for the monomer unit): ^{1}H NMR (500 MHz, DMSO-d_6): δ (ppm) 7.82 (br, 1H), 7.42–6.63 (m, 3H), 5.71–3.97 (m, 8H), 3.97–3.43 (m, 3H), 2.25–0.92 (m, 10H). FT-IR (KBr): ν (cm^{-1}) 3420, 3019, 2963, 2940, 2863, 1715, 1624, 1496, 1471, 1456, 1416, 1384, 1362, 1340, 1323, 1207, 1149, 1114, 1079, 1057, 1003, 892, 860, 829, 754, 721, 693, 665, 648, 638, 603, 580, 555, 527, 509, 496, 480, 469, 456, 443, 432, 426, 416. Analytical data (^{1}H NMR and FT-IR spectra) of poly-**1a** are shown in Figures S108–S109.

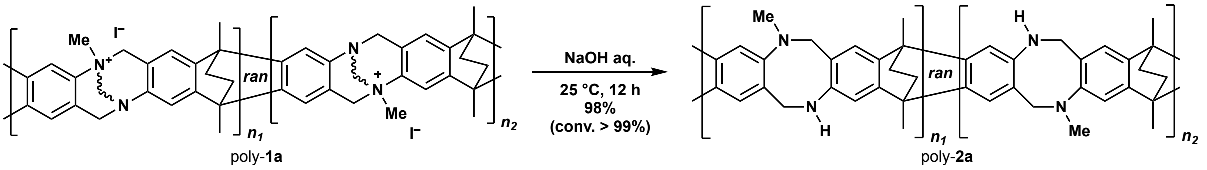

Poly-**2a**:[2] An aqueous suspension of poly-**1a** (83.5 mg, 189 μmol for the monomer unit) and NaOH (1.0 M, 5.0 mL) was stirred for 12 h at 25 °C. The resultant white precipitate was collected by filtration, washed with water, MeOH, and Et_2O, and dried under reduced pressure to afford poly-**2a** (98% yield) as an off-white powder (56.0 mg, 185 μmol for the monomer unit): ^{1}H NMR (500 MHz, $CDCl_3$): δ (ppm) 6.88 (br, 2H), 6.80 (br, 1H), 6.52 (br, 1H), 4.34 (br, 2H), 4.21 (br, 2H), 4.02 (br, 1H), 2.84 (br, 3H), 1.87 (br, 3H), 1.83 (br, 3H), 1.56 (br, 4H). ^{13}C NMR (125 MHz, $CDCl_3$): δ 148.2, 146.7, 146.2, 145.7, 137.3, 136.8, 136.4, 125.3, 122.9, 120.9, 110.6, 109.1, 108.5, 58.5, 51.5, 41.9, 41.6, 41.3, 41.1, 40.8, 40.2, 39.5, 36.3, 18.6. FT-IR (KBr): ν (cm^{-1}) 3612, 3406, 3251, 3016, 2958, 2932, 2897, 2873, 2856, 2786, 1670, 1614, 1577, 1560, 1502, 1476, 1457, 1408, 1375, 1334, 1321, 1278, 1254, 1229, 1190, 1156, 1103, 1064, 1036, 1013, 945, 915, 890, 840, 801, 746, 722, 694, 668, 659, 639, 606, 573, 527, 497, 476, 456, 444, 417. Analytical data (^{1}H and ^{13}C NMR and FT-IR spectra) of poly-**2a** are shown in Figures S110–S112.

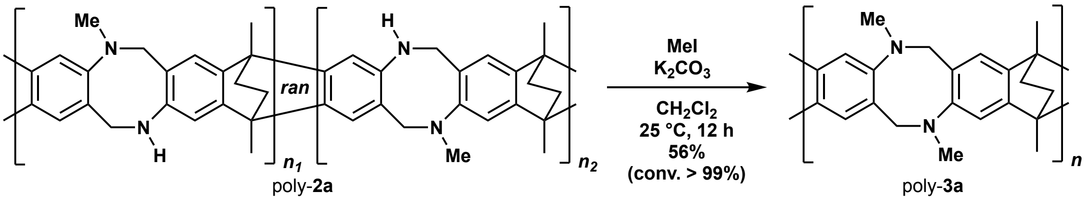

Poly-**3a**: MeI (33.5 μL, 539 μmol) was added at 25 °C to a CH_2Cl_2 solution (2.0 mL) of poly-**2a** (16.3 mg, 53.9 μmol for the monomer unit) and K_2CO_3 (38.7 mg, 280 μmol), and the mixture was stirred for 12 h at 25 °C. The reaction mixture was poured into MeOH, and the precipitate formed was collected by filtration, washed with water, MeOH, and Et_2O, and dried under reduced pressure to afford poly-**3a** (56% yield) as a beige powder (9.6 mg, 30.3 μmol for the monomer unit): ^{1}H NMR (500 MHz, $CDCl_3$) δ (ppm) 6.96 (br, 2H), 6.82 (br, 2H), 4.14 (br, 4H), 2.80 (br, 6H), 1.92 (br, 6H), 1.64 (br, 4H). ^{13}C NMR (125 MHz, $CDCl_3$): δ 148.6, 146.8, 136.5, 123.1, 108.5, 59.0, 45.5, 41.9, 41.1, 40.3, 39.7, 36.3, 18.6. FT-IR (KBr): ν (cm^{-1}) 3406, 3018, 2959, 2935, 2894, 2874, 2857, 2781, 1720, 1709, 1679, 1641, 1611, 1560, 1503, 1481, 1459, 1408, 1375, 1341, 1308, 1274, 1255, 1227, 1208, 1179, 1157, 1110, 1061, 1017, 953, 910, 889, 861, 852, 841, 801, 794, 783, 763, 754, 744, 686, 657, 631, 611, 573, 556, 547, 538, 529, 517, 510, 499, 487, 478, 470, 460, 451, 434, 423, 416, 406. Analytical data (^{1}H and ^{13}C NMR and FT-IR spectra) of poly-**3a** are shown in Figures S113–S115.

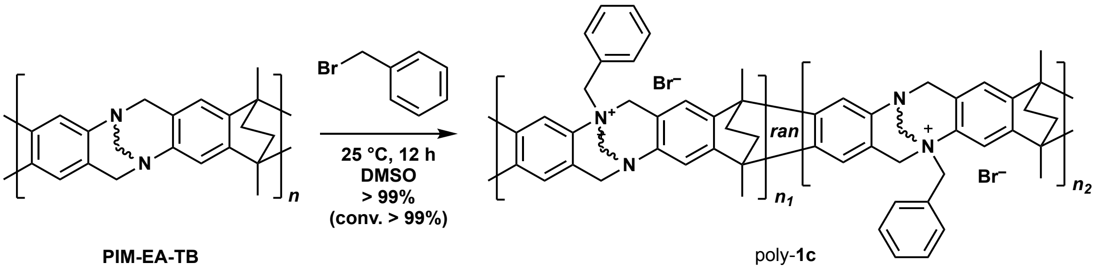

Poly-**1c**: Benzyl bromide (46.5 μL, 392 μmol) was added at 25 °C to a DMSO solution (2.0 mL) of **PIM-EA-TB** (23.7 mg, 78.9 mmol), and the mixture was stirred for 24 h at 25 °C. The reaction mixture was poured into Et_2O, and the precipitate formed was collected by filtration, washed with Et_2O and Et_2O/MeOH (1/1, v/v), and dried under reduced pressure to afford poly-**1c** (>99% yield) as a slightly brown powder (37.2 mg, 78.9 mmol for the monomer unit): ^{1}H NMR (500 MHz, DMSO-d_6): δ (ppm) 8.6–6.5 (br, 9H), 6.0–4.0 (br, 8H), 2.7–0.8 (br, 10H). FT-IR (KBr): ν (cm^{-1}) 3619, 3360, 3026, 3003, 2961, 2934, 2860, 2736, 1816, 1737, 1692, 1650, 1618, 1582, 1536, 1496, 1455, 1380, 1340, 1322, 1285, 1262, 1237, 1225, 1203, 1165, 1150, 1111, 1099, 1078, 1031, 1013, 994, 957, 937, 892, 850, 842, 811, 794, 752, 733, 700, 669, 648, 623, 602, 574, 566, 544, 527, 509, 500, 481, 461, 452, 443, 433, 425, 417, 405. Analytical data (^{1}H NMR and FT-IR spectra) of poly-**1c** are shown in Figures S116–S117.

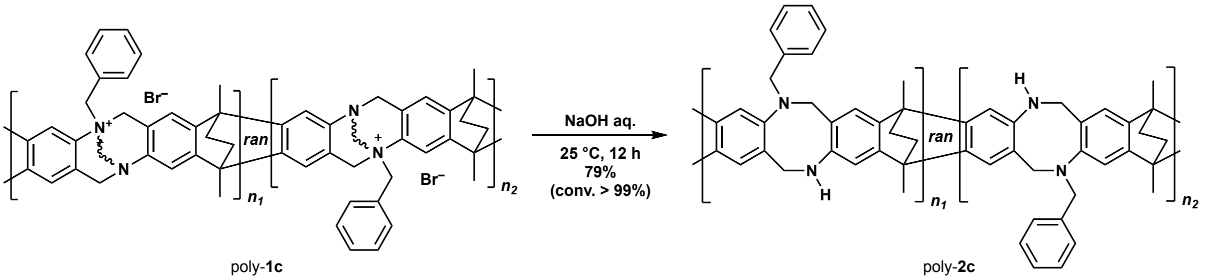

poly-**1c** poly-**2c**

Poly-**2c**: An aqueous suspension of poly-**1c** (41.6 mg, 88.2 μmol for the monomer unit) and NaOH (1.0 M, 5.0 mL) was stirred for 12 h at 25 °C. The resultant white precipitate was collected by filtration, washed with water, MeOH, and Et_2O, and dried under reduced pressure to afford poly-**2c** (79% yield) as a white powder (26.5 mg, 70.1 μmol for the monomer unit): ^{1}H NMR (500 MHz, DMSO-d_6): δ (ppm) 7.20 (br, 5H), 6.84 (br, 2H), 6.48 (br, 2H), 5.1-3.6 (br, 7H), 4.00 (br, 1H), 2.2-1.1 (br, 10H). ^{13}C NMR (125 MHz, $CDCl_3$): δ 148.0, 146.9, 146.3, 145.6, 145.5, 139.7, 137.5, 137.2, 136.6, 128.2, 128.1, 126.8, 125.6, 123.9, 122.7, 120.0, 111.1, 110.0, 57.0, 56.2, 55.0, 51.4, 41.6, 41.4, 41.2, 40.9, 40.8, 40.7, 40.6, 40.3, 40.2, 40.1, 36.3, 18.4. FT-IR (KBr): ν (cm^{-1}) 3397, 2953, 2925, 2855, 1612, 1590, 1549, 1509, 1467, 1453, 1436, 1410, 1379, 1326, 1228, 1169, 1113, 1040, 959, 899, 873, 809, 783, 724, 657, 614, 584. Analytical data (^{1}H and ^{13}C NMR and FT-IR spectra) of poly-**2c** are shown in Figures S118–S120.

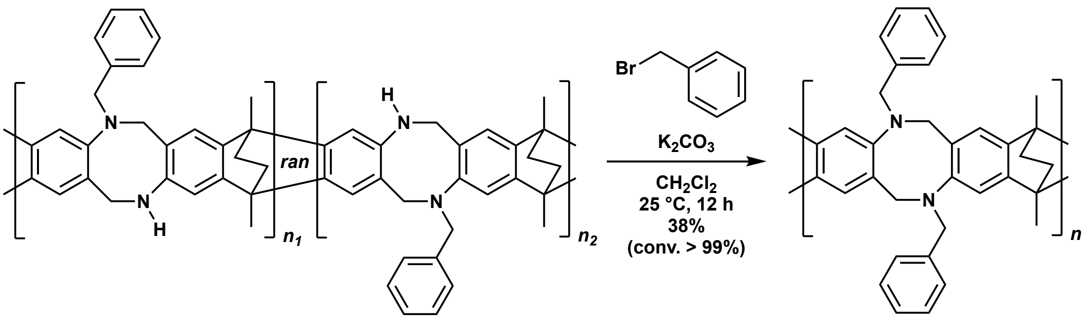

poly-**2c** poly-**3c**

Poly-**3c**: Benzyl bromide (25.0 μL, 210 μmol) was added at 25 °C to a CH_2Cl_2 solution (2.0 mL) of poly-**2c** (15.9 mg, 42.0 μmol for the monomer unit) and K_2CO_3 (30.8 mg, 223 μmol), and the mixture was stirred for 12 h at 25 °C. The reaction mixture was poured into MeOH, and the precipitate formed was collected by filtration, washed with water, MeOH, and Et_2O, and dried under reduced pressure to afford poly-**3c** (38% yield) as a slightly brown powder (7.5 mg, 16.0 μmol for the monomer unit): ^{1}H NMR (500 MHz, $CDCl_3$) δ (ppm) 7.20 (br, 10H), 6.82 (br, 2H), 6.55 (br, 2H), 4.27 (br, 8H), 1.59 (br, 10H). ^{13}C NMR (125 MHz, $CDCl_3$): δ 148.0, 146.7, 146.2, 139.7, 137.1, 128.2, 126.8, 123.8, 110.0, 56.0, 41.6, 40.9, 40.2, 36.4, 18.4. FT-IR (KBr): ν (cm^{-1}) 3345, 3102, 3083, 3060, 3024, 2957, 2932, 2892, 2872, 2856, 2801, 2726, 1945, 1874, 1863, 1834, 1805, 1786, 1777, 1737, 1727, 1701, 1679, 1658, 1641, 1610, 1585, 1557, 1536, 1493, 1480, 1454, 1413, 1374, 1356, 1340, 1317, 1274, 1252, 1225, 1203, 1155, 1076, 1045, 1027, 1000, 977, 947, 889, 854, 840, 800, 732, 697, 650, 620, 595, 585, 569, 546, 538, 531, 497, 479, 460, 443, 424, 417, 406. Analytical data (^{1}H and ^{13}C NMR and FT-IR spectra) of poly-**3c** are shown in Figures S121–S123.

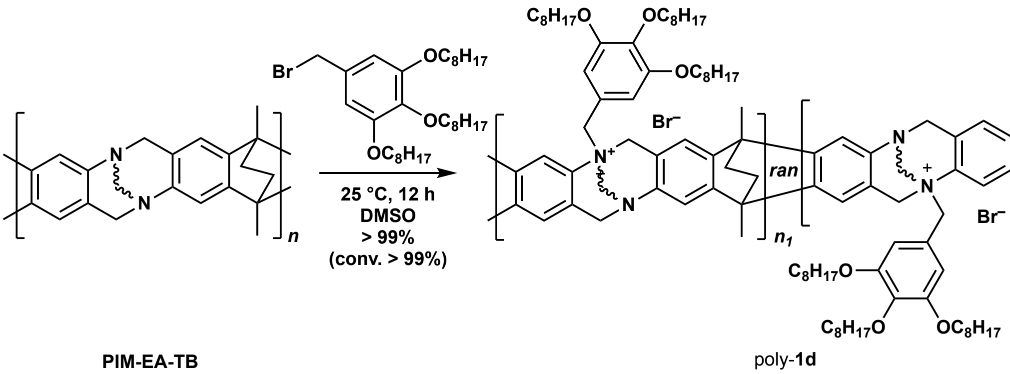

Poly-**1d**: 3,4,5-Trioctyloxybenzyl bromide (745 mg, 1340 μmol) was added at 25 °C to a DMSO solution (3.0 mL) of **PIM-EA-TB** (260 mg, 861 mmol), and the mixture was stirred for 12 h at 25 °C. The reaction mixture was poured into Et_2O, and the precipitate formed was collected by filtration, washed with Et_2O, and dried under reduced pressure to afford poly-**1d** (>99% yield) as an orange powder (785 mg, 915 μmol for the monomer unit): FT-IR (KBr): ν (cm^{-1}) 3404, 2955, 2925, 2855, 2731, 1733, 1686, 1652, 1615, 1588, 1541, 1500, 1456, 1438, 1379, 1331, 1232, 1145, 1112, 1018, 995, 958, 917, 894, 839, 809, 778, 751, 722, 696, 650, 606, 575, 519, 493, 465, 458, 442, 416, 402. Analytical data (^{1}H NMR and FT-IR spectra) of poly-**1d** are shown in Figures S124–S125.

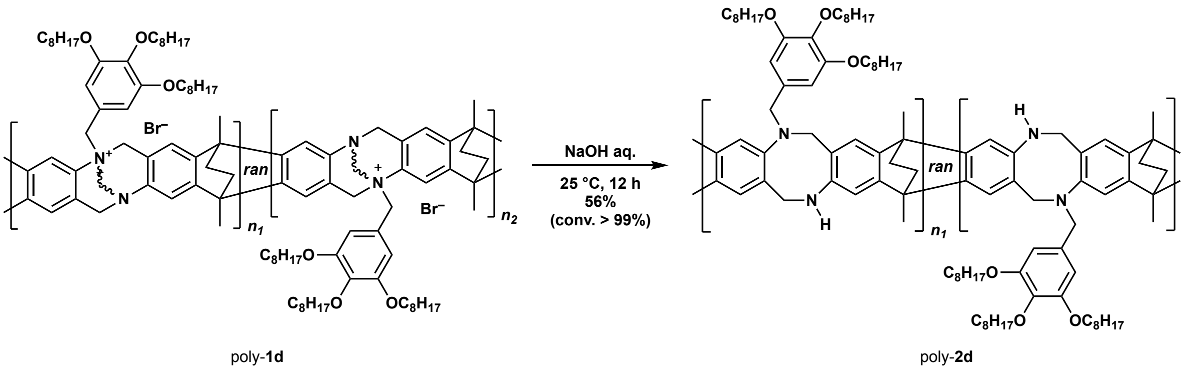

Poly-**2d**: An aqueous suspension of poly-**1d** (785 mg, 861 μmol for the monomer unit) and NaOH (1.0 M, 10 mL) was stirred for 12 h at 25 °C. The resultant orange precipitate was collected by filtration, washed with water, MeOH, tetrahydrofuran, and Et_2O, and dried under reduced pressure to afford poly-**2d** (56% yield) as an orange powder (373 mg, 489 μmol for the monomer unit): ^{1}H NMR (500 MHz, DMSO-d_6): δ (ppm) 6.90 (br, 2H), 6.74 (br, 2H), 6.61 (br, 2H), 4.59 (br, 3H), 3.97 (br, 10H), 1.72–1.28 (br, 50H), 0.88 (br, 9H). ^{13}C NMR

(125 MHz, $CDCl_3$): δ 153.2, 147.4, 144.9, 136.9, 123.8, 118.4, 105.5, 73.4, 69.2, 69.1, 57.0, 41.4, 31.8, 30.3, 25.6, 22.6, 18.2, 14.1. FT-IR (KBr): ν (cm^{-1}) 3420, 3011, 2953, 2926, 2855, 1683, 1617, 1588, 1559, 1541, 1498, 1456, 1437, 1419, 1377, 1332, 1283, 1231, 1203, 1144, 1110, 1066, 994, 957, 916, 893, 838, 806, 776, 748, 721, 694, 668, 639, 608, 575, 556, 528, 503, 473, 457, 443, 425, 417. Analytical data (^{1}H and ^{13}C NMR and FT-IR spectra) of poly-**2d** are shown in Figures S126–S128.

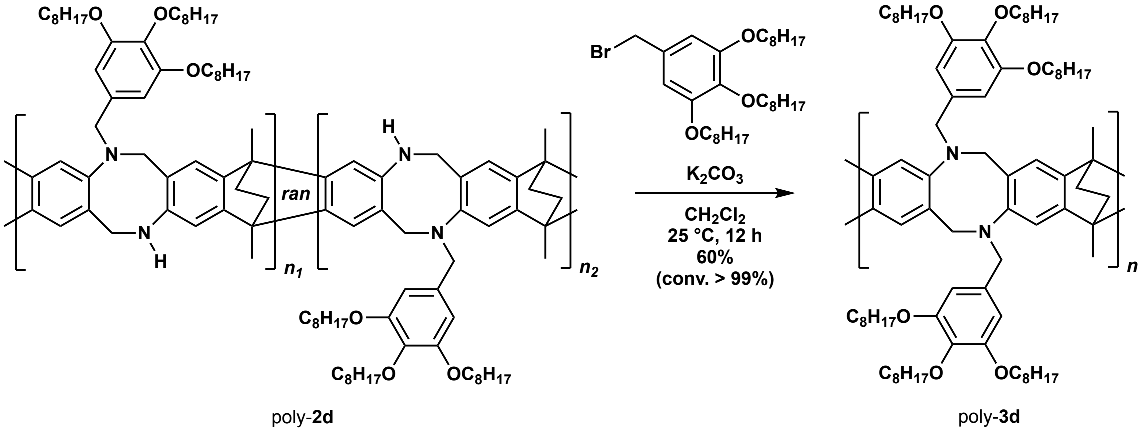

Poly-**3d**: 3,4,5-Trioctyloxybenzyl bromide (182 mg, 328 μmol) was added at 25 °C to a CH_2Cl_2 solution (5.0 mL) of poly-**2d** (50.0 mg, 66.2 μmol for the monomer unit) and K_2CO_3 (43.5 mg, 315 μmol), and the mixture was stirred for 12 h at 25 °C. The reaction mixture was poured into MeOH, and the precipitate formed was collected by filtration, washed with water, MeOH, and dried under reduced pressure to afford poly-**3d** (60% yield) as an off-white powder (49.1 mg, 39.7 μmol for the monomer unit): ^{1}H NMR (500 MHz, $CDCl_3$) δ (ppm) 6.84 (br, 4H), 6.36 (br, 4H), 4.12 (br, 8H), 3.92 (br, 4H), 3.84 (br, 12H), 1.72–1.28 (br, 90H), 0.88 (br, 18H). ^{13}C NMR (125 MHz, $CDCl_3$): δ 153.2, 146.8, 140.2, 136.9, 134.9, 123.9, 119.3, 106.3, 73.5, 69.1, 56.5, 40.9, 35.9, 31.9, 30.5, 29.5, 26.3, 22.8, 18.4, 14.2. FT-IR (KBr): ν (cm^{-1}) 3373, 3187, 3019, 2955, 2926, 2855, 2729, 1936, 1913, 1901, 1875, 1862, 1835, 1816, 1806, 1797, 1785, 1777, 1765, 1754, 1737, 1723, 1691, 1680, 1658, 1650, 1642, 1588, 1501, 1459, 1438, 1413, 1377, 1330, 1275, 1228, 1146, 1112, 1013, 993, 983, 964, 917, 891, 840, 832, 823, 812, 804, 794, 783, 773, 764, 753, 744, 724, 698, 669, 658, 650, 641, 632, 621, 612, 602, 595, 583, 574, 556, 537, 529, 519, 510, 498, 487, 479, 469, 461, 451, 437, 424, 415, 406. Analytical data (^{1}H and ^{13}C NMR and FT-IR spectra) of poly-**3d** are shown in Figures S129–S131.

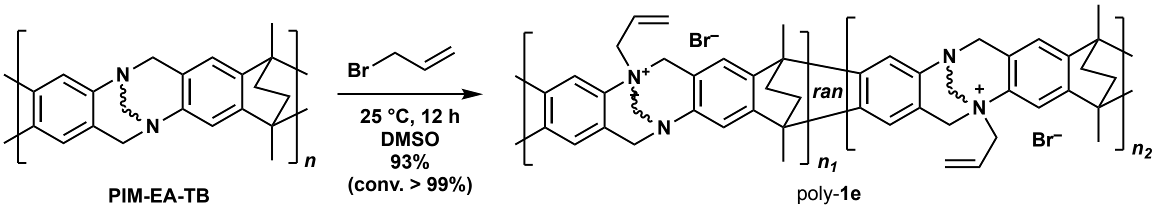

Poly-**1e**: Allyl bromide (33.9 μL, 401 μmol) was added at 25 °C to a DMSO solution (4.0 mL) of **PIM-EA-TB** (60.6 mg, 200 μmol), and the mixture was stirred for 12 h at 25 °C. The reaction mixture was poured into water, and the precipitate formed was collected by filtration, washed with water and Et_2O, and dried under reduced pressure to afford poly-**1e** (93% yield) as an off-white powder (78.5 mg, 186 μmol for the monomer unit): ^{1}H NMR (500 MHz, DMSO-d_6): δ (ppm) 7.77 (br, 1H), 7.12 (br, 3H), 5.62–4.79 (br, 11H), 1.83 (br, 6H), 1.49 (br, 4H). FT-IR (KBr): ν (cm^{-1}) 3407, 2962, 2938, 2862, 2052, 1715, 1619, 1582, 1498, 1456, 1382, 1339, 1321, 1258, 1199, 1170, 1149, 1108, 1020, 997, 952, 896, 806, 749, 694, 638, 608, 575, 527, 503, 473, 445, 419. Analytical data (^{1}H NMR and FT-IR spectra) of poly-**1e** are shown in Figures S132–S133.

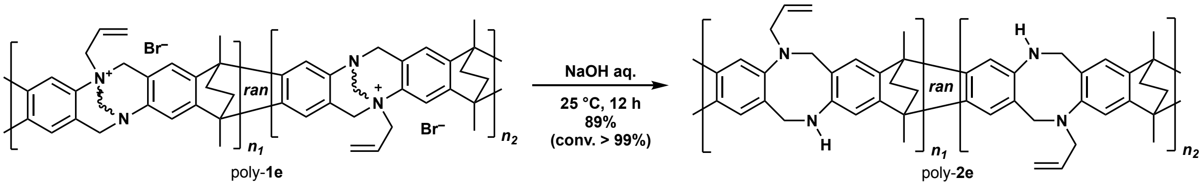

Poly-**2e**: An aqueous suspension of poly-**1e** (72.6 mg, 242 μmol for the monomer unit) and NaOH (1.0 M, 5.0 mL) was stirred for 12 h at 25 °C. The resultant white precipitate was collected by filtration, washed with Et_2O, and dried under reduced pressure to afford poly-**2e** (89% yield) as an off-white powder (68.5 mg, 208 μmol for the monomer unit): ^{1}H NMR (500 MHz, DMSO-d_6): δ (ppm) 6.82 (br, 3H), 6.49 (br, 1H), 5.88 (br, 1H), 5.19 (br, 2H), 4.33 (br, 4H), 4.06 (br, 1H), 3.67 (br, 2H), 1.82 (br, 10H). FT-IR (KBr): ν (cm^{-1}) 3747, 3407, 3237, 3073, 3016, 2959, 2934, 2857, 1732, 1716, 1615, 1559, 1500, 1475, 1457, 1411, 1375, 1321, 1255, 1228, 1157, 1064, 994, 947, 916, 890, 861, 839, 803, 777, 748, 720, 693, 659, 607, 574, 527, 501, 473, 459, 443, 416. Analytical data (^{1}H NMR and FT-IR spectra) of poly-**2e** are shown in Figures S134–S135.

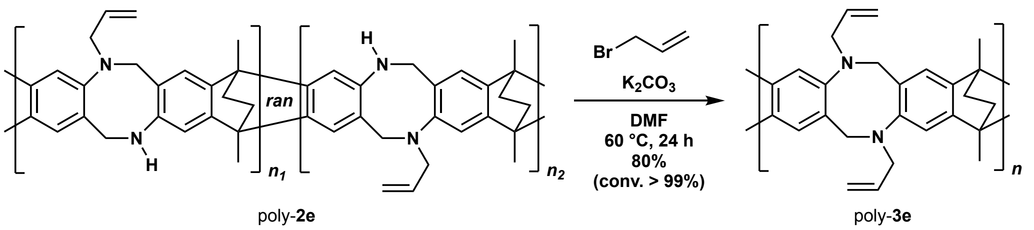

Poly-**3e**: Under nitrogen, allyl bromide (18.5 μL, 219 μmol) was added at 25 °C to a DMF solution (2.0 mL) of poly-**2e** (14.4 mg, 43.8 μmol for the monomer unit) and K_2CO_3 (33.5 mg, 242 μmol), and the mixture was stirred for 24 h at 100 °C. The reaction mixture was poured into water, and the precipitate formed was collected by filtration, washed with water, MeOH, and Et_2O, and dried under reduced pressure to afford poly-**3e** (80% yield) as an off-white powder (13.9 mg, 34.9 μmol for the monomer unit): ^{1}H NMR (500 MHz, $CDCl_3$) δ (ppm) 6.86 (br, 4H), 5.84 (br, 2H), 5.17 (br, 4H), 4.22 (br, 4H), 3.61 (br, 4H), 1.87–1.40 (br, 10H). FT-IR (KBr): ν (cm^{-1}) 3337, 3073, 2959, 2934, 2857, 2801, 1725, 1665, 1611, 1572, 1551, 1501, 1478, 1459, 1411, 1375, 1322, 1227, 1157, 1041, 974, 918, 898, 803, 773, 745, 669, 649, 602, 574, 500, 461, 451, 424, 416, 406. Analytical data (^{1}H NMR and FT-IR spectra) of poly-**3e** are shown in Figures S136–S137.

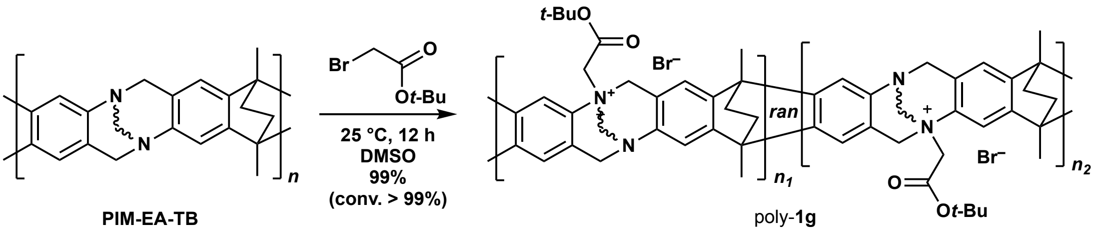

Poly-**1g**: *tert*-Butyl bromoacetate (60.6 μL, 410 μmol) was added at 25 °C to a DMSO solution (2.0 mL) of **PIM-EA-TB** (62.0 mg, 205 mmol), and the mixture was stirred for 12 h at 25 °C. The reaction mixture was poured into Et_2O, and the precipitate formed was collected by filtration, washed with Et_2O, and dried under reduced pressure to afford poly-**1g** (99% yield) as an off-white powder (96.8 mg, 202 μmol for the monomer unit): ^{1}H NMR (500 MHz, DMSO-d_6): δ (ppm) 7.77 (br, 1H), 7.12 (br, 3H), 6.0–4.0 (br, 8H), 1.83–1.49 (br, 19H). FT-IR (KBr): ν (cm^{-1}) 3409, 2965, 2936, 2864, 2039, 1735, 1653, 1622, 1586, 1540, 1498, 1456, 1431, 1396, 1370, 1340, 1319, 1286, 1251, 1152, 1102, 1078, 1028, 995, 967, 952, 897, 839, 809, 746, 695, 669, 638, 607, 575, 558, 526, 507, 473, 462, 454, 443, 425, 414. Analytical data (^{1}H NMR and FT-IR spectra) of poly-**1g** are shown in Figures S138–S139.

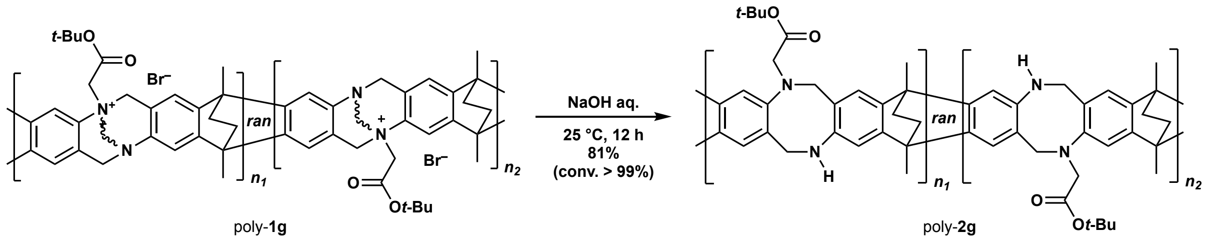

Poly-**2g**: An aqueous suspension of poly-**1g** (95.0 mg, 192 μmol for the monomer unit) and NaOH (1.0 M, 5.0 mL) was stirred for 12 h at 25 °C. The resultant white precipitate was collected by filtration, washed with water and MeOH, and dried under reduced pressure to afford poly-**2g** (81% yield) as an off-white powder (62.8 mg, 156 μmol for the monomer unit): ^{1}H NMR (500 MHz, DMSO-d_6): δ (ppm) 6.86 (br, 2H), 6.64 (br, 1H), 6.50 (br, 1H), 4.70–3.70 (br, 7H), 3.57 (br, 2H), 1.82–1.42 (br, 19H). FT-IR (KBr): ν (cm^{-1}) 3603, 3407, 3015, 2960, 2934, 2858, 1731, 1615, 1561, 1500, 1475, 1458, 1414, 1394, 1369, 1334, 1254, 1226, 1152, 1065, 982, 955, 915, 893, 843, 803, 777, 749, 693, 668, 607, 575, 526, 505, 473, 458, 445, 435, 416. Analytical data (^{1}H NMR and FT-IR spectra) of poly-**2g** are shown in Figures S140–S141.

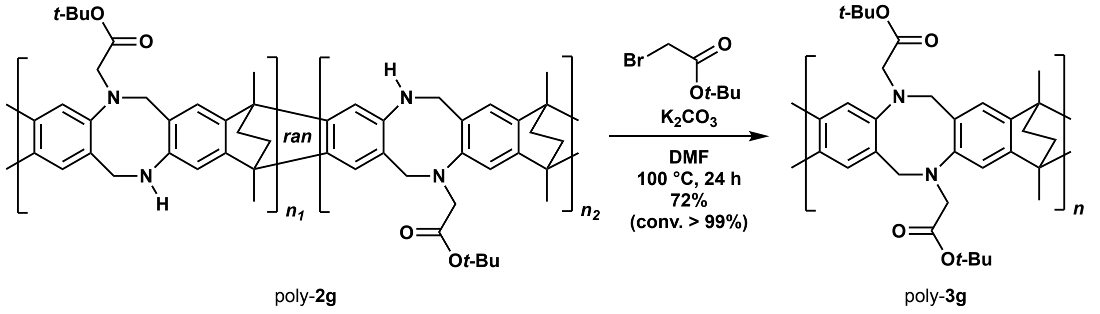

Poly-**3g**: Under nitrogen, *tert*-butyl bromoacetate (31.4 μL, 212 mmol) was added at 25 °C to a DMF solution (2.0 mL) of poly-**2g** (17.1 mg, 42.5 μmol for the monomer unit) and K_2CO_3 (32.4 mg, 234 μmol), and the mixture was stirred for 24 h at 100 °C. The reaction mixture was poured into water, and the precipitate formed was collected by filtration, washed with water, MeOH, and Et_2O, and dried under reduced pressure to afford poly-**3g** (72% yield) as a slightly brown powder (15.7 mg, 30.4 μmol for the monomer unit): ^{1}H NMR (500 MHz, $CDCl_3$) δ (ppm) 6.91 (br, 2H), 6.60 (br, 2H), 4.35 (br, 4H), 3.49 (br, 4H), 1.82–1.50 (br, 28H). ^{13}C NMR (125 MHz, $CDCl_3$): δ 171.9, 147.0, 137.4, 123.4, 122.4, 109.7, 81.2, 55.6, 53.8, 41.7, 41.0, 40.4, 36.6, 28.3, 18.5. FT-IR (KBr): ν (cm^{-1}) 2963, 2935, 2875, 2859, 1739, 1728, 1678, 1642, 1613, 1563, 1503, 1481, 1460, 1415, 1392, 1368, 1343, 1305, 1255, 1218, 1150, 1056, 985, 957, 891, 844, 794, 784, 746, 706, 669, 650, 632, 613, 575, 538, 526, 518, 499, 490, 479, 462, 452, 435, 418, 407. Analytical data (^{1}H and ^{13}C NMR and FT-IR spectra) of poly-**3g** are shown in Figures S142–S144.

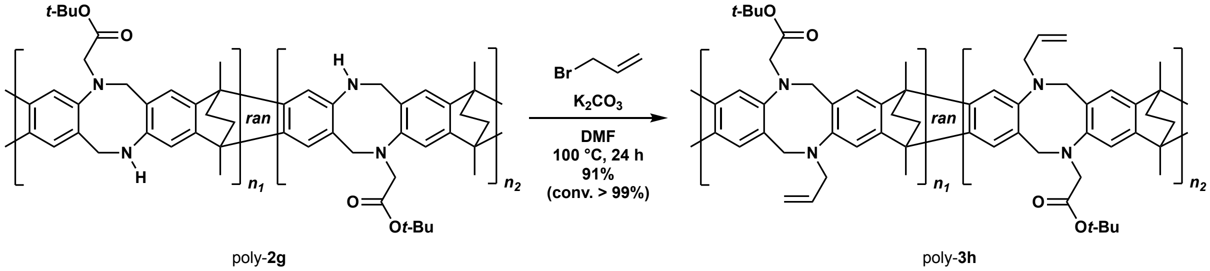

Poly-**3h**: Under nitrogen, allyl bromide (22.3 μL, 264 μmol) was added at 25 °C to a DMF solution (2.0 mL) of poly-**2g** (21.3 mg, 52.9 μmol for the monomer unit) and K_2CO_3 (36.5 mg, 264 μmol), and the mixture was stirred for 24 h at 100 °C. The reaction mixture was poured into water, and the precipitate formed was collected by filtration, washed with water, MeOH, and Et_2O, and dried under reduced pressure to afford poly-**3h** (91% yield) as a slightly brown powder (21.3 mg, 48.12 μmol for the monomer unit): ^{1}H NMR (500 MHz, $CDCl_3$) δ (ppm) 6.91 (br, 3H), 6.63 (br, 1H), 5.84 (br, 1H), 5.18 (br, 2H), 4.39 (br, 4H), 3.60 (br, 4H), 1.86–1.52 (br, 19H). ^{13}C NMR (125 MHz, $CDCl_3$): δ 172.0, 146.8, 135.8, 123.7, 118.1, 116.2, 109.8, 81.1, 53.8, 41.7, 41.0, 40.3, 36.3, 28.3, 18.5. FT-IR (KBr): ν (cm^{-1}) 3409, 3074, 2960, 2934, 2858, 1728, 1679, 1642, 1612, 1563, 1502, 1479, 1460, 1414, 1392, 1368, 1343, 1323, 1254, 1219, 1152, 1081, 1054, 982, 917, 892, 843, 802, 784, 765, 745, 697, 658, 632, 603, 575, 548, 538, 527, 509, 499, 490, 479, 461, 435, 425, 417, 406. Analytical data (^{1}H and ^{13}C NMR and FT-IR spectra) of poly-**3h** are shown in Figures S145–S147.

Supplementary figures

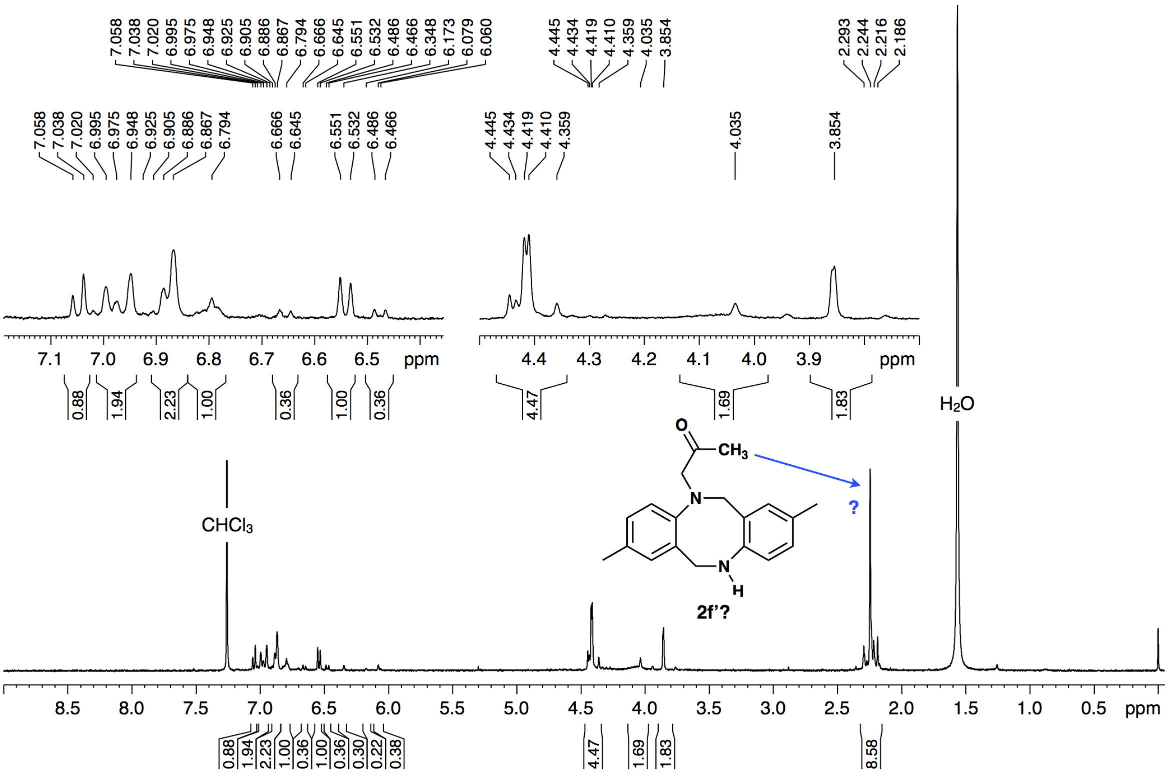

Fig. S1. ^{1}H NMR spectrum (500 MHz) of the crude material in the synthesis of **2f** in CDCl$_3$ at 25 °C.

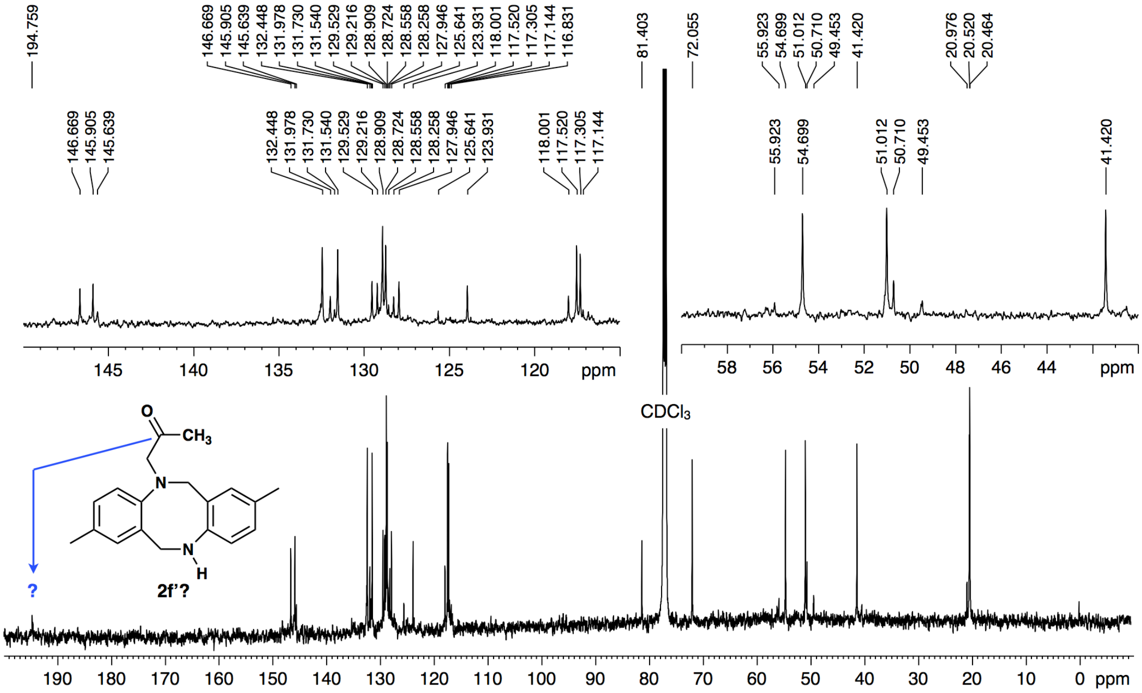

Fig. S2. ^{13}C NMR spectrum (125 MHz) of the crude material in the synthesis of **2f** in CDCl$_3$ at 25 °C.

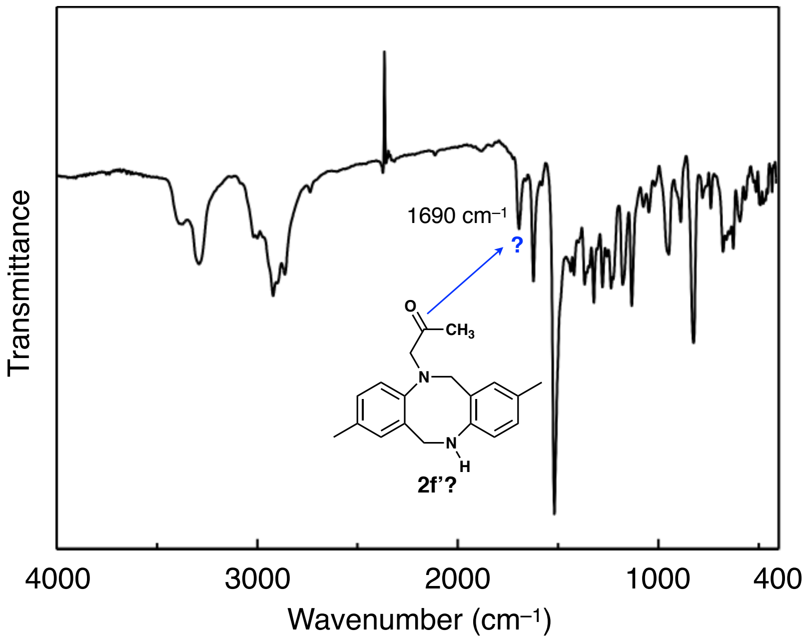

Fig. S3. FT-IR spectrum of the crude material in the synthesis of **2f** at 25 °C (KBr).

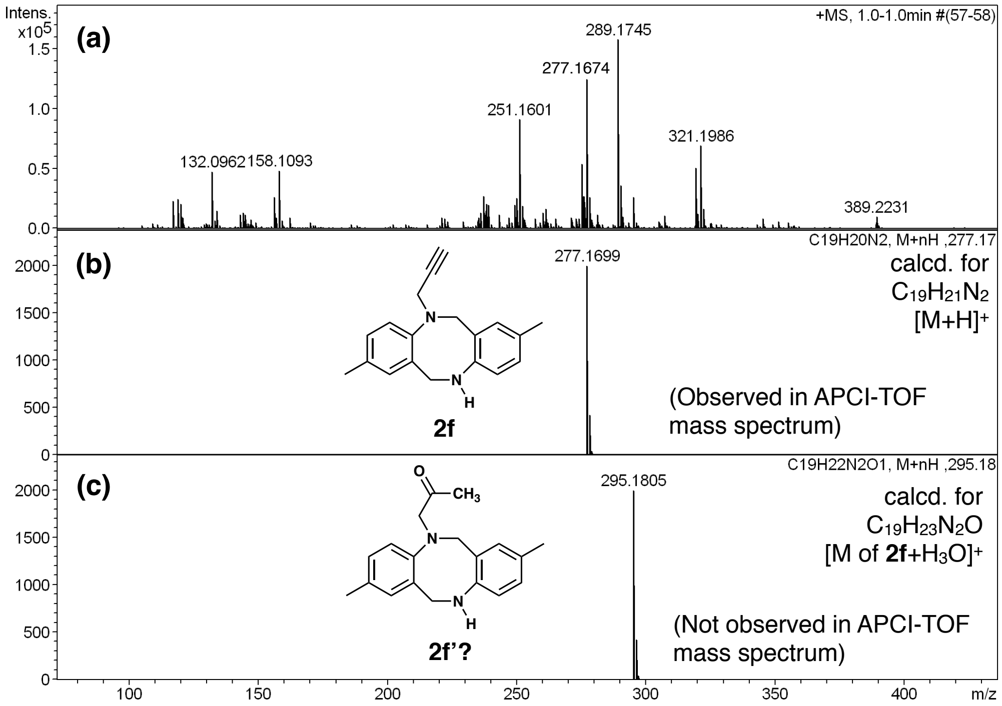

Fig. S4. APCI-TOF mass spectrum of (a) the crude material in the synthesis of **2f** and simulated mass spectra of (b) **2f**+H$^+$ and (c) **2f'**+H$^+$ (= **2f**+H$_2$O+H$^+$).

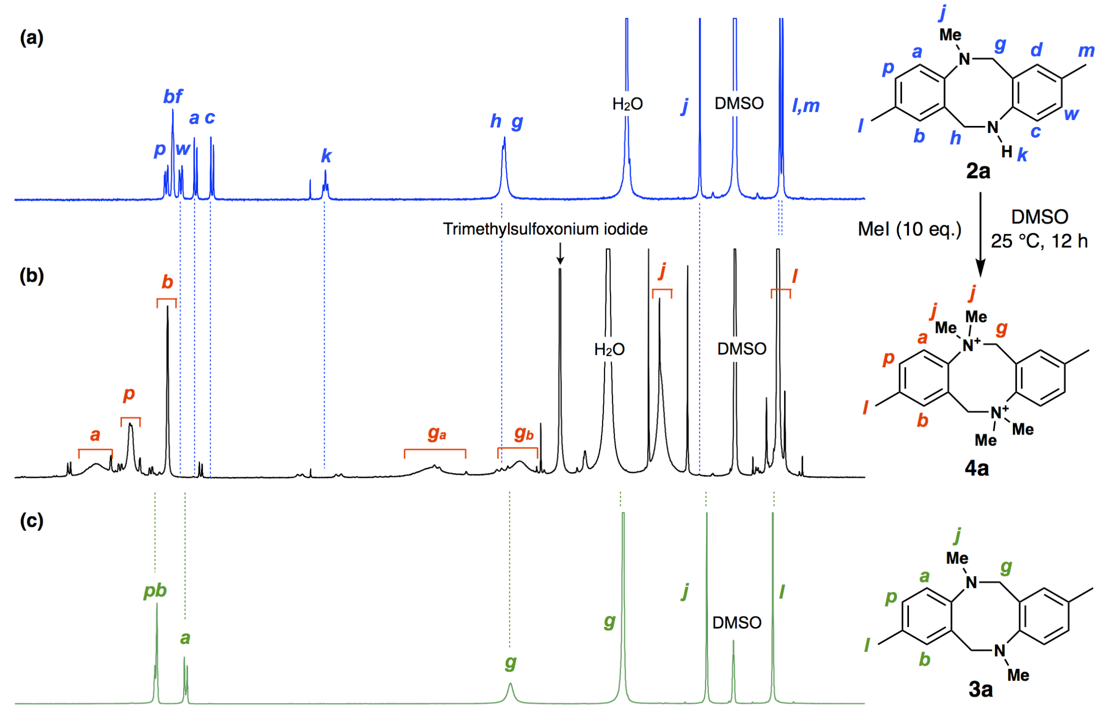

Fig. S5. ^{1}H NMR spectra (500 MHz, at 25 °C, in DMSO-d_6,) of **2a**, **4a** (the crude material after treating **2a** with 10 eq. of MeI in DMSO at 25 °C for 12 h) and **3a**.

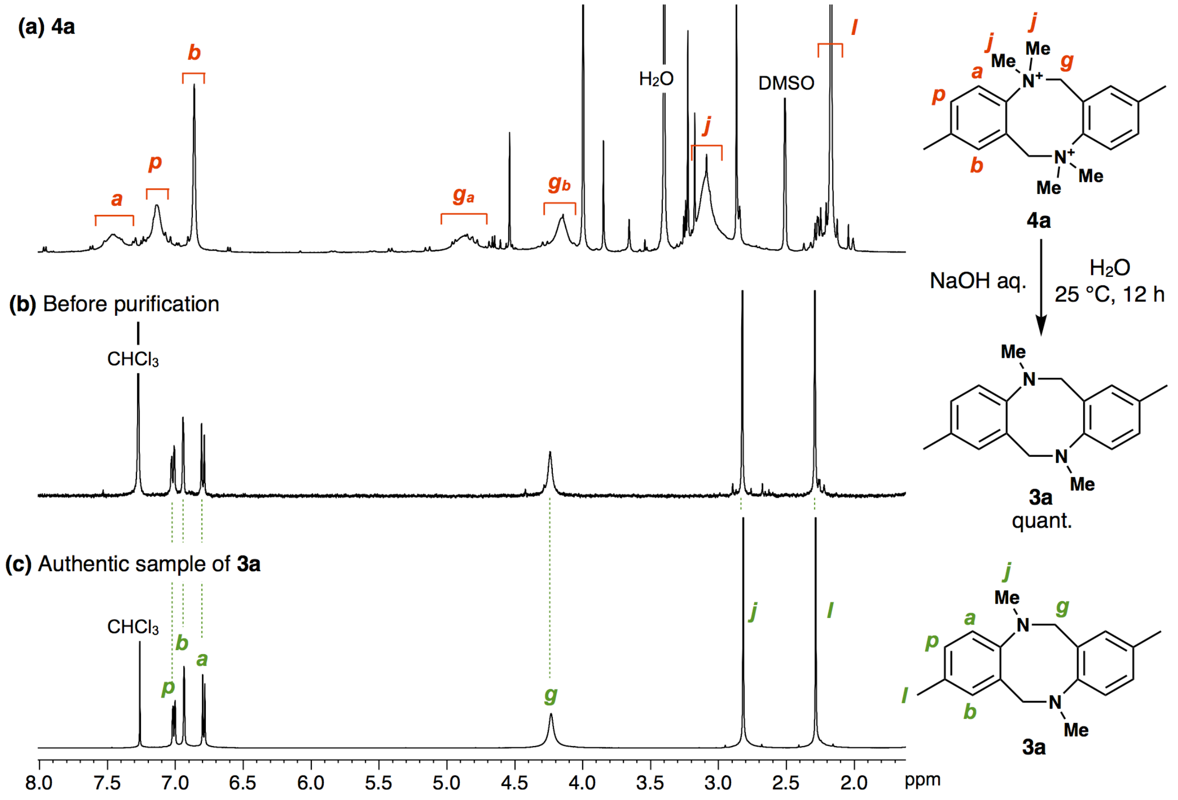

Fig. S6. ^{1}H NMR spectra [500 MHz, at 25 °C, (a) in DMSO-d_6, (b,c) in $CDCl_3$] of (a) **4a**, (b) the crude material after treating **4a** with NaOH aq. at 25 °C for 12 h and (c) **3a**.

Analytical data

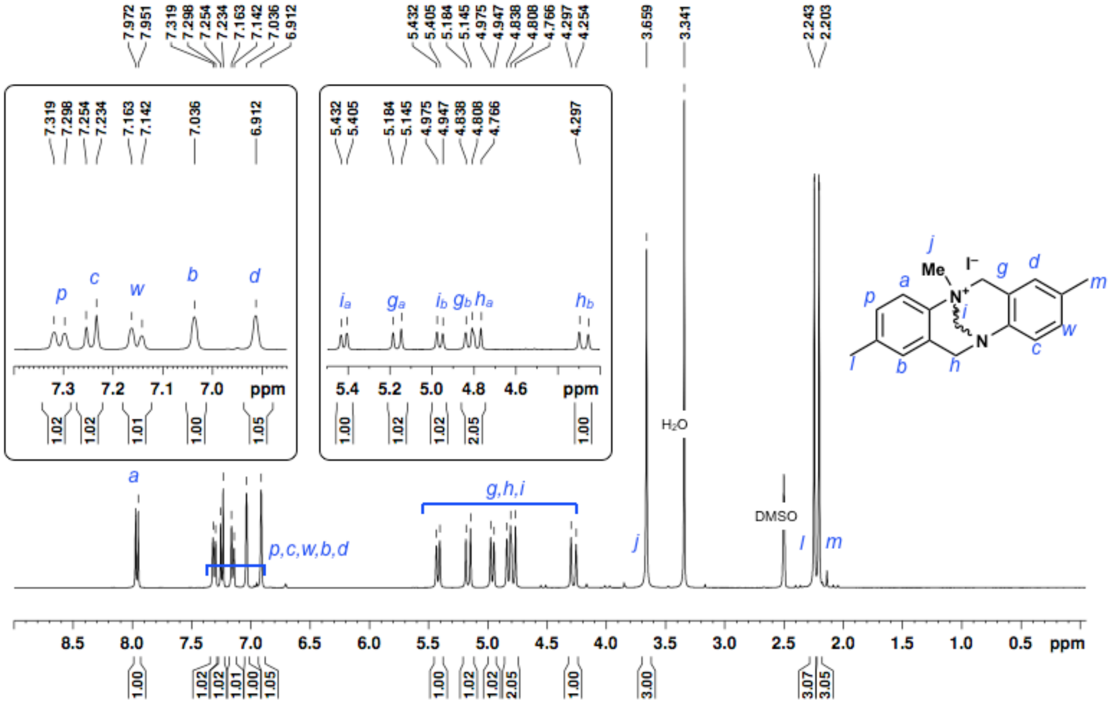

Fig. S7. ^{1}H NMR spectrum (500 MHz) of **1a** in DMSO-d_6 at 25 °C.

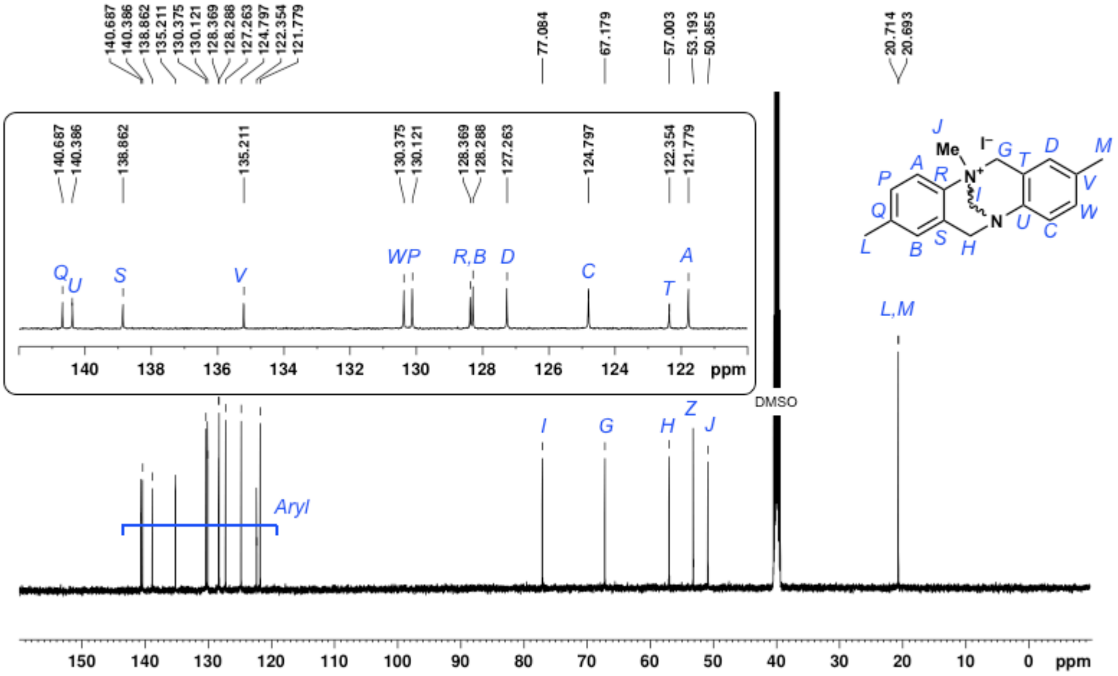

Fig. S8. ^{13}C NMR spectrum (125 MHz) of **1a** in DMSO-d_6 at 25 °C.

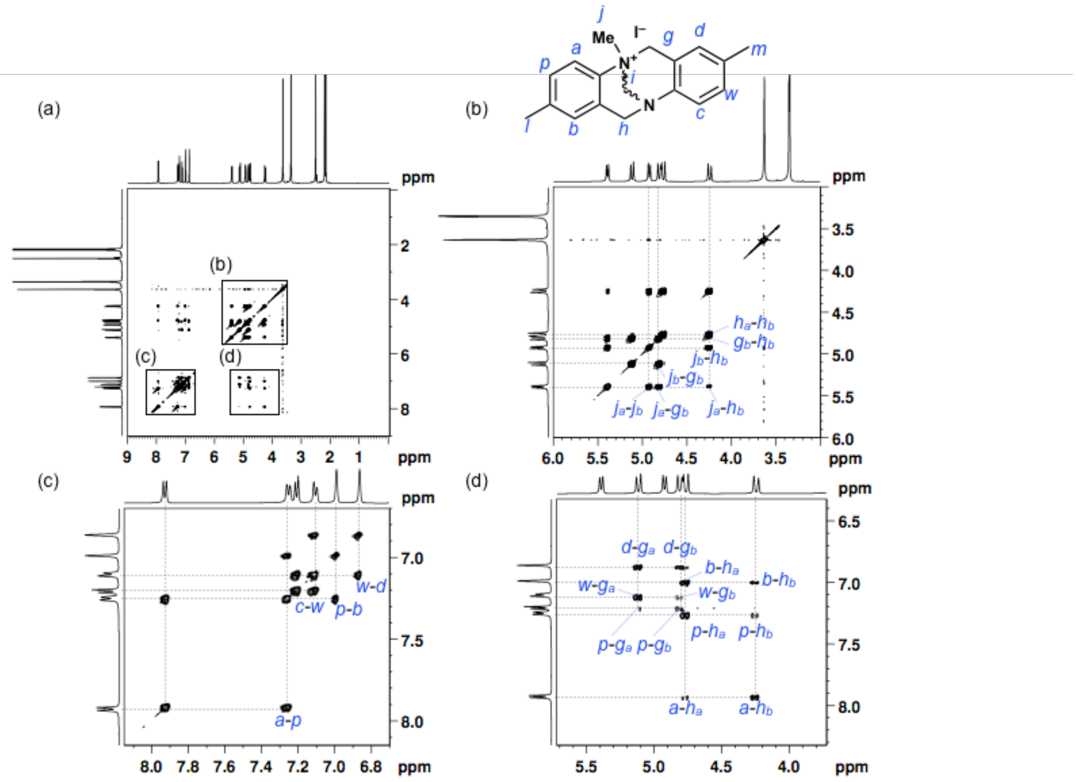

Fig. S9. H-H COSY correlations (500 MHz) of **1a** in DMSO-d_6 at 25 °C.

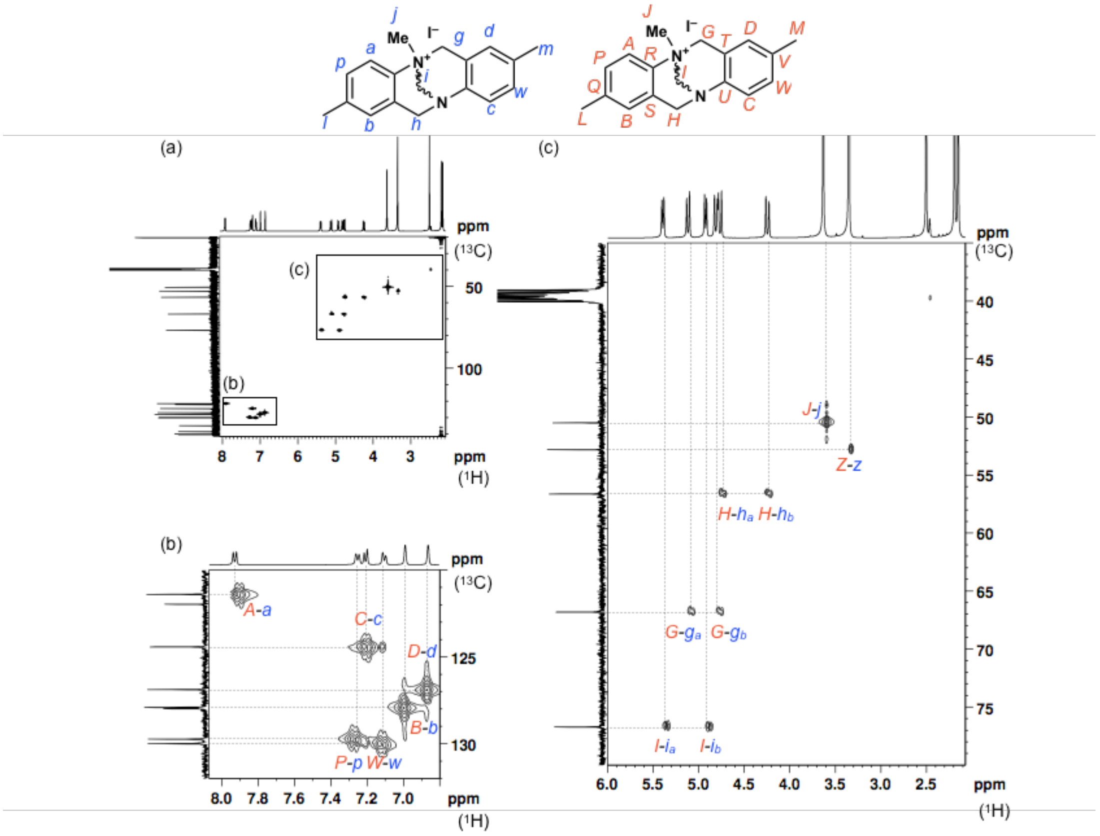

Fig. S10. HMQC correlations (^{1}H: 500 MHz, ^{13}C: 125 MHz) of **1a** in DMSO-d_6 at 25 °C.

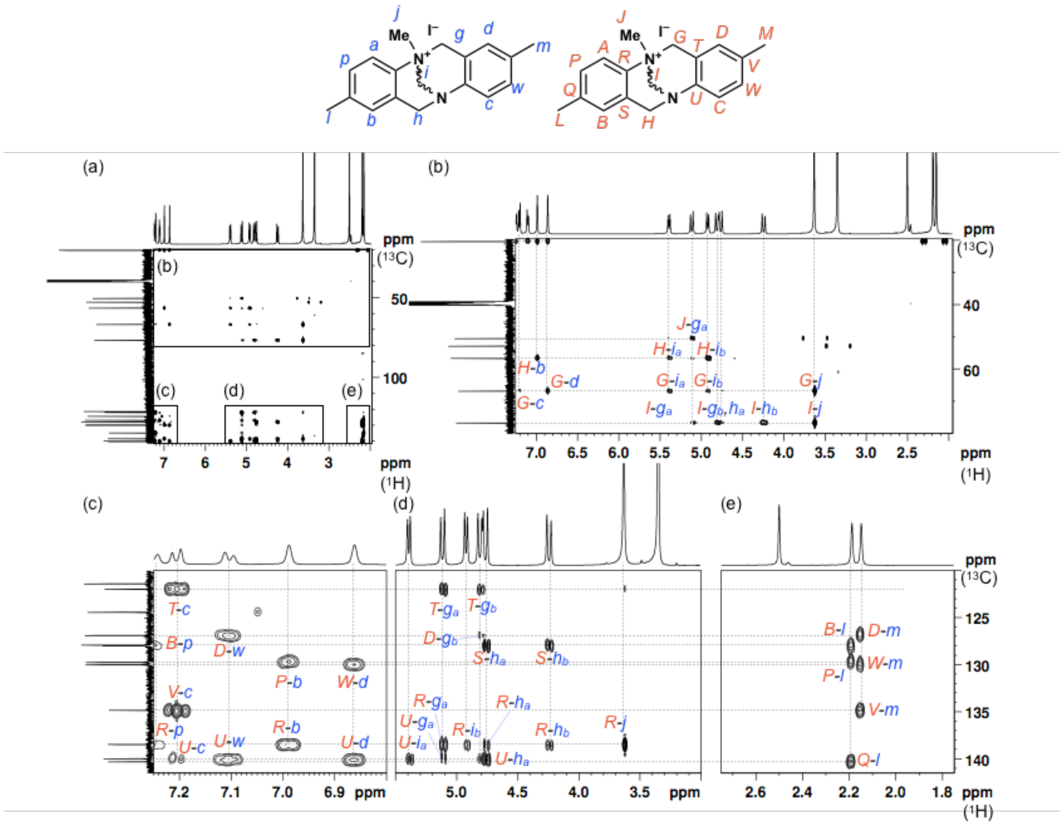

Fig. S11. HMBC correlations (^{1}H: 500 MHz, ^{13}C: 125 MHz) of **1a** in DMSO-d_6 at 25 °C.

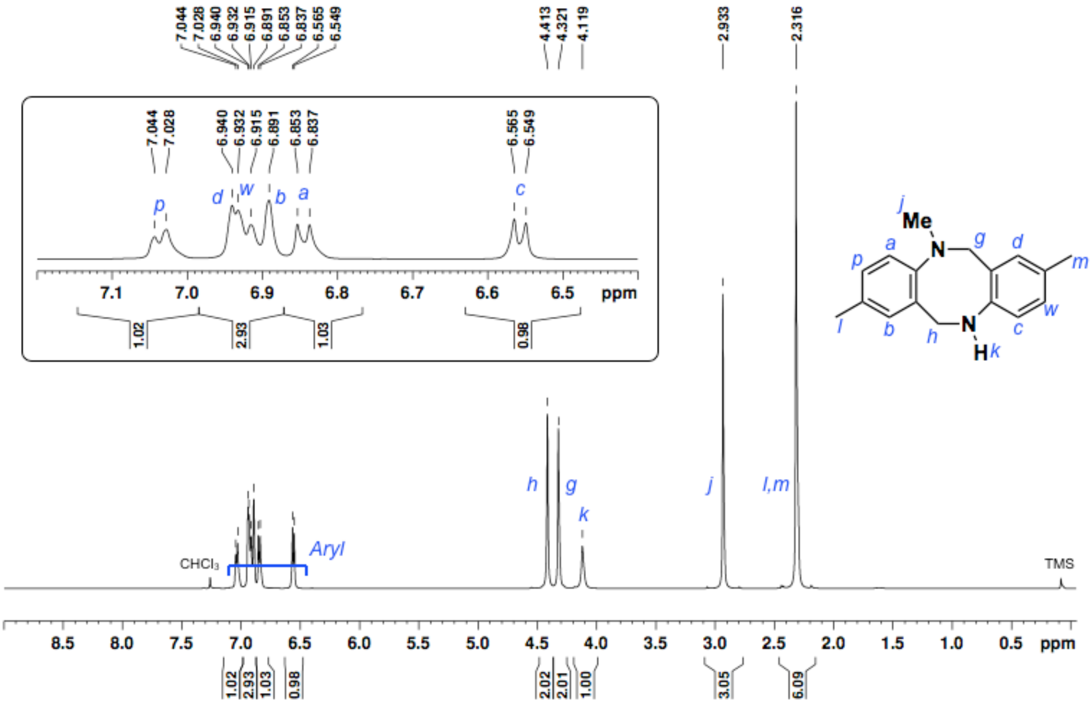

Fig. S12. ^{1}H NMR spectrum (500 MHz) of **2a** in CDCl$_3$ at 25 °C.

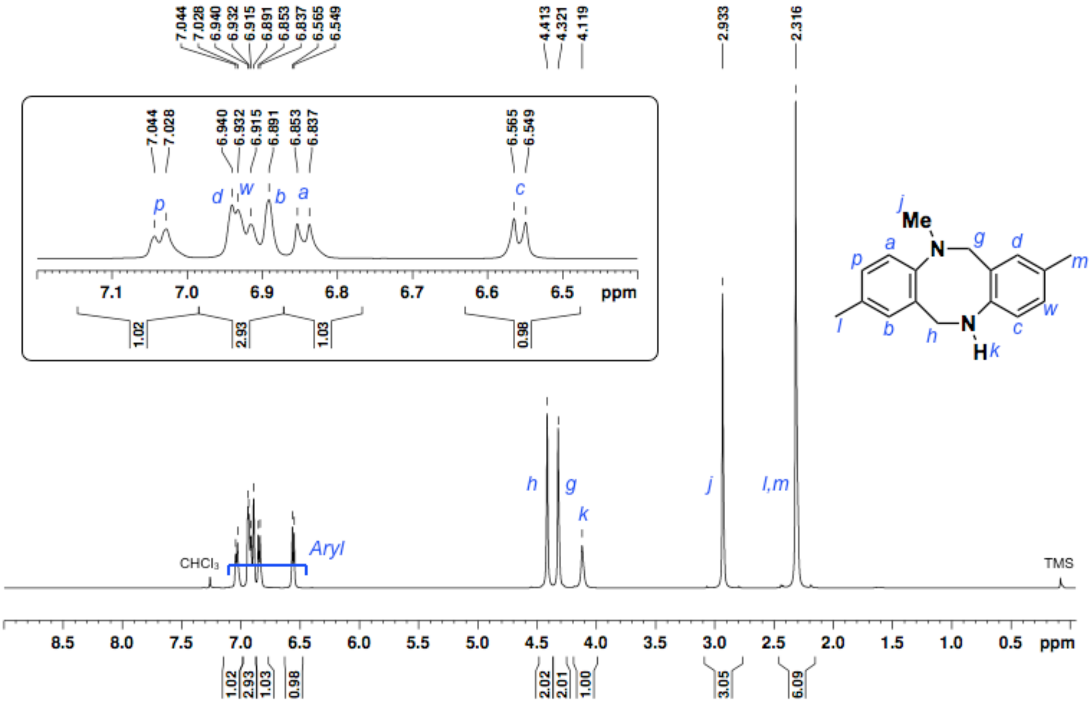

Fig. S13. ^{13}C NMR spectrum (125 MHz) of **2a** in $CDCl_3$ at 25 °C.

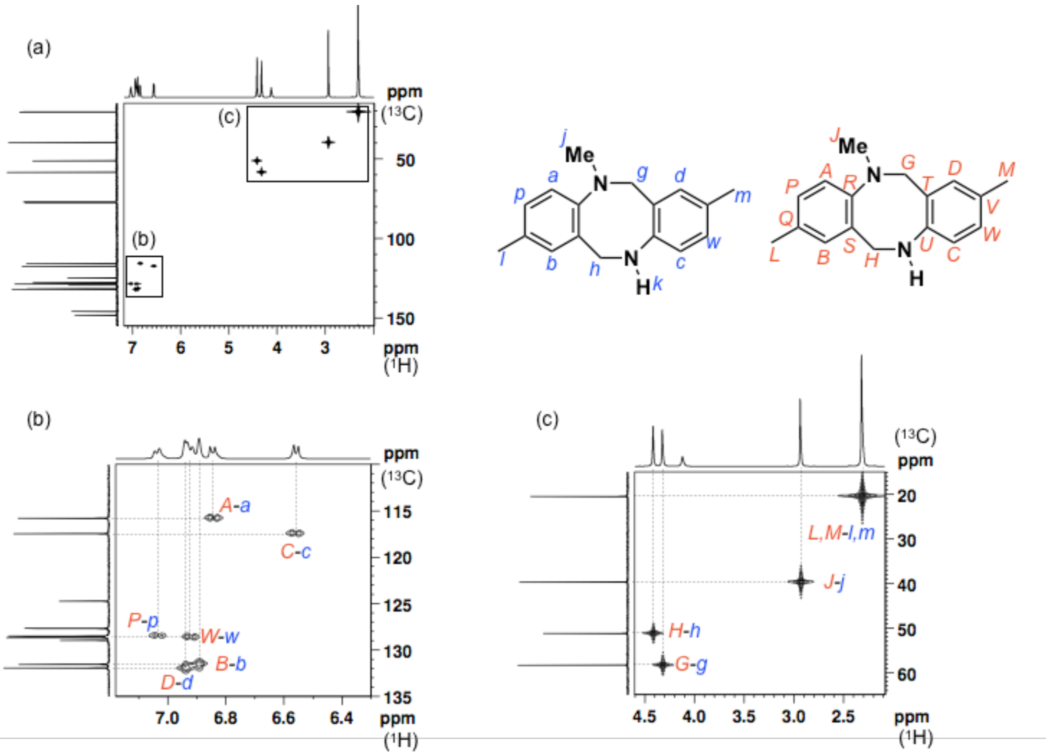

Fig. S14. HMQC correlations (^{1}H: 500 MHz, ^{13}C: 125 MHz) of **2a** in $CDCl_3$ at 25 °C.

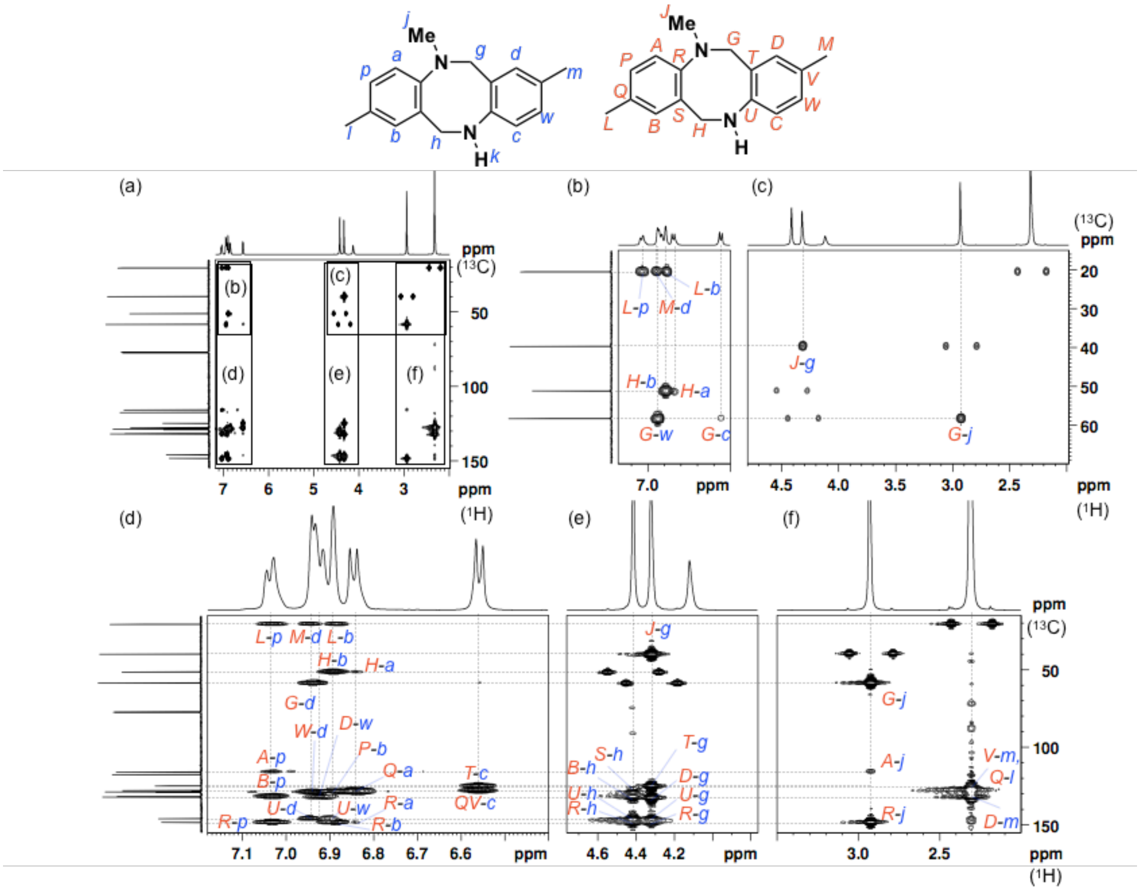

Fig. S15. HMBC correlations (^{1}H: 500 MHz, ^{13}C: 125 MHz) of **2a** in CDCl$_3$ at 25 °C.

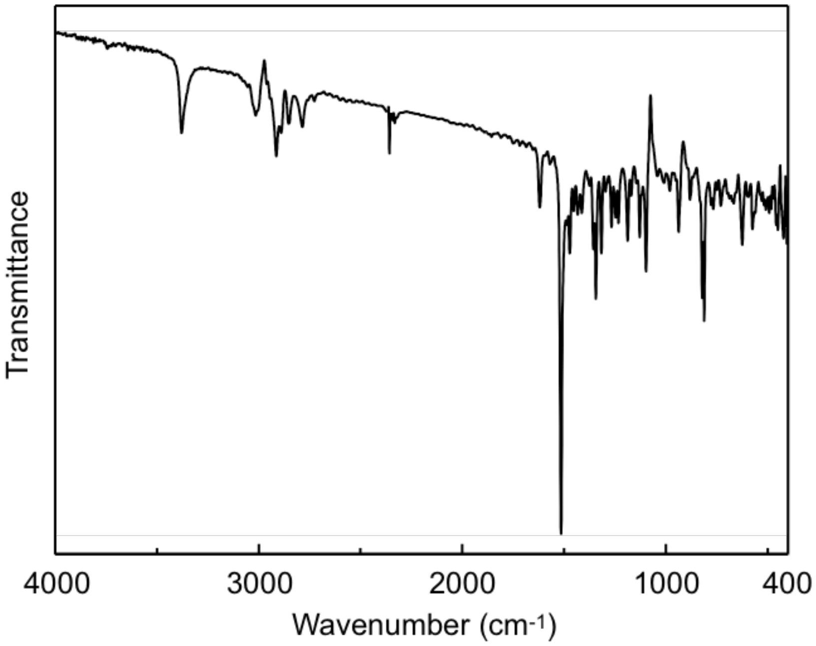

Fig. S16. FT-IR spectrum of **2a** at 25 °C (KBr).

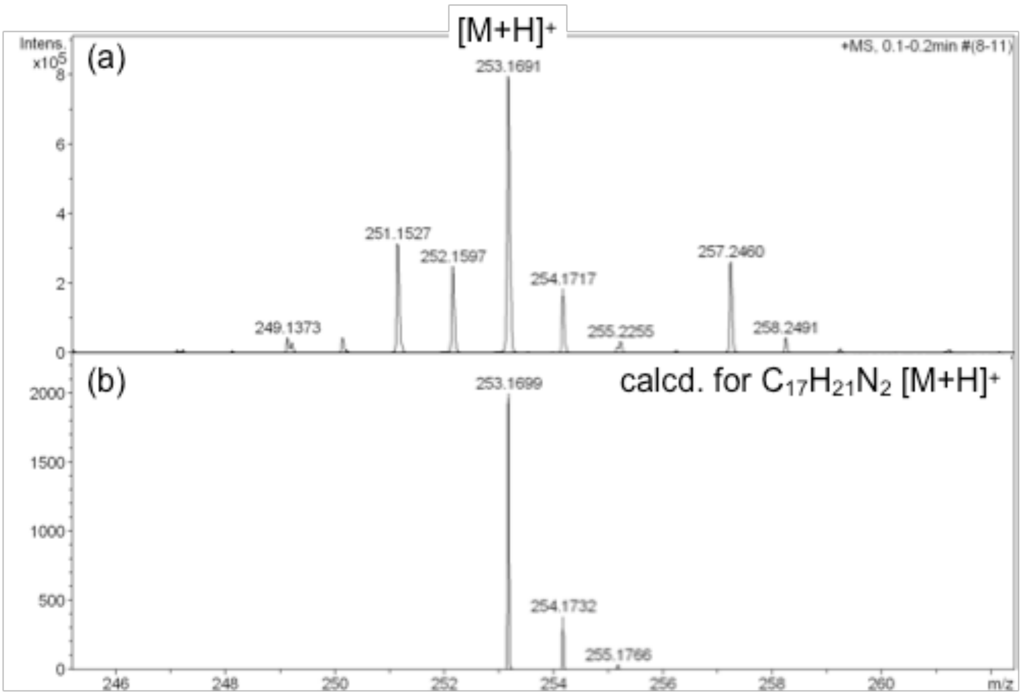

Fig. S17. (a) Observed and (b) simulated high-resolution APCI-TOF mass spectra of **2a**.

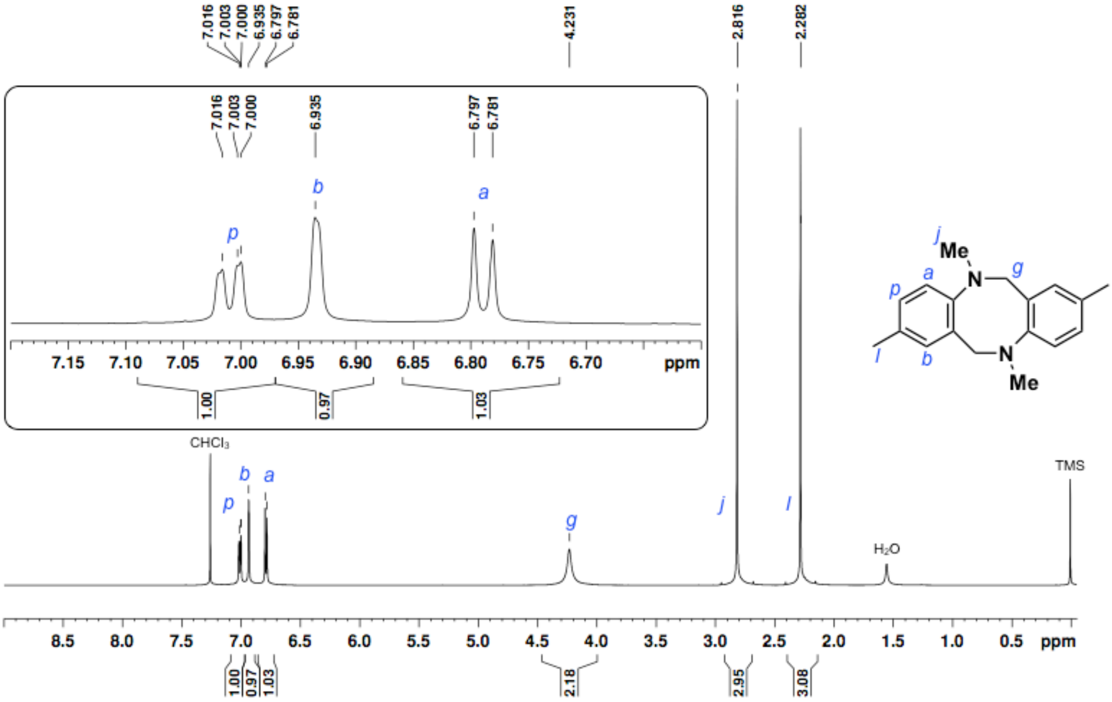

Fig. S18. ^{1}H NMR spectrum (500 MHz) of **3a** in $CDCl_3$ at 25 °C.

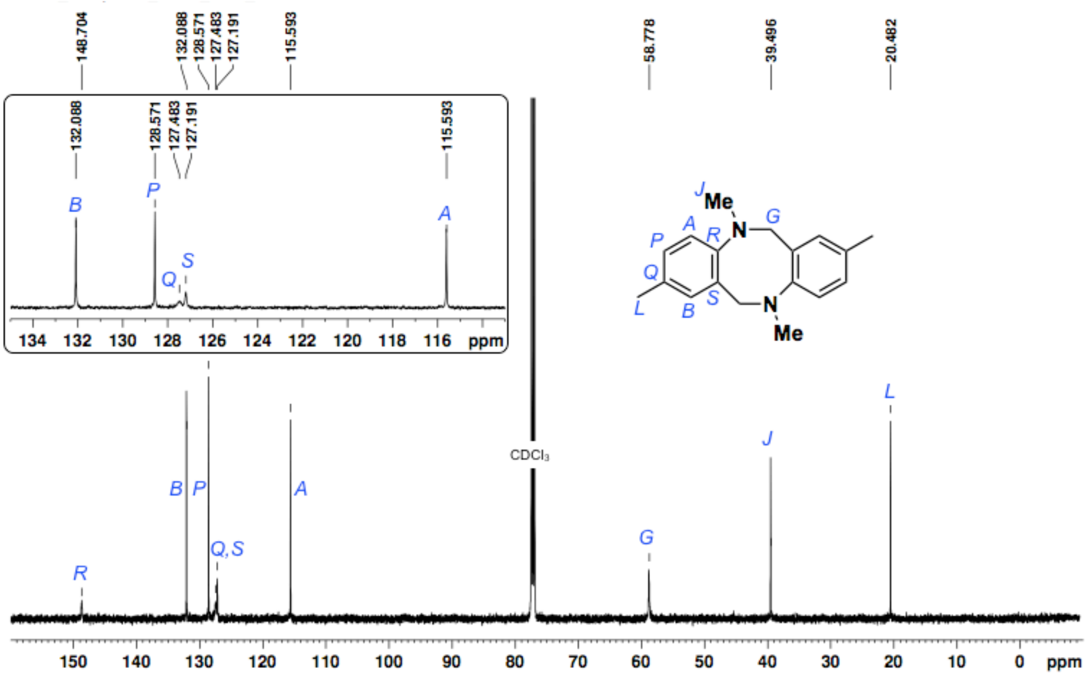

Fig. S19. ^{13}C NMR spectrum (125 MHz) of **3a** in CDCl$_3$ at 25 °C.

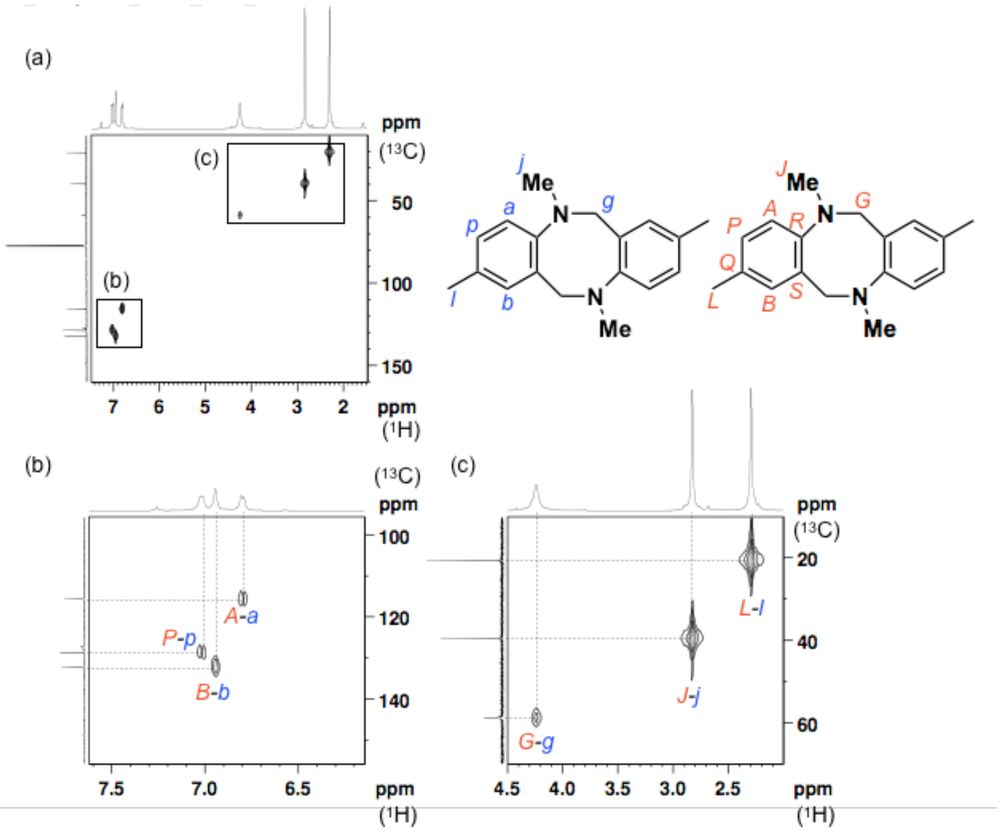

Fig. S20. HMQC correlations (^{1}H: 500 MHz, ^{13}C: 125 MHz) of **3a** in CDCl$_3$ at 25 °C.

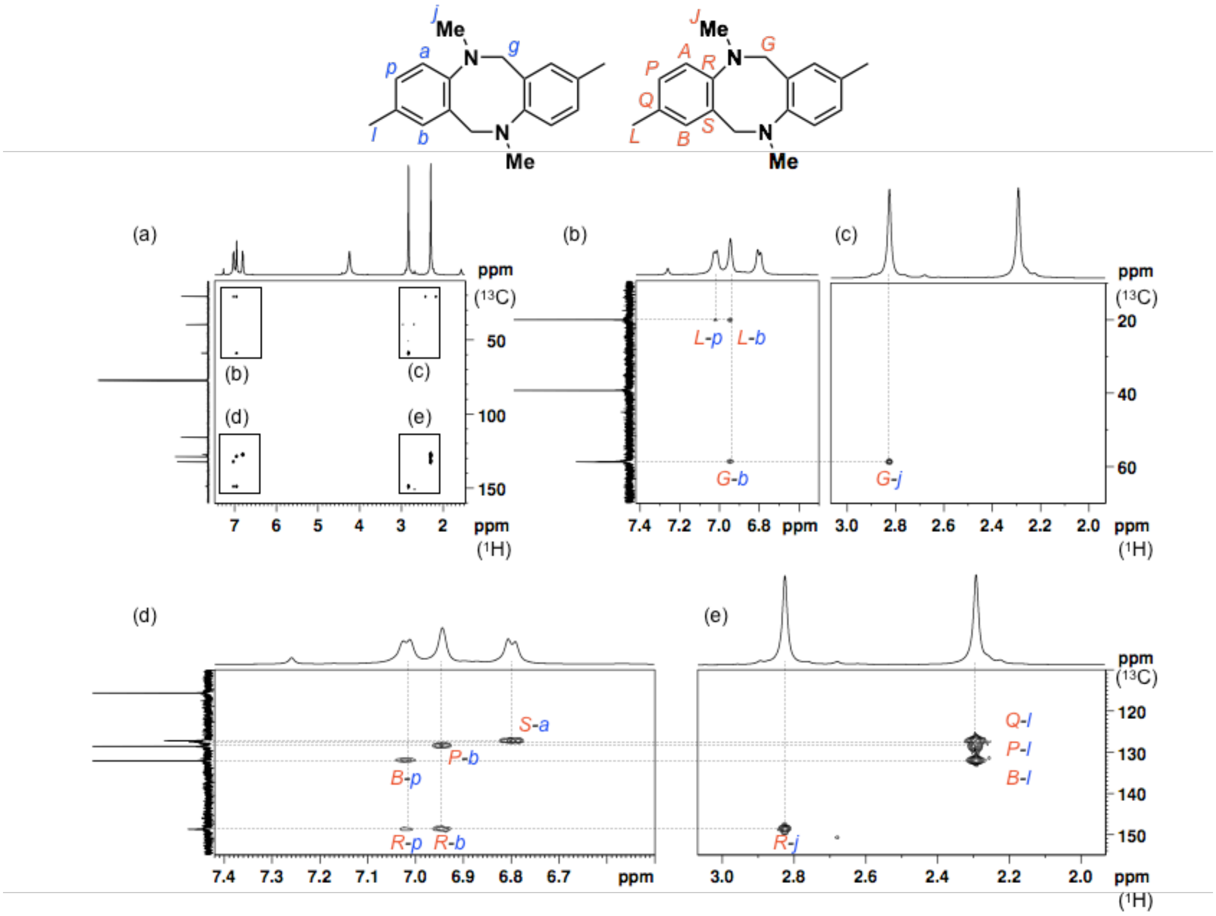

Fig. S21. HMBC correlations (^{1}H: 500 MHz, ^{13}C: 125 MHz) of **3a** in CDCl$_3$ at 25 °C.

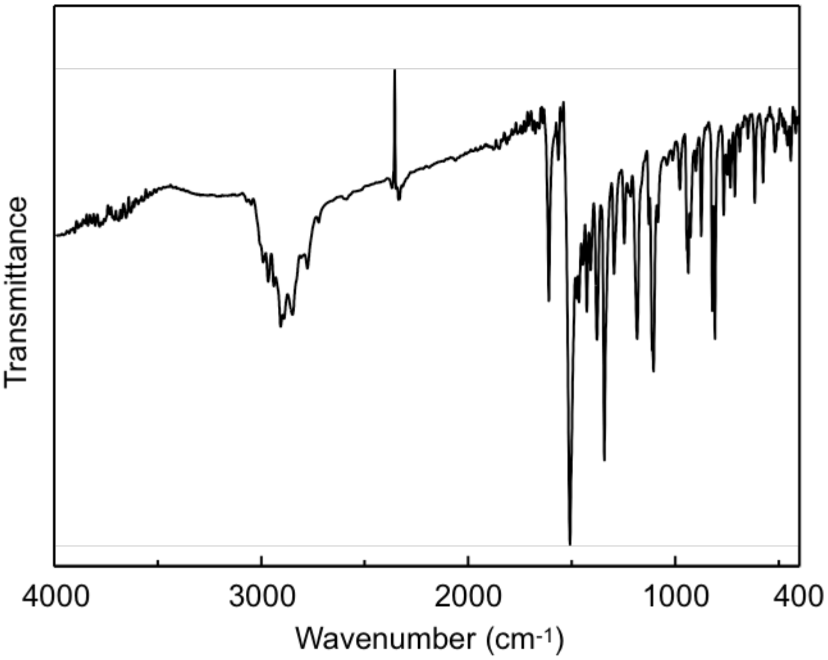

Fig. S22. FT-IR spectrum of **3a** at 25 °C (KBr).

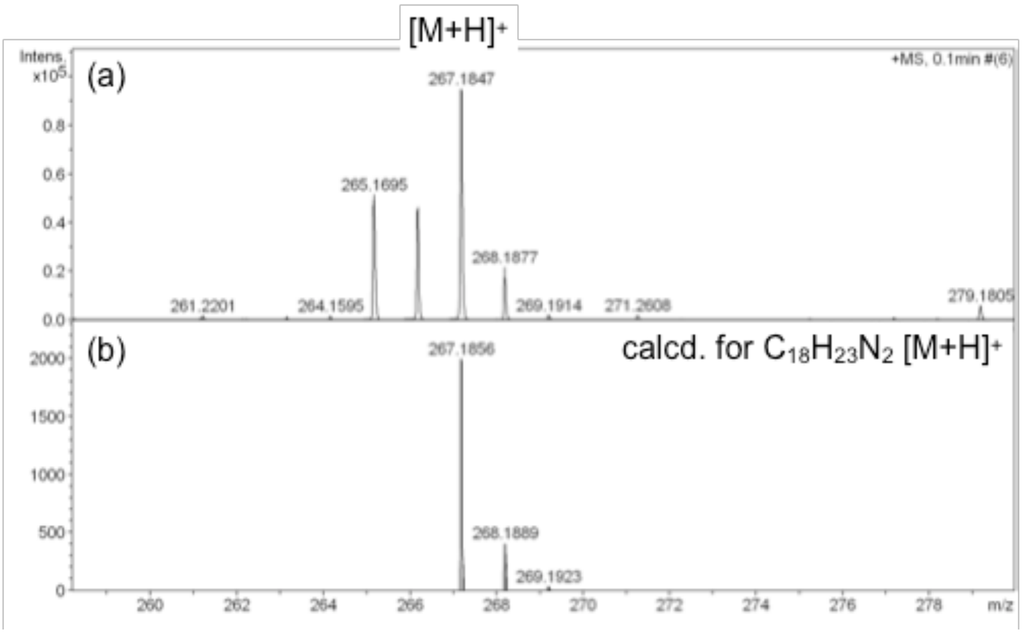

Fig. S23. (a) Observed and (b) simulated high-resolution APCI-TOF mass spectra of **3a**.

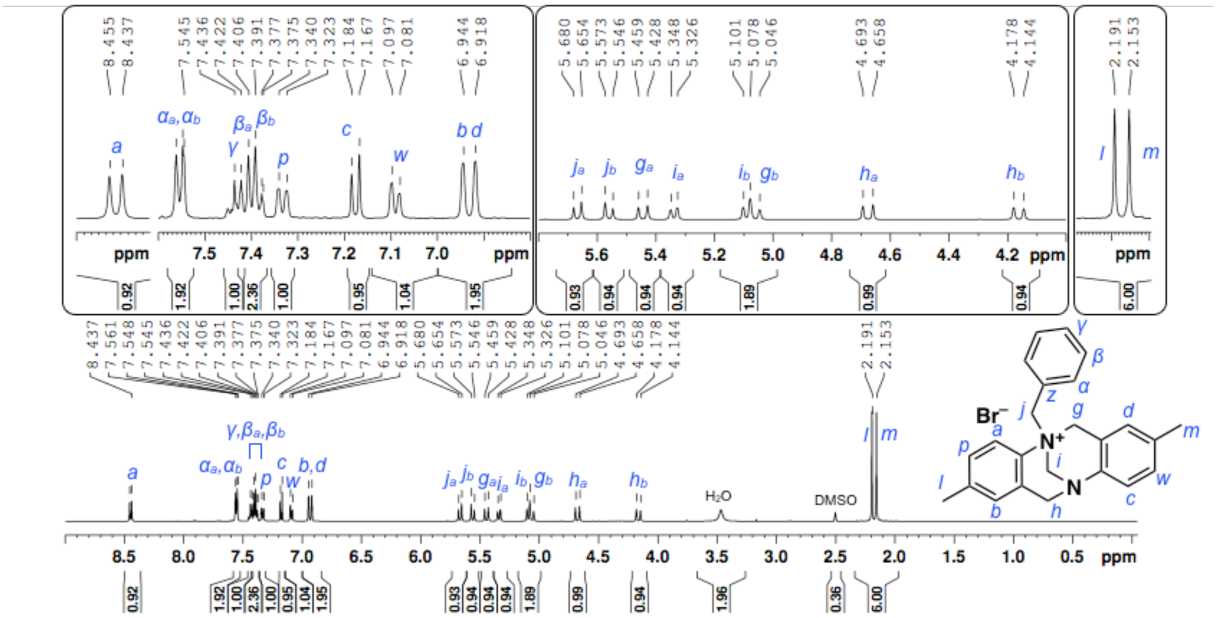

Fig. S24. ^{1}H NMR spectrum (500 MHz) of **1c** in DMSO-d_6 at 25 °C.

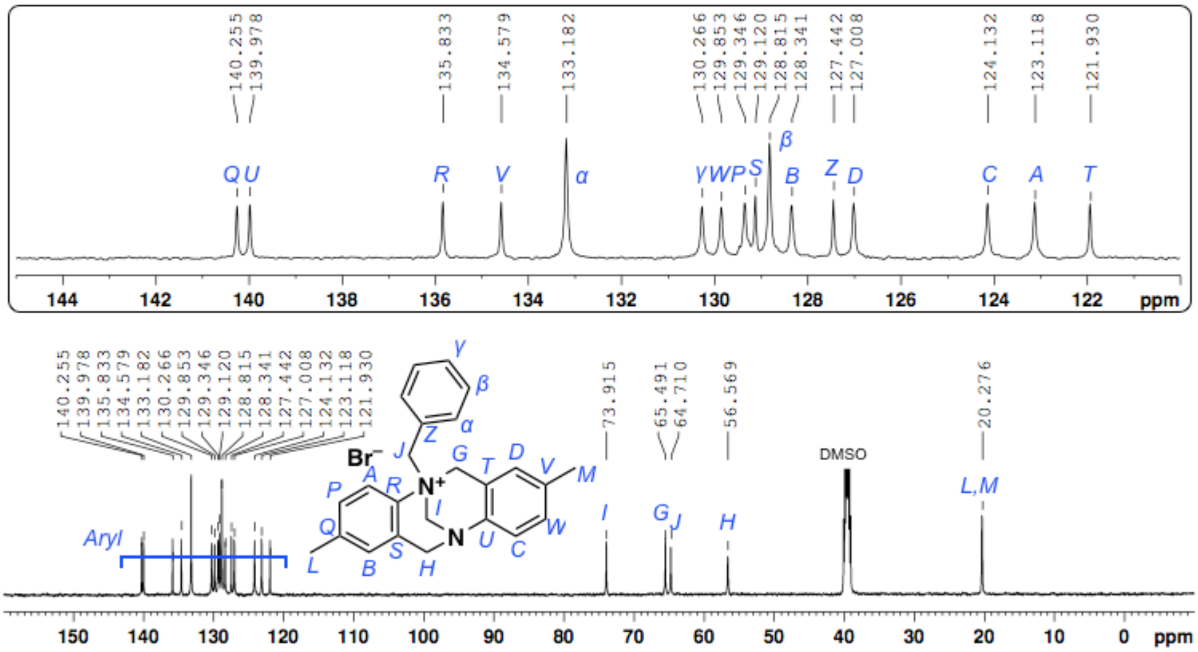

Fig. S25. ^{13}C NMR spectrum (500 MHz) of **1c** in DMSO-d_6 at 25 °C.

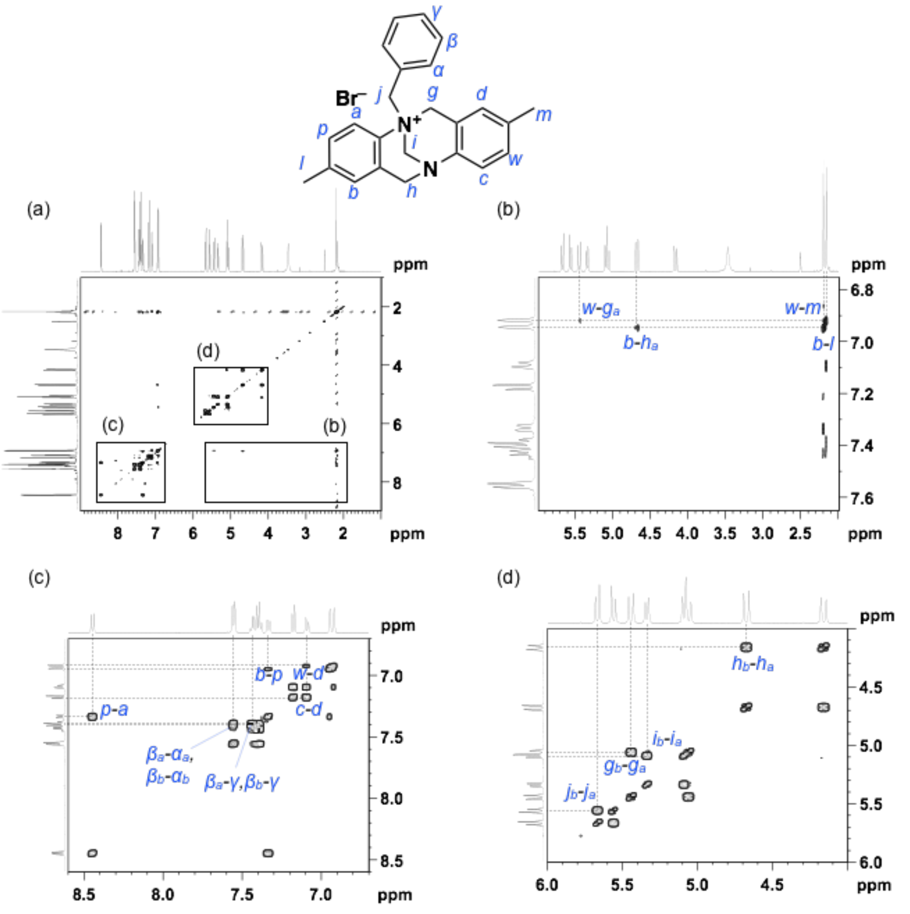

Fig. S26. H-H COSY correlations (500 MHz) of **1c** in DMSO-d_6 at 25 °C.

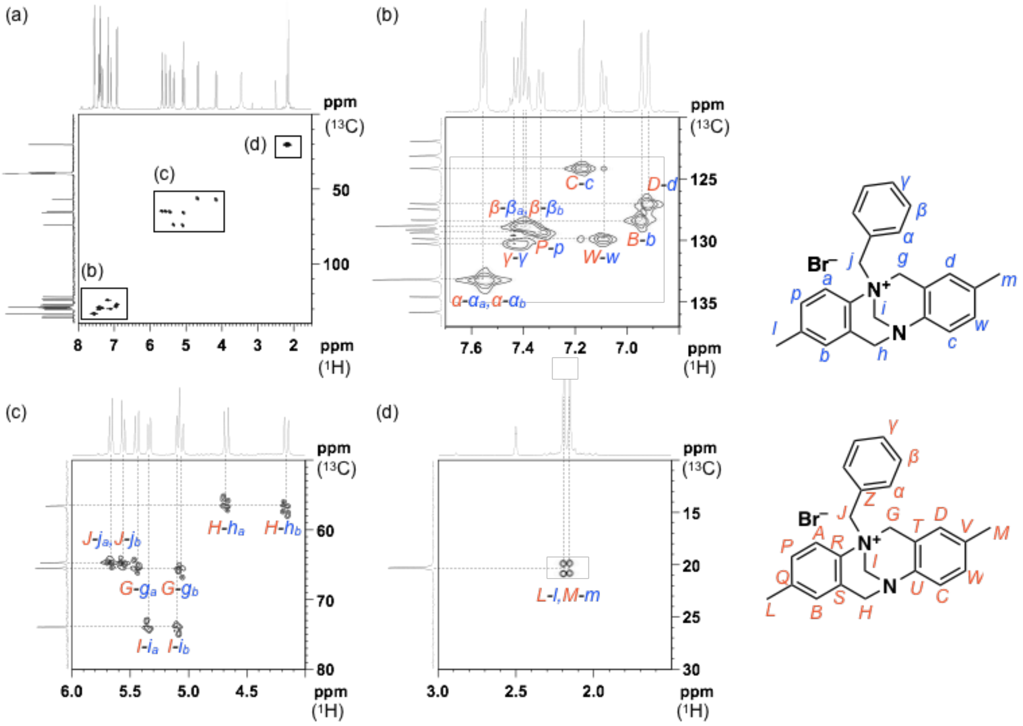

Fig. S27. HMQC correlations (^{1}H: 500 MHz, ^{13}C: 125 MHz) of **1c** in DMSO-d_6 at 25 °C.

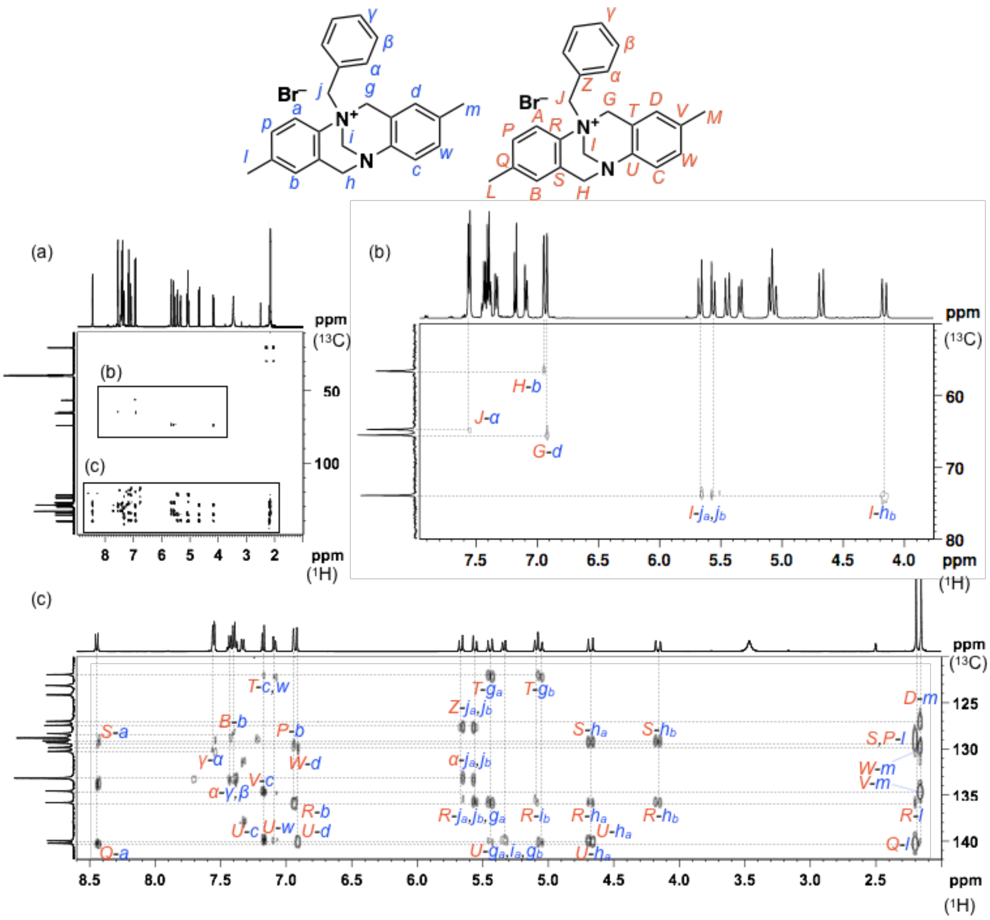

Fig. S28. HMBC correlations (^{1}H: 500 MHz, ^{13}C: 125 MHz) of **1c** in DMSO-d_6 at 25 °C.

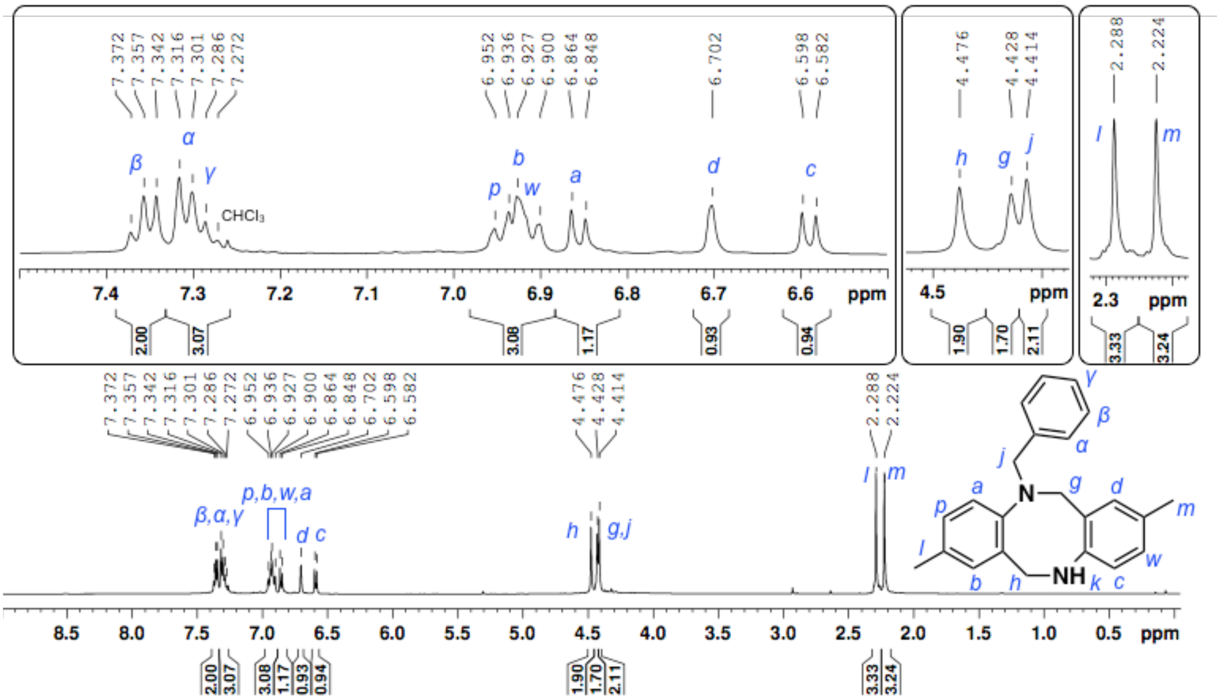

Fig. S29. ^{1}H NMR spectrum (500 MHz) of **2c** in CDCl$_3$ at 25 °C.

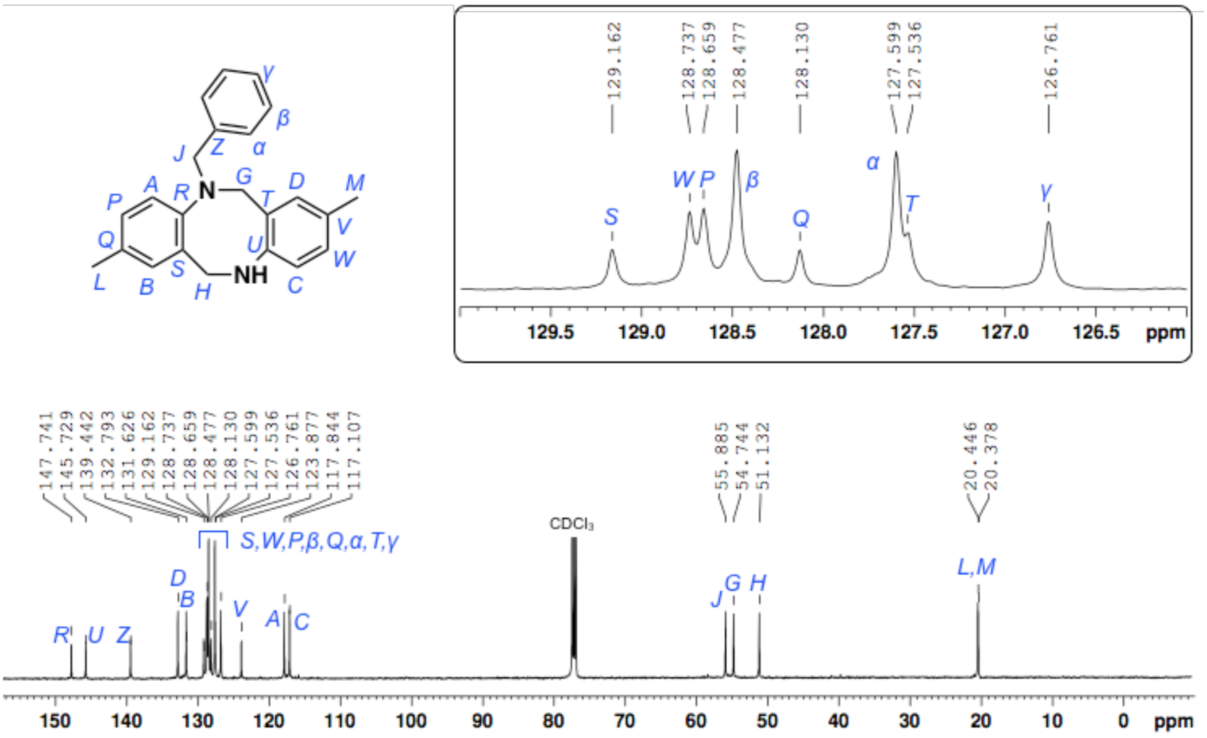

Fig. S30. ^{13}C NMR spectrum (125 MHz) of **2c** in CDCl$_3$ at 25 °C.

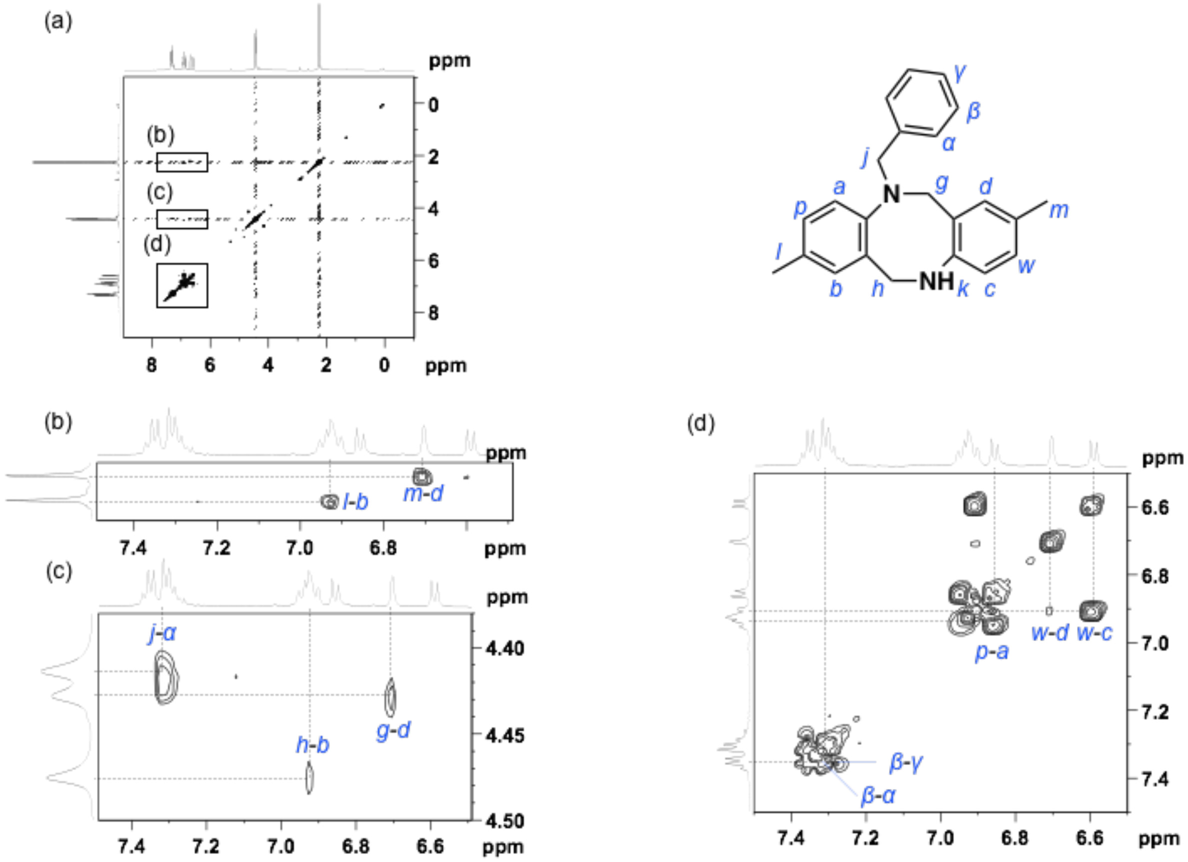

Fig. S31. H-H COSY correlations (500 MHz) of **2c** in $CDCl_3$ at 25 °C.

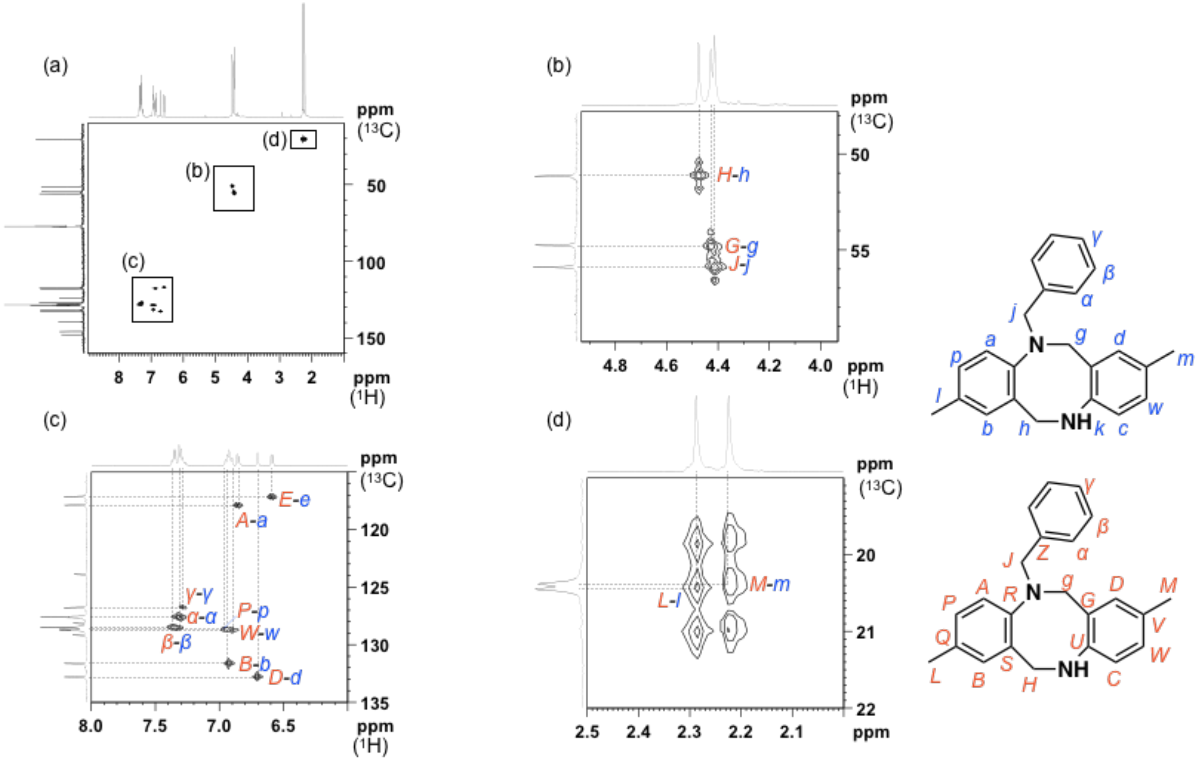

Fig. S32. HMQC correlations (^1H: 500 MHz, ^{13}C: 125 MHz) of **2c** in $CDCl_3$ at 25 °C.

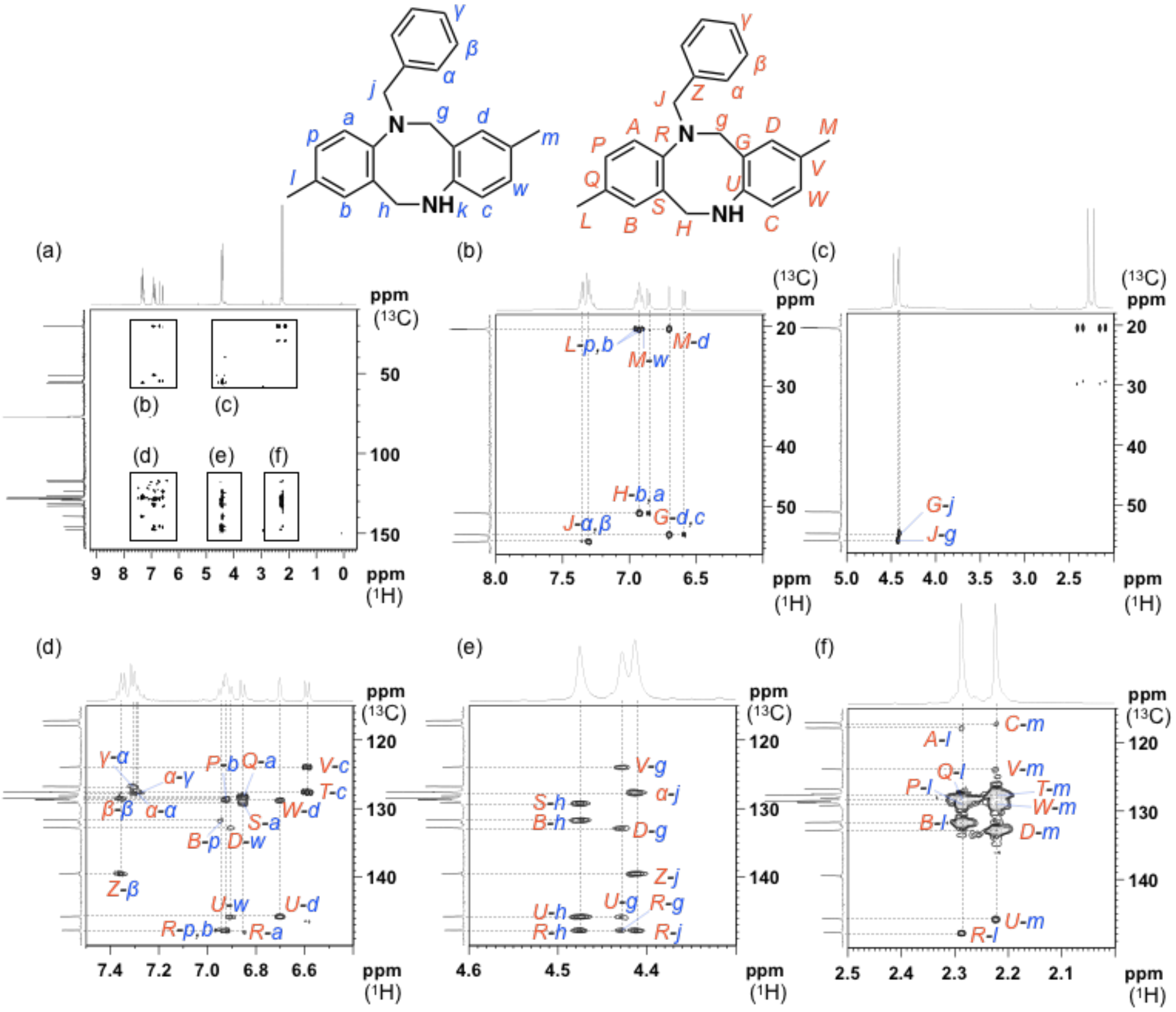

Fig. S33. HMBC correlations (^{1}H: 500 MHz, ^{13}C: 125 MHz) of **2c** in $CDCl_3$ at 25 °C.

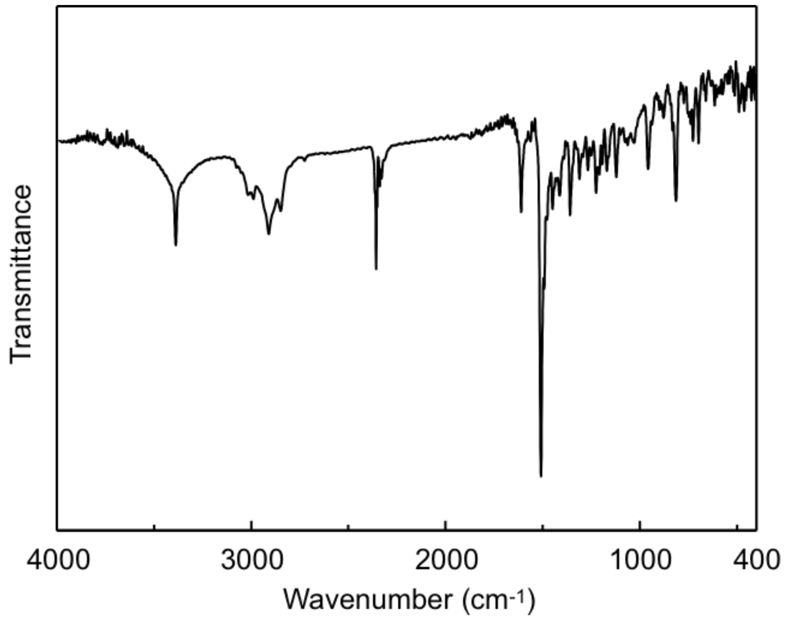

Fig. S34. FT-IR spectrum of **2c** at 25 °C (KBr).

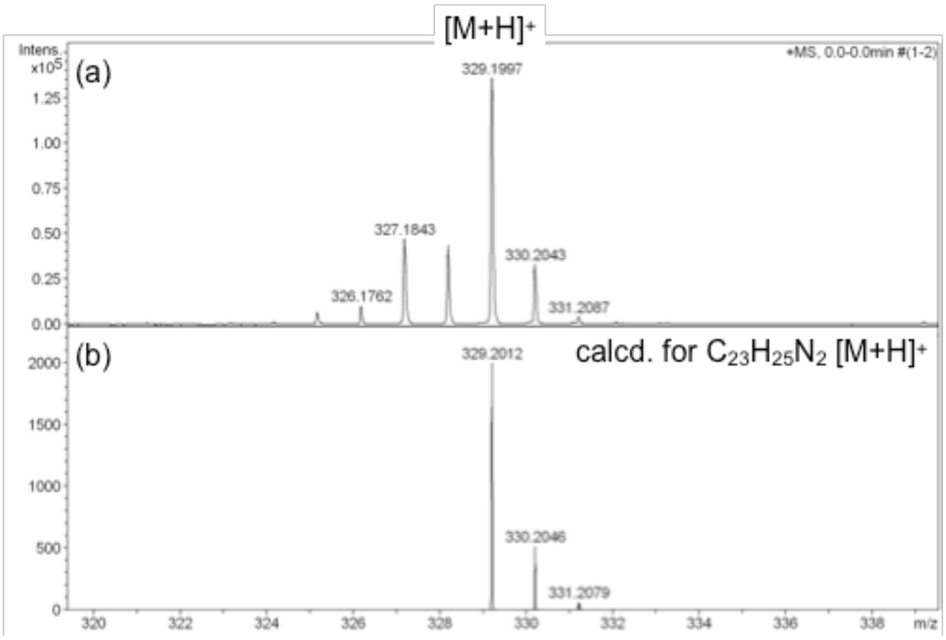

Fig. S35. (a) Observed and (b) simulated high-resolution APCI-TOF mass spectra of **2c**.

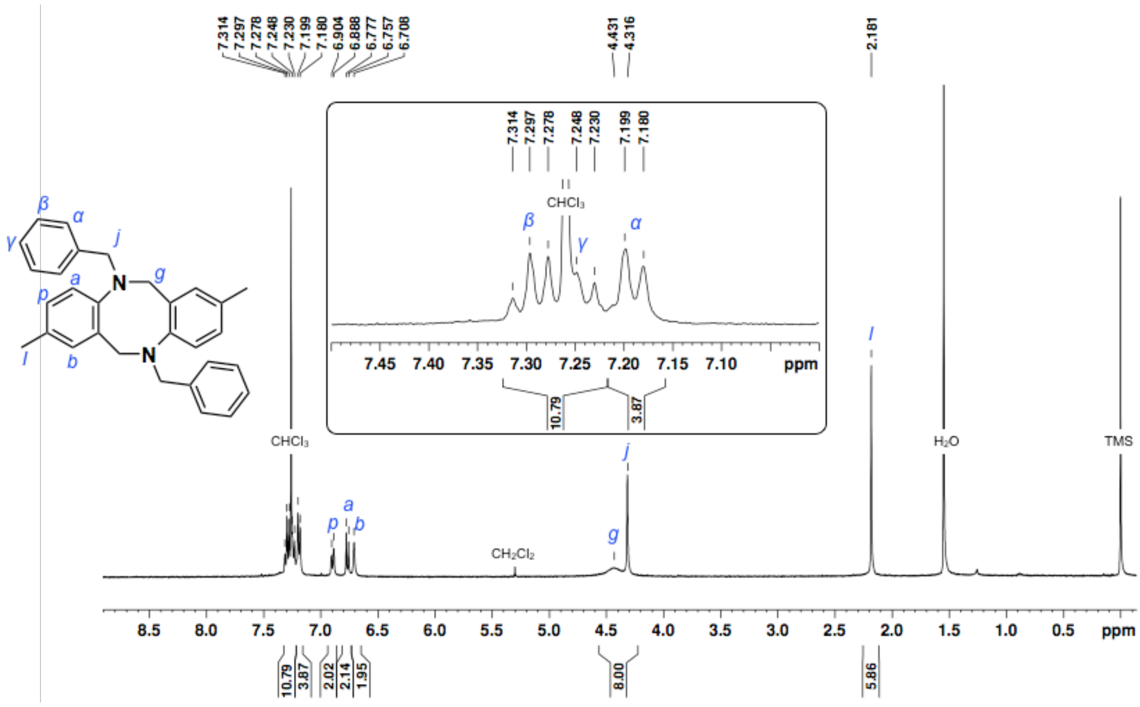

Fig. S36. ^{1}H NMR spectrum (500 MHz) of **3c** in $CDCl_3$ at 25 °C.

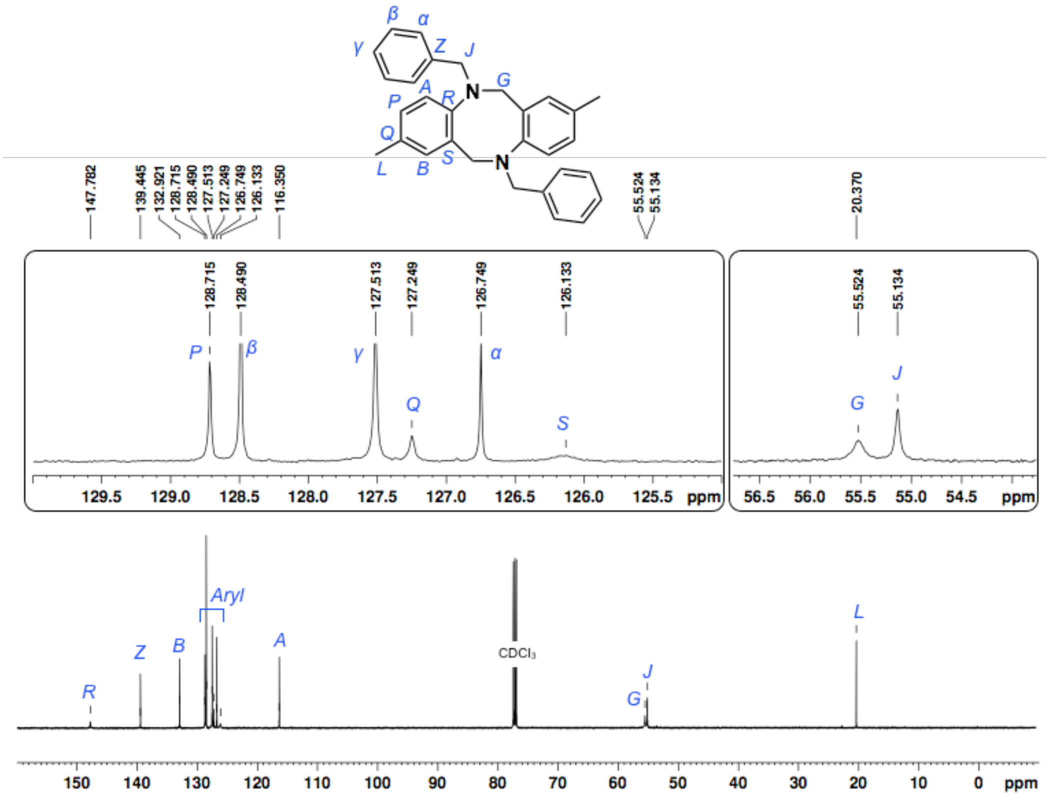

Fig. S37. ^{13}C NMR spectrum (125 MHz) of **3c** in $CDCl_3$ at 25 °C.

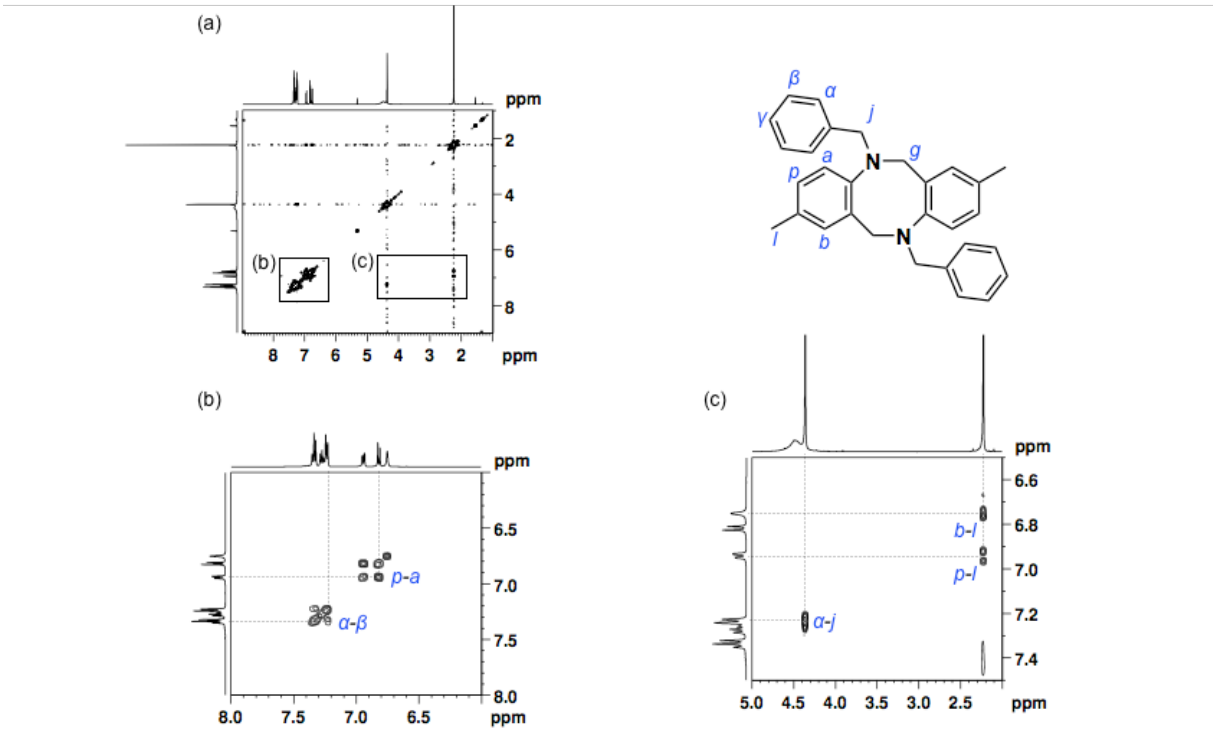

Fig. S38. H-H COSY correlations (500 MHz) of **3c** in $CDCl_3$ at 25 °C.

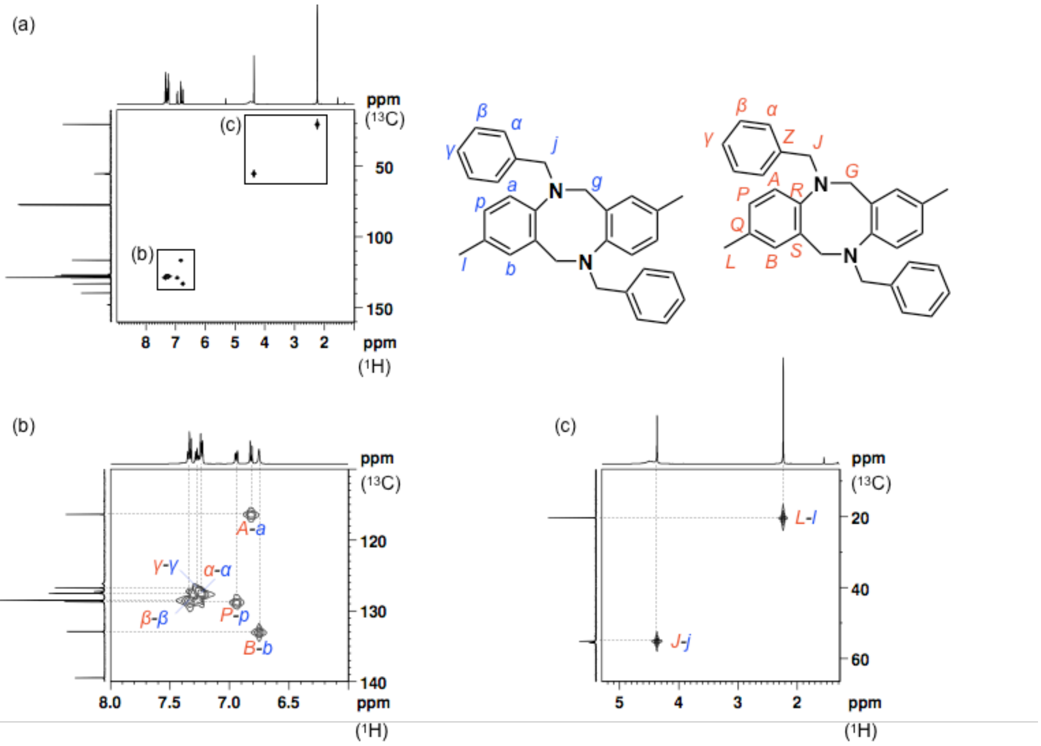

Fig. S39. HMQC correlations (^{1}H: 500 MHz, ^{13}C: 125 MHz) of **3c** in $CDCl_3$ at 25 °C.

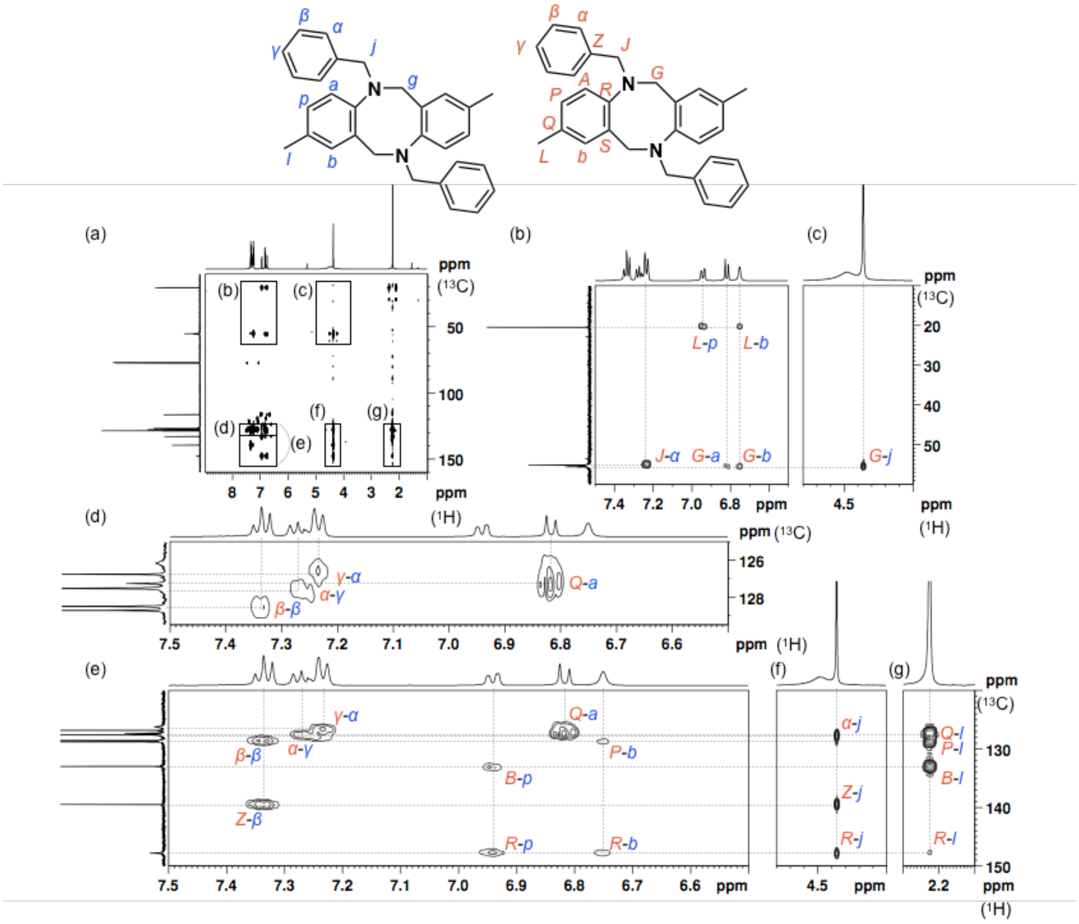

Fig. S40. HMBC correlations (^{1}H: 500 MHz, ^{13}C: 125 MHz) of **3c** in $CDCl_3$ at 25 °C.

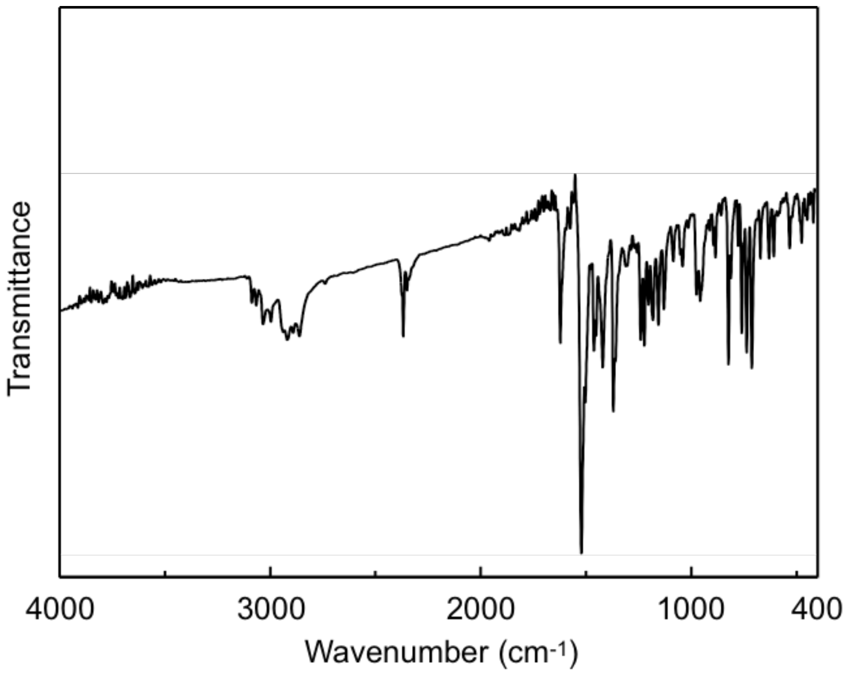

Fig. S41. FT-IR spectrum of **3c** at 25 °C (KBr).

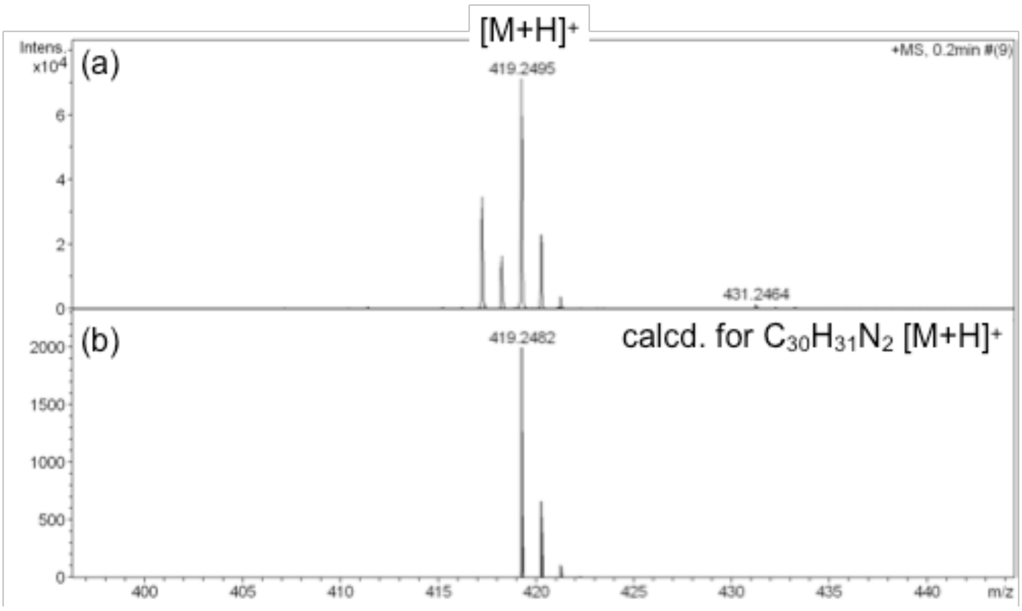

Fig. S42. (a) Observed and (b) simulated high-resolution APCI-TOF mass spectra of **3c**.

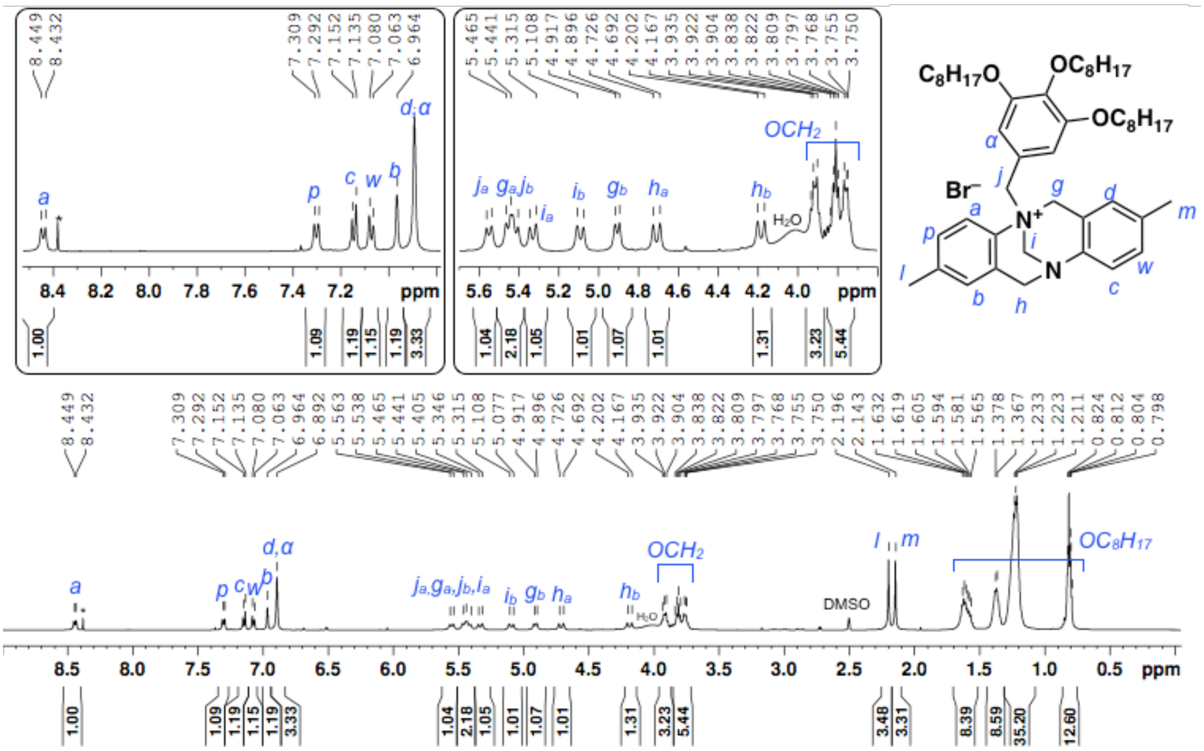

Fig. S43. ^{1}H NMR spectrum (500 MHz) of **1d** in DMSO-d_6 at 25 °C.

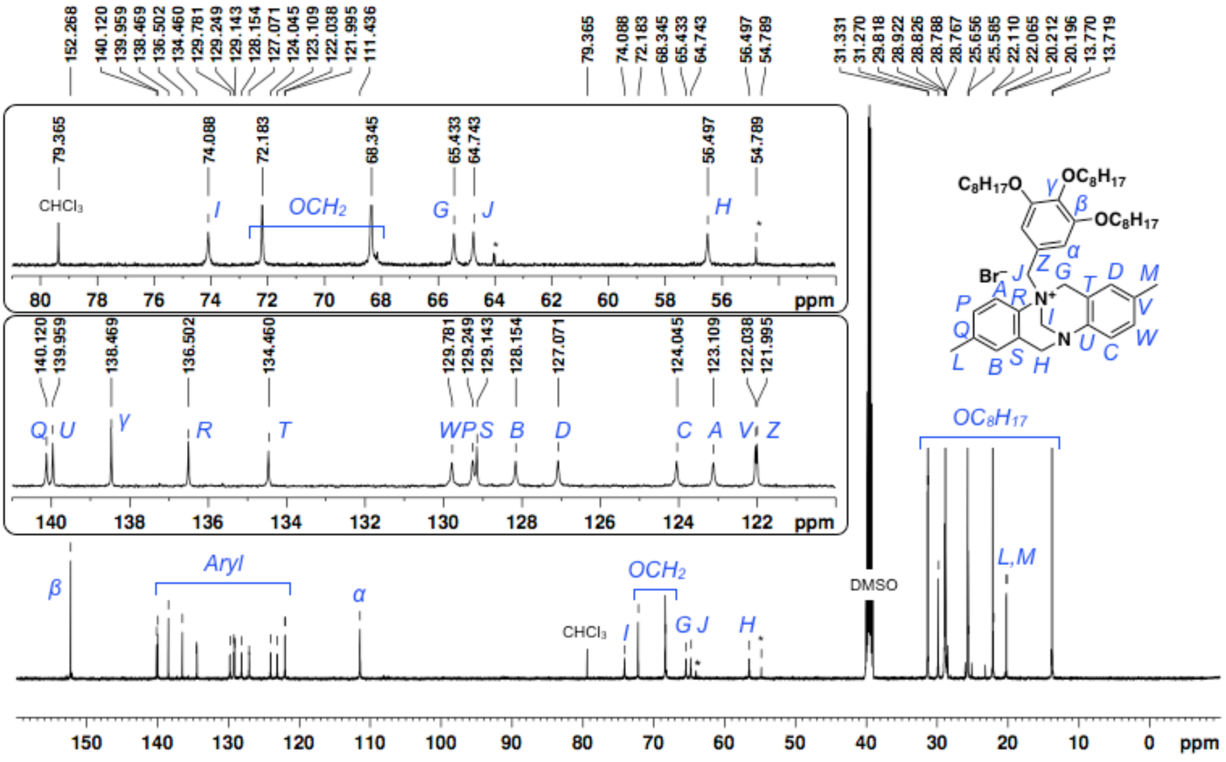

Fig. S44. ^{13}C NMR spectrum (500 MHz) of **1d** in DMSO-d_6 at 25 °C.

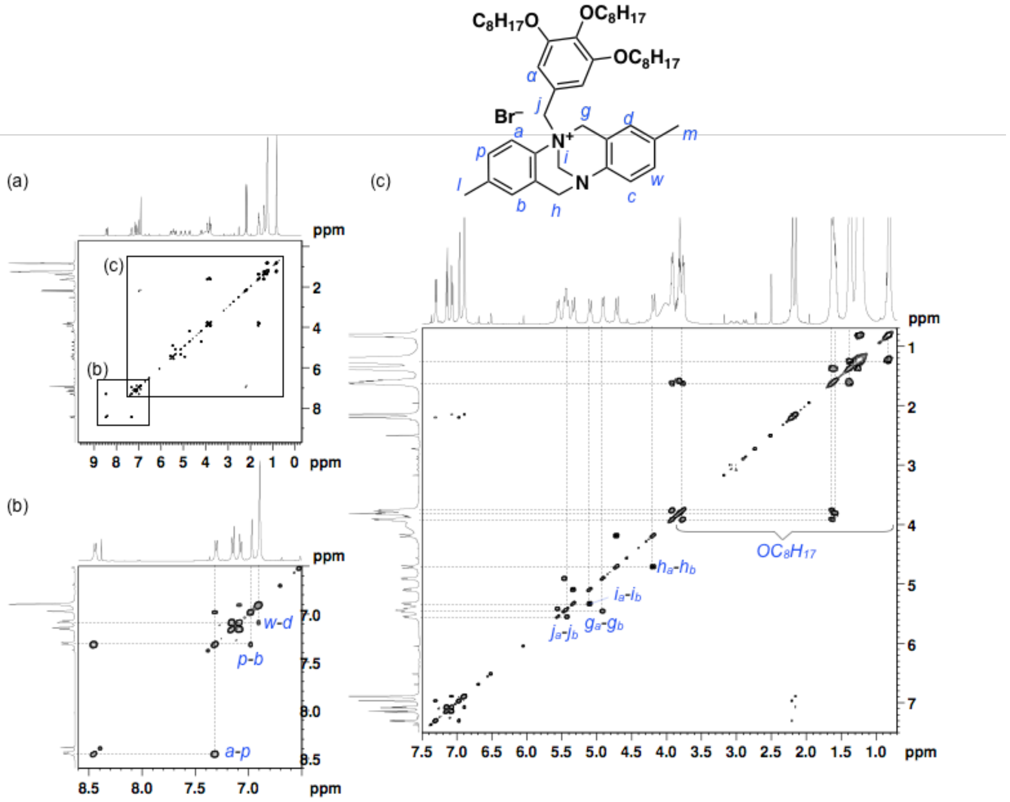

Fig. S45. H-H COSY correlations (^{1}H: 500 MHz, ^{13}C: 125 MHz) of **1d** in DMSO-d_6 at 25 °C.

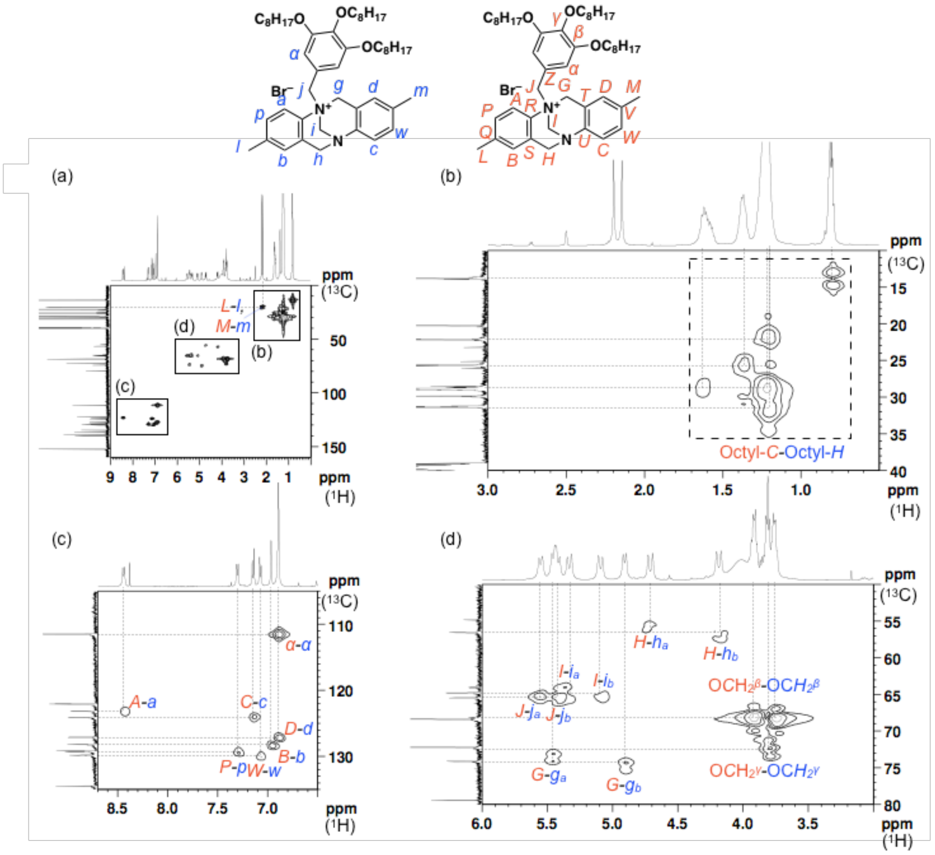

Fig. S46. HMQC correlations (^{1}H: 500 MHz, ^{13}C: 125 MHz) of **1d** in DMSO-d_6 at 25 °C.

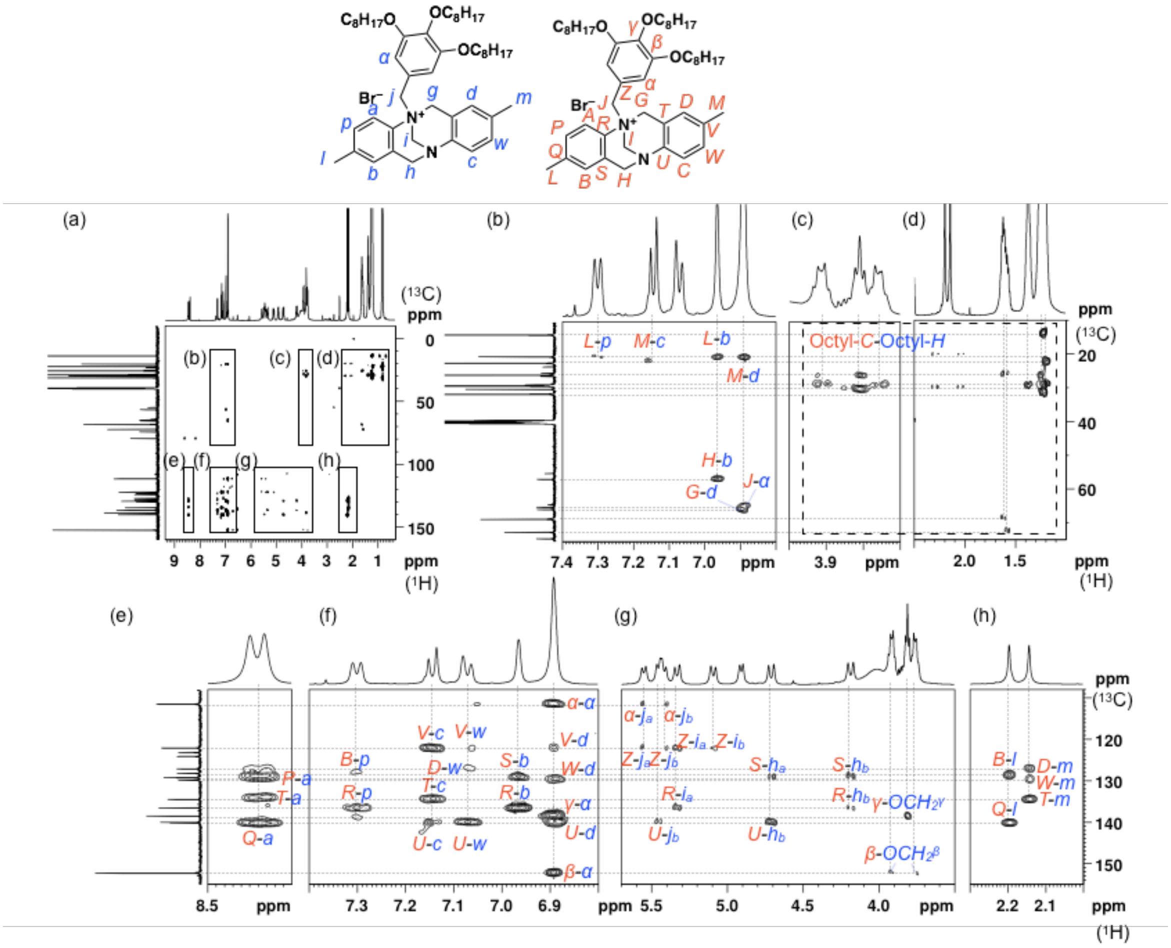

Fig. S47. HMBC correlations (^{1}H: 500 MHz, ^{13}C: 125 MHz) of **1d** in DMSO-d_6 at 25 °C.

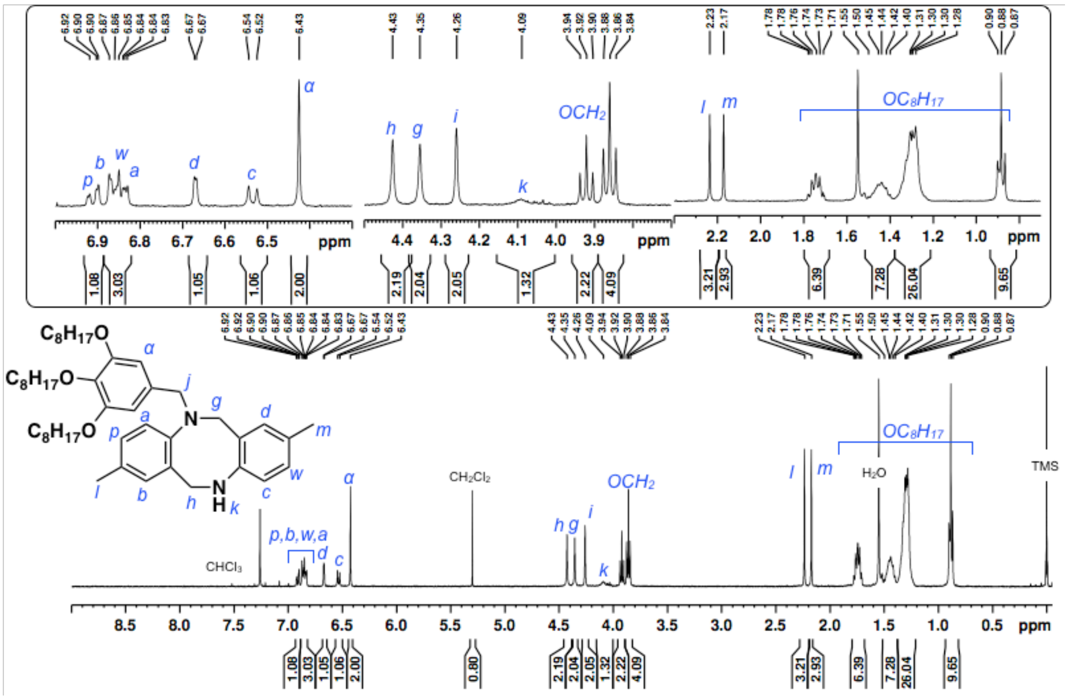

Fig. S48. ^{1}H NMR spectrum (500 MHz) of **2d** in $CDCl_3$ at 25 °C.

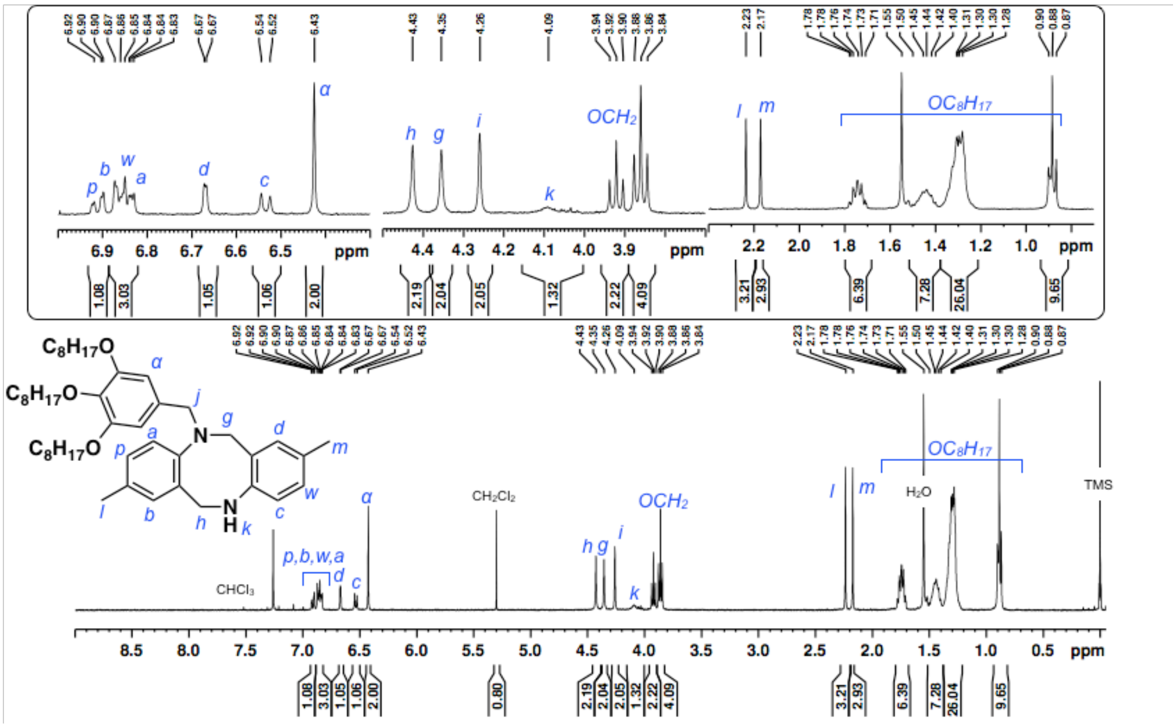

Fig. S49. ^{13}C NMR spectrum (125 MHz) of **2d** in $CDCl_3$ at 25 °C.

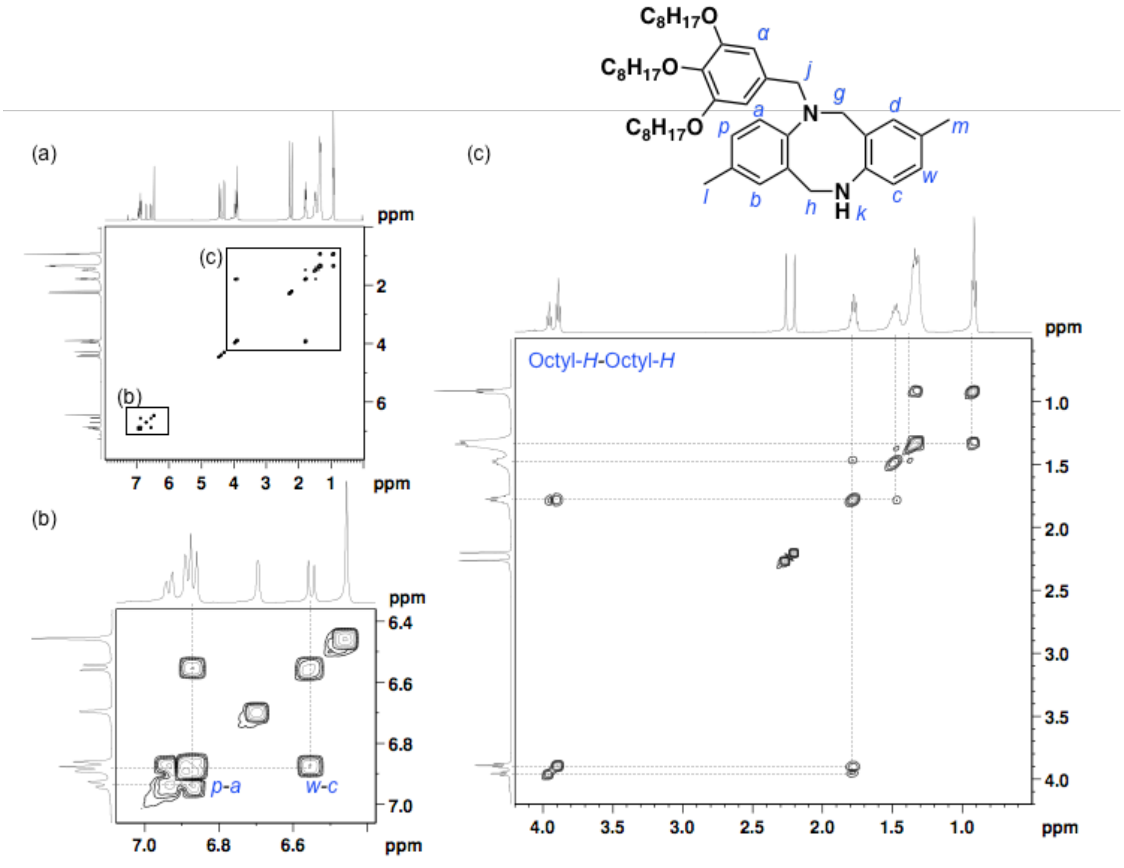

Fig. S50. H-H COSY correlations (500 MHz) of **2d** in $CDCl_3$ at 25 °C.

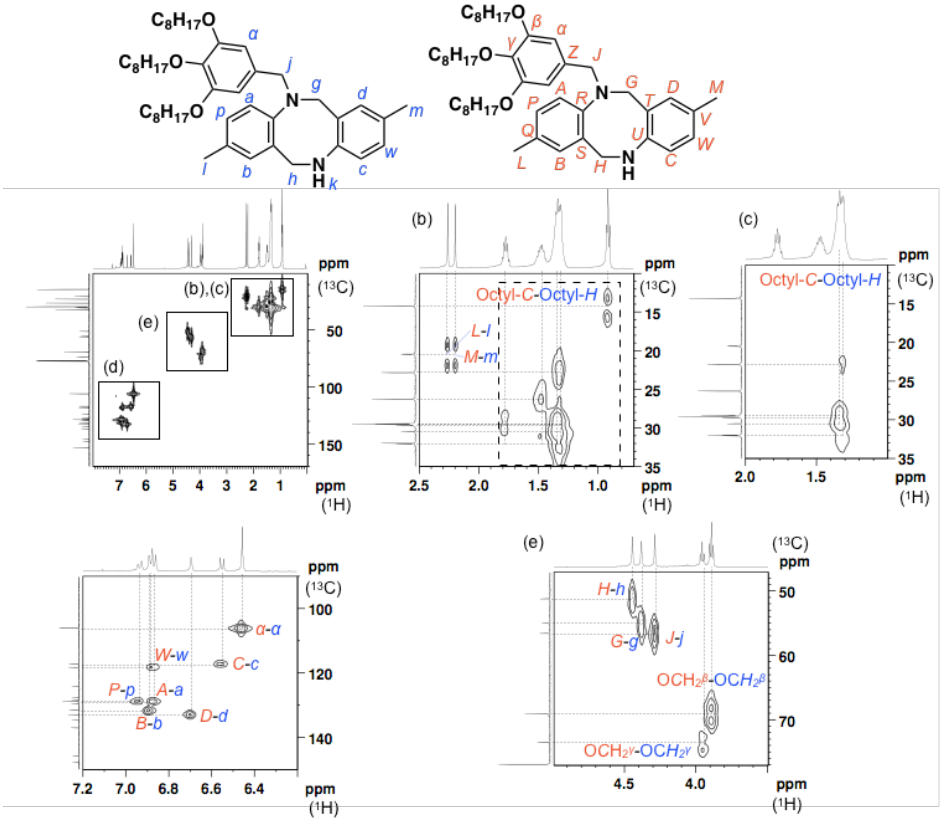

Fig. S51. HMQC correlations (^{1}H: 500 MHz, ^{13}C: 125 MHz) of **2d** in $CDCl_3$ at 25 °C.

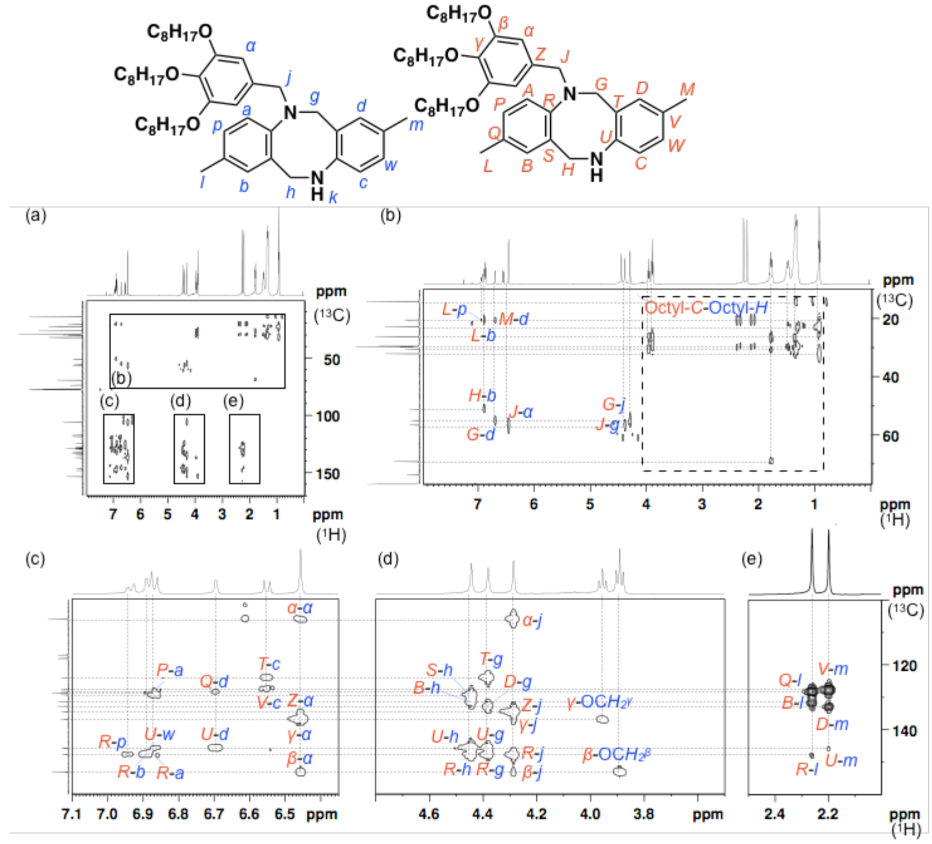

Fig. S52. HMBC correlations (^{1}H: 500 MHz, ^{13}C: 125 MHz) of **2d** in $CDCl_3$ at 25 °C.

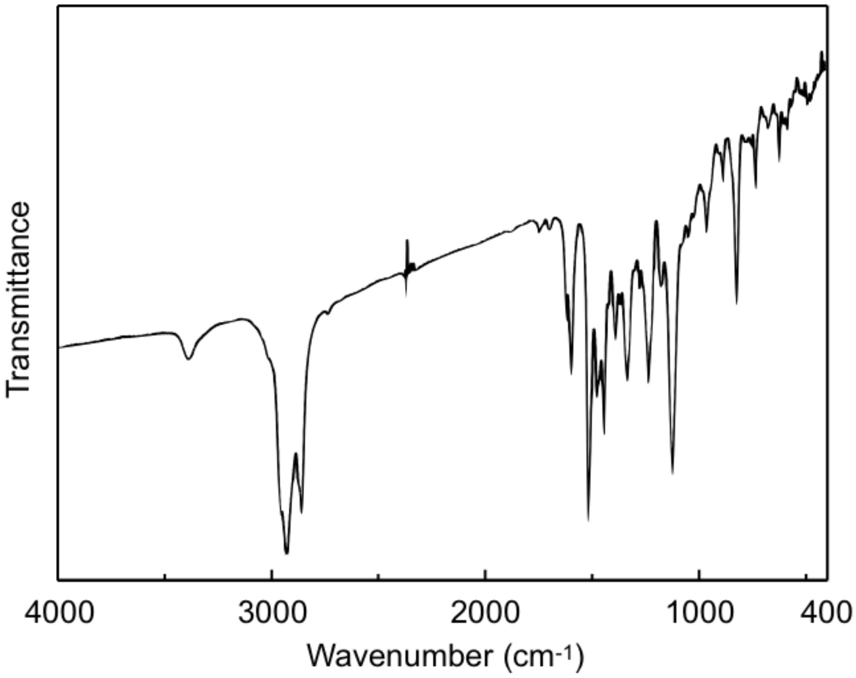

Fig. S53. FT-IR spectrum of **2d** at 25 °C (KBr).

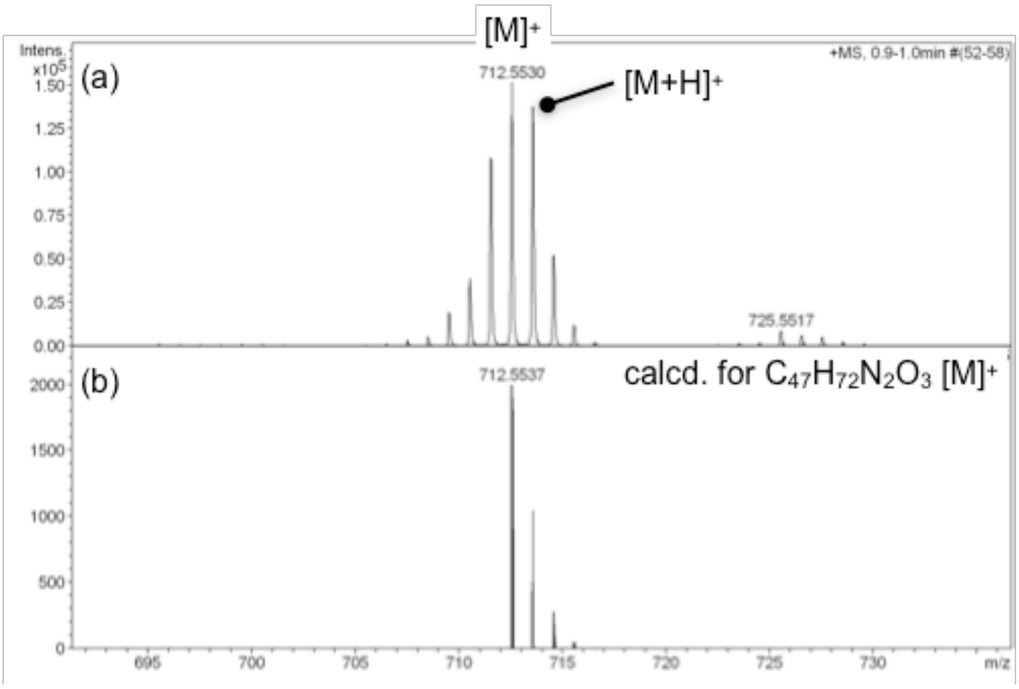

Fig. S54. (a) Observed and (b) simulated high-resolution APCI-TOF mass spectra of **2d**.

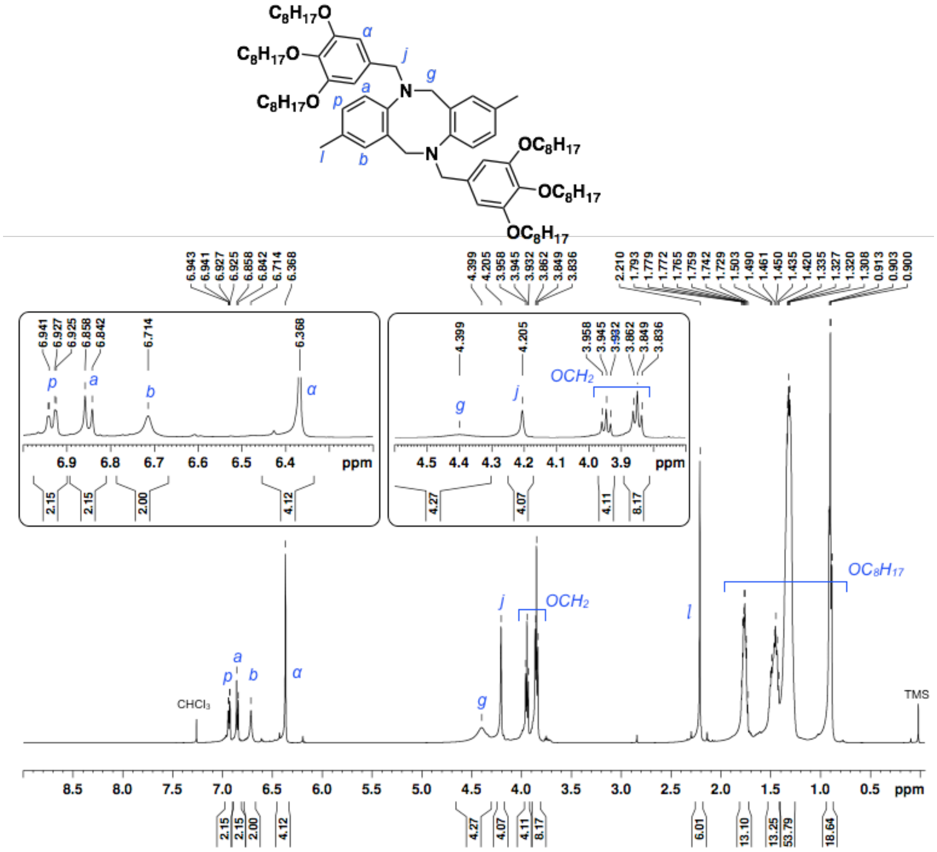

Fig. S55. ^{1}H NMR spectrum (500 MHz) of **3d** in $CDCl_3$ at 25 °C.

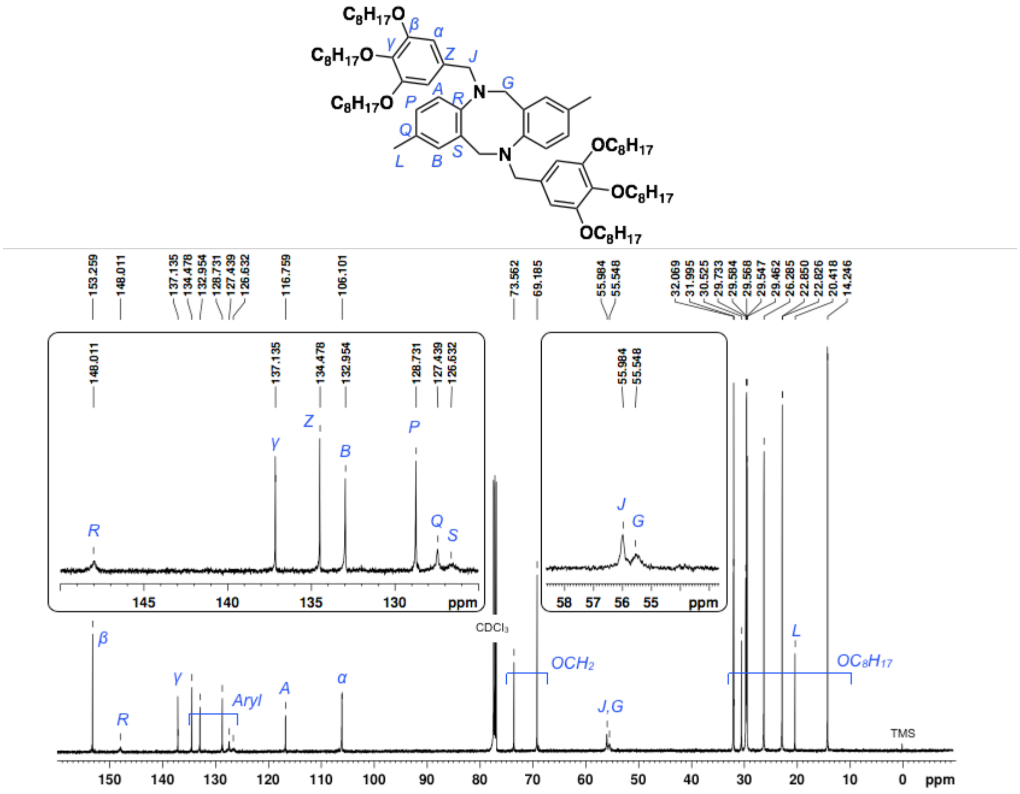

Fig. S56. ^{13}C NMR spectrum (125 MHz) of **3d** in $CDCl_3$ at 25 °C.

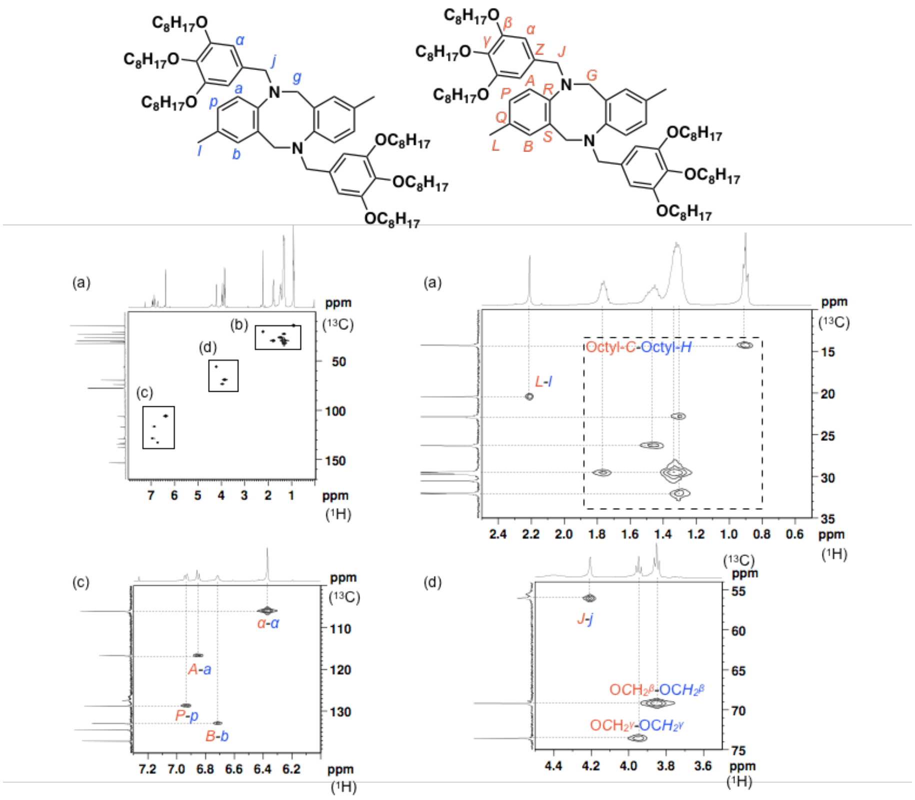

Fig. S57. HMQC correlations (^{1}H: 500 MHz, ^{13}C: 125 MHz) of **3d** in $\mathrm{CDCl_3}$ at 25 °C.

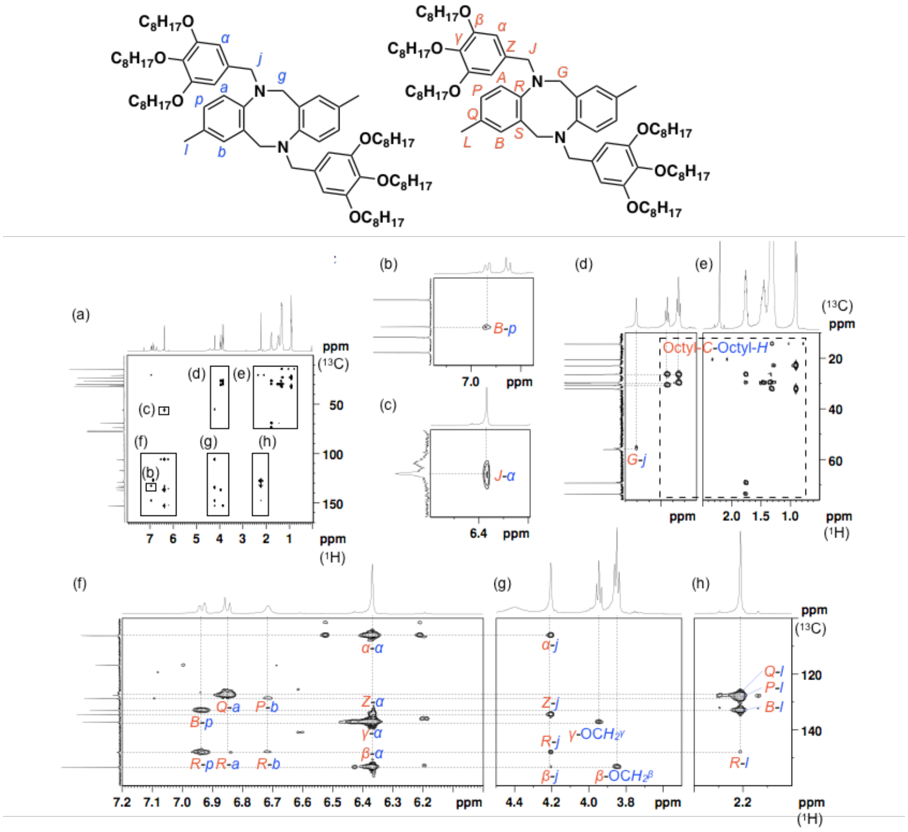

Fig. S58. HMBC correlations (^{1}H: 500 MHz, ^{13}C: 125 MHz) of **3d** in $\mathrm{CDCl_3}$ at 25 °C.

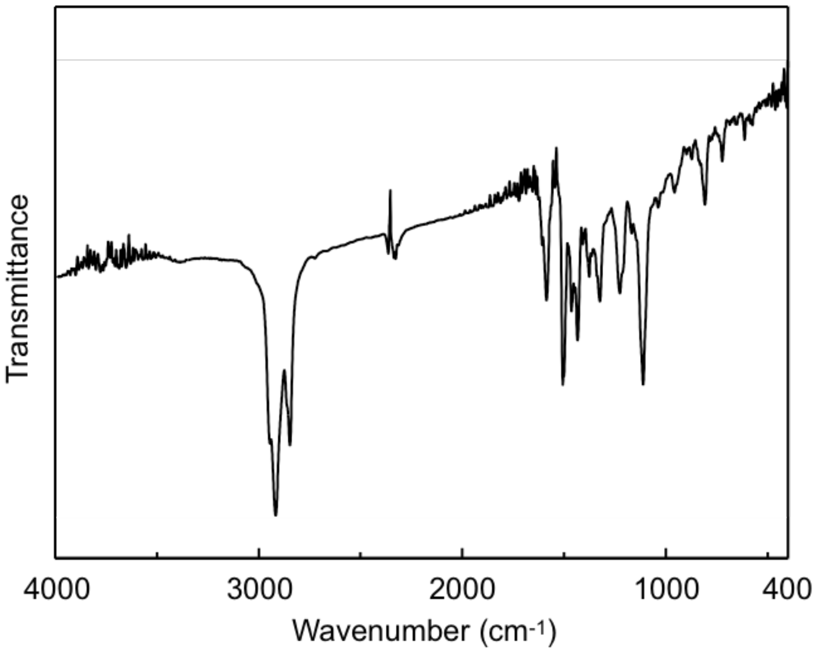

Fig. S59. FT-IR spectrum of **3d** at 25 °C (KBr).

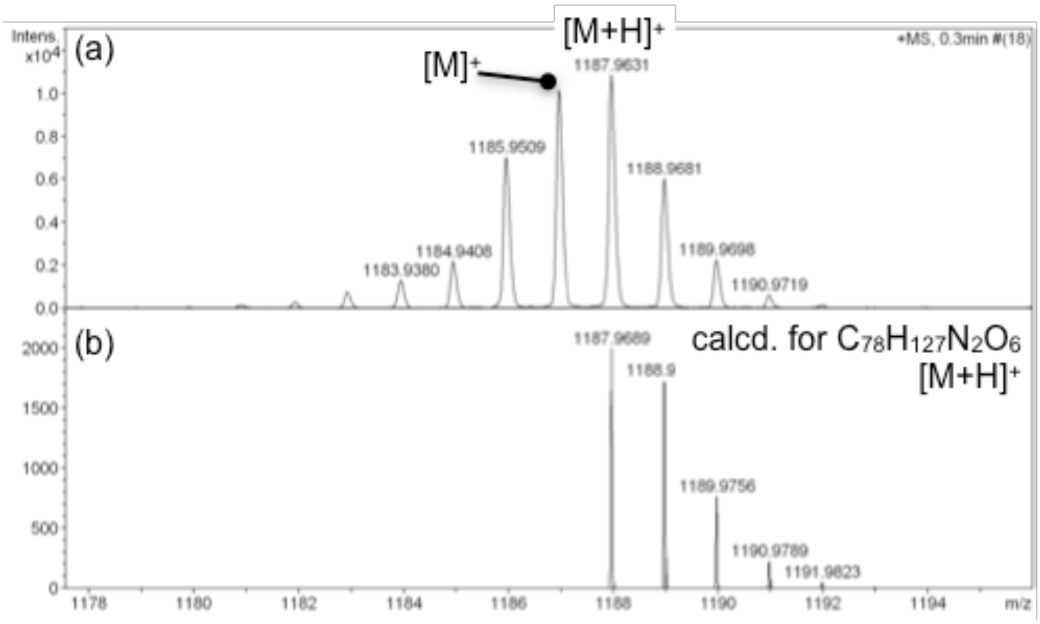

Fig. S60. (a) Observed and (b) simulated high-resolution APCI-TOF mass spectra of **3d**.

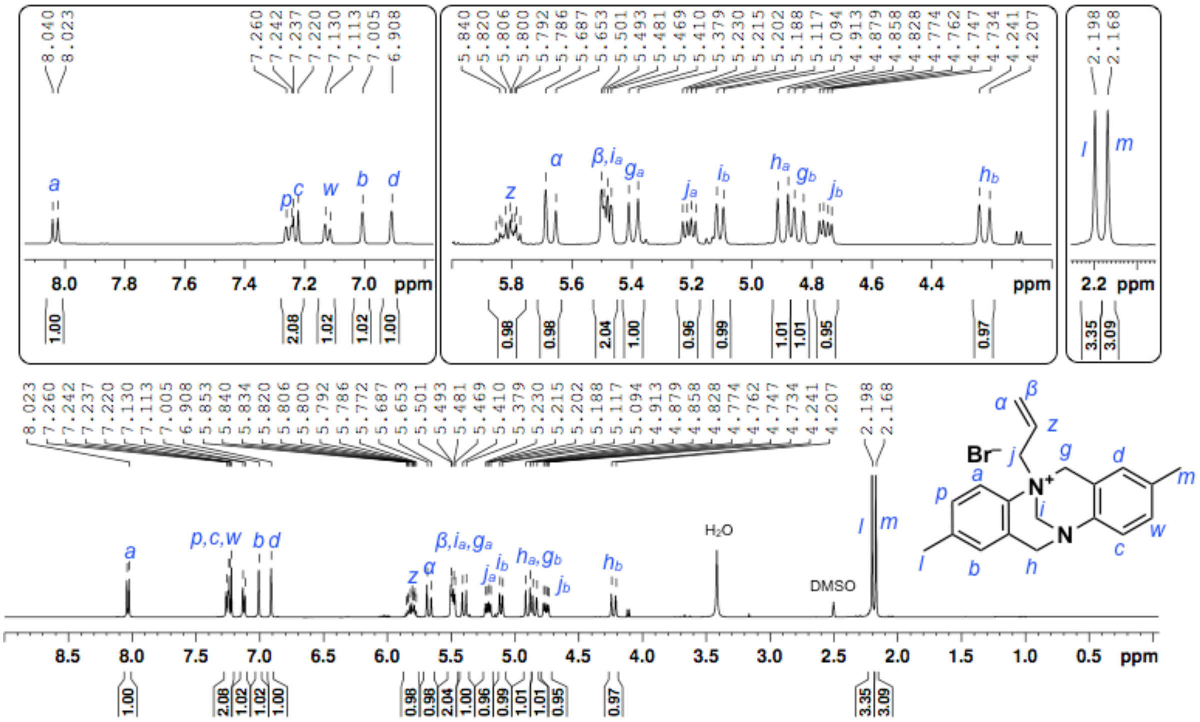

Fig. S61. ^{1}H NMR spectrum (500 MHz) of **1e** in DMSO-d_6 at 25 °C.

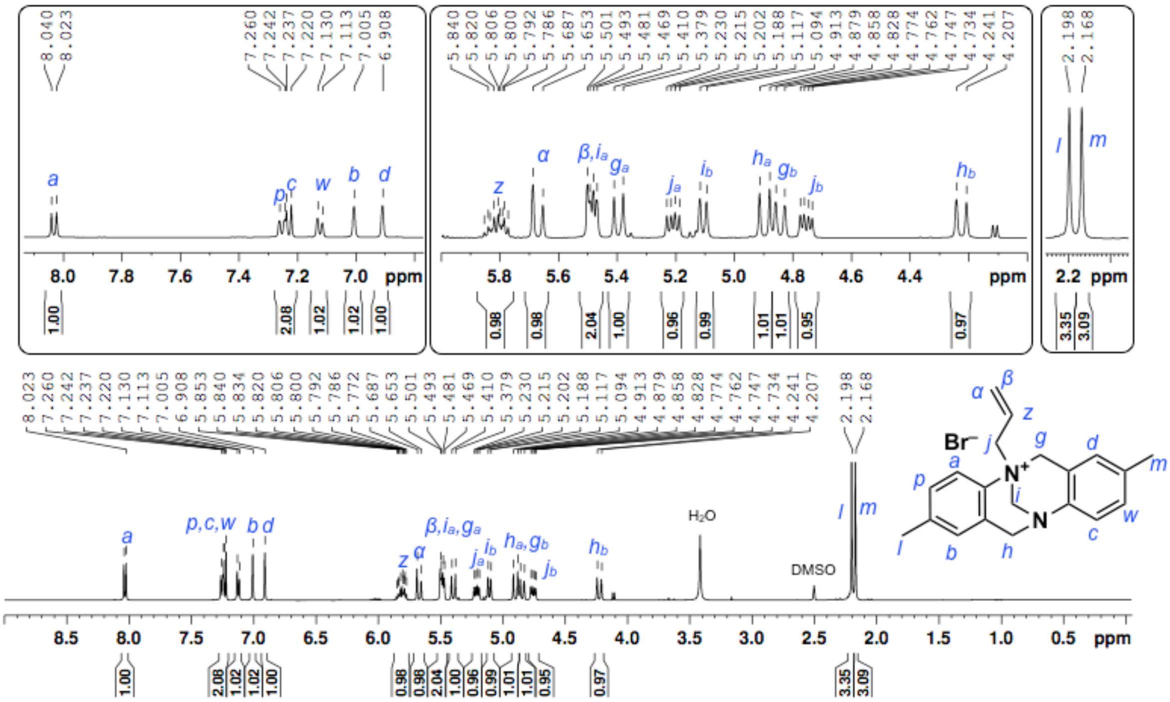

Fig. S62. ^{13}C NMR spectrum (125 MHz) of **1e** in DMSO-d_6 at 25 °C.

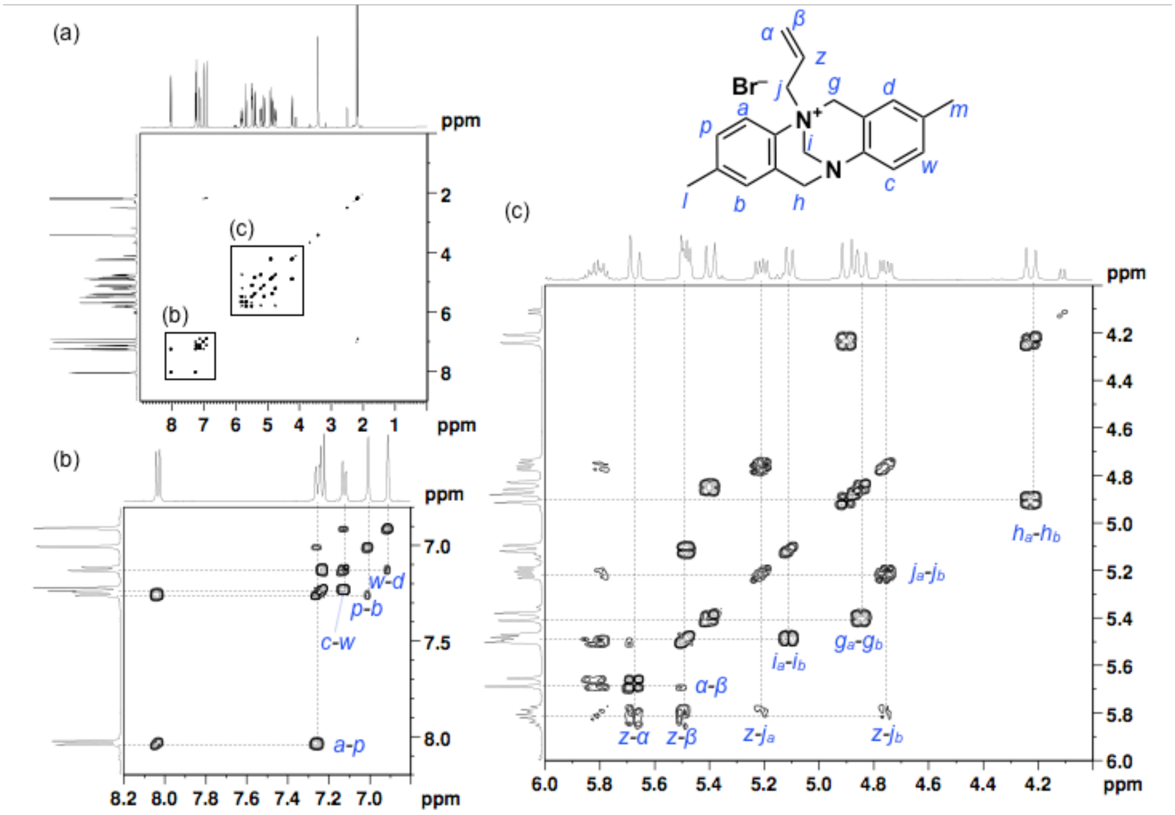

Fig. S63. H-H COSY correlations (500 MHz) of **1e** in DMSO-d_6 at 25 °C.

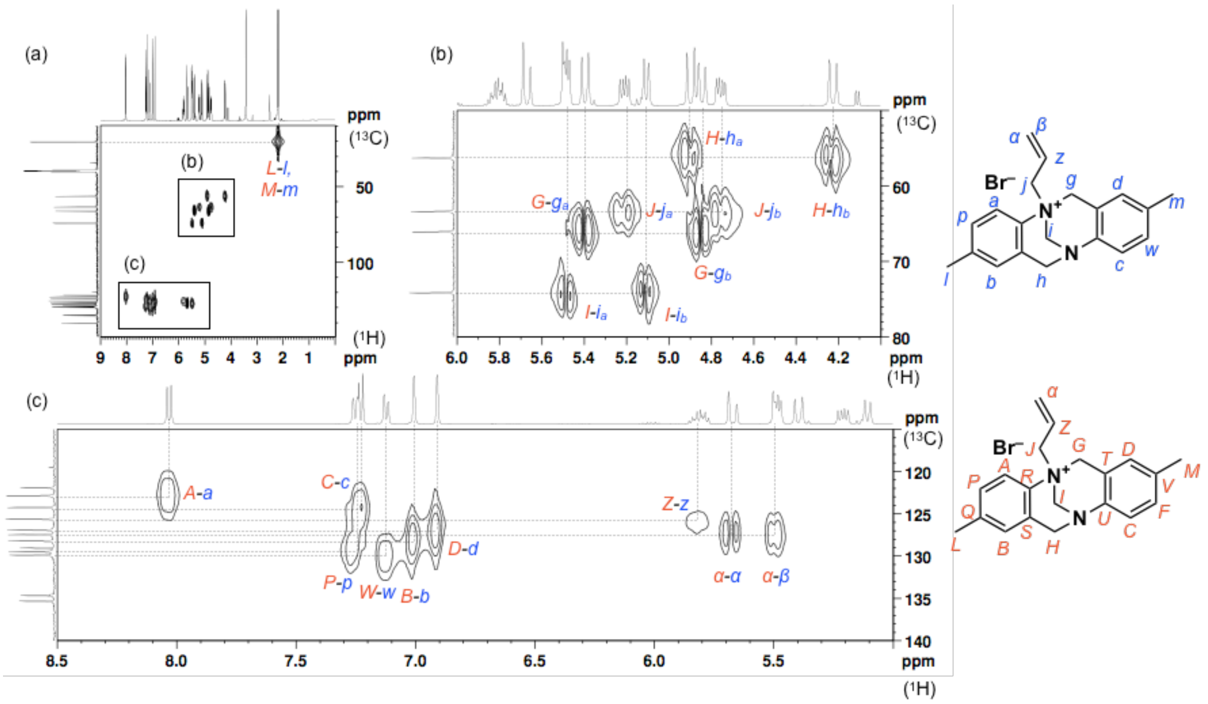

Fig. S64. HMQC correlations (^{1}H: 500 MHz, ^{13}C: 125 MHz) of **1e** in DMSO-d_6 at 25 °C.

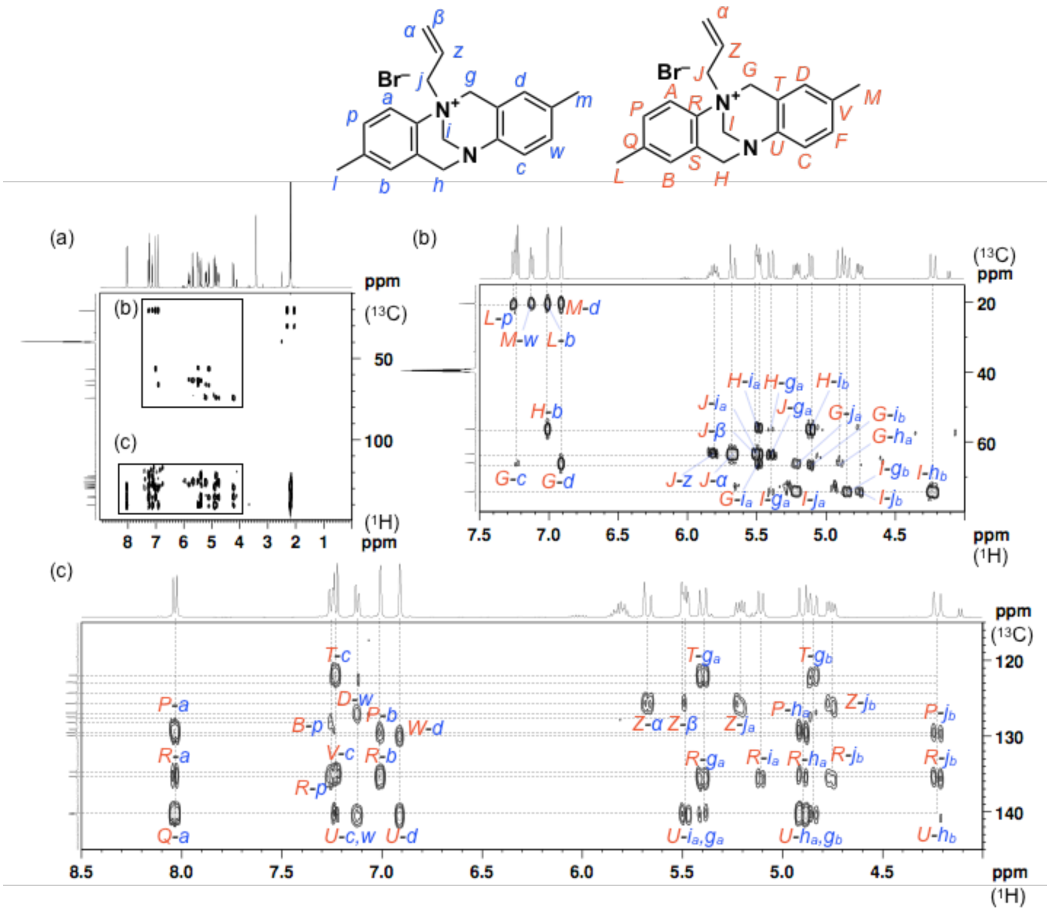

Fig. S65. HMBC correlations (^{1}H: 500 MHz, ^{13}C: 125 MHz) of **1e** in DMSO-d_6 at 25 °C.

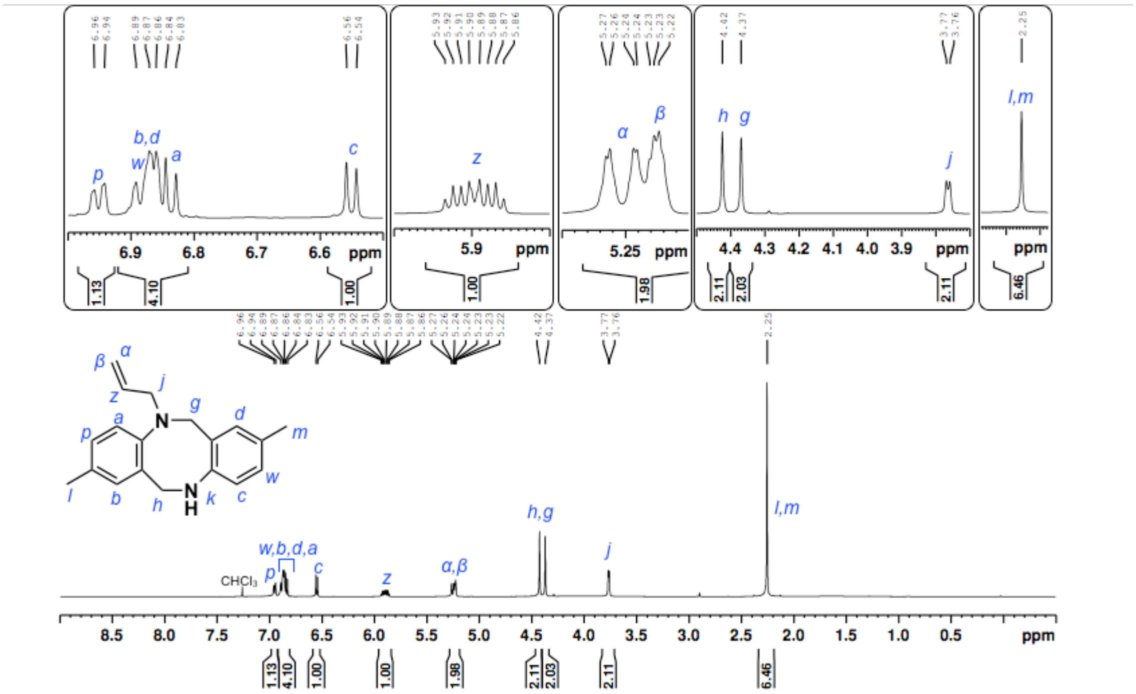

Fig. S66. ^{1}H NMR spectrum (500 MHz) of **2e** in CDCl$_3$ at 25 °C.

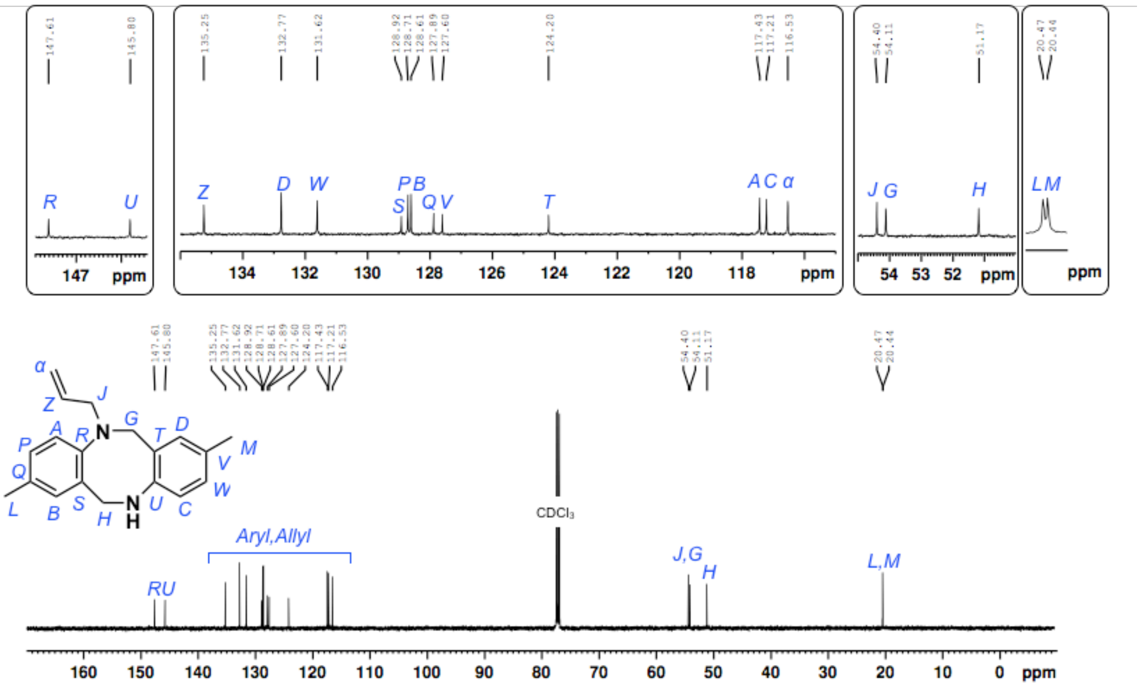

Fig. S67. ^{13}C NMR spectrum (125 MHz) of **2e** in $CDCl_3$ at 25 °C.

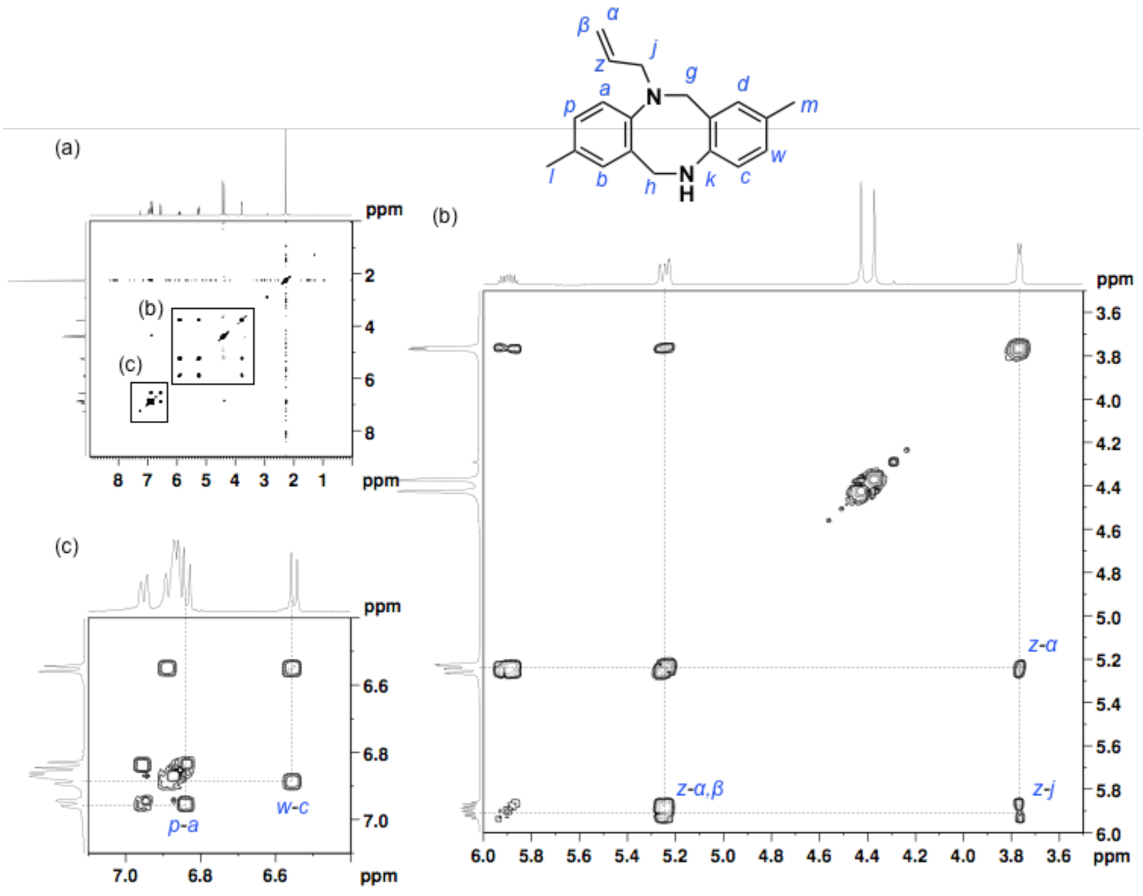

Fig. S68. H-H COSY correlations (500 MHz) of **2e** in $CDCl_3$ at 25 °C.

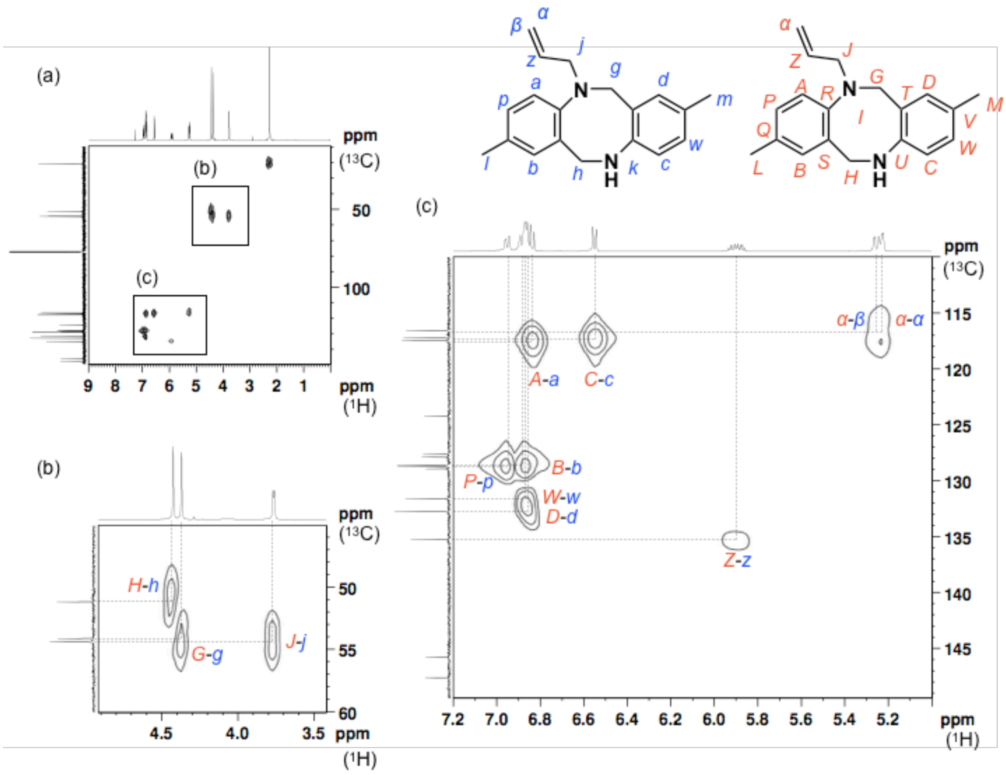

Fig. S69. HMQC correlations (^{1}H: 500 MHz, ^{13}C: 125 MHz) of **2e** in CDCl$_3$ at 25 °C.

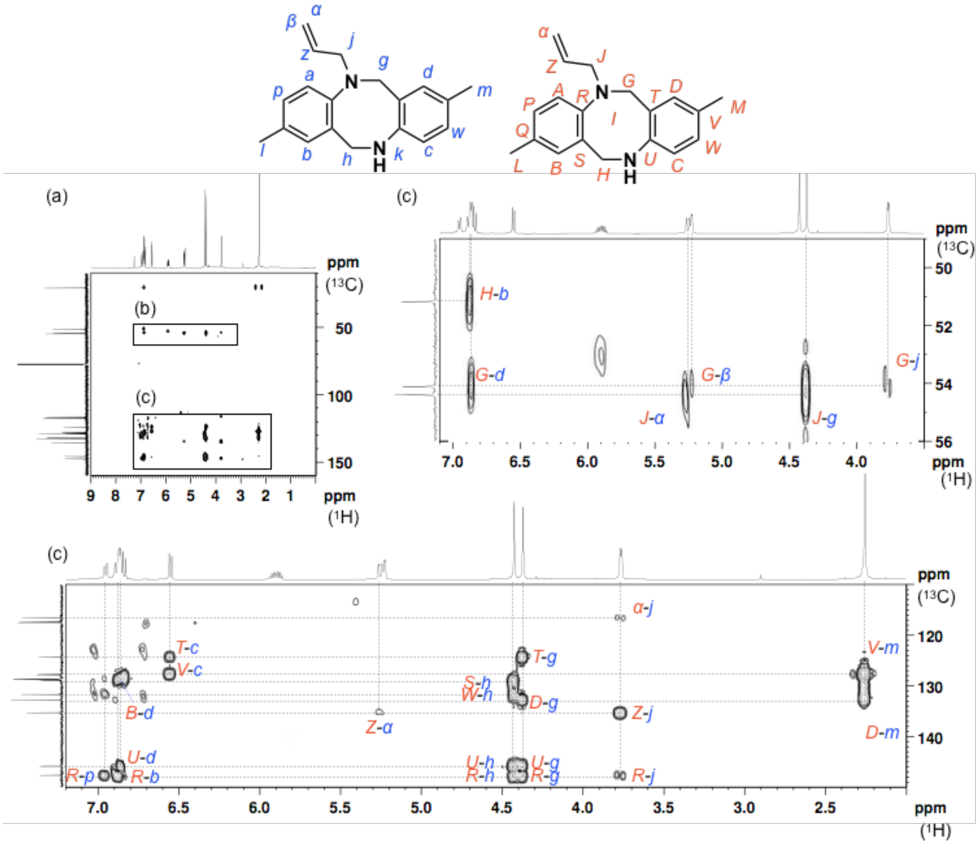

Fig. S70. HMBC correlations (^{1}H: 500 MHz, ^{13}C: 125 MHz) of **2e** in CDCl$_3$ at 25 °C.

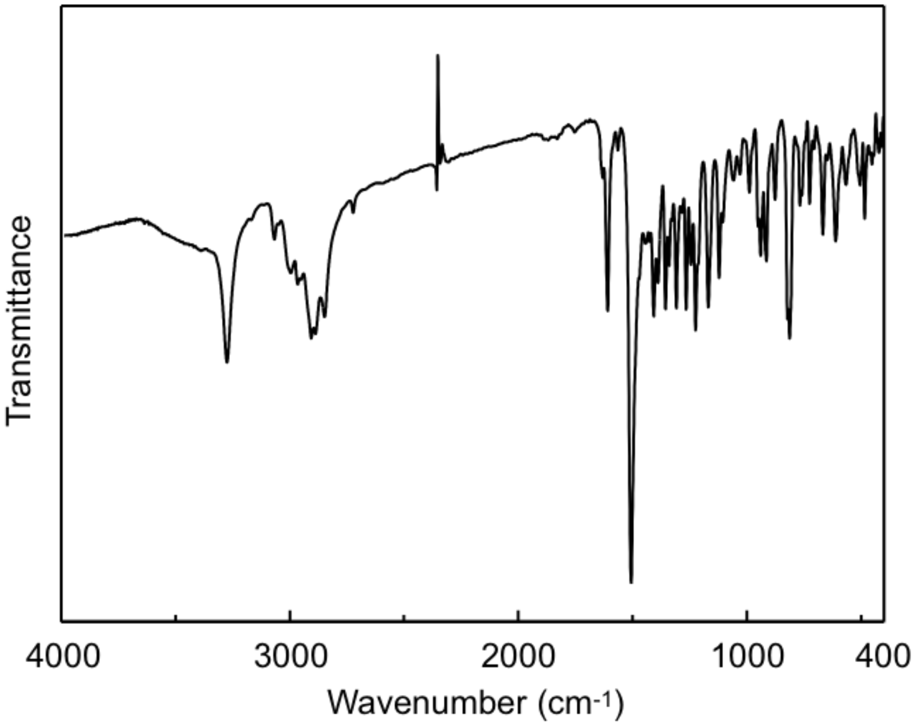

Fig. S71. FT-IR spectrum of **2e** at 25 °C (KBr).

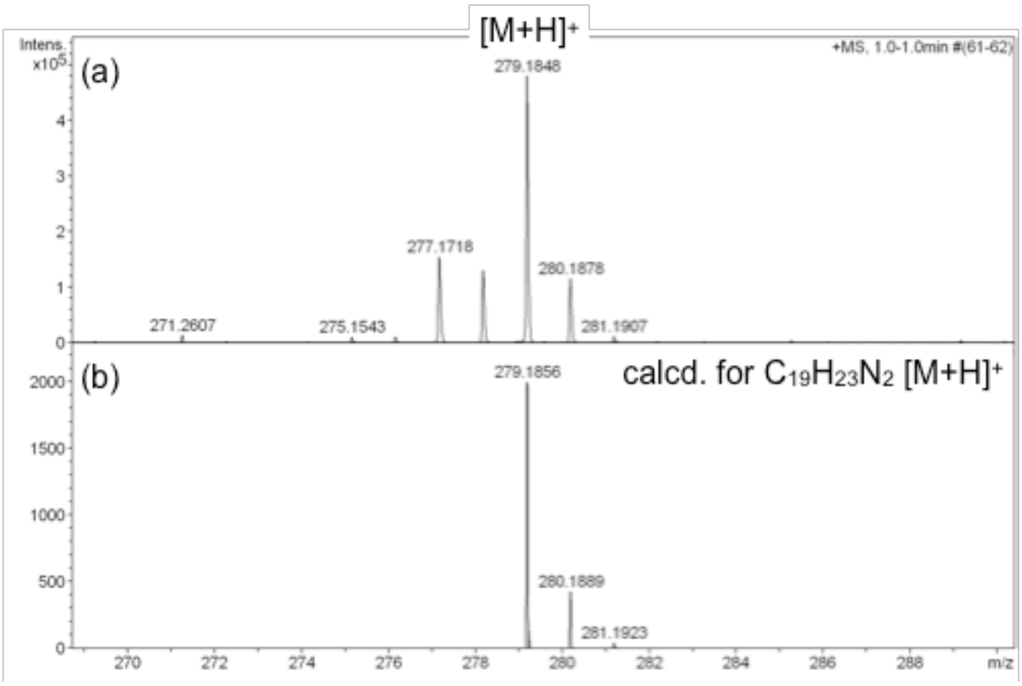

Fig. S72. (a) Observed and (b) simulated high-resolution APCI-TOF mass spectra of **2e**.

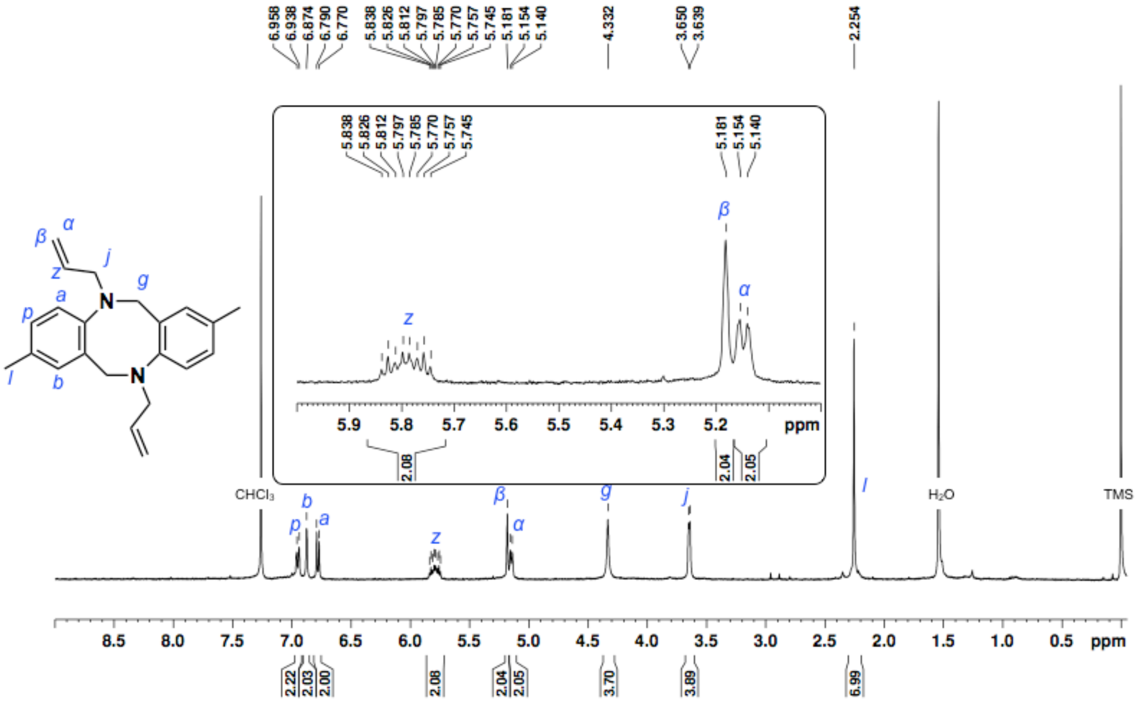

Fig. S73. ^{1}H NMR spectrum (500 MHz) of **3e** in CDCl$_3$ at 25 °C.

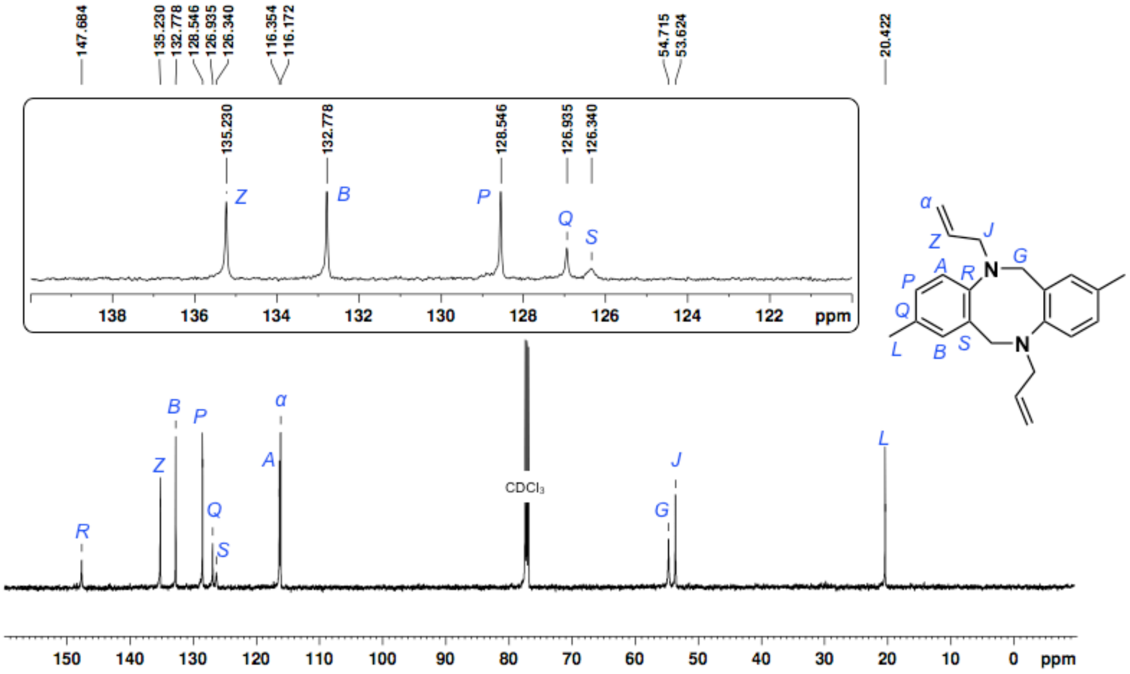

Fig. S74. ^{13}C NMR spectrum (125 MHz) of **3e** in CDCl$_3$ at 25 °C.

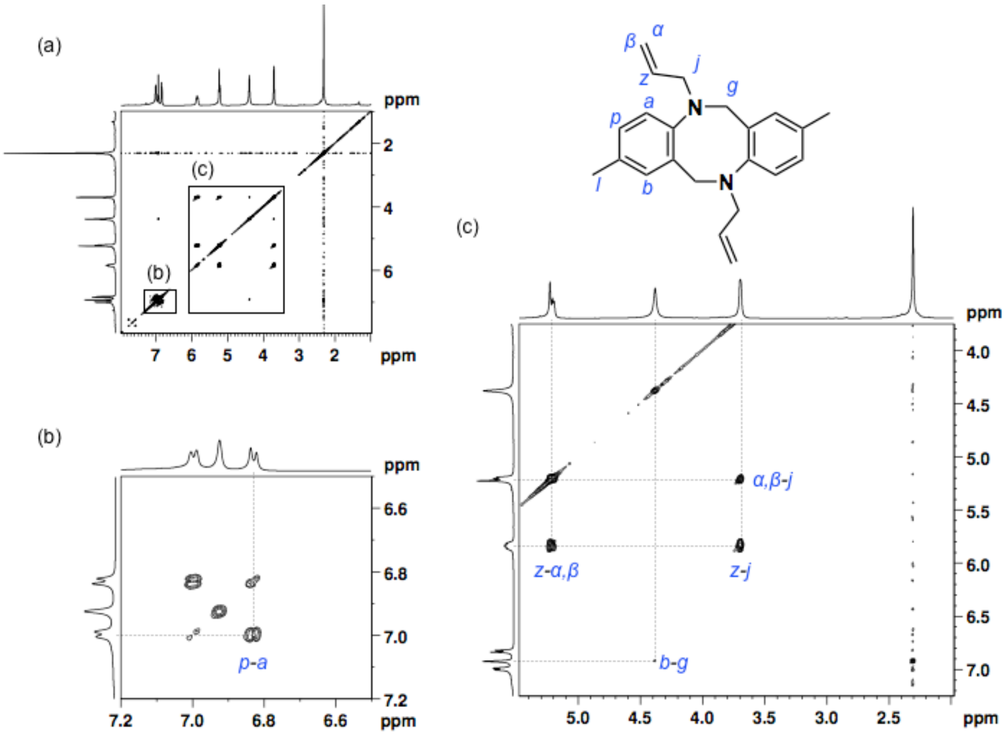

Fig. S75. H-H COSY correlations (500 MHz) of **3e** in $CDCl_3$ at 25 °C.

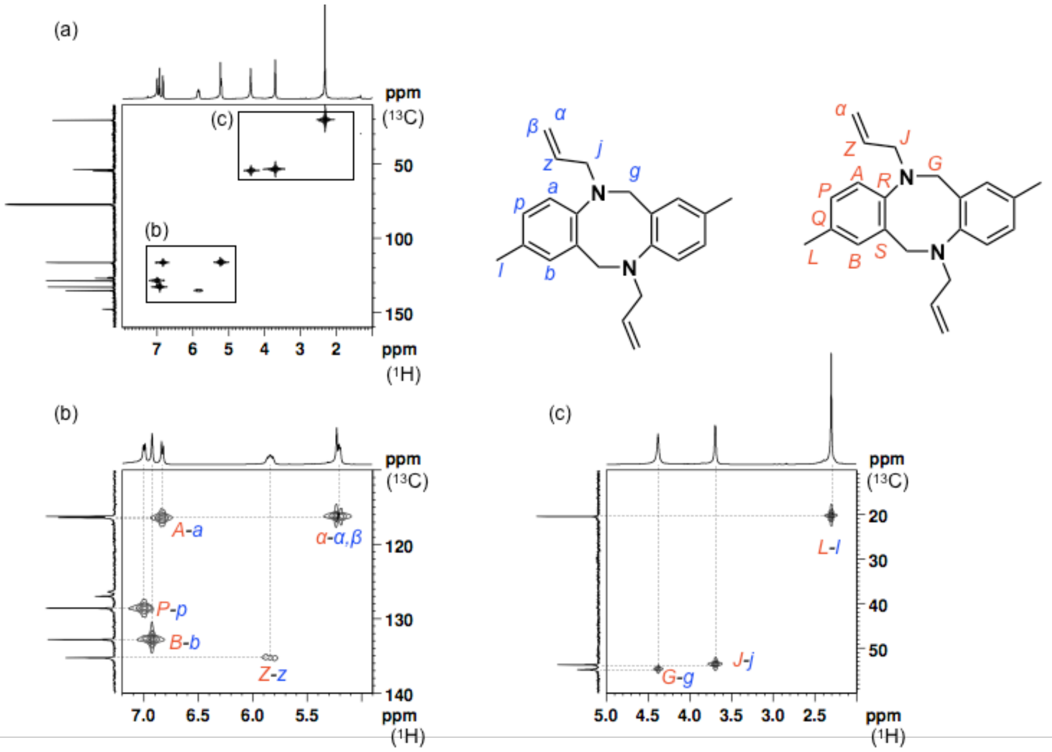

Fig. S76. HMQC correlations (^{1}H: 500 MHz, ^{13}C: 125 MHz) of **3e** in $CDCl_3$ at 25 °C.

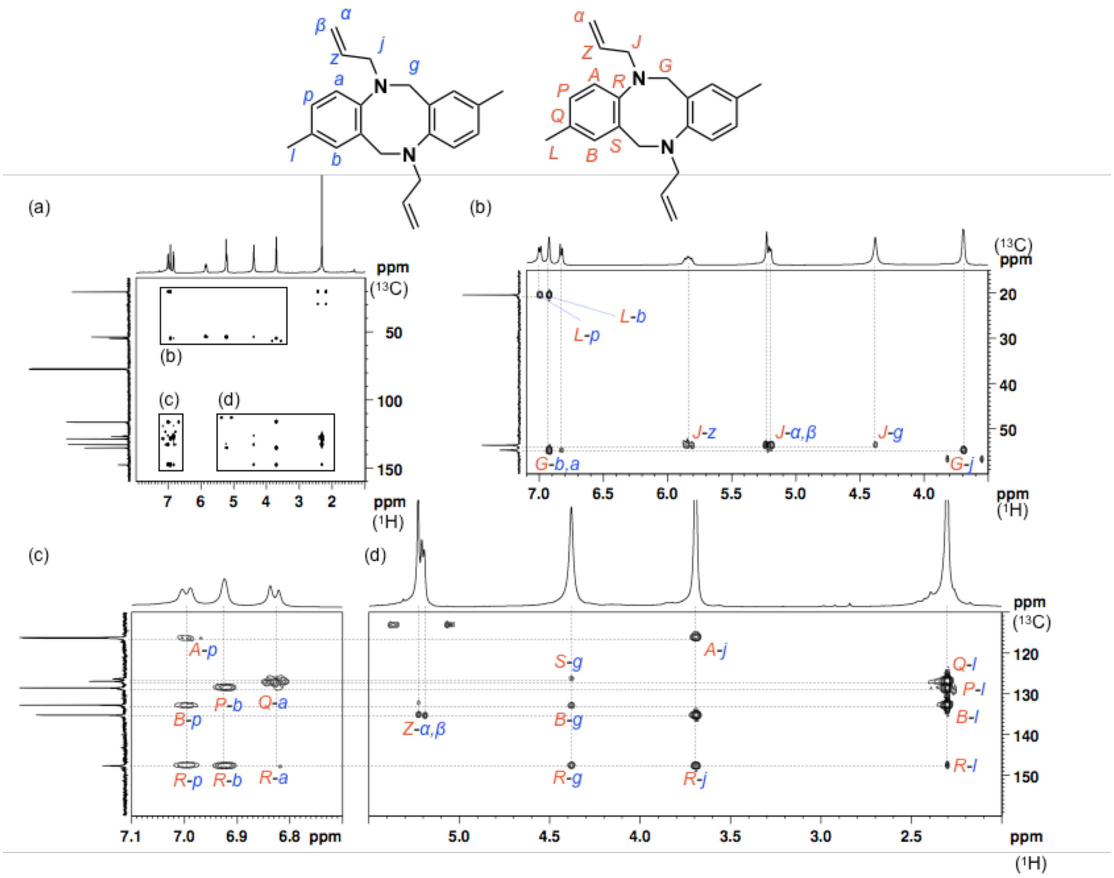

Fig. S77. HMBC correlations (^{1}H: 500 MHz, ^{13}C: 125 MHz) of **3e** in $CDCl_3$ at 25 °C.

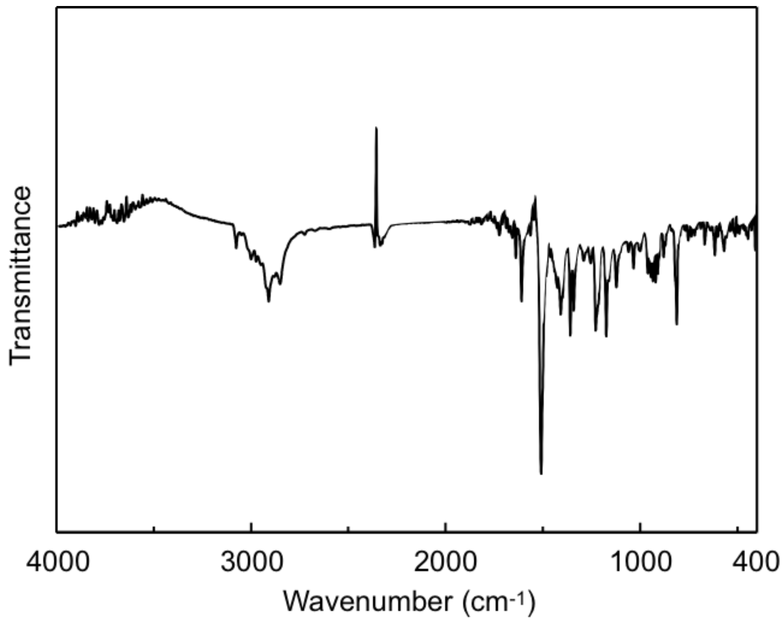

Fig. S78. FT-IR spectrum of **3e** at 25 °C (KBr).

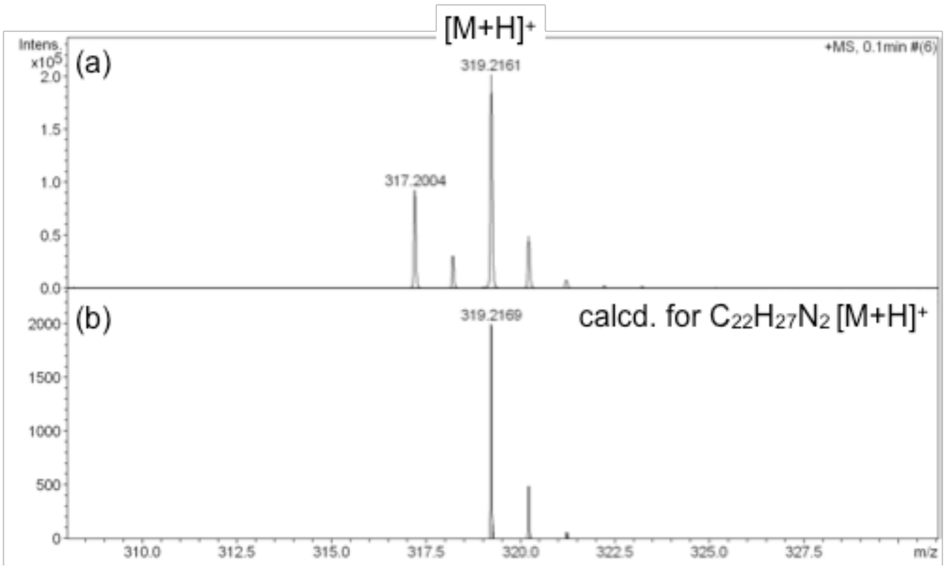

Fig. S79. (a) Observed and (b) simulated high-resolution APCI-TOF mass spectra of **3e**.

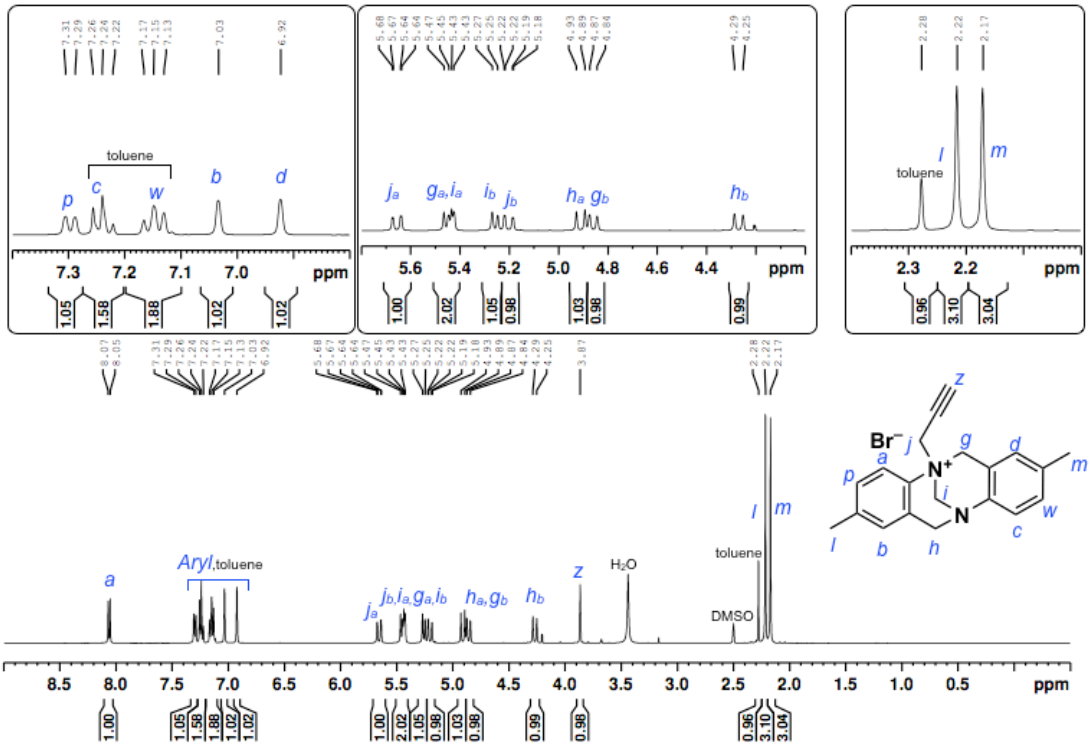

Fig. S80. ^{1}H NMR spectrum (500 MHz) of **1f** in DMSO-d_6 at 25 °C.

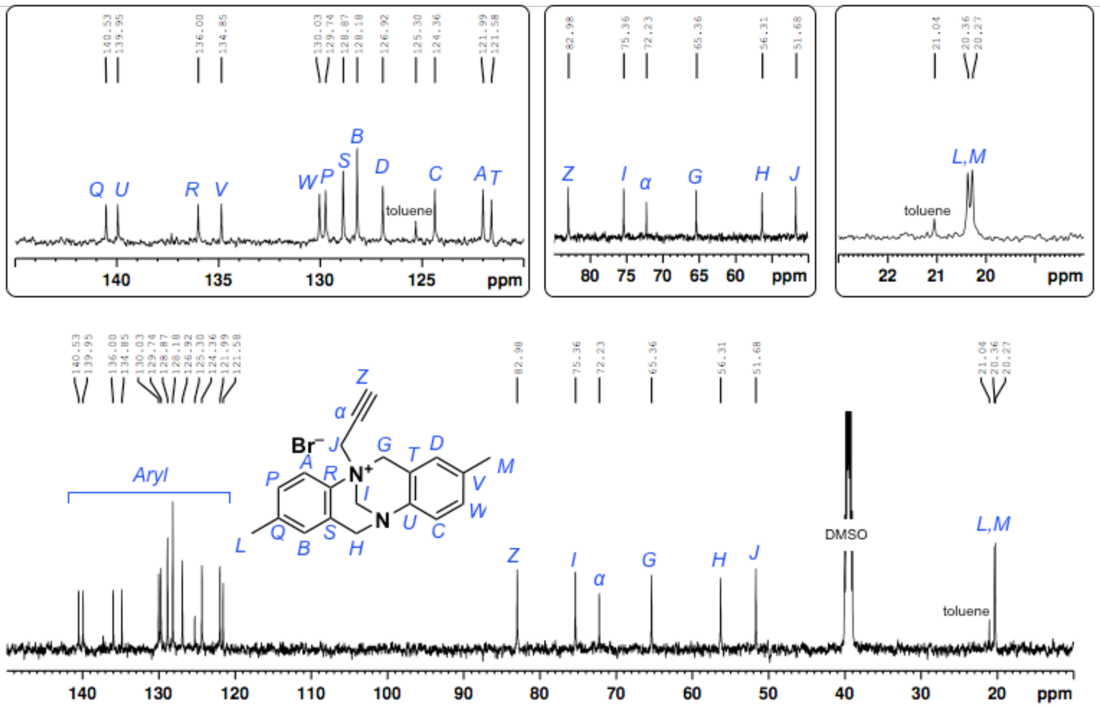

Fig. S81. ^{13}C NMR spectrum (125 MHz) of **1f** in DMSO-d_6 at 25 °C.

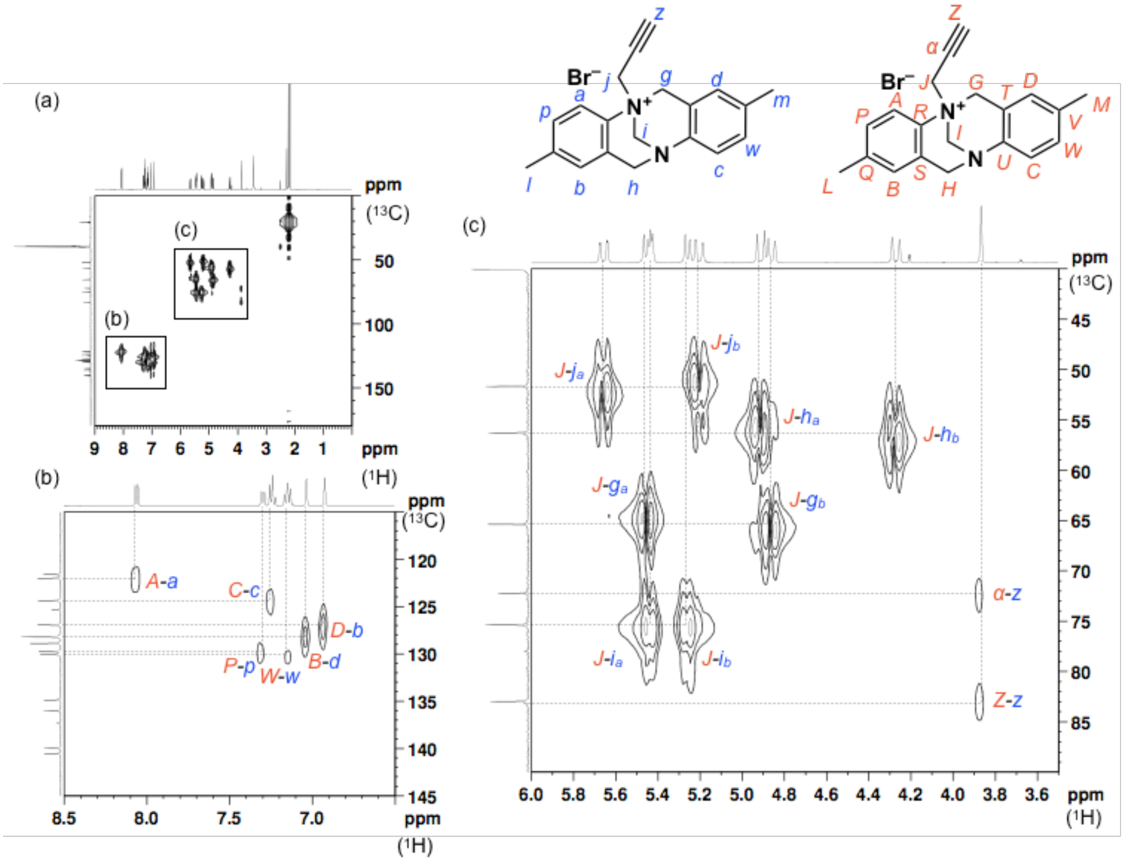

Fig. S82. HMQC correlations (^{1}H: 500 MHz, ^{13}C: 125 MHz) of **1f** in DMSO-d_6 at 25 °C.

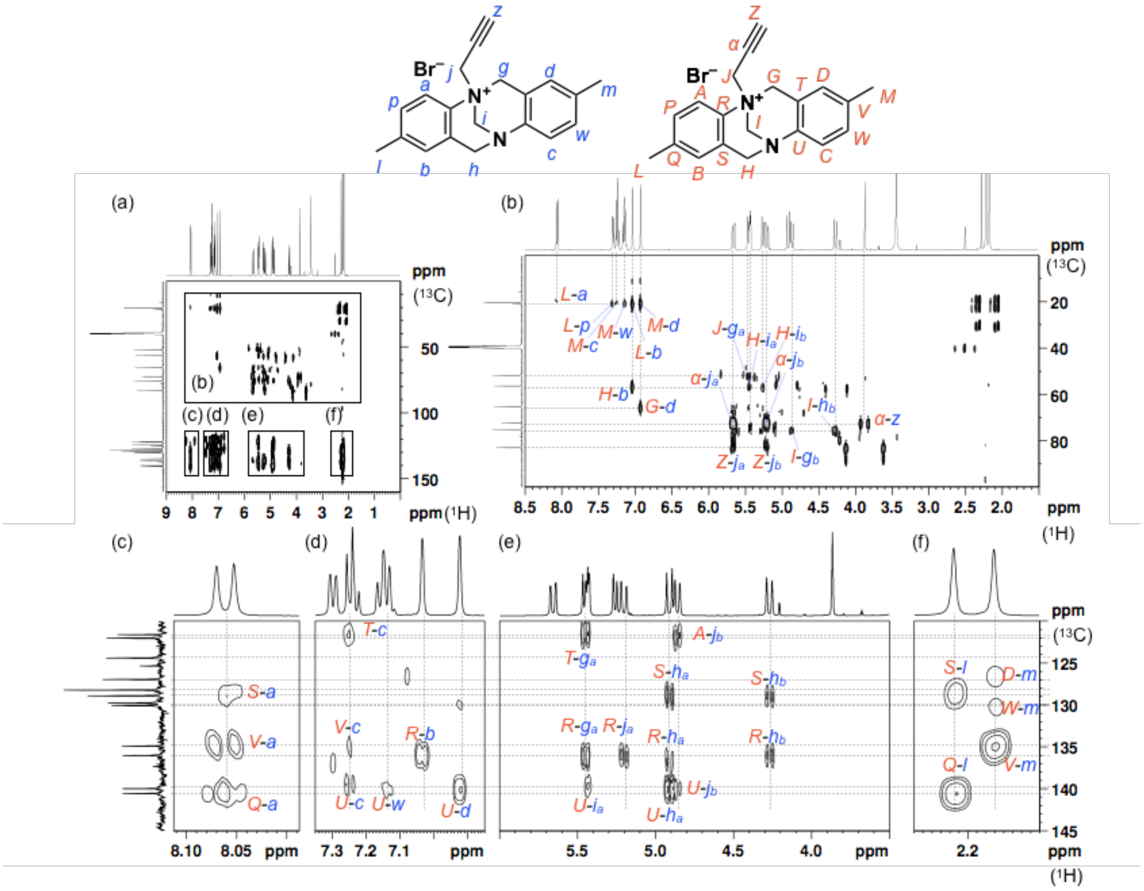

Fig. S83. HMBC correlations (^{1}H: 500 MHz, ^{13}C: 125 MHz) of **1f** in DMSO-d_6 at 25 °C.

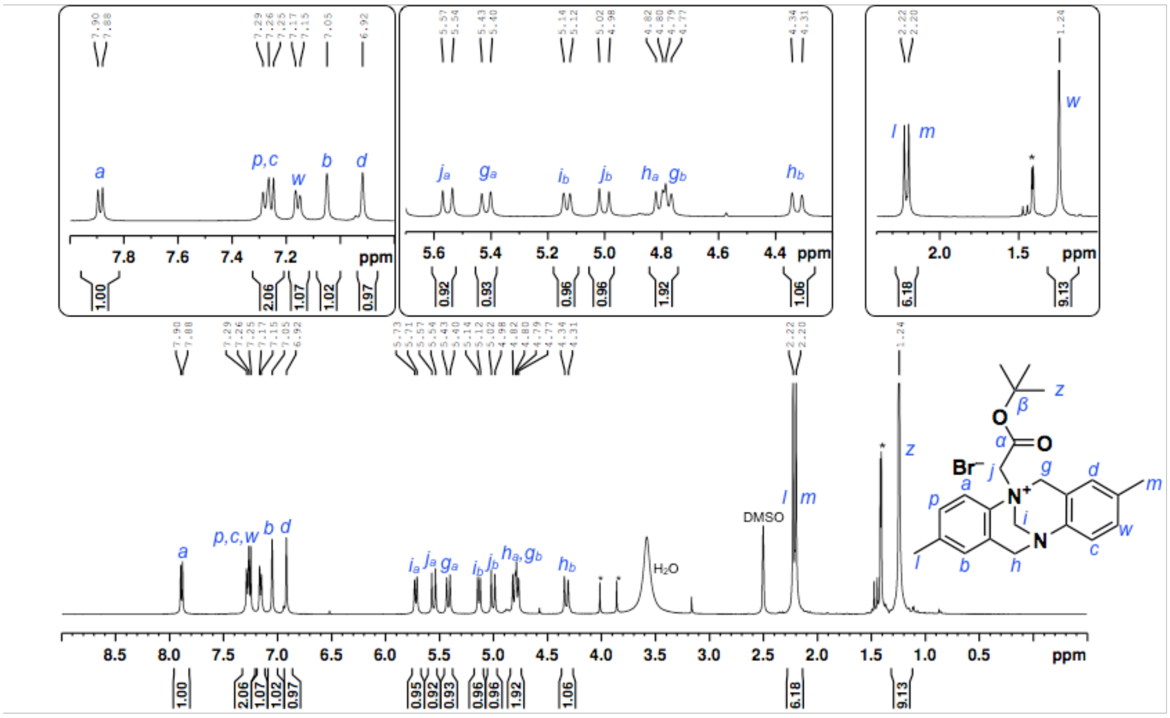

*residual *tert*-butoxy α-bromo-acetate

Fig. S84. ^{1}H NMR spectrum (500 MHz) of **1g** in DMSO-d_6 at 25 °C.

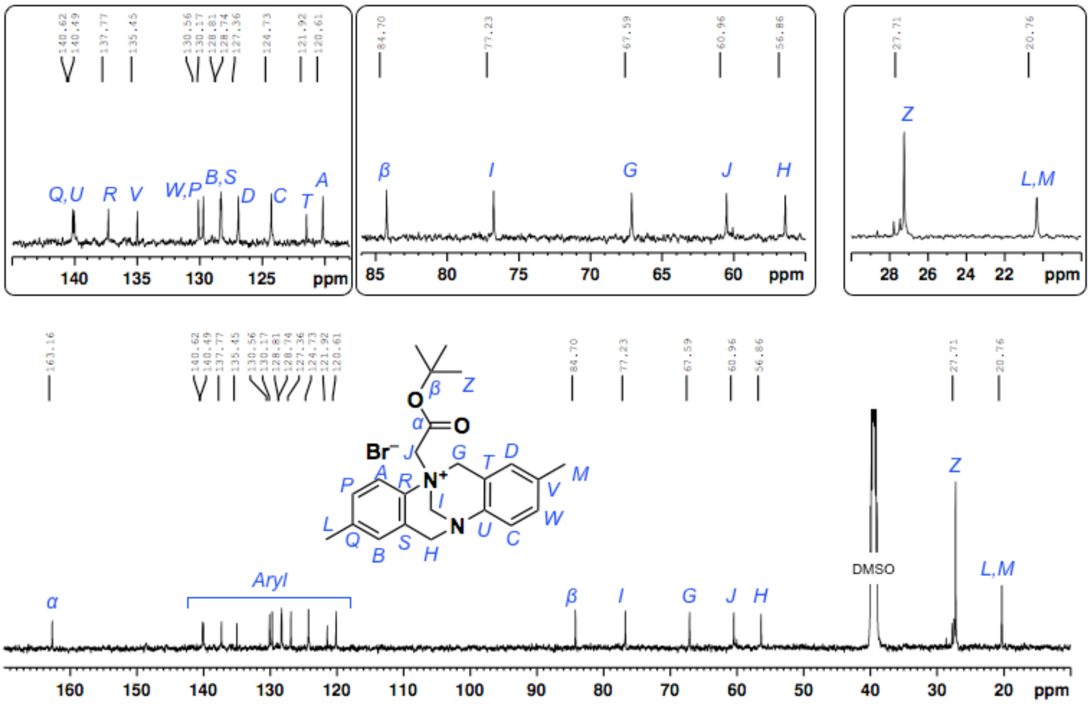

Fig. S85. ^{13}C NMR spectrum (125 MHz) of **1g** in DMSO-d_6 at 25 °C.

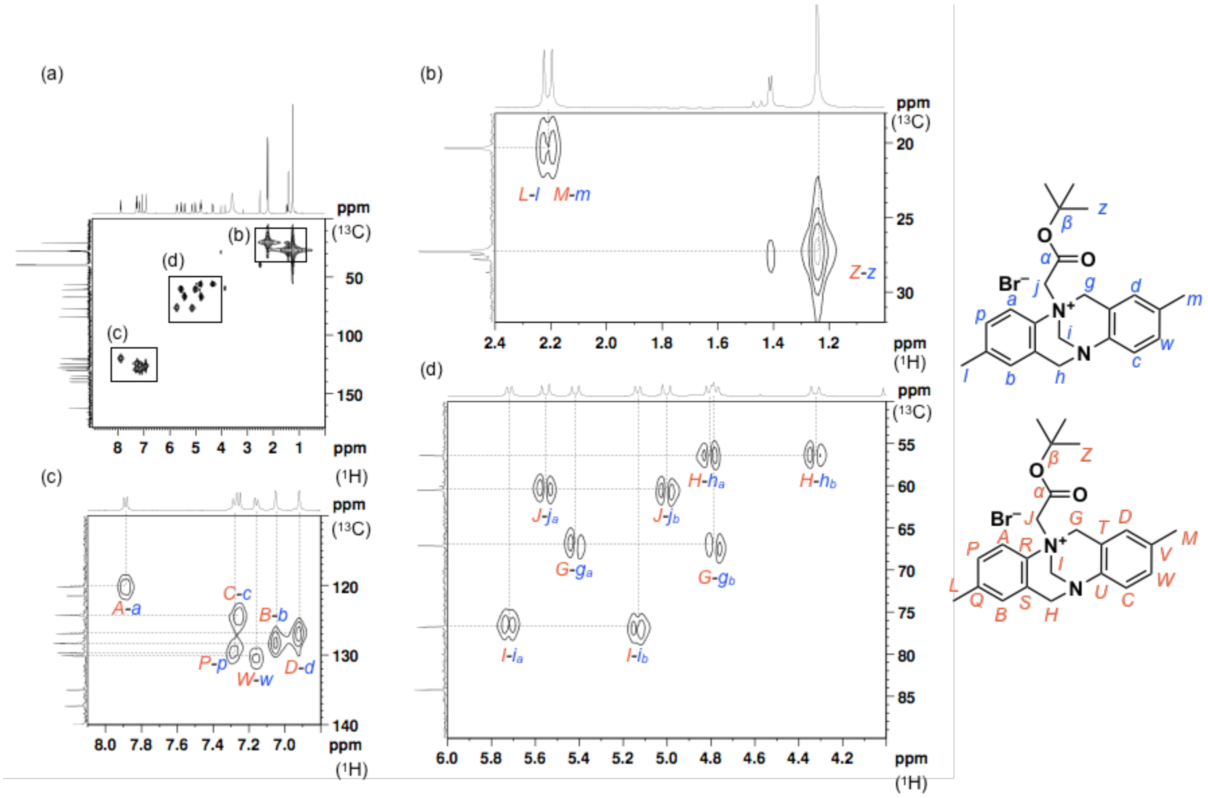

Fig. S86. HMQC correlations (^{1}H: 500 MHz, ^{13}C: 125 MHz) of **1g** in DMSO-d_6 at 25 °C.

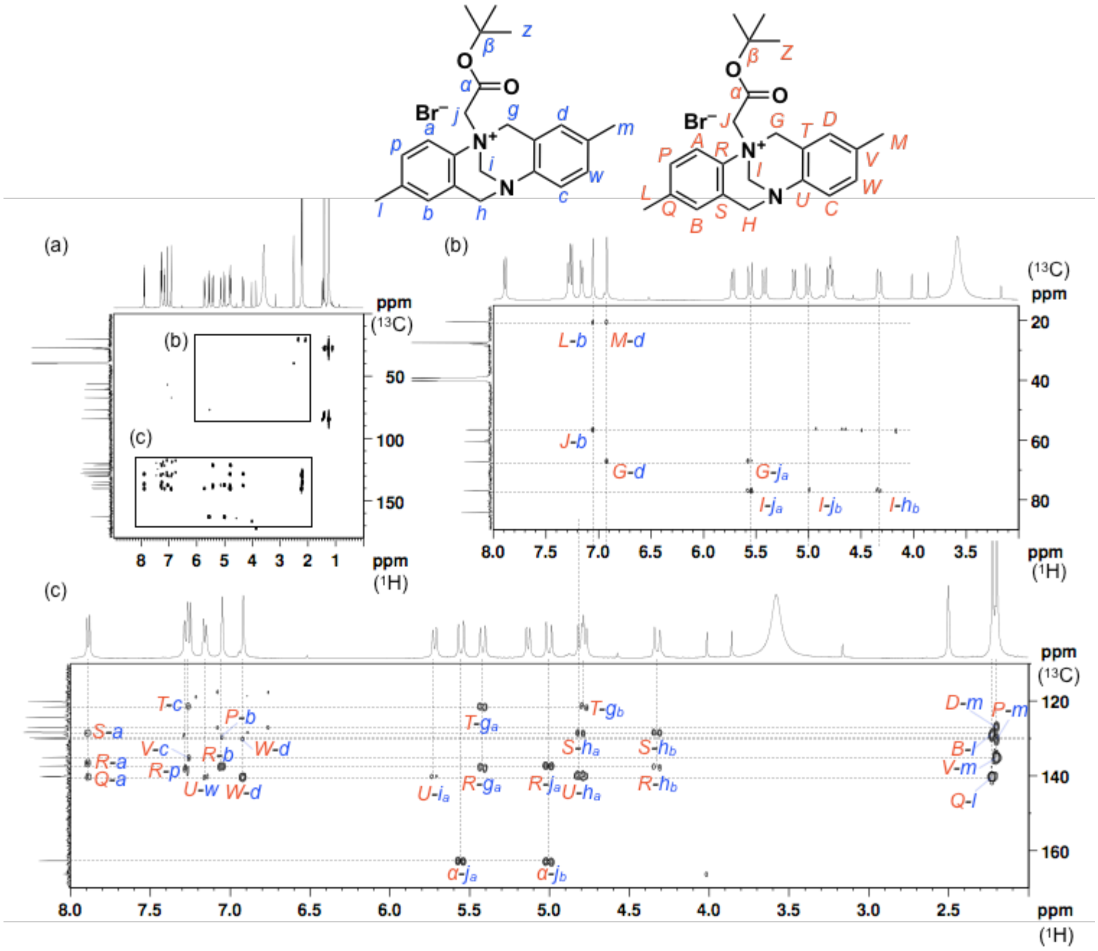

Fig. S87. HMBC correlations (^{1}H: 500 MHz, ^{13}C: 125 MHz) of **1g** in DMSO-d_6 at 25 °C.

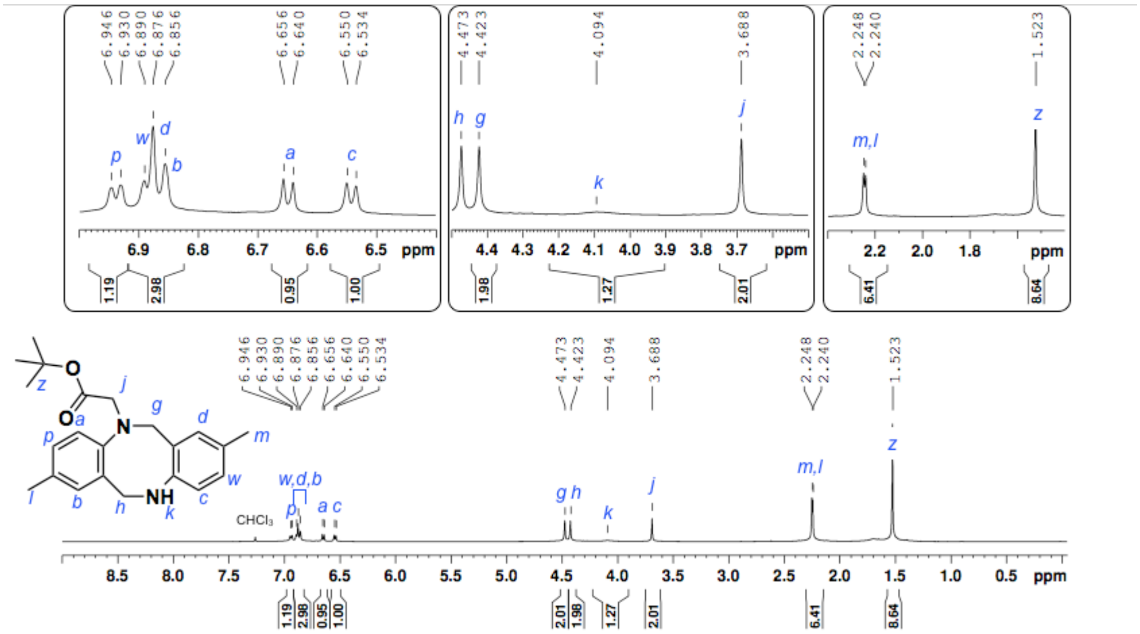

Fig. S88. ^{1}H NMR spectrum (500 MHz) of **2g** in CDCl$_3$ at 25 °C.

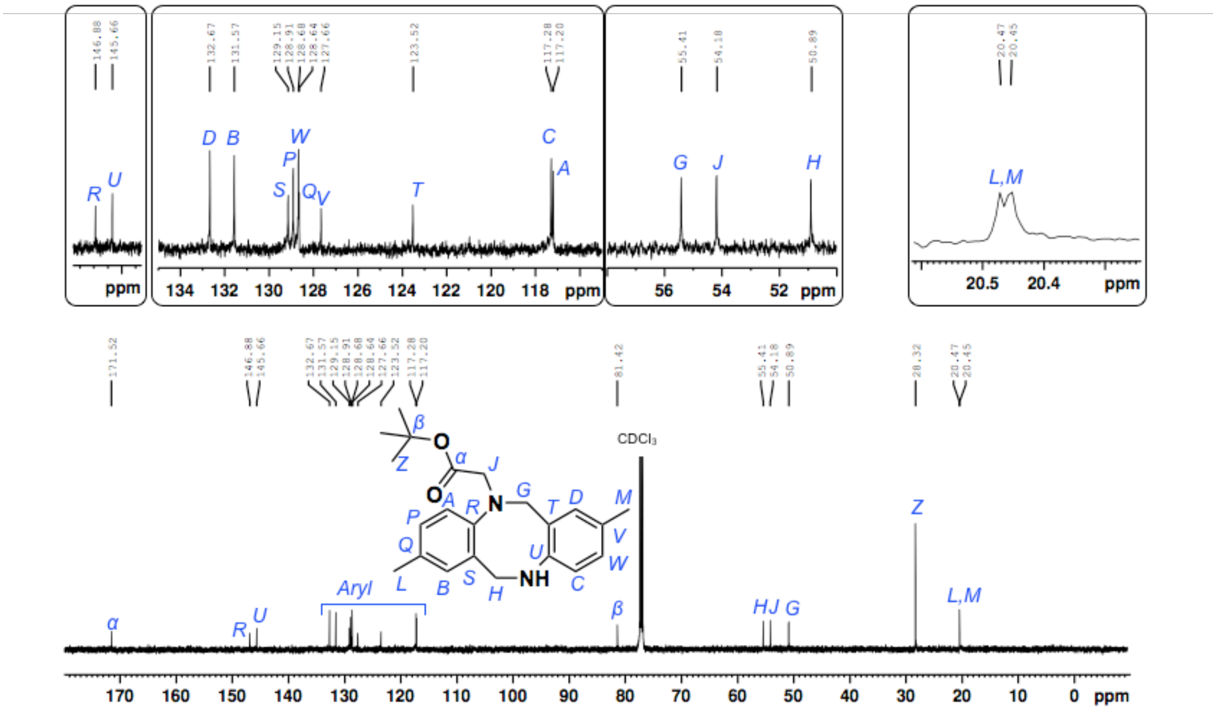

Fig. S89. ^{13}C NMR spectrum (125 MHz) of **2g** in CDCl$_3$ at 25 °C.

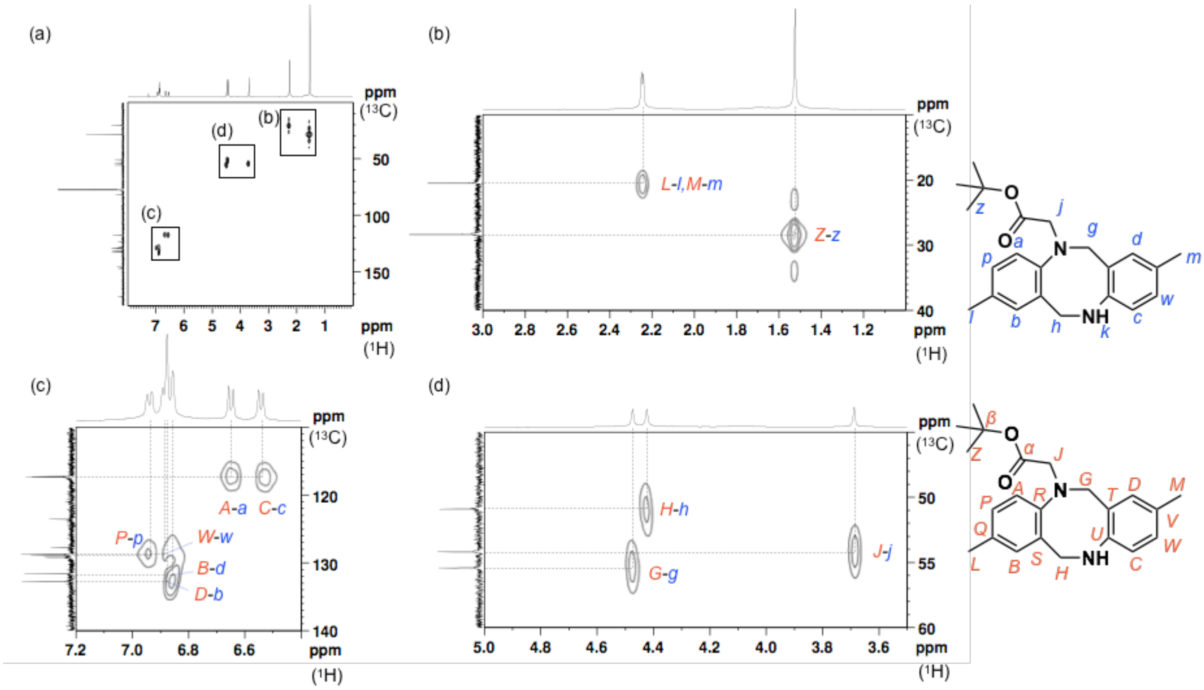

Fig. S90. HMQC correlations (^{1}H: 500 MHz, ^{13}C: 125 MHz) of **2g** in CDCl$_3$ at 25 °C.

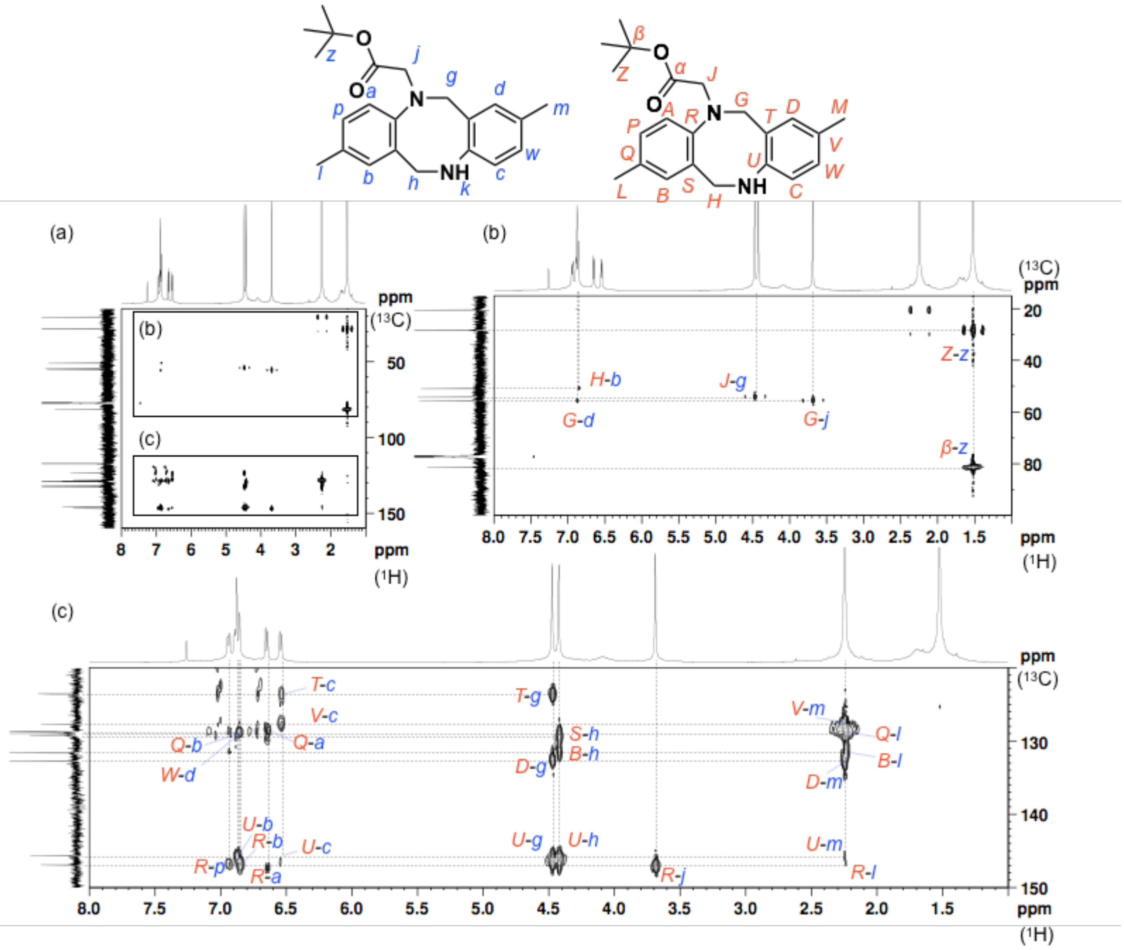

Fig. S91. HMBC correlations (^{1}H: 500 MHz, ^{13}C: 125 MHz) of **2g** in CDCl$_3$ at 25 °C.

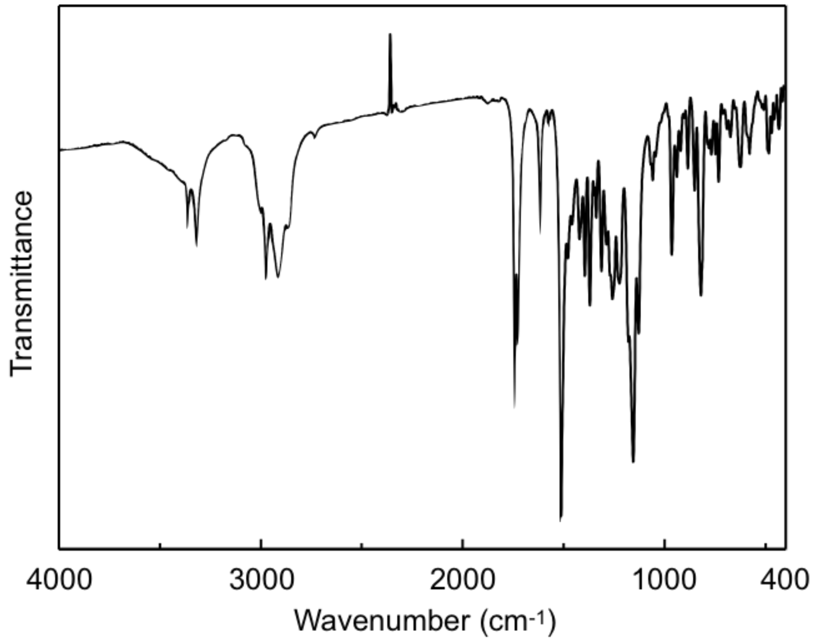

Fig. S92. FT-IR spectrum of **2g** at 25 °C (KBr).

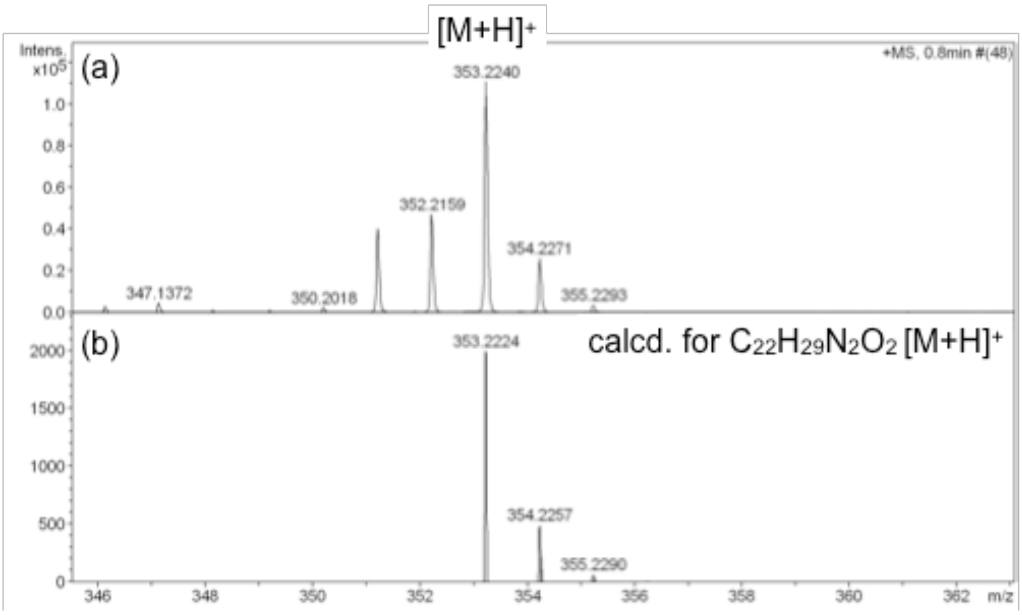

Fig. S93. (a) Observed and (b) simulated high-resolution APCI-TOF mass spectra of **2g**.

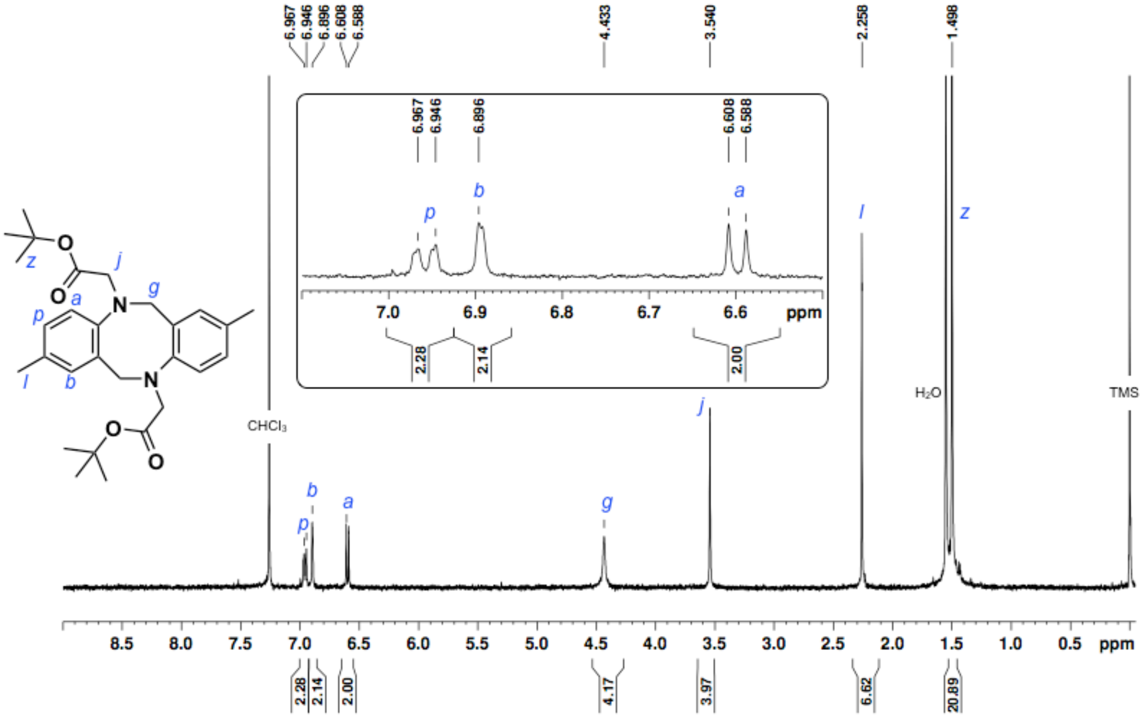

Fig. S94. ^{1}H NMR spectrum (500 MHz) of **3g** in $CDCl_3$ at 25 °C.

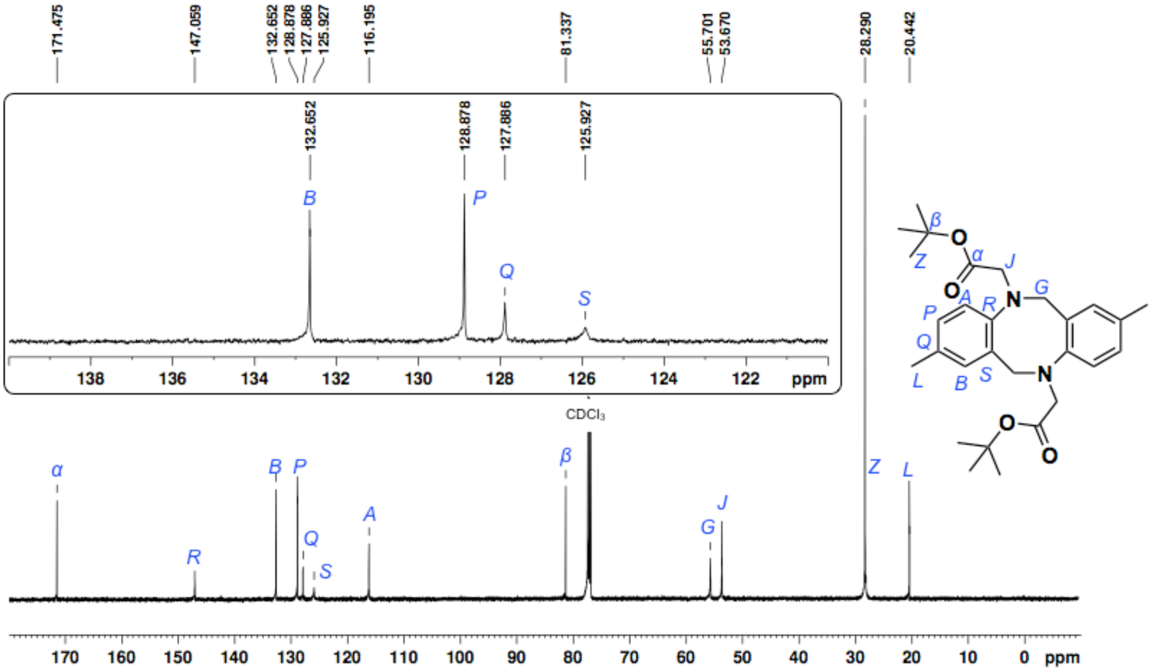

Fig. S95. ^{13}C NMR spectrum (125 MHz) of **3g** in $CDCl_3$ at 25 °C.

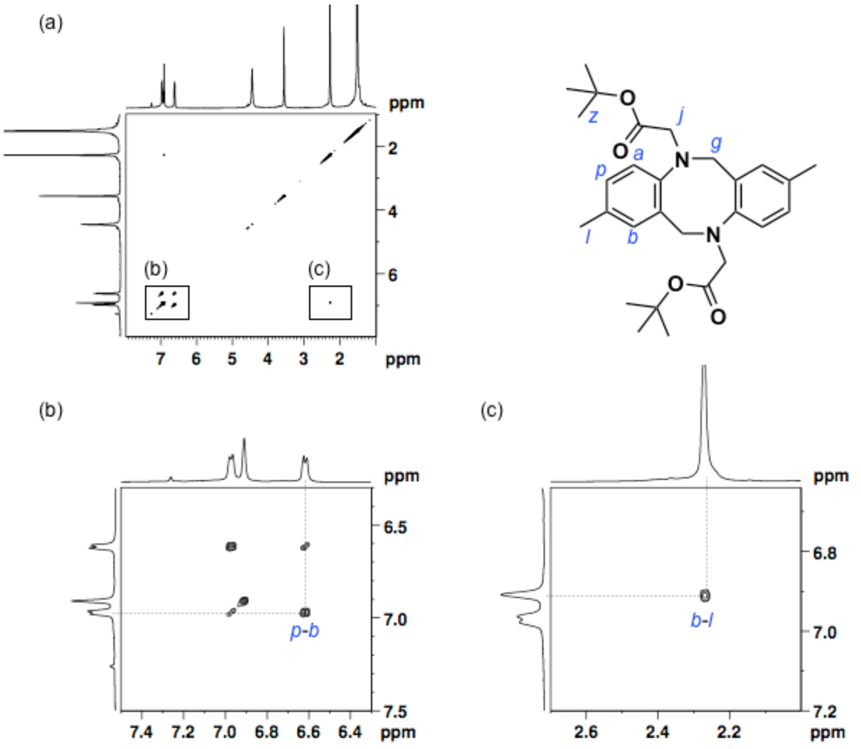

Fig. S96. H-H COSY correlations (500 MHz) of **3g** in $CDCl_3$ at 25 °C.

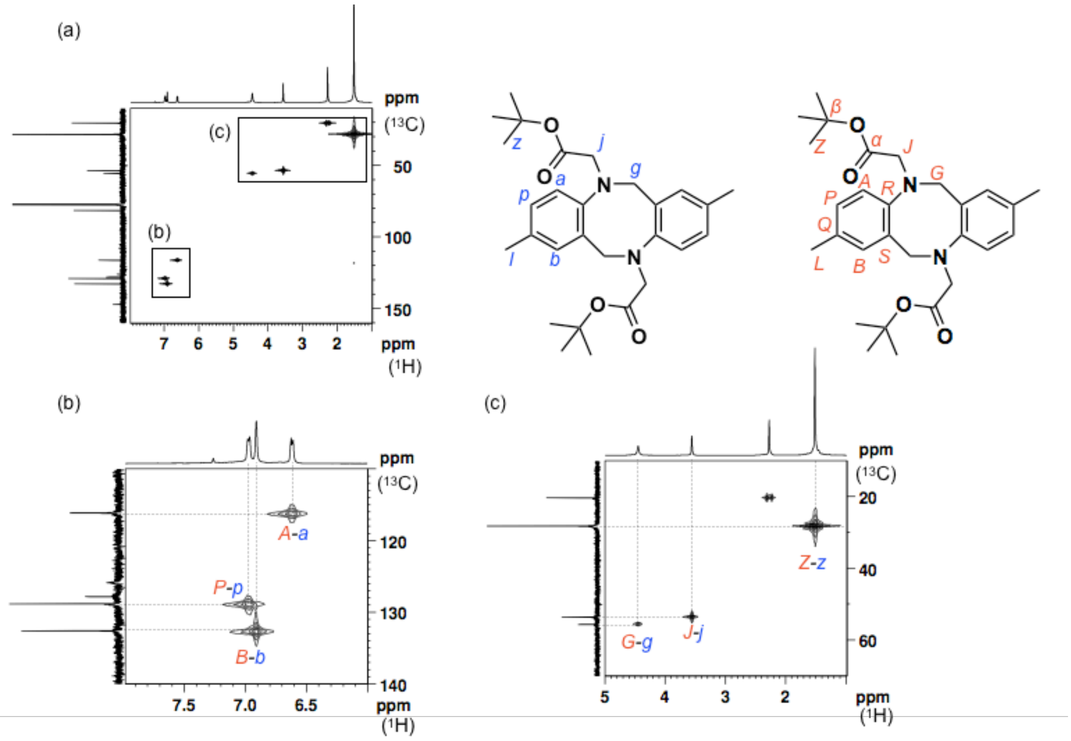

Fig. S97. HMQC correlations (^{1}H: 500 MHz, ^{13}C: 125 MHz) of **3g** in CDCl$_3$ at 25 °C.

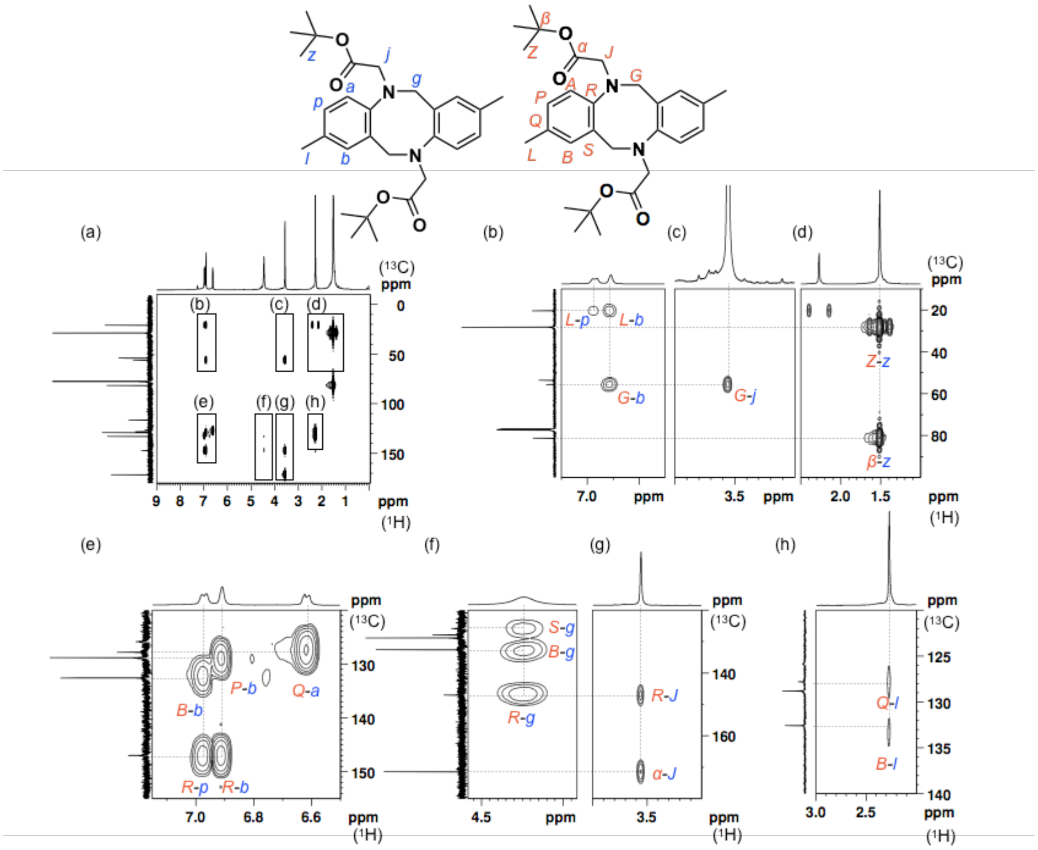

Fig. S98. HMBC correlations (^{1}H: 500 MHz, ^{13}C: 125 MHz) of **3g** in CDCl$_3$ at 25 °C.

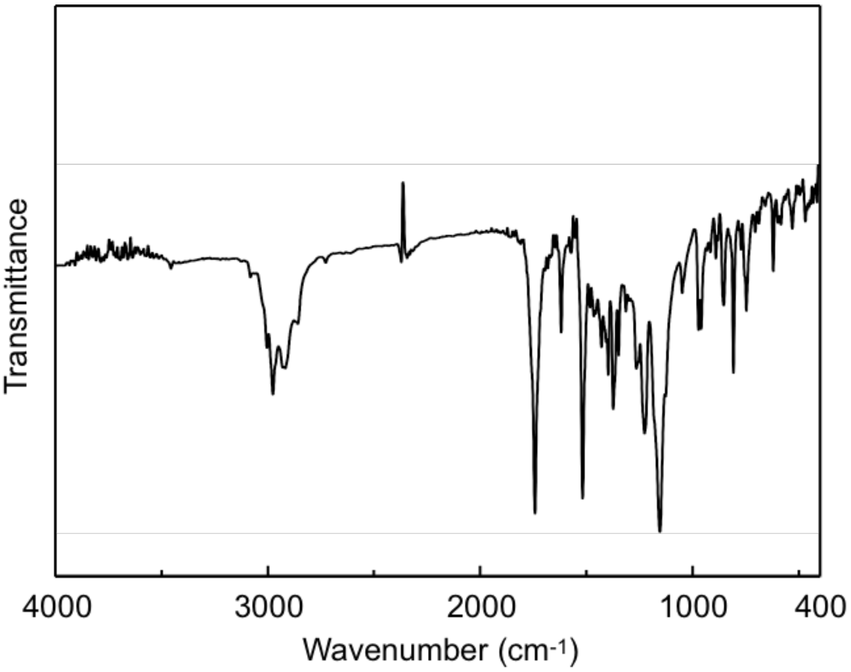

Fig. S99. FT-IR spectrum of **3g** at 25 °C (KBr).

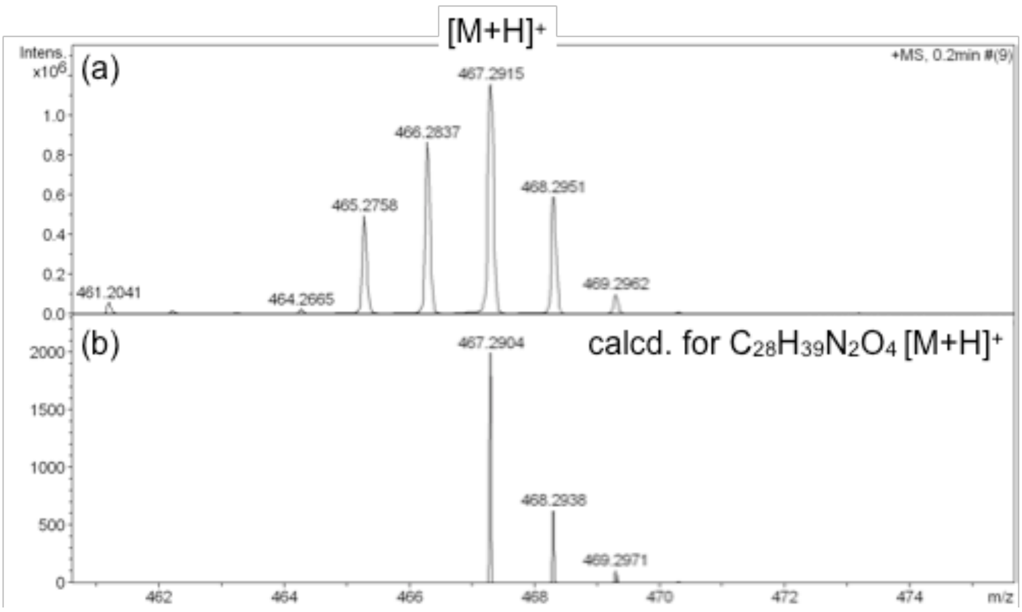

Fig. S100. (a) Observed and (b) simulated high-resolution APCI-TOF mass spectra of **3g**.

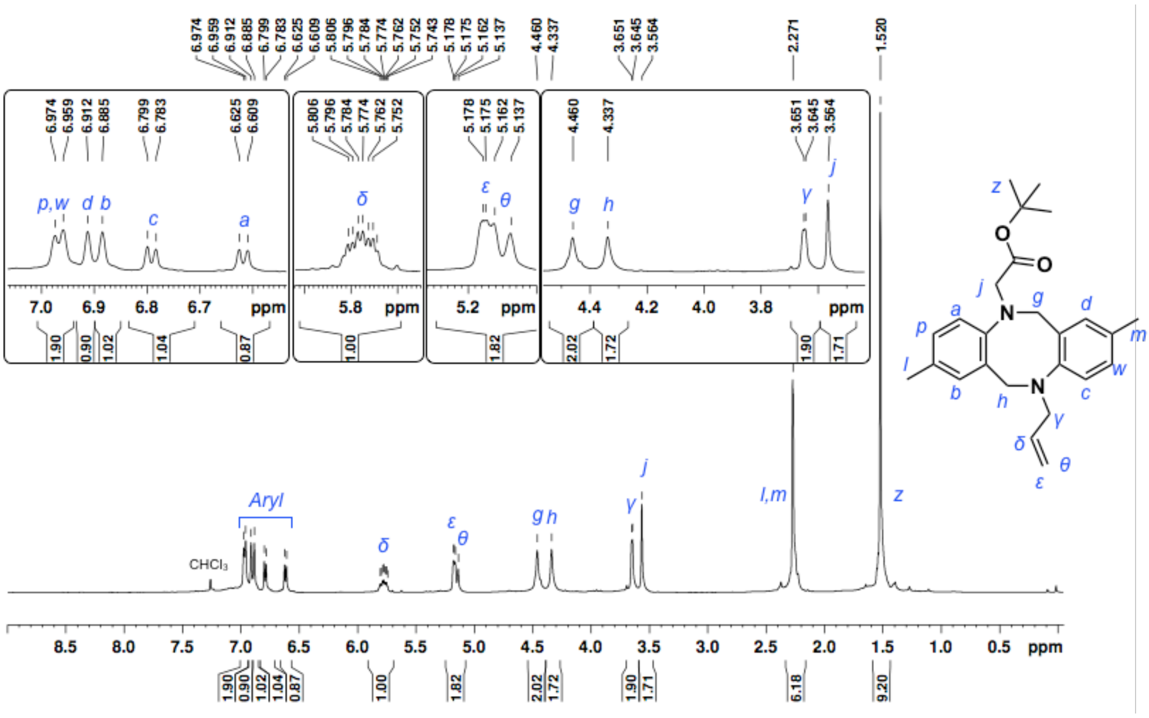

Fig. S101. ^{1}H NMR spectrum (500 MHz) of **3h** in $CDCl_3$ at 25 °C.

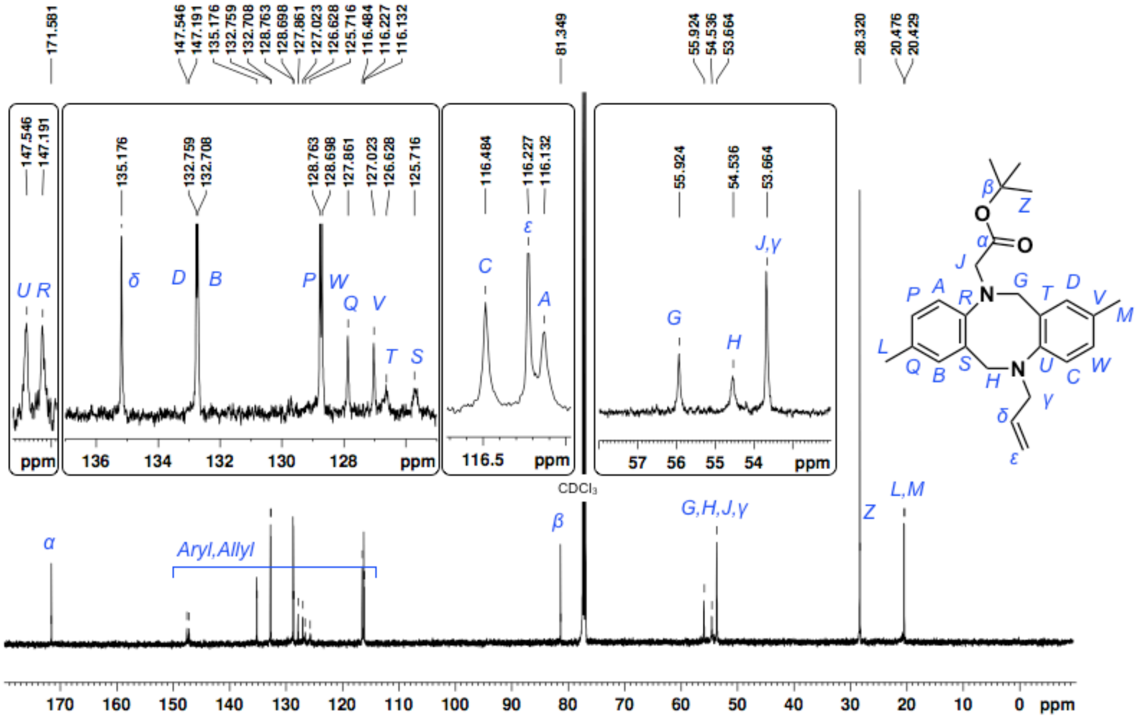

Fig. S102. ^{13}C NMR spectrum (125 MHz) of **3h** in $CDCl_3$ at 25 °C.

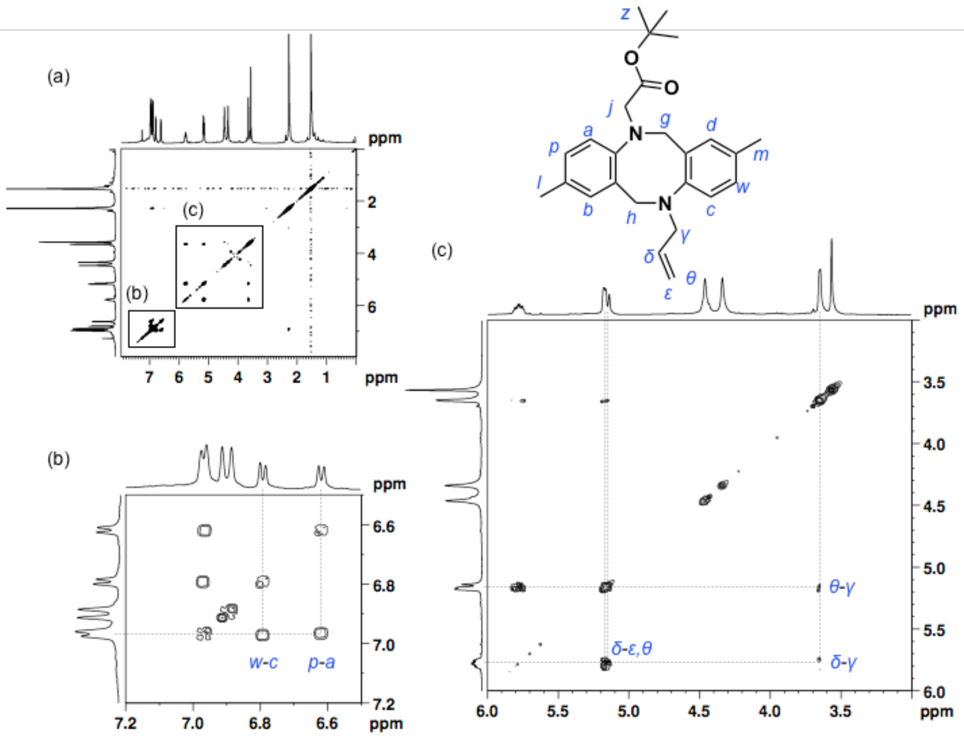

Fig. S103. H-H COSY correlations (500 MHz) of **3h** in $CDCl_3$ at 25 °C.

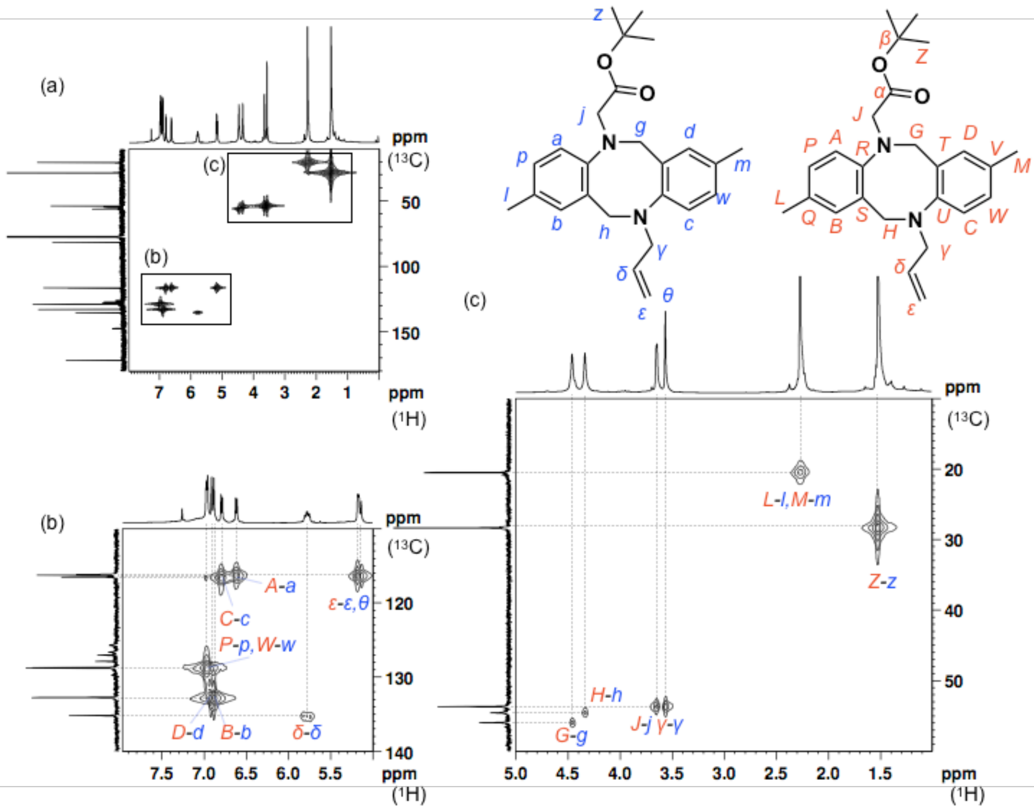

Fig. S104. HMQC correlations (^{1}H: 500 MHz, ^{13}C: 125 MHz) of **3h** in $CDCl_3$ at 25 °C.

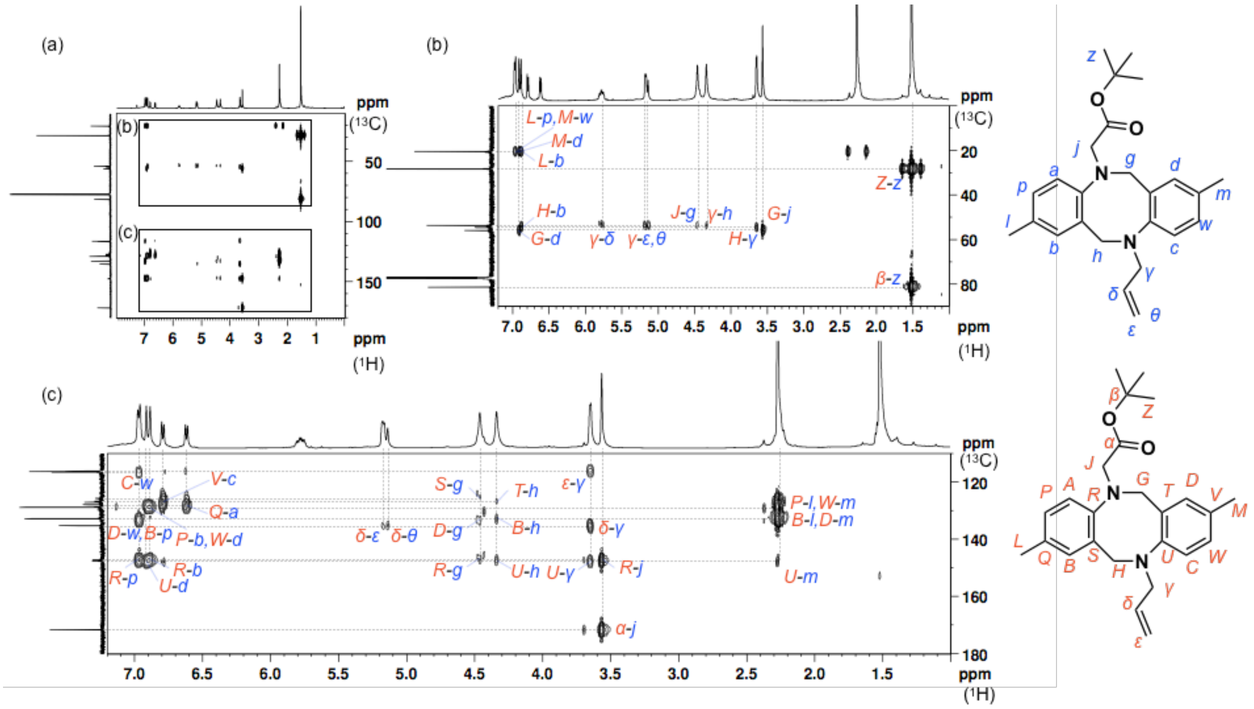

Fig. S105. HMBC correlations (^{1}H: 500 MHz, ^{13}C: 125 MHz) of **3h** in CDCl$_3$ at 25 °C.

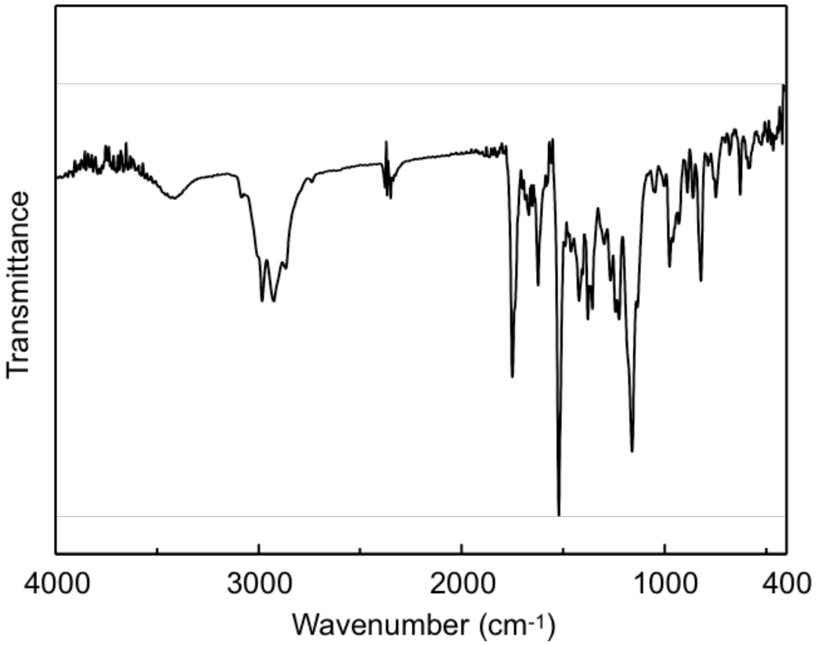

Fig. S106. FT-IR spectrum of **3h** at 25 °C (KBr).

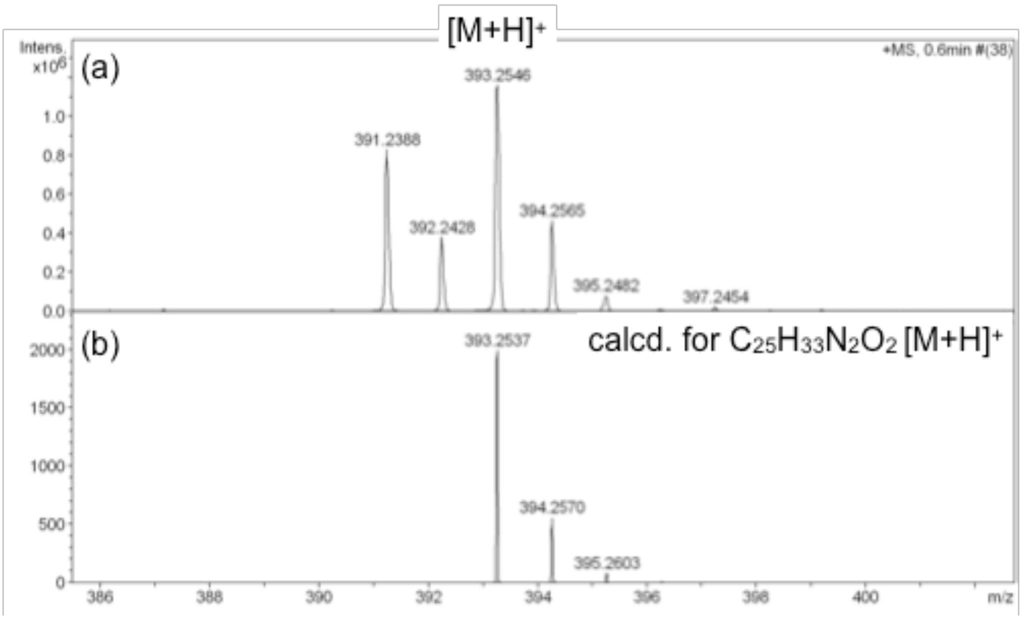

Fig. S107. (a) Observed and (b) simulated high-resolution APCI-TOF mass spectra of **3h**.

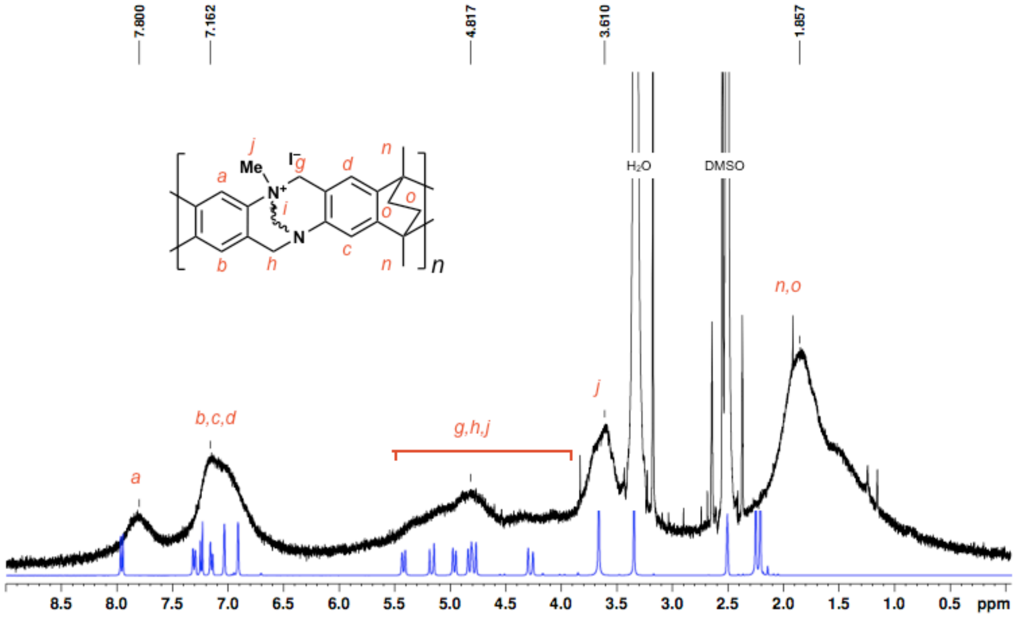

Fig. S108. ^{1}H NMR spectra (500 MHz) of poly-**1a** (black) and **1a** (blue) in DMSO-d_6 at 25 °C.

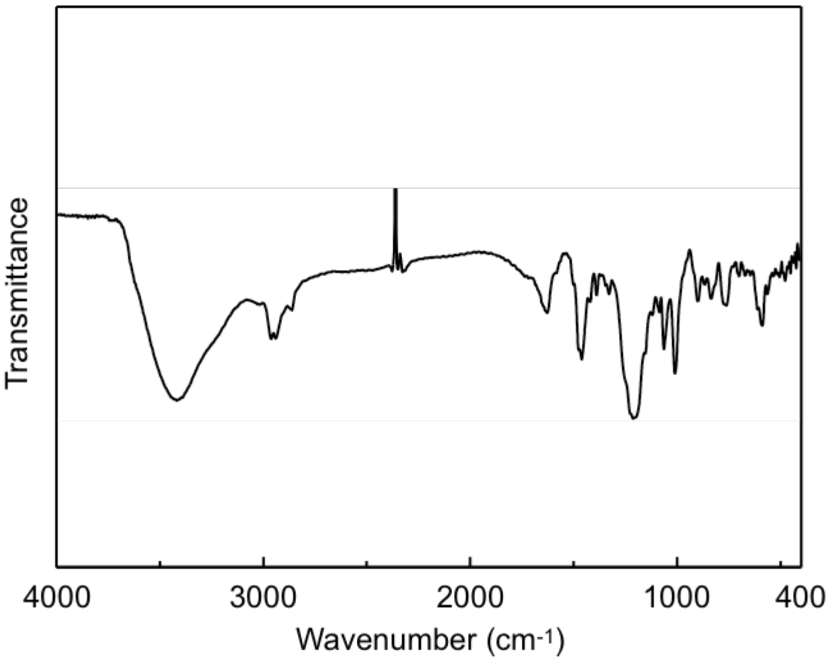

Fig. S109. FT-IR spectrum of poly-**1a** at 25 °C (KBr).

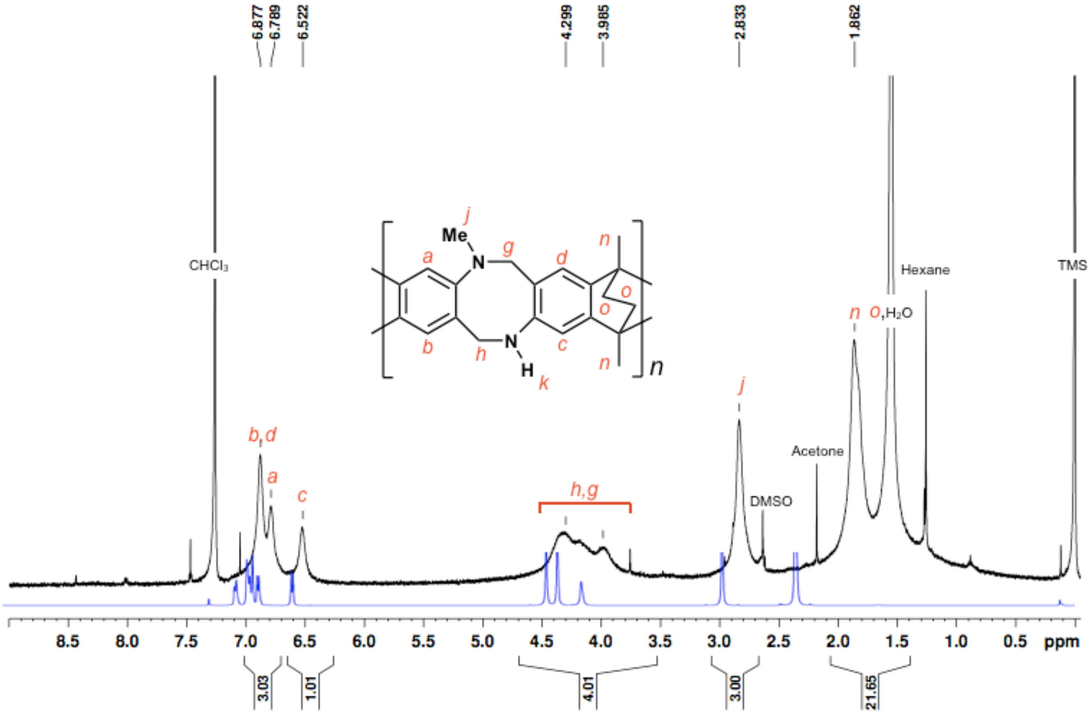

Fig. S110. ^{1}H NMR spectra (500 MHz) of poly-**2a** (black) and **2a** (blue) in $CDCl_3$ at 25 °C.

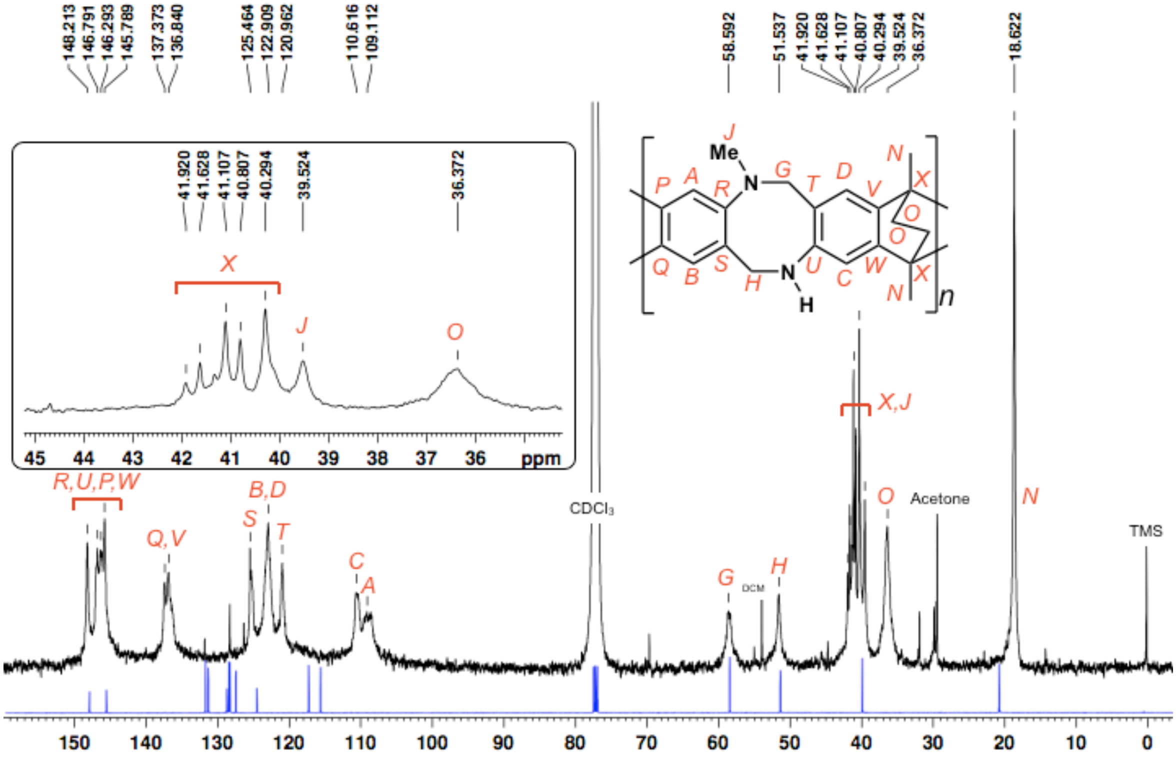

Fig. S111. ^{13}C NMR spectra (125 MHz) of poly-**2a** (black) and **2a** (blue) in CDCl$_3$ at 25 °C.

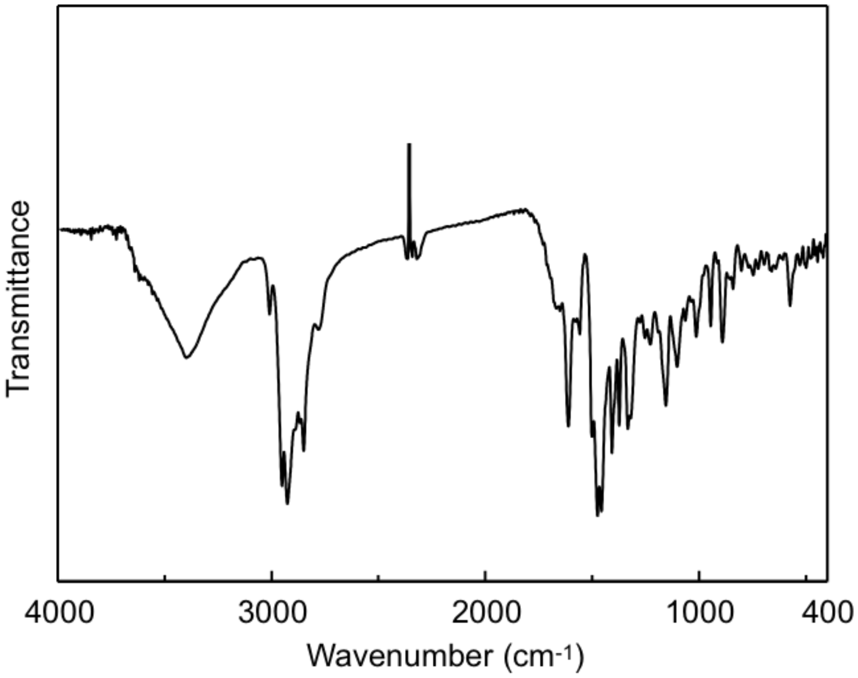

Fig. S112. FT-IR spectrum of poly-**2a** in at 25 °C (KBr).

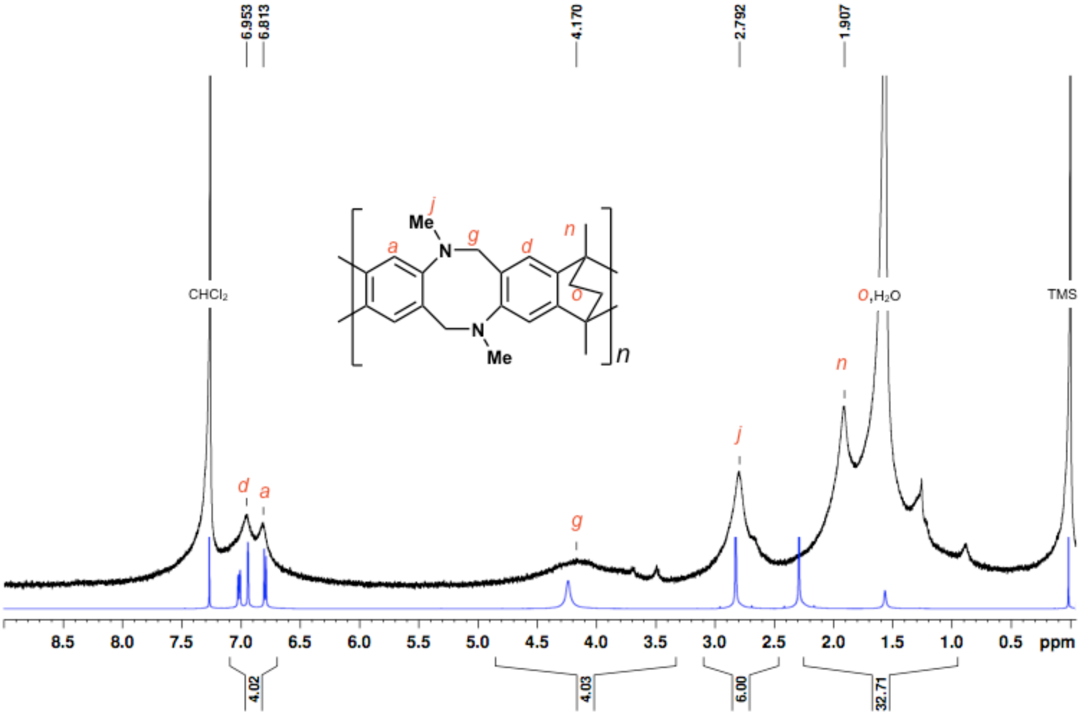

Fig. S113. ^{1}H NMR spectra (500 MHz) of poly-**3a** (black) and **3a** (blue) in CDCl$_3$ at 25 °C.

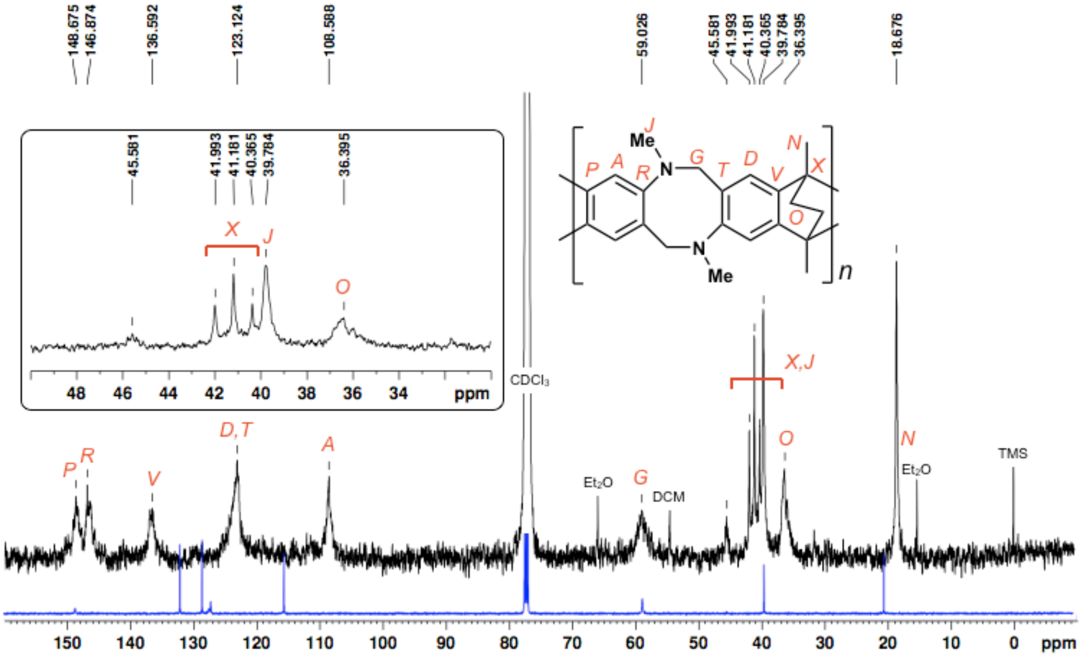

Fig. S114. ^{13}C NMR spectra (125 MHz) of poly-**3a** (black) and **3a** (blue) in CDCl$_3$ at 25 °C.

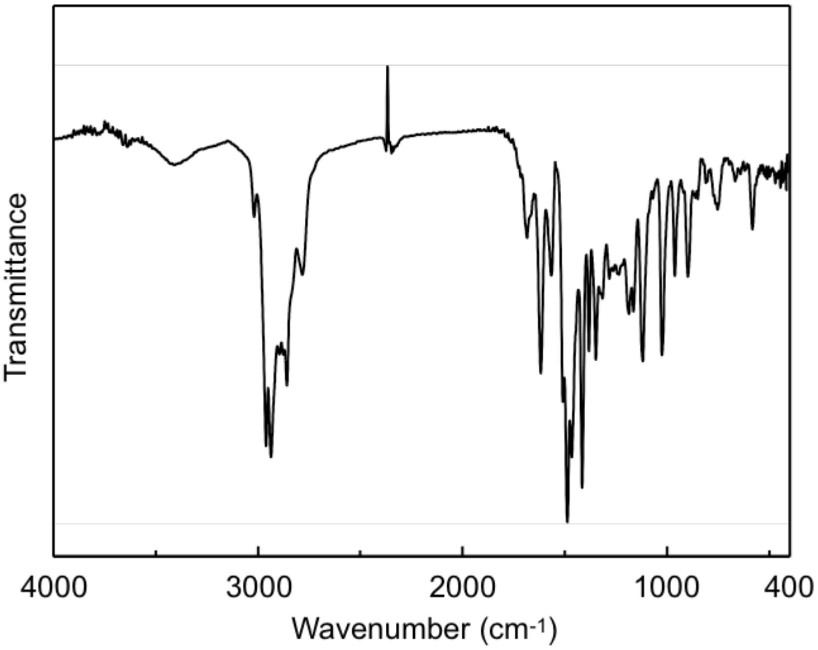

Fig. S115. FT-IR spectrum of poly-**3a** at 25 °C (KBr).

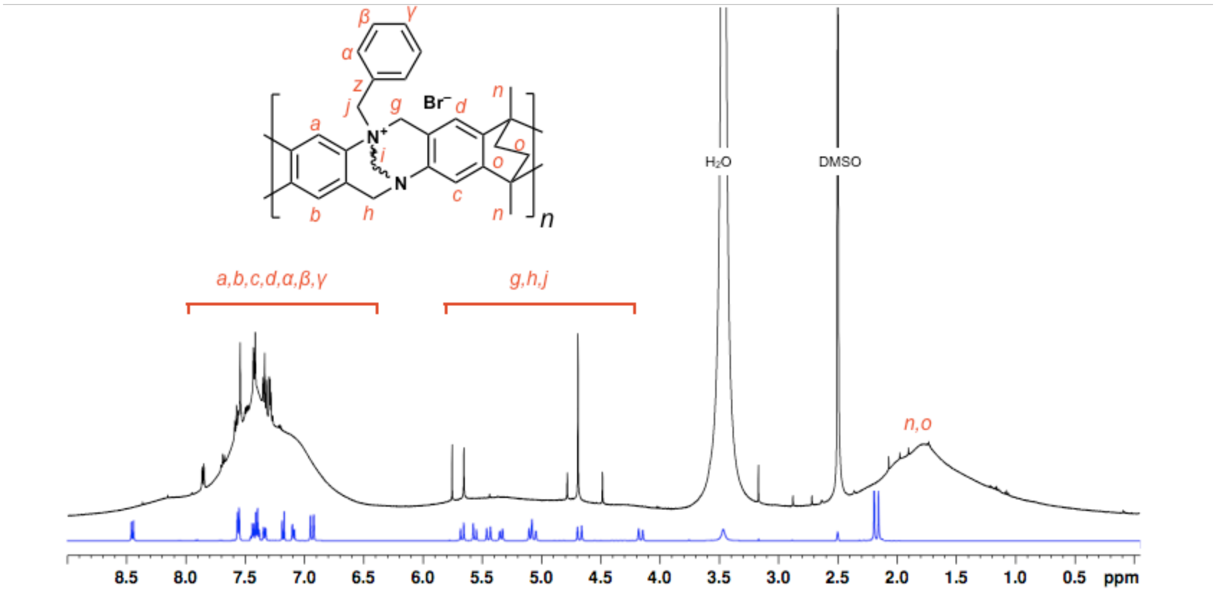

Fig. S116. ^{1}H NMR spectra (500 MHz) of poly-**1c** (black) and **1c** (blue) in DMSO-d_6 at 25 °C.

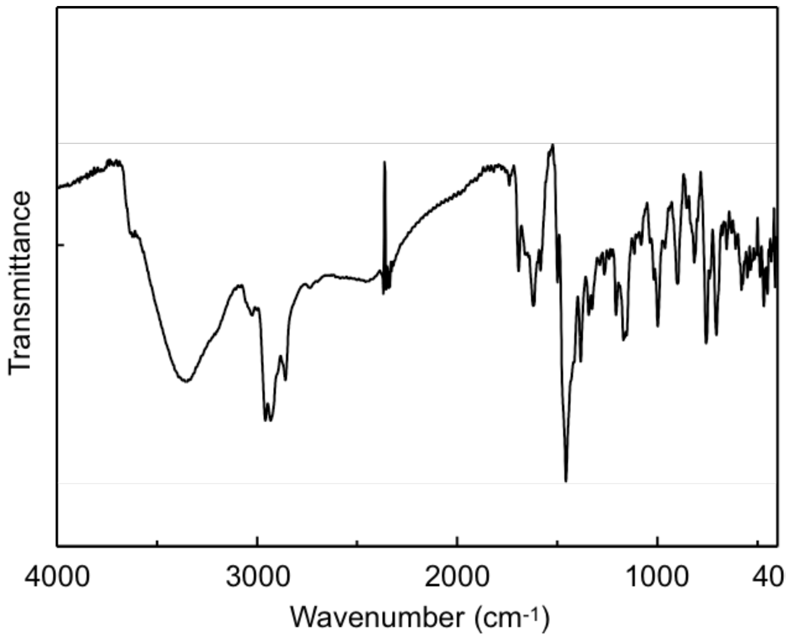

Fig. S117. FT-IR spectrum of poly-**2c** at 25 °C (KBr).

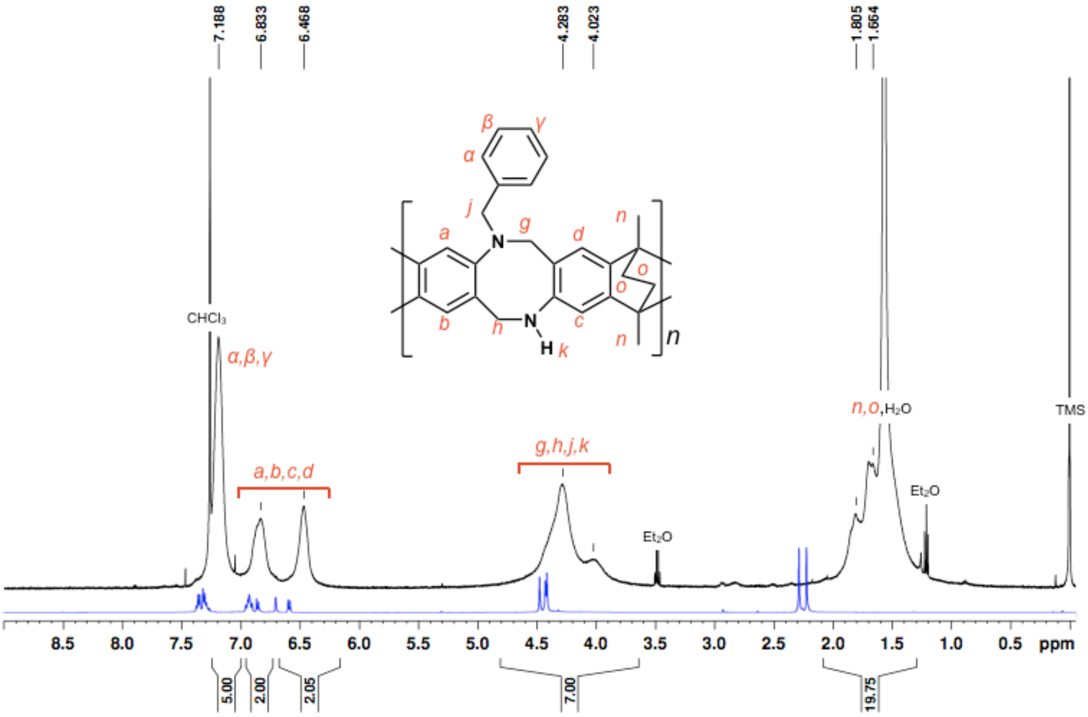

Fig. S118. ^{1}H NMR spectra (500 MHz) of poly-**2c** (black) and **2c** (blue) in $CDCl_3$ at 25 °C.

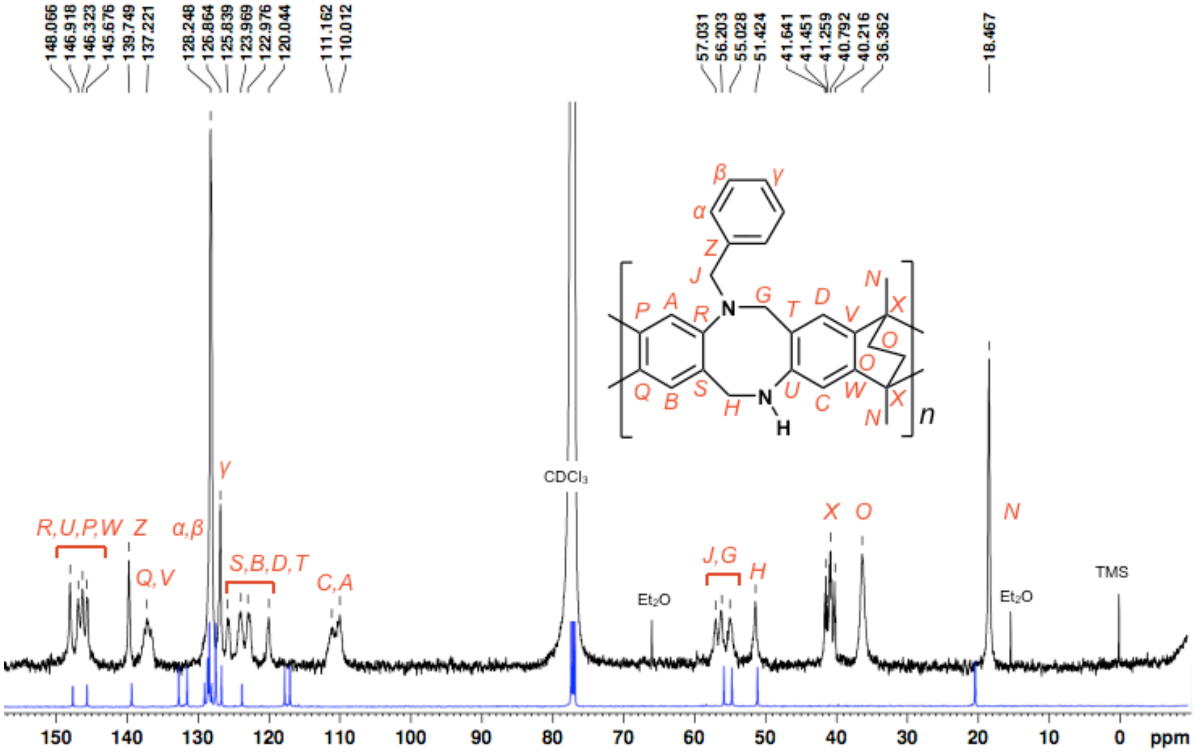

Fig. S119. ^{13}C NMR spectra (125 MHz) of poly-**2c** (black) and **2c** (blue) in $CDCl_3$ at 25 °C.

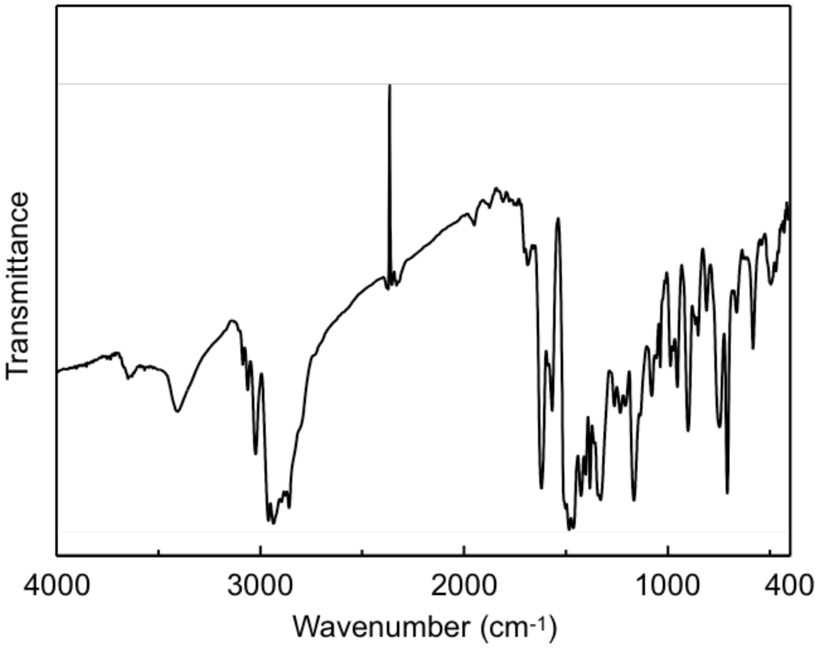

Fig. S120. FT-IR spectrum of poly-**2c** at 25 °C (KBr).

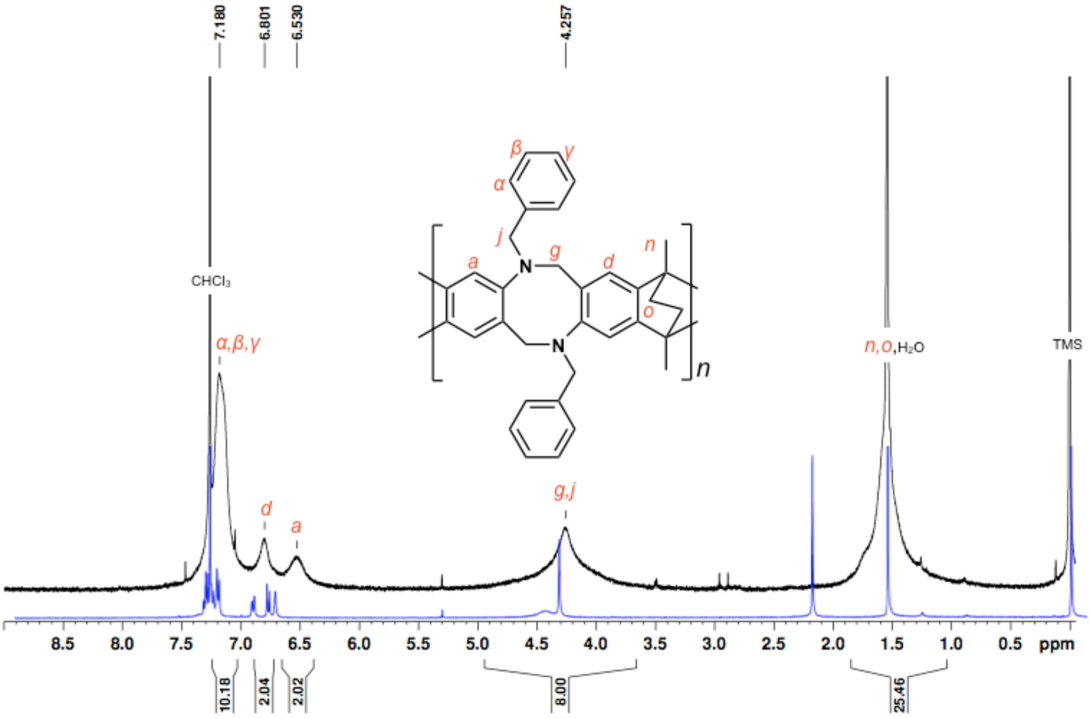

Fig. S121. ^{1}H NMR spectra (500 MHz) of poly-**3c** (black) and **3c** (blue) in $CDCl_3$ at 25 °C.

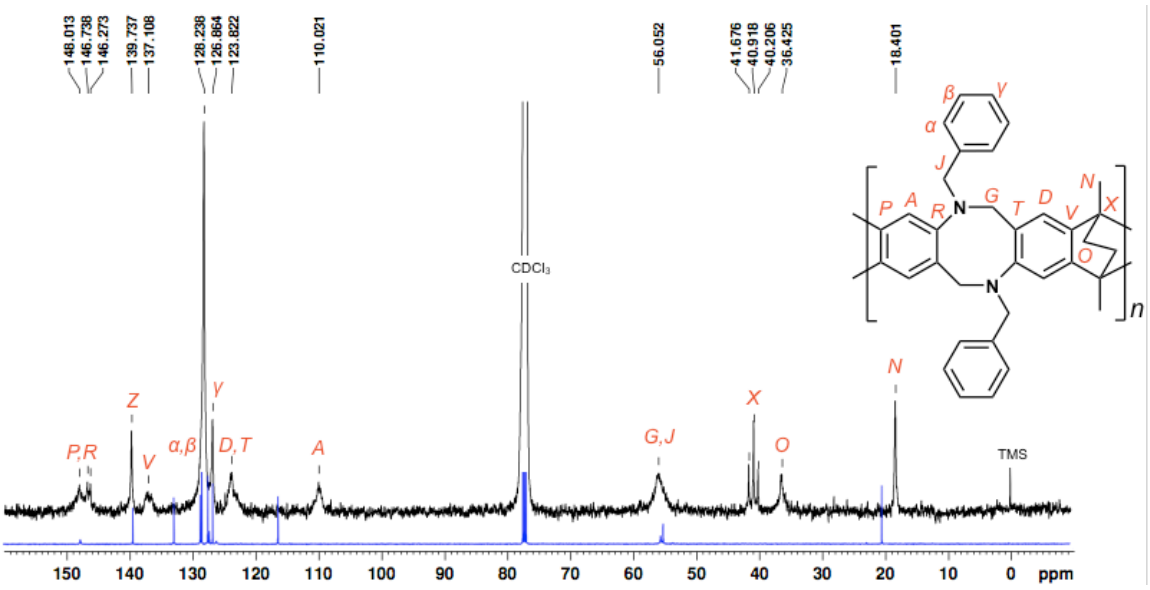

Fig. S122. ^{13}C NMR spectra (125 MHz) of poly-**3c** (black) and **3c** (blue) in $CDCl_3$ at 25 °C.

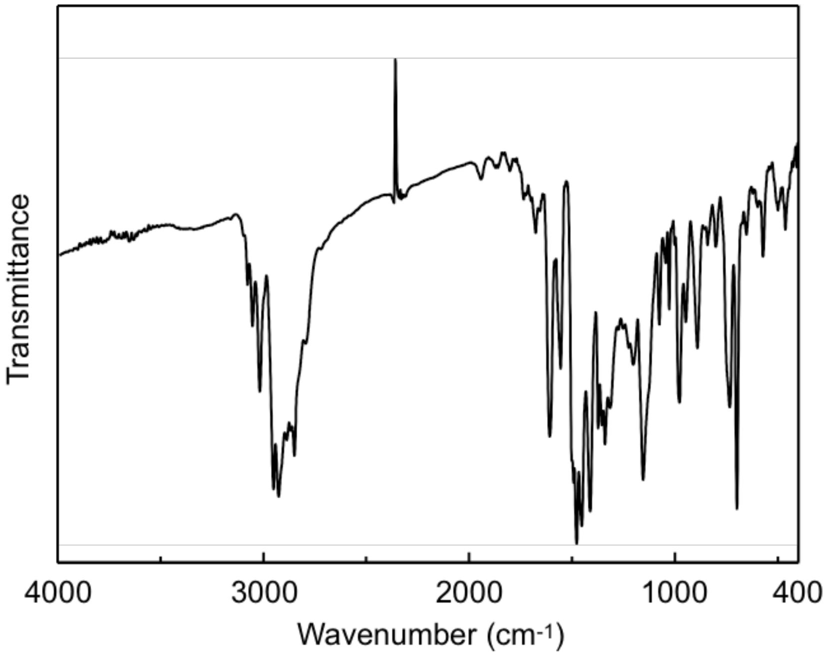

Fig. S123. FT-IR spectrum of poly-**3c** at 25 °C (KBr).

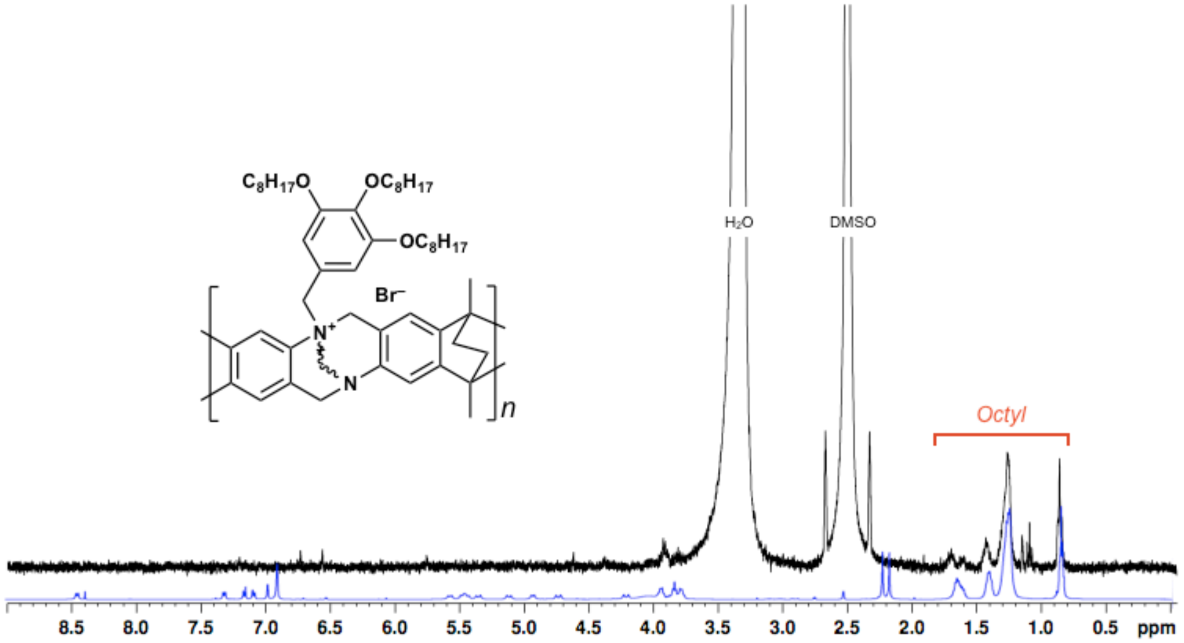

Fig. S124. ^{1}H NMR spectra (500 MHz) of poly-**1d** (black) and **1d** (blue) in DMSO-d_6 at 25 °C.

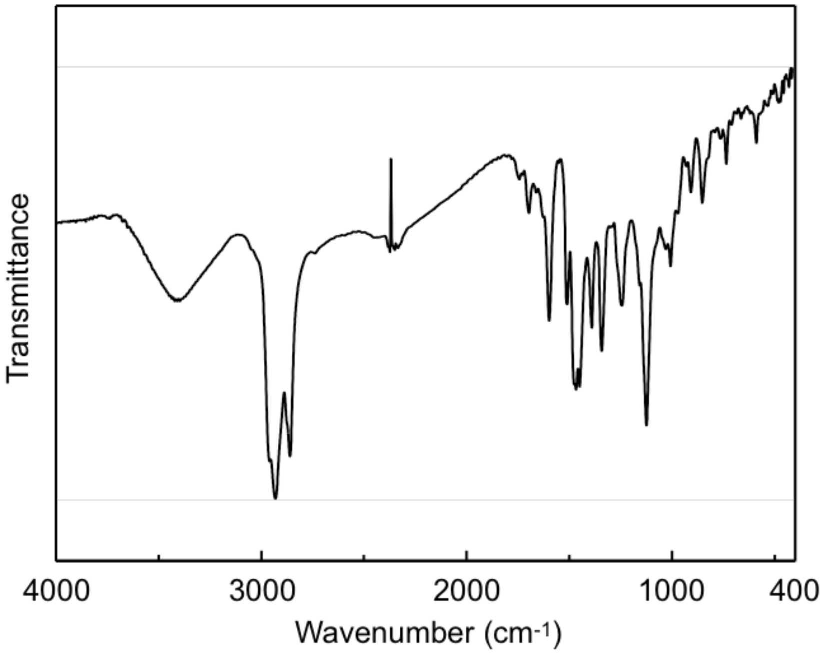

Fig. S125. FT-IR spectrum of poly-**1d** at 25 °C (KBr).

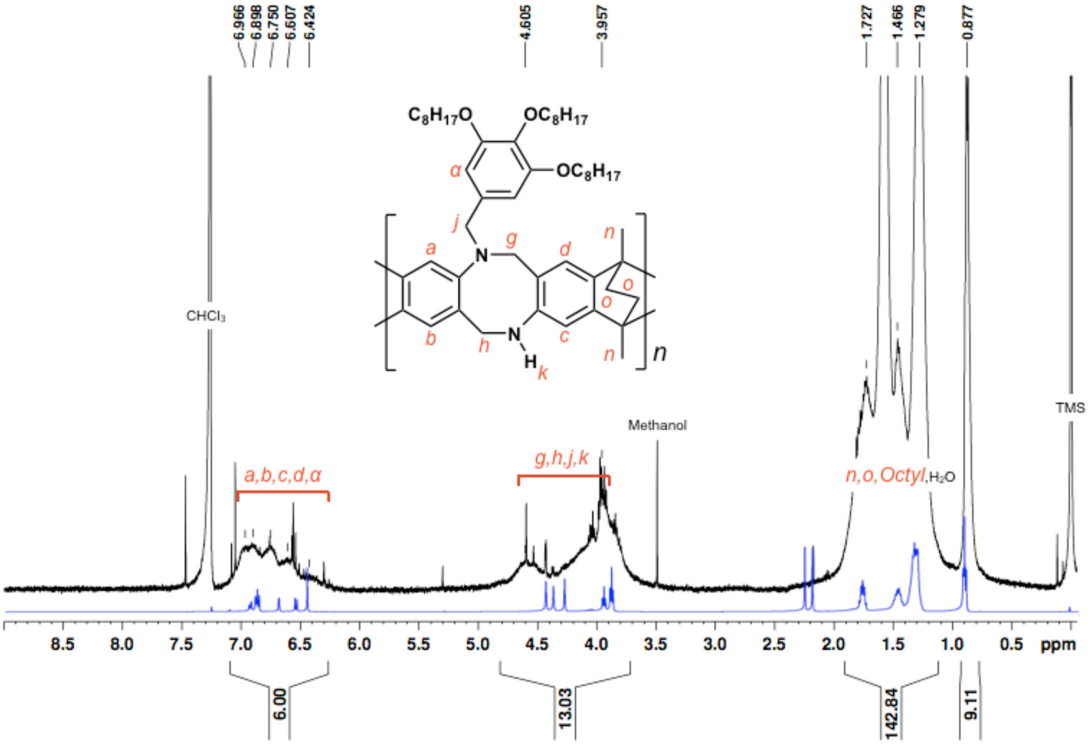

Fig. S126. ^{1}H NMR spectra (500 MHz) of poly-**2d** (black) and **2d** (blue) in $CDCl_3$ at 25 °C.

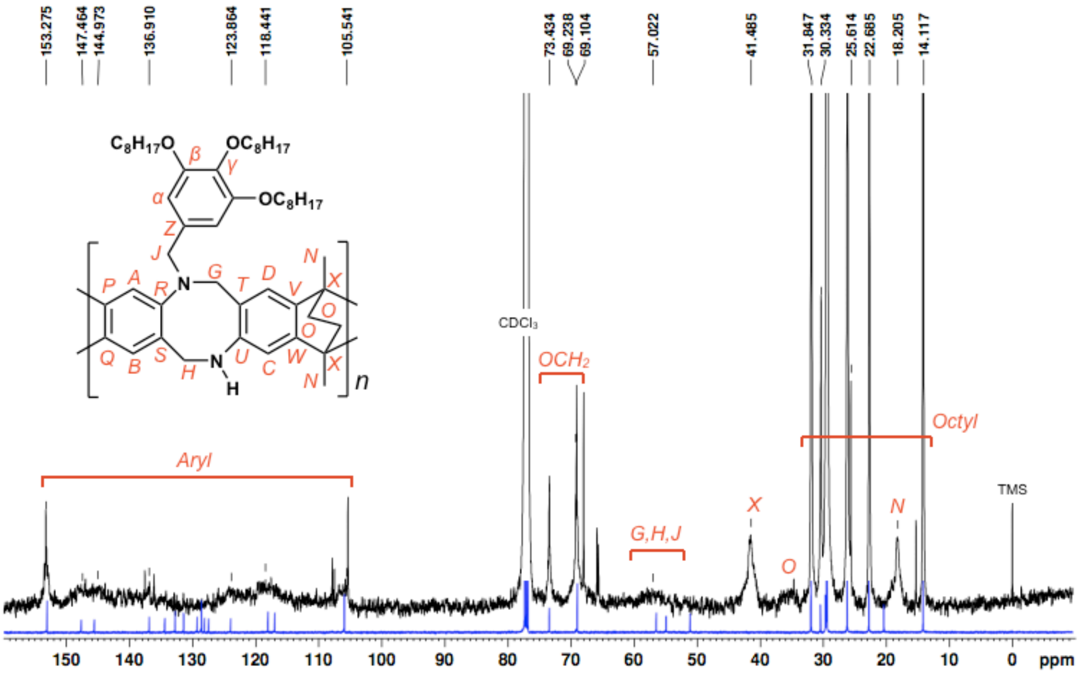

Fig. S127. ^{13}C NMR spectra (125 MHz) of poly-**2d** (black) and **2d** (blue) in $CDCl_3$ at 25 °C.

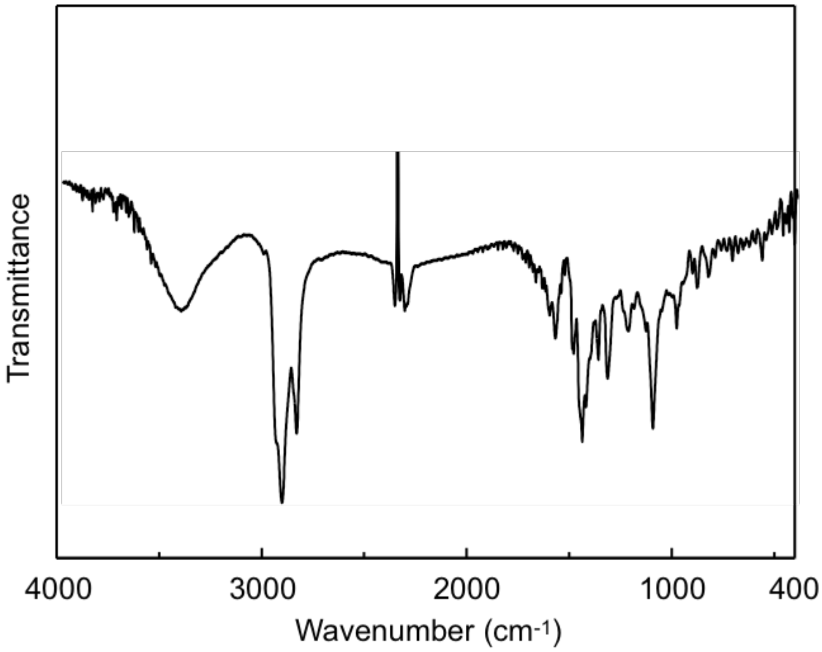

Fig. S128. FT-IR spectrum of poly-**2d** at 25 °C (KBr).

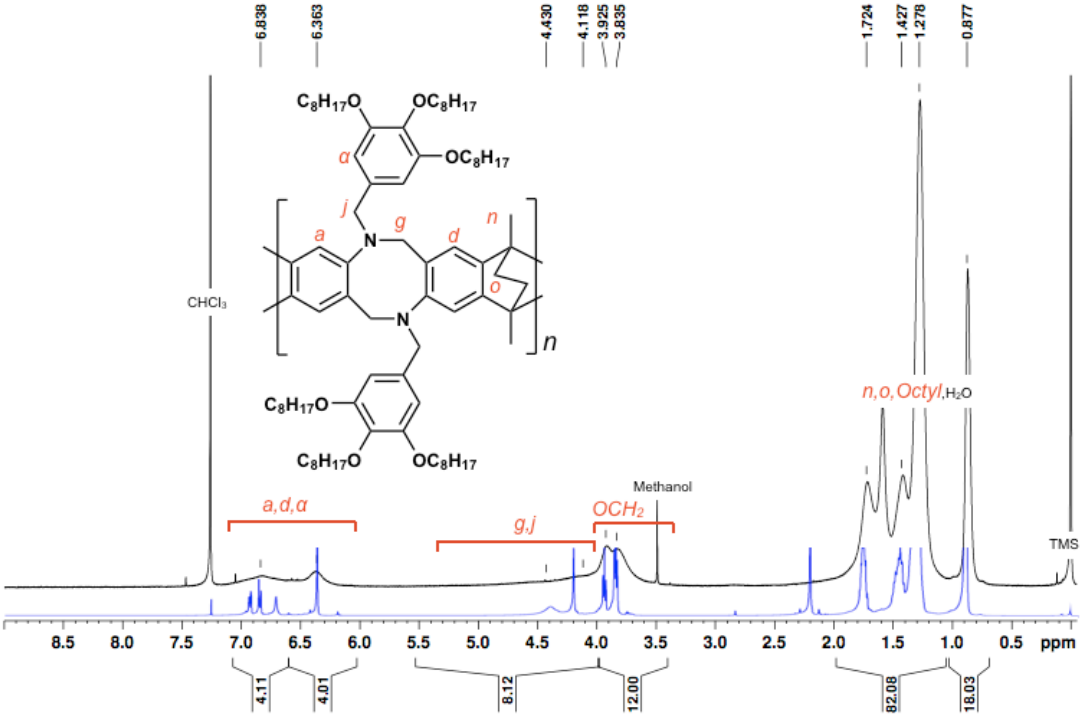

Fig. S129. ^{1}H NMR spectra (500 MHz) of poly-**3d** (black) and **3d** (blue) in $CDCl_3$ at 25 °C.

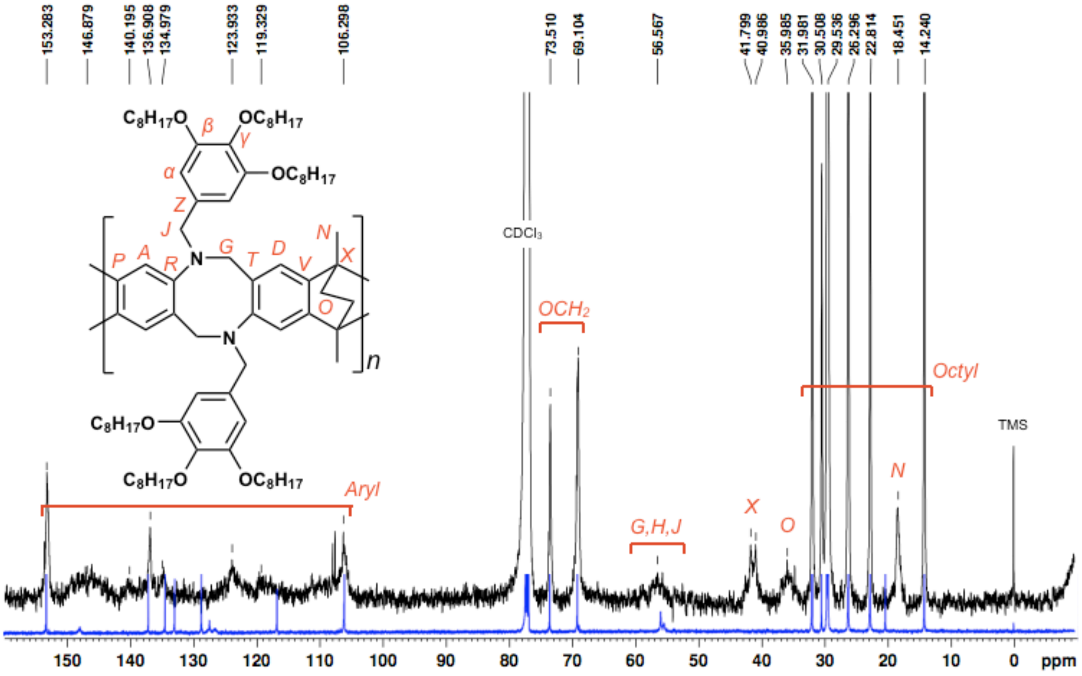

Fig. S130. ^{13}C NMR spectra (125 MHz) of poly-**3d** (black) and **3d** (blue) in $CDCl_3$ at 25 °C.

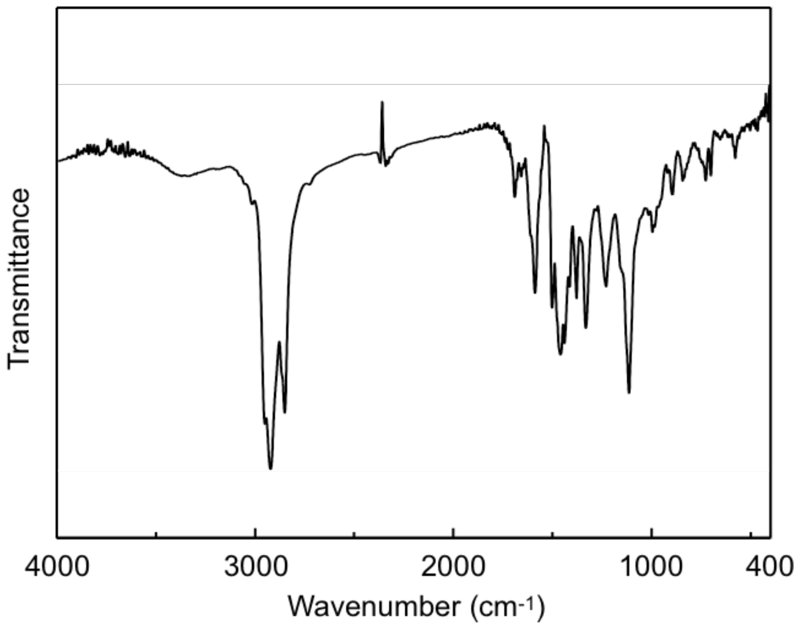

Fig. S131. FT-IR spectrum of poly-**3d** at 25 °C (KBr).

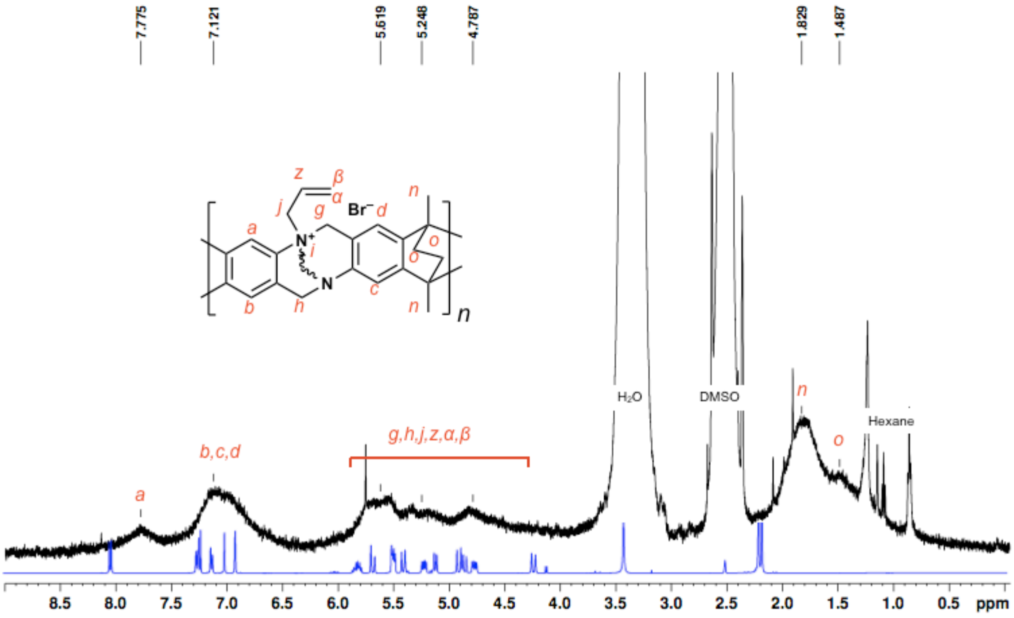

Fig. S132. ^{1}H NMR spectra (500 MHz) of poly-**1e** (black) and **1e** (blue) in DMSO-d_6 at 25 °C.

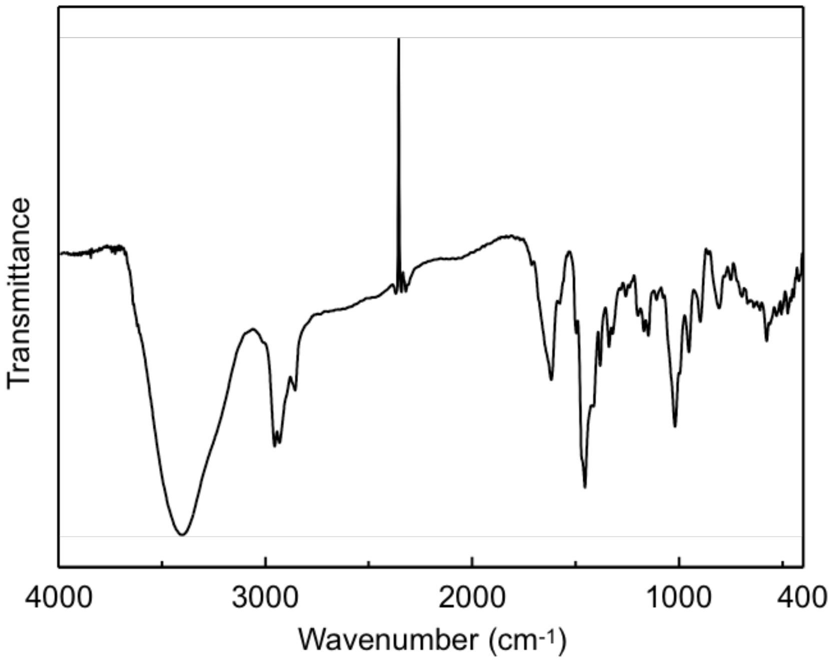

Fig. S133. FT-IR spectrum of poly-**1e** at 25 °C (KBr).

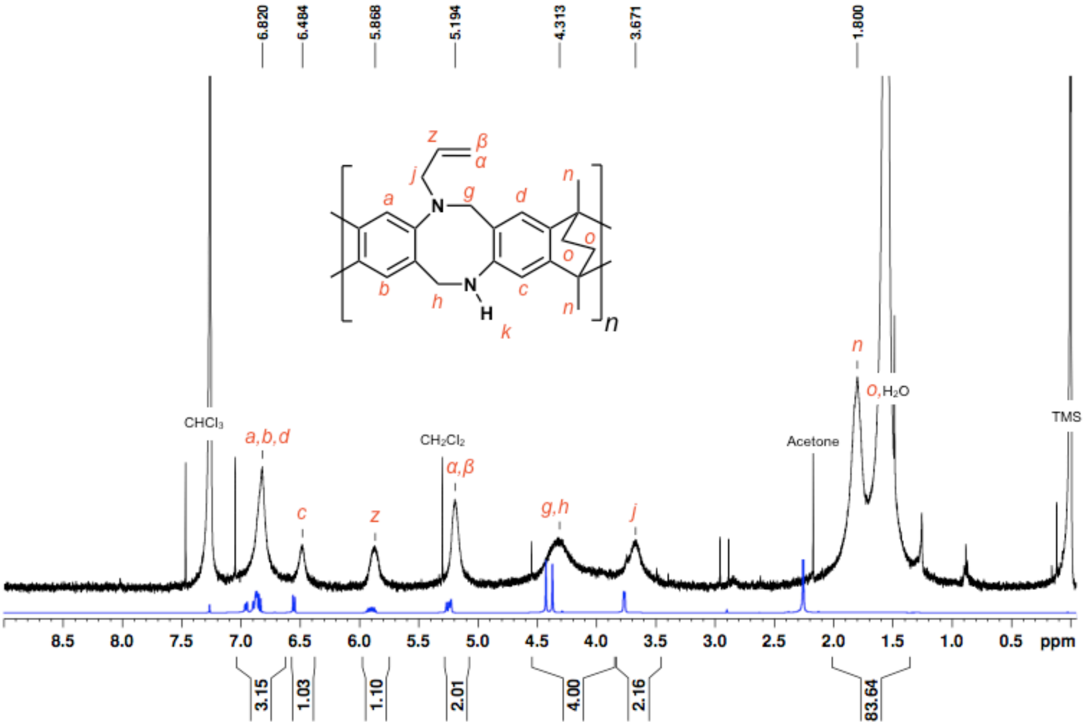

Fig. S134. ^{1}H NMR spectra (500 MHz) of poly-**2e** (black) and **2e** (blue) in $CDCl_3$ at 25 °C.

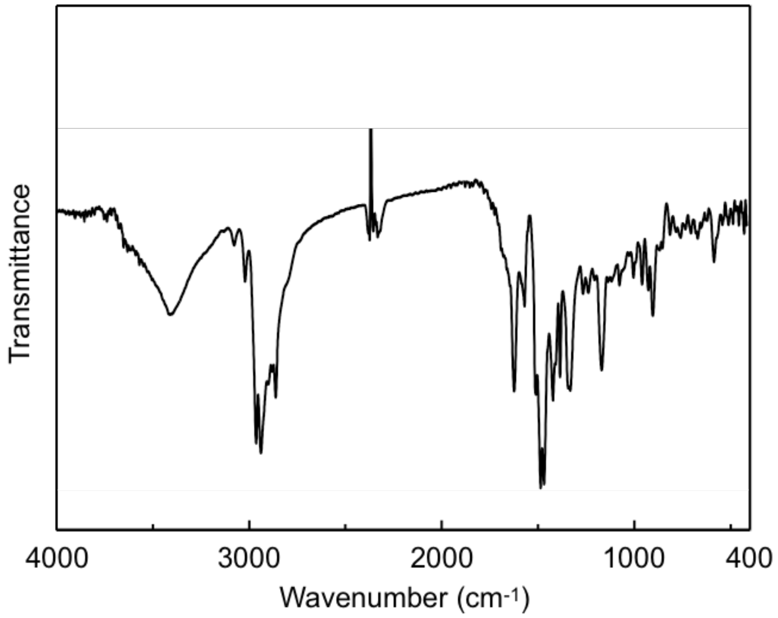

Fig. S135. FT-IR spectrum of poly-**2e** at 25 °C (KBr).

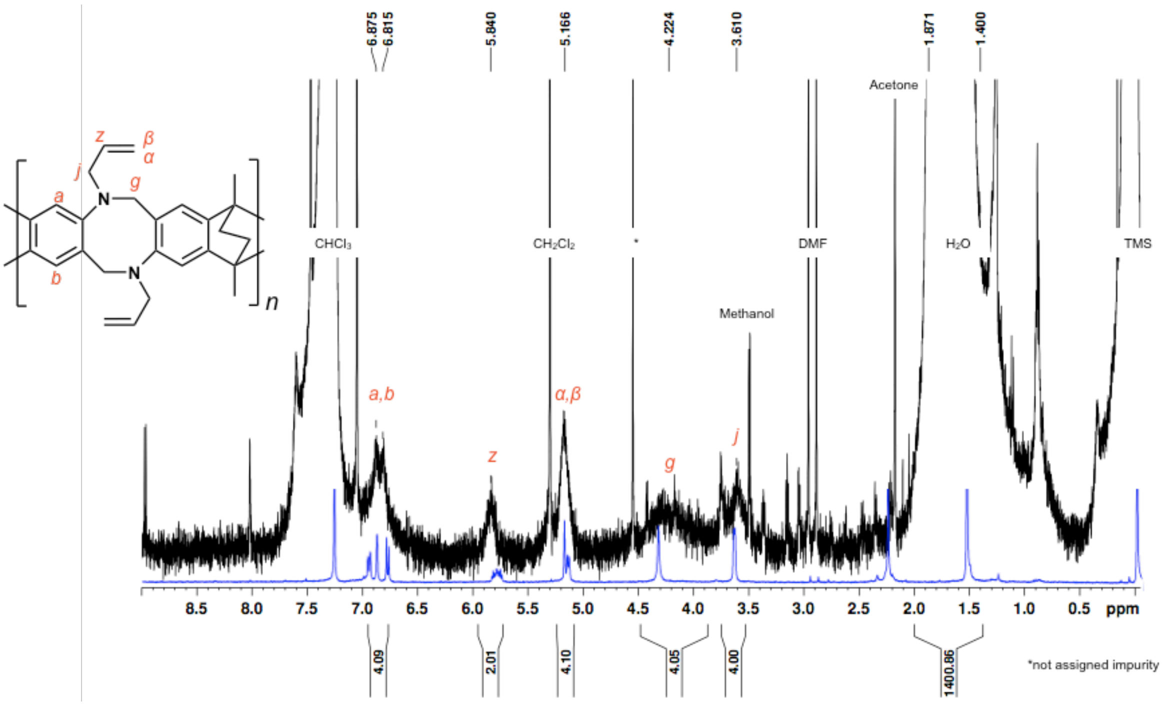

Fig. S136. ^{1}H NMR spectra (500 MHz) of poly-**3e** (black) and **3e** (blue) in $CDCl_3$ at 25 °C.

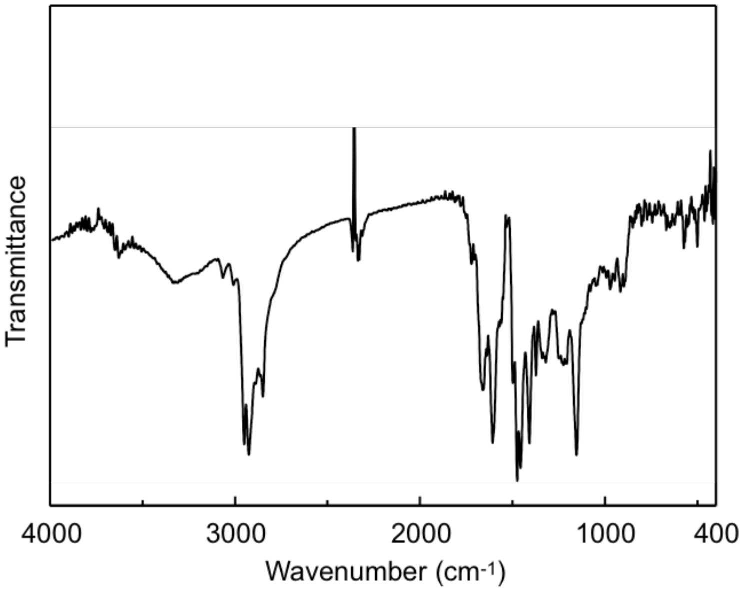

Fig. S137. FT-IR spectrum of poly-**3e** at 25 °C (KBr).

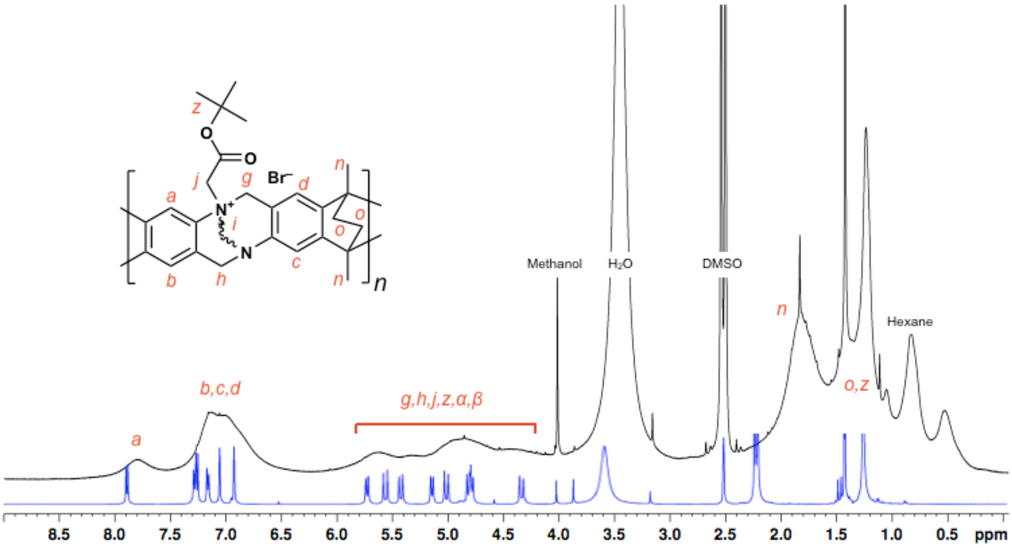

Fig. S138. ^{1}H NMR spectra (500 MHz) of poly-**1g** (black) and **1g** (blue) in DMSO-d_6 at 25 °C.

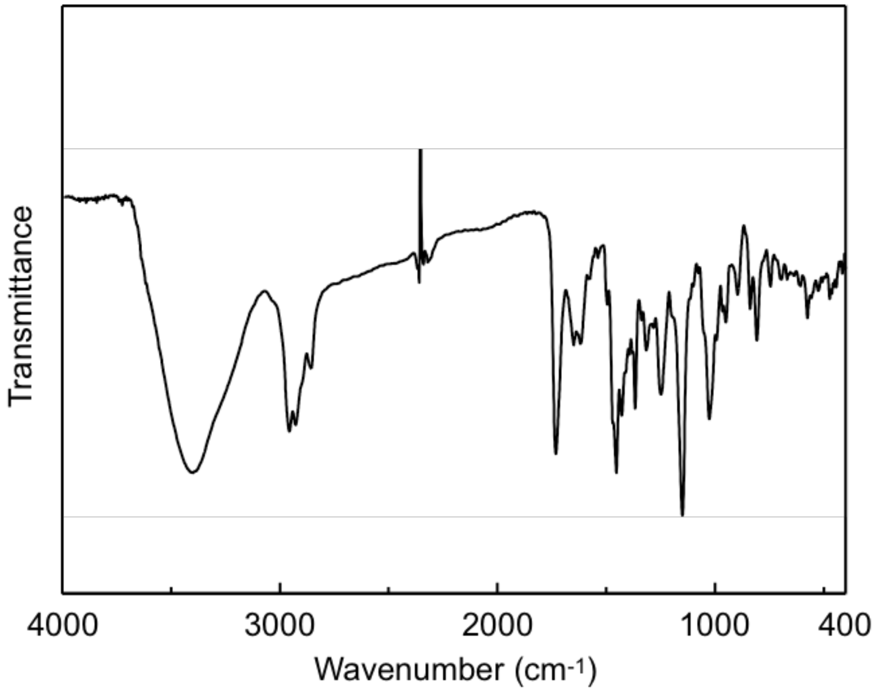

Fig. S139. FT-IR spectrum of poly-**1g** at 25 °C (KBr).

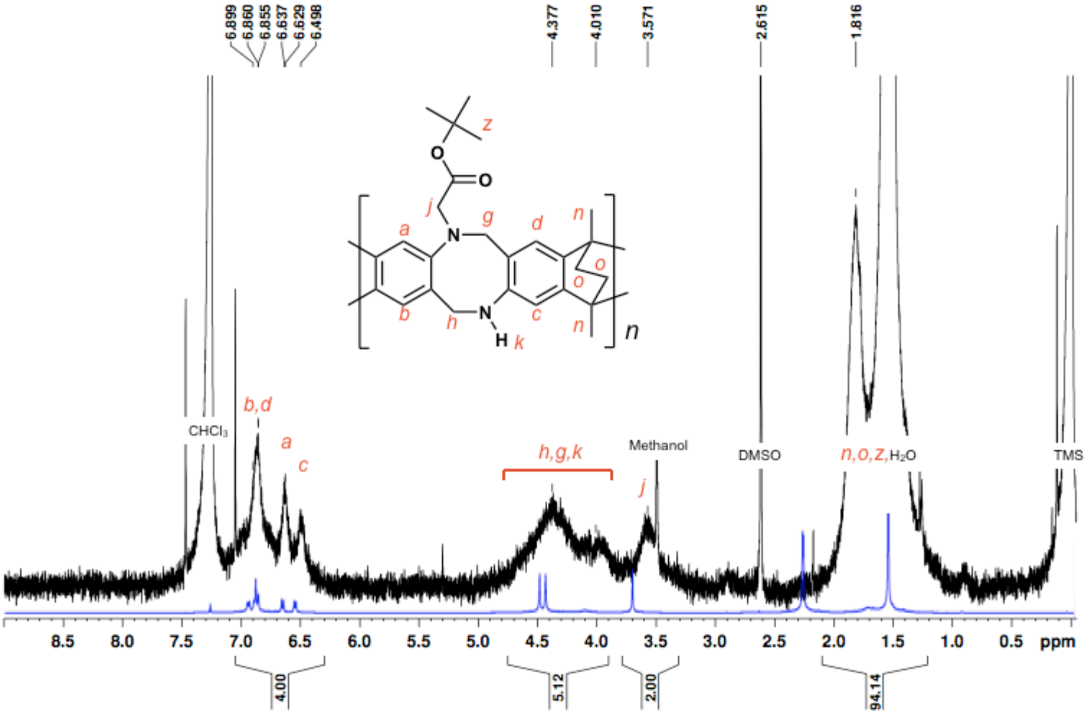

Fig. S140. ^{1}H NMR spectra (500 MHz) of poly-**2g** (black) and **2g** (blue) in $CDCl_3$ at 25 °C.

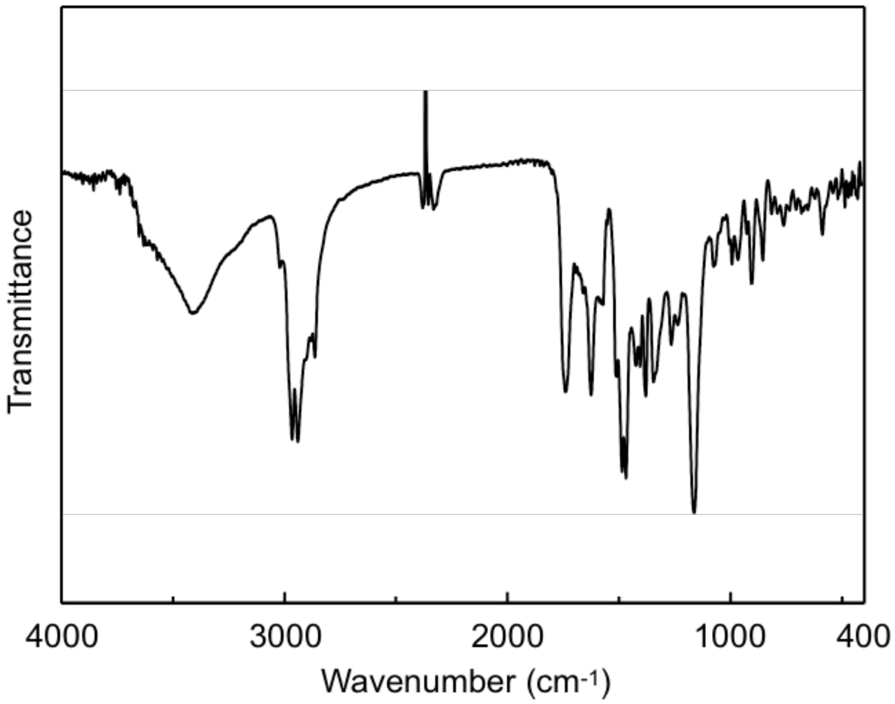

Fig. S141. FT-IR spectrum of poly-**2g** at 25 °C (KBr).

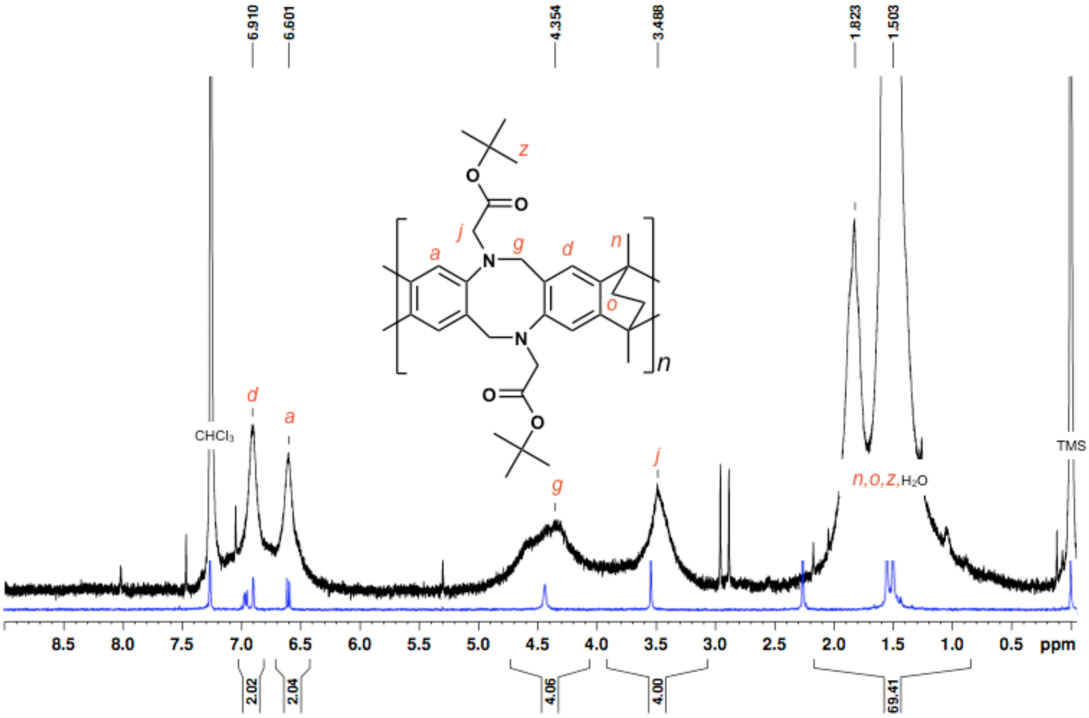

Fig. S142. ^{1}H NMR spectra (500 MHz) of poly-**3g** (black) and **3g** (blue) in $CDCl_3$ at 25 °C.

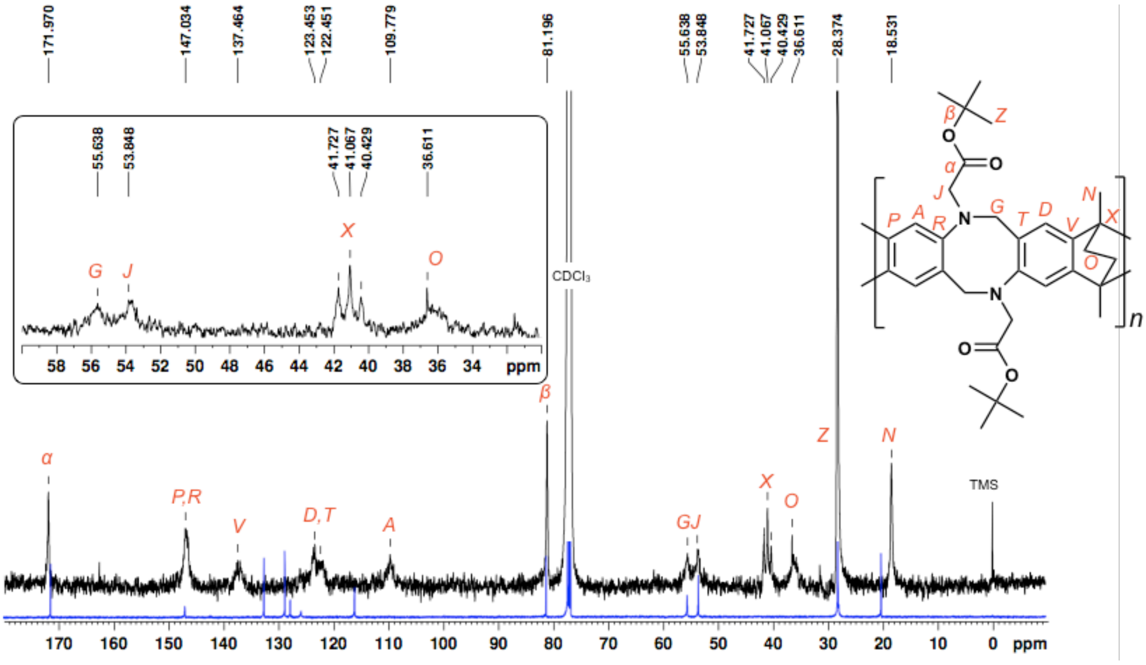

Fig. S143. ^{13}C NMR spectra (125 MHz) of poly-**3g** (black) and **3g** (blue) in $CDCl_3$ at 25 °C.

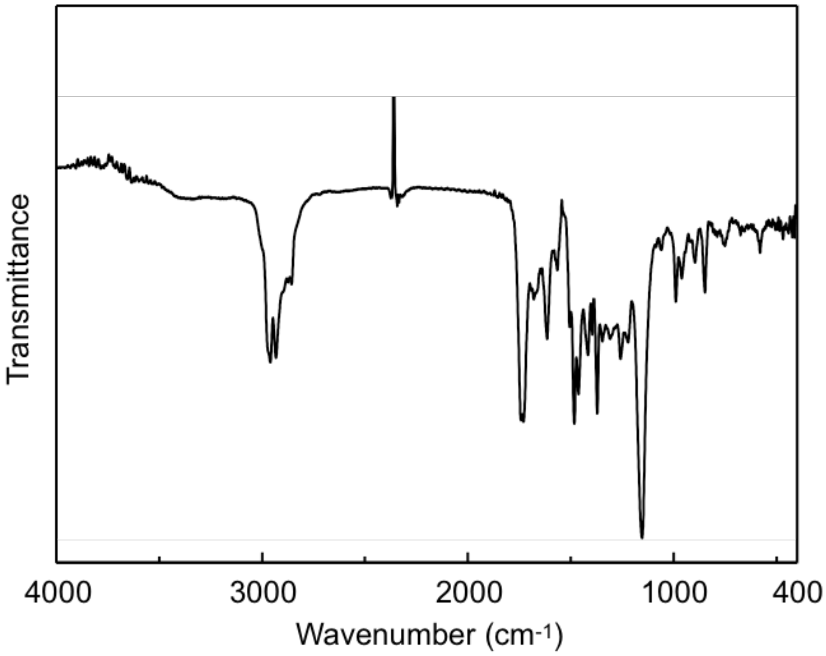

Fig. S144. FT-IR spectrum of poly-**3g** at 25 °C (KBr).

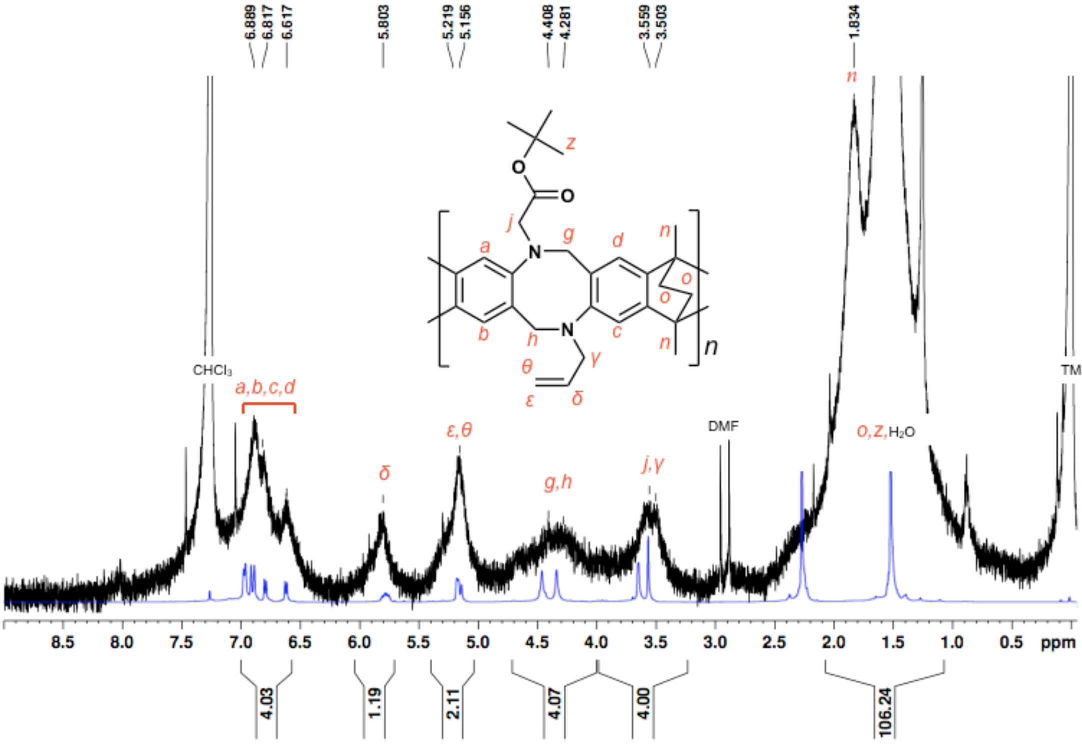

Fig. S145. ^{1}H NMR spectra (500 MHz) of poly-**3h** (black) and **3h** (blue) in CDCl$_3$ at 25 °C.

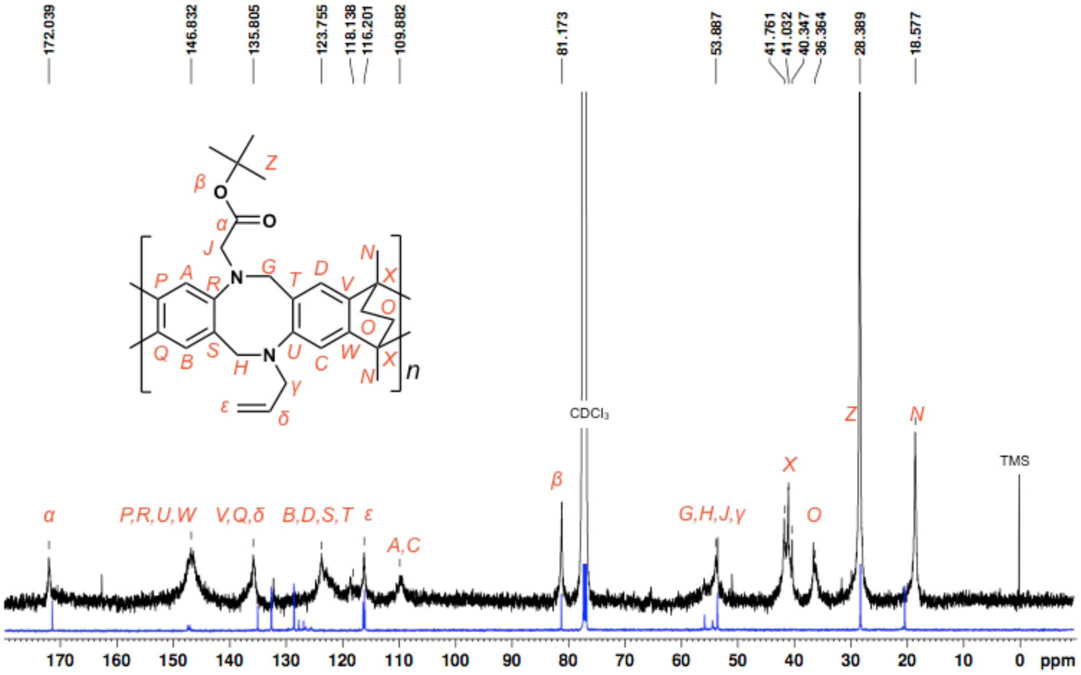

Fig. S146. ^{13}C NMR spectra (125 MHz) of poly-**3h** (black) and **3h** (blue) in CDCl$_3$ at 25 °C.

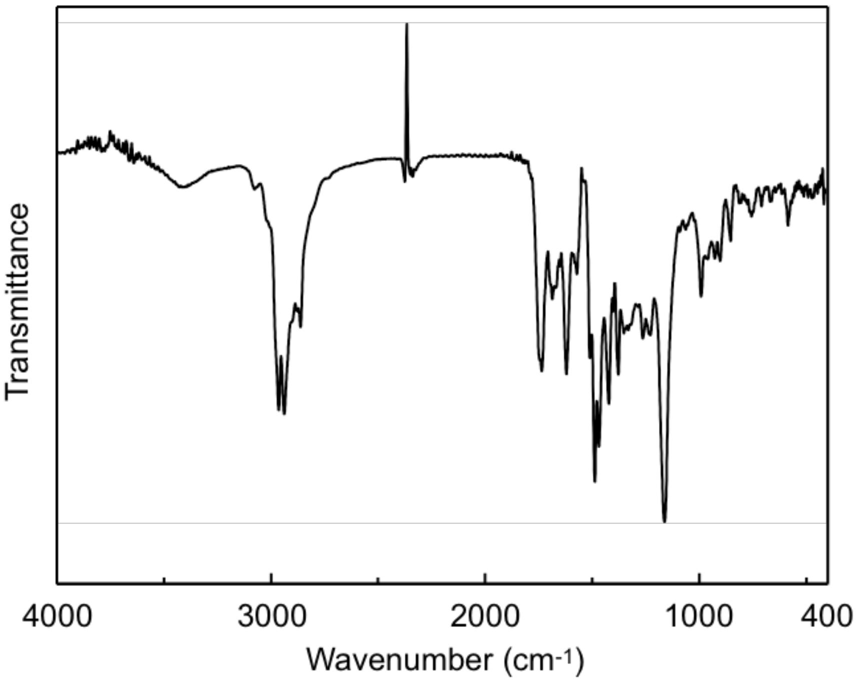

Fig. S147. FT-IR spectrum of poly-**3h** at 25 °C (KBr).

References

1. M. Carta, R. Malpass-Evans, M. Croad, Y. Rogan, J. C. Jansen, P. Bernardo, F. Bazzarelli and N. B. McKeown, *Science*, 2013, **339**, 303.
2. F. Ishiwari, N. Takeuchi, T. Sato, H. Yamazaki, R. Osuga, J. N. Kondo and T. Fukushima, *ACS Macro Lett*., 2017, **6**, 775.
3. M. Häring, *Helv. Chim. Acta*, 1963, **46**, 2970.
4. S. Kohrt, N. Santschi and J. Cvengroš, *Chem. Eur. J*., 2016, **22**, 390.
5. E. Weber, U. Muller, D. Worsch, F. Vogtle, G. Will and A. Kirfel, *J. Chem. Soc*., 1985, 1578.
6. C. Michon, M. H. Gonçalves and J. Lacour, *Chirality*, 2009, **21**, 809.
7. C. Michon, A. Sharma, G. Bernardinelli, E. Francotte and J. Lacour, *Chem. Commun*., 2010, **46**, 2206.